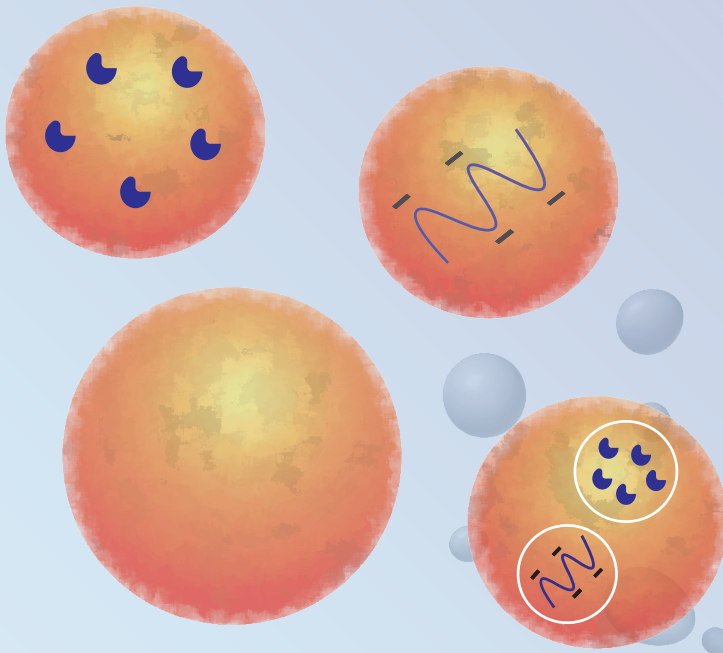


EARLY LIFE

COW'S MILK ALLERGY PREVENTION:

**PLGA Nanoparticles for the Oral Delivery
of β -Lactoglobulin Derived Peptide
and CpG Oligodeoxynucleotides**



Mengshan Liu

**EARLY LIFE COW'S MILK ALLERGY
PREVENTION: PLGA Nanoparticles for the
Oral Delivery of β -Lactoglobulin Derived
Peptide and CpG Oligodeoxynucleotides**

Mengshan Liu
2023

EARLY LIFE COW'S MILK ALLERGY PREVENTION: PLGA Nanoparticles for the Oral Delivery of β -Lactoglobulin Derived Peptide and CpG Oligodeoxynucleotides

Mengshan Liu

Division of Pharmaceutics, Utrecht University, Utrecht, the Netherlands

Division of Pharmacology, Utrecht University, Utrecht, the Netherlands

ISBN: 978-94-6473-212-2

Author: Mengshan Liu

Printing: Ipskamp Printing

Cover design: Mengshan Liu

Layout: Mengshan Liu

Copyright 2023 © by Mengshan Liu

The Netherlands. All rights reserved. No parts of this thesis may be reproduced, stored in a retrieval system or transmitted in any form by any means without permission of the author.

EARLY LIFE COW'S MILK ALLERGY PREVENTION: PLGA Nanoparticles for the Oral Delivery of β -Lactoglobulin Derived Peptide and CpG Oligodeoxynucleotides

**PREVENTIE VAN KOEMELKALLERGIE IN HET VROEGE LEVEN: PLGA-
nanodeeltjes voor de orale toediening van β -lactoglobuline afgeleid
peptide en CpG-oligodeoxynucleotiden**
(met een samenvatting in het Nederlands)

Proefschrift

ter verkrijging van de graad van doctor aan de
Universiteit Utrecht
op gezag van de
rector magnificus, prof.dr. H.R.B.M. Kummeling,
ingevolge het besluit van het college voor promoties
in het openbaar te verdedigen op

maandag 2 oktober 2023 des ochtends te 10.15 uur

door

MENGSHAN LIU

geboren op 4 januari 1991
te GUANGDONG, China

Promotoren:

Prof. dr. J. Garssen
Prof. dr. W.E. Hennink

Copromotoren:

Dr. C.F. van Nostrum
Dr. L.E.M. Willemsen

Beoordelingscommissie:

Prof. dr. F. Broere
Prof. dr. R.J. Kok
Prof. dr. J. Siepmann
Dr. R. van Ree
Prof. dr. H. Wichers

Dit proefschrift werd (mede) mogelijk gemaakt met financiële steun van China Scholarship Council.

TABLE OF CONTENTS

Chapter 1	General introduction	8
Chapter 2	Inhibition of cow's milk allergy development in mice by oral delivery of β -lactoglobulin derived peptides loaded PLGA nanoparticles is associated with systemic whey-specific immune silencing	19
Chapter 3	Oral pretreatment with β -lactoglobulin derived peptide and CpG co-encapsulated in PLGA nanoparticles prior to sensitizations attenuates cow's milk allergy development in mice	54
Chapter 4	Live cell imaging by Förster Resonance Energy Transfer fluorescence to study trafficking of PLGA nanoparticles and the release of a loaded peptide in dendritic cells	88
Chapter 5	<i>In vitro</i> immunostimulatory effects of CpG-ODN encapsulated PLGA nanoparticles on human monocytes derived dendritic cells and their T-cells priming capacity using an allogeneic DC-T-cell model	125
Chapter 6	Summary and perspectives	152
Appendices		171
	Nederlandse samenvatting	172
	中文总结	177
	Curriculum vitae	181
	List of publications	183
	Acknowledgements	185

CHAPTER 1

General Introduction

Cow's milk allergy (CMA) is one of the most common food allergies with a prevalence of roughly 2-4.5% in infants [1]. Unlike the non-IgE mediated type, the IgE-mediated CMA is less likely to be outgrown [2]. Following ingestion of a small amount of cow's milk protein, sometimes within minutes but mostly within an hour IgE-mediated CMA manifests symptoms including urticaria, angioedema, nausea, vomiting, diarrhea, rhino conjunctivitis, wheeze, or in severe cases life-threatening anaphylaxis. The prognosis of CMA was regarded as less serious when compared to the highly persistent peanut allergy, since 80% of the patients will naturally be resolved by the age of 4-year-old [3]. Nevertheless, a more recent study casted doubts on the early natural tolerance development and reported 40% of CMA cases persisted until the age of 5 [4]. Furthermore, CMA children suffering from CMA have a higher risk to develop asthma and other atopic diseases later on in their life [5]. To date, no treatment is recommended for CMA and the main guideline for the clinicians advises on cow's milk avoidance and the use of suitable milk substitutes [6]. However, the guideline for strict allergen avoidance imposes psychological stress on CMA patients as well as their caretakes and compromises their quality of life [7]. Furthermore, allergen avoidance can be associated with a higher risk of allergy development due to failure to establish oral tolerance to allergenic proteins [8].

Oral tolerance was first defined in 1946 by Chase *et al.* [9] as an active inhibition of the antigen-specific immune response that is generated via oral pre-exposure to the same antigen. Breakdown of oral tolerance or failure of oral tolerance induction was hypothesized as a cause for food hypersensitivity [10]. Hence, oral tolerance induction is considered as a pivotal intervention approach for prevention of food allergy. Early life has been shown as a window of opportunity for the induction of oral tolerance for several allergenic food components. The gut forms the largest immunological organ in the body and is the gatekeeper protecting the host from pathogens, while facilitating immune non-responsiveness for harmless antigens such as food proteins [10]. The early-life development and maturation of the gut-associated lymphoid tissue (GALT) is regarded as a window of opportunity for the induction of oral tolerance using preventive strategies [11]. For instance, in the Learning Early About Peanut Allergy (LEAP) study published in 2015, it was shown that introduction of peanuts into the diet of high-risk infants between 4 to 11 months of age, effectively lowered prevalence of peanut allergy to 10.6% as compared to 35.3% of the avoidance group [12]. Similarly, ingestion of egg proteins by 4-6 months-old infants reduced their risk to develop hen's

egg allergy [13]. Furthermore, an earlier timing for cow's milk proteins introduction in the Enquiring About Tolerance (EAT) observational study, effectively protected the breastfed infants between 14 days to 3 months of age [14] were effectively protected against CMA development [14, 15]. Noteworthy, early introduction of cow's milk proteins (*i.e.* whole whey protein) might provoke adverse allergic reactions in infants that have been sensitized after environmental exposure by the skin earlier [16]. This also necessitates early introduction of cow's milk proteins via oral ingestion [16]. In case breastfeeding is not possible, cow's milk formula or hydrolyzed formula milk might be given to the infants at high-risk of CMA development [17]. However, both formula milk did not effectively prevent CMA development [17]. Thus, the development of a safe and effective approach for CMA prevention is highly needed.

To induce oral tolerance for cow's milk proteins, T-cell recognition of the allergen-derived T-cell epitopes is required. Noteworthy, cow's milk consists of more than 25 different proteins [18], among which only some are allergenic, namely caseins and whey proteins. In the whey fraction of CM, α -lactalbumin and β -lactoglobulin are the major allergens [19, 20]. Particularly, in the whey fraction, β -lactoglobulin (BLG) is one of the major allergenic proteins. In this regard, van Esch *et al.* [21] reported that oral pre-exposure to the partially hydrolyzed whey protein prior to sensitization with whole whey protein, conferred protection of these mice against acute allergic skin reactivity upon intradermal challenge with whole whey protein. These whey hydrolysates contain multiple T-cell epitopes including those derived from α -lactalbumin and β -lactoglobulin. These small peptides may possess tolerance inducing capacities and can be further developed aiming to enhance the chances of developing oral tolerance for cow's milk particularly in high-risk infants who are fed with these hydrolyzed formula milk.

Far too often, environmental exposure of the newborns to cow's milk proteins through the skin may induce sensitization [16] unbeknownst to their caretakers. Therefore, to avoid potential risk of these adverse reactions, safer and more effective allergy preventive approaches are urgently needed. Noteworthy, T-cell receptors can recognize peptides of 8-12 amino acids (AA) [22], whereas peptides of 35-AA or longer are capable of crosslinking two effector cell-bound IgE molecules [23], which then trigger degranulation of mast cells and mediate allergic symptoms [24]. Thus, many attempts have been proposed and investigated to select T-cell epitopes-containing peptides ranging from 9 to 35 AA to fulfill the demands for both T-cell recognition and

avoidance of adverse reactions. As an example, Meulenbroek *et al.* [25] selected a mixture of synthetic BLG-peptides of 18-AA based on their capacity to activate human whey responsive T-cell lines and studied their preventive effects against whey-sensitizations in a prophylactic murine CMA model. In a follow up study, Kostadinova *et al.* [26] further identified four 18-AA long peptide sequences of the BLG protein that are effective in inducing oral tolerance against this protein in mice. Furthermore, these BLG derived peptides possess a reduced sensitizing capacity as compared to the intact BLG protein [27], likely because these peptides are too small to induce allergic symptoms and sensitization. Therefore, these peptides are potentially safe to be used for both prevention and treatment of children at risk for CMA, and might thus be added to infant milk formula.

Notwithstanding their improved safety profile, these BLG derived peptides (BLG-peptides) administered via oral route are susceptible to proteolytic degradation in the gastrointestinal tract which subsequently compromise their efficacy in tolerance induction. In light of these considerations, nanoparticles-based oral immunotherapy has gained increasingly attention for its efficacy in instructing allergen-specific tolerance [28-30]. Noteworthy, nanoparticles (NP) based on poly(lactic-*co*-glycolic acid) (PLGA) have been extensively investigated for development of oral vaccines [31, 32]. These particles protect the loaded peptides against enzymatic degradation in the GI tract [33-35]. Importantly, PLGA NPs can be taken up by antigen presenting cells (*i.e.*, dendritic cells) and subsequently and ideally intracellularly release their content in a sustained manner. These particles also have a good safety profile and a number of PLGA based drug products have been approved by the FDA and EMA [31, 36, 37]. From a pharmaceutical point of view, it is remarked that the size of the particles can be tailored for the aimed application by the formulation and processing conditions. Finally, the surface properties of PLGA NPs can be modulated by decoration with *e.g.*, PEG and targeting ligands to avoid non-specific uptake by cells and render them specific for the target cells [38, 39]. As a proof of concept, Kostadinova *et al.* [40] demonstrated using a mouse model that oral pretreatment with a mixture of PLGA NP loaded with two selected BLG-peptides and 2 additional soluble BLG-peptides lowered acute allergic skin response to whole whey protein as compared to the Empty NP pretreated mice.

Despite early-life development and maturation of the gut-associated lymphoid tissue (GALT) there is a window of opportunity for oral tolerance induction [11], since

the neonatal GALT is prone to development of Th2 immunity [41]. Therefore, environmental stimuli (*i.e.*, intestinal microbial diversity) as Th1- and Treg- adjuvants are indispensable to skew away from allergic type 2 immunity. Nevertheless, improved hygiene conditions and use of antibiotics affect intestinal microbial diversity and commensal microbiota composition [42, 43]. Hanski *et al.* [42] and Stefka *et al.* [43] hypothesized that these changes give rise to an immune imbalance leading to an increased risk in allergic disease development (*i.e.*, food allergy). Bacteria and viruses are captured by APCs and their building blocks are degraded into small molecules and evolutionary conserved cellular structures like peptidoglycans, lipopolysaccharides (LPS) and bacterial DNA (pathogen-associated molecular patterns, PAMPs) which can be recognized via different type of pattern recognition receptors (PRRs) [44, 45]. In this regard, bacterial DNA rich in unmethylated cytosine-guanosine dinucleotides (CpG) act as Toll-like receptor-9 (TLR-9) agonists. These bind to and subsequently activate TLR-9, a receptor expressed on activated intestinal epithelial cells [46] or in endosomal compartments of human plasmacytoid dendritic cells (pDCs) [47] and B lymphocytes (B-cells) [48, 49]. In particular, DCs play a crucial role in shaping immunity and tolerance [50]. Upon binding to TLR-9 in DCs, bacterial CpG motives activate the TLR-9 signaling cascade, which drives differentiation of the DCs. Matured DCs are able to instruct naïve T-cells to develop into effector cells such as T helper 1- (Th1) and a regulatory T-cell (Treg) response in case of functional shaping of DCs by CpG DNA [28, 51]. If these CpG primed DCs subsequently capture food antigens from the intestinal lumen, these antigens are presented by these DCs which may direct the allergen specific T-cell response towards a Th1 and/or Treg prone phenotype skewing away from the allergic Th2 phenotype. To exploit this Th1 and/or Treg skewing effect, synthetic CpG oligodeoxynucleotides (CpG-ODN) that contain unmethylated CpG-ODN motifs, mimicking the structure of bacterial CpG DNA [51], have been exploited as Th1- and Treg- adjuvants for PLGA NP loaded with allergens [28, 52]. Srivastava *et al.* [28] reported that oral immunotherapy using peanut extract loaded in CpG-ODN surface-conjugated PLGA nanoparticles effectively protected peanut allergic mice from anaphylaxis and alleviated peanut-allergic phenotypes. Instead of surface conjugation of CpG-ODN, we aimed for an easier approach, namely, to co-encapsulate both the antigen and CpG-ODN into the PLGA nanoparticles to improve the allergen-specific oral tolerance induction efficacy. Henceforth, the allergen-specific tolerogenic outcomes *in vivo* and immunomodulatory effect of these PLGA NP loaded with peptide and/or CpG-

ODN payload on the major antigen-presenting cells (*i.e.*, dendritic cells), should be elucidated.

Aim And Outline Of This Thesis

This thesis aimed to develop PLGA NP for delivery T-cell epitope containing peptides and/or CpG-ODN for CMA prevention *in vivo* and to investigate the immunomodulatory effects mediated by these NP on a cellular level.

Instead of a mixture of 4 selected BLG-peptides as reported previously [40], only two BLG-peptides were chosen for oral tolerance induction in mice. **Chapter 2** describes the tolerance induction effect and dose-related effect of oral pre-treatments using the two selected BLG-peptides encapsulated PLGA nanoparticles in a prophylactic CMA murine model. The nanoparticles encapsulating the BLG-peptides were optimized in terms of NP size and BLG-peptides loading. The allergen-specific tolerogenic outcomes were evaluated for acute allergic skin response to whole whey protein, sera allergen-specific immunoglobulins, *ex vivo* allergen-restimulated cytokine release by splenocytes and percentage of different splenic T-cell subsets.

In light of the relevance of environmental stimuli during allergen-exposure, co-delivery of CpG-ODN as immune adjuvant may help to improve allergen-specific oral tolerance induction. **Chapter 3** studies allergen-specific tolerogenic effect of the oral pretreatment using PLGA nanoparticles loaded with a selected BLG-peptide and/or CpG-ODN in the same prophylactic CMA murine model as used in Chapter 2. These PLGA nanoparticles were prepared with similar size and surface physicochemical properties using double emulsion solvent evaporation method. The allergen-specific tolerogenic outcomes were evaluated the same way as described in Chapter 2 and additional analysis of surface expression of activation markers on dendritic cells from mesenteric lymph nodes and spleen.

Dendritic cells (DC) as a major antigen presenting cell type, play a pivotal role in allergen-specific oral tolerance induction. Hence, investigation of the interaction between orally administered PLGA NPs loaded with BLG-peptides and dendritic cells may shed light onto the mechanism(s) via which PLGA nanocarriers promote oral tolerance induction. To this end, in **Chapter 4** the intracellular trafficking of PLGA nanoparticles and the release of a loaded peptide in dendritic cells was studied using

Förster Resonance Energy Transfer (FRET) analysis. Donor dye (Cy3) conjugated BLG-peptide and acceptor dye (Cy5) conjugated PLGA were synthesized and characterized. FRET NPs, consisting of the labeled polymer and peptide were prepared and optimized for size and FRET efficiency. The obtained FRET NPs were exploited to study their stability and integrity in a biorelevant simulated gastric fluid. Uptake of Pep-Cy3 loaded in PLGA-Cy5 NP by human monocytes derived dendritic cells (human moDCs) was studied via live imaging and quantified using flow cytometry. FRET was exploited to determine the intracellular fate of BLG-peptide encapsulated PLGA NP and the release of loaded peptide.

Following *in vivo* study of antigen and/or class B-CpG-ODN loaded PLGA nanoparticles oral tolerance induction (in **Chapter 3**), comprehensive understanding of the adjuvant action of CpG-ODN in relation to the functional outcome of DC and T-cell interaction relevant for tolerance induction is warranted. **Chapter 5** describes *in vitro* investigation of the immunomodulatory effects of different classes of CpG-ODN encapsulated PLGA nanoparticles on DC and their T-cell polarizing capacity using an allogeneic DC-T-cell model. After 2-days-incubation with the different NPs, surface expression of activation markers and cytokine release by the primed moDC were determined. The primed moDCs were co-cultured with allogeneic naïve T-cells for 5 days and their T-cell priming capacity was investigated.

Chapter 6 summarizes and discusses the findings of this thesis and provides future perspectives for development of PLGA nanoparticles-based approaches for prevention of early life cow's milk allergy.

References

- [1] J.L. Brozek, R.T. Firmino, A. Bognanni, S. Arasi, I. Ansotegui, A.H. Assa'ad, S.L. Bahna, R.B. Canani, M. Bozzola, D.K. Chu, L. Dahdah, C. Dupont, P. Dziechciarz, M. Ebisawa, E. Galli, A. Horvath, R. Kamenwa, G. Lack, H. Li, A. Martelli, A. Nowak-Wegrzyn, N.G. Papadopoulos, R. Pawankar, Y. Roldan, M. Said, M. Sanchez-Borges, R. Shamir, J.M. Spergel, H. Szajewska, L. Terracciano, Y. Vandenplas, C. Venter, S. Waffenschmidt, S. Wasserman, A. Warner, G.W.K. Wong, A. Fiocchi, H.J. Schunemann, World Allergy Organization (WAO) Diagnosis and Rationale for Action against Cow's Milk Allergy (DRACMA) Guideline update - XIV - Recommendations on CMA immunotherapy, *World Allergy Organ J*, 15 (2022) 100646.
- [2] A.A. Schoemaker, A.B. Sprikkelman, K.E. Grimshaw, G. Roberts, L. Grabenhenrich, L. Rosenfeld, S. Siegert, R. Dubakiene, O. Rudzeviciene, M. Reche, A. Fiandor, N.G. Papadopoulos, A. Malamitsi-Puchner, A. Fiocchi, L. Dahdah, S.T. Sigurdardottir, M. Clausen, A. Stanczyk-Przyluska, K. Zeman, E.N. Mills, D. McBride, T. Keil, K. Beyer, Incidence and natural history of challenge-proven cow's milk allergy in European children--EuroPrevall birth cohort, *Allergy*, 70 (2015) 963-972.
- [3] A. Host, S. Halken, A prospective study of cow milk allergy in Danish infants during the first 3 years of life. Clinical course in relation to clinical and immunological type of hypersensitivity reaction, *Allergy*, 45 (1990) 587-596.
- [4] A. Elizur, N. Rajuan, M.R. Goldberg, M. Leshno, A. Cohen, Y. Katz, Natural course and risk factors for persistence of IgE-mediated cow's milk allergy, *J Pediatr*, 161 (2012) 482-487 e481.
- [5] L. Yang, J. Fu, Y. Zhou, Research Progress in Atopic March, *Front Immunol*, 11 (2020) 1907.
- [6] D. Luyt, H. Ball, N. Makwana, M.R. Green, K. Bravin, S.M. Nasser, A.T. Clark, A. Standards of Care Committee of the British Society for, I. Clinical, BSACI guideline for the diagnosis and management of cow's milk allergy, *Clin Exp Allergy*, 44 (2014) 642-672.
- [7] A.J. Cummings, R.C. Knibb, R.M. King, J.S. Lucas, The psychosocial impact of food allergy and food hypersensitivity in children, adolescents and their families: a review, *Allergy*, 65 (2010) 933-945.
- [8] M. van Splunter, L. Liu, R.J.J. van Neerven, H.J. Wichers, K.A. Hettinga, N.W. de Jong, Mechanisms Underlying the Skin-Gut Cross Talk in the Development of IgE-Mediated Food Allergy, *Nutrients*, 12 (2020).
- [9] M.W. Chase, Inhibition of experimental drug allergy by prior feeding of the sensitizing agent, *Proc Soc Exp Biol Med*, 61 (1946) 257-259.
- [10] M. Chehade, L. Mayer, Oral tolerance and its relation to food hypersensitivities, *J Allergy Clin Immunol*, 115 (2005) 3-12; quiz 13.
- [11] B. Weström, E. Arévalo Sureda, K. Pierzynowska, S.G. Pierzynowski, F.-J. Pérez-Cano, The Immature Gut Barrier and Its Importance in Establishing Immunity in Newborn Mammals, *Frontiers in Immunology*, 11 (2020).
- [12] G. Du Toit, G. Roberts, P.H. Sayre, H.T. Bahnson, S. Radulovic, A.F. Santos, H.A. Brough, D. Phippard, M. Basting, M. Feeney, V. Turcanu, M.L. Sever, M. Gomez Lorenzo, M. Plaut, G. Lack, L.S. Team, Randomized trial of peanut consumption in infants at risk for peanut allergy, *N Engl J Med*, 372 (2015) 803-813.
- [13] J.J. Koplin, N.J. Osborne, M. Wake, P.E. Martin, L.C. Gurrin, M.N. Robinson, D. Tey, M. Slaa, L. Thiele, L. Miles, D. Anderson, T. Tan, T.D. Dang, D.J. Hill, A.J. Lowe, M.C. Matheson, A.L. Ponsonby, M.L. Tang, S.C. Dharmage, K.J. Allen, Can early introduction of egg prevent egg allergy in infants? A population-based study, *J Allergy Clin Immunol*, 126 (2010) 807-813.
- [14] Y. Katz, N. Rajuan, M.R. Goldberg, E. Eisenberg, E. Heyman, A. Cohen, M. Leshno, Early exposure to cow's milk protein is protective against IgE-mediated cow's milk protein allergy, *J Allergy Clin Immunol*, 126 (2010) 77-82 e71.
- [15] R.L. Peters, J.J. Koplin, S.C. Dharmage, M.L.K. Tang, V.L. McWilliam, L.C. Gurrin, M.R. Neeland, A.J. Lowe, A.L. Ponsonby, K.J. Allen, Early Exposure to Cow's Milk Protein Is Associated with a Reduced Risk of Cow's Milk Allergic Outcomes, *J Allergy Clin Immunol Pract*, 7 (2019) 462-470 e461.
- [16] G. Lack, Epidemiologic risks for food allergy, *J Allergy Clin Immunol*, 121 (2008) 1331-1336.
- [17] S. Halken, A. Muraro, D. de Silva, E. Khaleva, E. Angier, S. Arasi, H. Arshad, H.T. Bahnson, K. Beyer, R. Boyle, G. du Toit, M. Ebisawa, P. Eigenmann, K. Grimshaw, A. Hoest, C. Jones, G. Lack, K. Nadeau, L. O'Mahony, H. Szajewska, C. Venter, V. Verhasselt, G.W.K. Wong, G. Roberts, A. European Academy of, A. Clinical Immunology Food, G. Anaphylaxis Guidelines, EAACI guideline: Preventing the development of food allergy in infants and young children (2020 update), *Pediatr Allergy Immunol*, 32 (2021) 843-858.
- [18] S. Taniuchi, M. Takahashi, K. Soejima, Y. Hatano, H. Minami, Immunotherapy for cow's milk allergy, *Hum Vaccin Immunother*, 13 (2017) 2443-2451.

- [19] R.F. G. H. Docena, F. G. Chirido, C. A. Fossati, Identification of casein as the major allergenic and antigenic protein of cow's milk, *Allergy*, 51 (1996) 412-416.
- [20] Jean-Michel Wal, Bovine milk allergenicity, *Annals of allergy, asthma & immunology*, 93 (2004) 2-11.
- [21] B.C.A.M. van Esch, A.I. Kostadinova, J. Garssen, L.E.M. Willemsen, L.M.J. Knippels, A dietary intervention with non-digestible oligosaccharides and partial hydrolysed whey protein prevents the onset of food allergic symptoms in mice, *PharmaNutrition*, 5 (2017) 1-7.
- [22] C.J. Holland, D.K. Cole, A. Godkin, Re-Directing CD4(+) T Cell Responses with the Flanking Residues of MHC Class II-Bound Peptides: The Core is Not Enough, *Front Immunol*, 4 (2013) 172.
- [23] R.C. Aalberse, R. Cramer, IgE-binding epitopes: a reappraisal, *Allergy*, 66 (2011) 1261-1274.
- [24] M. Larche, Peptide therapy for allergic diseases: basic mechanisms and new clinical approaches, *Pharmacol Ther*, 108 (2005) 353-361.
- [25] L.A. Meulenbroek, B.C. van Esch, G.A. Hofman, C.F. den Hartog Jager, A.J. Nauta, L.E. Willemsen, C.A. Bruijnzeel-Koomen, J. Garssen, E. van Hoffen, L.M. Knippels, Oral treatment with beta-lactoglobulin peptides prevents clinical symptoms in a mouse model for cow's milk allergy, *Pediatr Allergy Immunol*, 24 (2013) 656-664.
- [26] A.I. Kostadinova, A. Pablos-Tanarro, M.A.P. Diks, B. van Esch, J. Garssen, L.M.J. Knippels, L.E.M. Willemsen, Dietary Intervention with beta-Lactoglobulin-Derived Peptides and a Specific Mixture of Fructo-Oligosaccharides and *Bifidobacterium breve* M-16V Facilitates the Prevention of Whey-Induced Allergy in Mice by Supporting a Tolerance-Prone Immune Environment, *Front Immunol*, 8 (2017) 1303.
- [27] K.L. Bogh, V. Barkholt, C.B. Madsen, The sensitising capacity of intact beta-lactoglobulin is reduced by co-administration with digested beta-lactoglobulin, *Int Arch Allergy Immunol*, 161 (2013) 21-36.
- [28] K.D. Srivastava, A. Siefert, T.M. Fahmy, M.J. Caplan, X.M. Li, H.A. Sampson, Investigation of peanut oral immunotherapy with CpG/peanut nanoparticles in a murine model of peanut allergy, *J Allergy Clin Immunol*, 138 (2016) 536-543 e534.
- [29] K.R. Hughes, M.N. Saunders, J.J. Landers, K.W. Janczak, H. Turkistani, L.M. Rad, S.D. Miller, J.R. Podojil, L.D. Shea, J.J. O'Konek, Masked Delivery of Allergen in Nanoparticles Safely Attenuates Anaphylactic Response in Murine Models of Peanut Allergy, *Frontiers in Allergy*, 3 (2022).
- [30] H. Pohlit, I. Bellinghausen, H. Frey, J. Saloga, Recent advances in the use of nanoparticles for allergen-specific immunotherapy, *Allergy*, 72 (2017) 1461-1474.
- [31] G. Cappellano, C. Comi, A. Chiochetti, U. Dianzani, Exploiting PLGA-Based Biocompatible Nanoparticles for Next-Generation Tolerogenic Vaccines against Autoimmune Disease, *Int J Mol Sci*, 20 (2019).
- [32] J. Koerner, D. Horvath, M. Groettrup, Harnessing Dendritic Cells for Poly (D,L-lactide-co-glycolide) Microspheres (PLGA MS)-Mediated Anti-tumor Therapy, *Front Immunol*, 10 (2019) 707.
- [33] F. Sarti, G. Perera, F. Hintzen, K. Kotti, V. Karageorgiou, O. Kammona, C. Kiparissides, A. Bernkop-Schnürch, In vivo evidence of oral vaccination with PLGA nanoparticles containing the immunostimulant monophosphoryl lipid A, *Biomaterials*, 32 (2011) 4052-4057.
- [34] D.R.R. Daqing Wang, Glen S. Kwon and John Samuel, Encapsulation of plasmid DNA in biodegradable poly(D,L-lactic-coglycolic acid) microspheres as a novel approach for immunogene delivery, *Journal of Controlled Release* 57 (1999) 9-18.
- [35] J.M. Carreno, C. Perez-Shibayama, C. Gil-Cruz, A. Printz, R. Pastelin, A. Isibasi, D. Chariatte, Y. Tanoue, C. Lopez-Macias, B. Gander, B. Ludewig, PLGA-microencapsulation protects *Salmonella typhi* outer membrane proteins from acidic degradation and increases their mucosal immunogenicity, *Vaccine*, 34 (2016) 4263-4269.
- [36] H.K. Makadia, S.J. Siegel, Poly Lactic-co-Glycolic Acid (PLGA) as Biodegradable Controlled Drug Delivery Carrier, *Polymers (Basel)*, 3 (2011) 1377-1397.
- [37] B.K. Lee, Y. Yun, K. Park, PLA micro- and nano-particles, *Adv Drug Deliv Rev*, 107 (2016) 176-191.
- [38] F. Danhier, E. Ansorena, J.M. Silva, R. Coco, A. Le Breton, V. Preat, PLGA-based nanoparticles: an overview of biomedical applications, *J Control Release*, 161 (2012) 505-522.
- [39] N. Benne, J. van Duijn, J. Kuiper, W. Jiskoot, B. Slutter, Orchestrating immune responses: How size, shape and rigidity affect the immunogenicity of particulate vaccines, *J Control Release*, 234 (2016) 124-134.
- [40] A.I. Kostadinova, J. Middelburg, M. Ciulla, J. Garssen, W.E. Hennink, L.M.J. Knippels, C.F. van Nostrum, L.E.M. Willemsen, PLGA nanoparticles loaded with beta-lactoglobulin-derived peptides modulate mucosal immunity and may facilitate cow's milk allergy prevention, *Eur J Pharmacol*, 818 (2018) 211-220.
- [41] H. Zaghoulani, C.M. Hoeman, B. Adkins, Neonatal immunity: faulty T-helpers and the shortcomings of dendritic cells, *Trends Immunol*, 30 (2009) 585-591.

- [42] I. Hanski, L. von Hertzen, N. Fyhrquist, K. Koskinen, K. Torppa, T. Laatikainen, P. Karisola, P. Auvinen, L. Paulin, M.J. Makela, E. Vartiainen, T.U. Kosunen, H. Alenius, T. Haahtela, Environmental biodiversity, human microbiota, and allergy are interrelated, *Proc Natl Acad Sci U S A*, 109 (2012) 8334-8339.
- [43] A.T. Stefka, T. Feehley, P. Tripathi, J. Qiu, K. McCoy, S.K. Mazmanian, M.Y. Tjota, G.Y. Seo, S. Cao, B.R. Theriault, D.A. Antonopoulos, L. Zhou, E.B. Chang, Y.X. Fu, C.R. Nagler, Commensal bacteria protect against food allergen sensitization, *Proc Natl Acad Sci U S A*, 111 (2014) 13145-13150.
- [44] T.H. Mogensen, Pathogen recognition and inflammatory signaling in innate immune defenses, *Clin Microbiol Rev*, 22 (2009) 240-273, Table of Contents.
- [45] M.L. Saiz, V. Rocha-Perugini, F. Sanchez-Madrid, Tetraspanins as Organizers of Antigen-Presenting Cell Function, *Front Immunol*, 9 (2018) 1074.
- [46] G. Pedersen, L. Andresen, M.W. Matthiessen, J. Rask-Madsen, J. Brynskov, Expression of Toll-like receptor 9 and response to bacterial CpG oligodeoxynucleotides in human intestinal epithelium, *Clin Exp Immunol*, 141 (2005) 298-306.
- [47] H. Wagner, The immunobiology of the TLR9 subfamily, *Trends Immunol*, 25 (2004) 381-386.
- [48] V. Hornung, S. Rothenfusser, S. Britsch, A. Krug, B. Jahrsdorfer, T. Giese, S. Endres, G. Hartmann, Quantitative expression of toll-like receptor 1-10 mRNA in cellular subsets of human peripheral blood mononuclear cells and sensitivity to CpG oligodeoxynucleotides, *J Immunol*, 168 (2002) 4531-4537.
- [49] A. Iwasaki, R. Medzhitov, Toll-like receptor control of the adaptive immune responses, *Nat Immunol*, 5 (2004) 987-995.
- [50] M.P. Domogalla, P.V. Rostan, V.K. Raker, K. Steinbrink, Tolerance through Education: How Tolerogenic Dendritic Cells Shape Immunity, *Front Immunol*, 8 (2017) 1764.
- [51] G. Montamat, C. Leonard, A. Poli, L. Klimek, M. Ollert, CpG Adjuvant in Allergen-Specific Immunotherapy: Finding the Sweet Spot for the Induction of Immune Tolerance, *Front Immunol*, 12 (2021) 590054.
- [52] M. Ebrahimian, M. Hashemi, M. Maleki, G. Hashemitabar, K. Abnous, M. Ramezani, A. Haghparast, Co-delivery of Dual Toll-Like Receptor Agonists and Antigen in Poly(Lactic-Co-Glycolic) Acid/Polyethylenimine Cationic Hybrid Nanoparticles Promote Efficient In Vivo Immune Responses, *Front Immunol*, 8 (2017) 1077.

CHAPTER 2

Inhibition Of Cow's Milk Allergy Development In Mice By Oral Delivery Of β -Lactoglobulin Derived Peptides Loaded PLGA Nanoparticles Is Associated With Systemic Whey-Specific Immune Silencing

M. (Mengshan) Liu^{1,2}, S.(Suzan) Thijssen², C.F. (Cornelus) van Nostrum¹, W.E. (Wim) Hennink¹, J. (Johan) Garssen^{1,3}, L.E.M. (Linette) Willemsen^{2*}

1. Division of Pharmaceutics, Utrecht Institute for Pharmaceutical Sciences, Utrecht University, Utrecht, the Netherlands

2. Division of Pharmacology, Utrecht Institute for Pharmaceutical Sciences, Utrecht University, Utrecht, the Netherlands

3. Department of Immunology, Nutricia Research B.V., Utrecht, the Netherlands

This chapter is published in *Clin Exp Allergy*. 2022;52(1):137-148.

Abstract

Background. 2-4% Of infants are affected by cow's milk allergy (CMA), which persists in 20% of cases. Intervention approaches using early oral exposure to cow's milk protein or hydrolyzed cow's milk formula are being studied for CMA prevention. Yet, concerns regarding safety and/or efficacy remain to be tackled in particular for high-risk non-exclusively breastfed infants. Therefore, safe and effective strategies to improve early life oral tolerance induction may be considered. **Objective.** We aim to investigate the efficacy of CMA prevention using oral pre-exposure of two selected 18-AA β -lactoglobulin derived peptides loaded poly (lactic-co-glycolic acid) (PLGA) nanoparticles (NPs) in a whey-protein induced CMA murine model. **Methods.** The peptides were loaded in PLGA NPs via a double emulsion solvent evaporation technique. *In vivo*, 3-week old female C3H/HeOJ mice received 6 daily gavages with PBS, whey, Peptide-mix, a high or low dose Peptide-NPs, or empty-NP plus Peptide-mix, prior to 5 weekly oral sensitizations with cholera toxin plus whey or PBS (sham). One week after the last sensitization, the challenge induced acute allergic skin response, anaphylactic shock score, allergen-specific serum immunoglobulins and *ex vivo* whey-stimulated cytokine release by splenocytes was measured. **Results.** Mice pretreated with high-dose Peptide-NPs but not low-dose or empty-NP plus Peptide-mix, were protected from anaphylaxis and showed a significantly lower acute allergic skin response upon intradermal whey challenge compared to whey-sensitized mice. Compared with the Peptide-mix or empty-NP plus Peptide-mix pretreatment, the high-dose Peptide-NPs-pretreatment inhibited *ex vivo* whey-stimulated pro-inflammatory cytokine TNF- α release by splenocytes. **Conclusion & Clinical relevance.** Oral pre-exposure of mice to two β -lactoglobulin derived peptides loaded PLGA NPs induced a dose-related partial prevention of CMA symptoms upon challenge to whole whey protein and silenced whey-specific systemic immune response. These findings encourage further development of the concept of peptide-loaded PLGA NPs for CMA prevention towards clinical application.

ABBREVIATION

CMA: cow's milk allergy; BLG: β -lactoglobulin; PLGA: poly(lactic-co-glycolic acid)

Introduction

Cow's milk allergy is one of the most prevalent food allergies in newborns, afflicting an estimate of 1.8-7.5% of infants in the first year of life [1]. CMA infants show symptoms including atopic dermatitis, rhinitis, diarrhea and even anaphylactic shock upon ingestion of cow's milk contaminated food. Currently, dietary avoidance remains as a major approach for CMA management [2]. Whereas, children with CMA tend to develop allergy to other mammalian milk proteins, due to their structural similarity with cow's milk proteins and/or their atopic constitution [3]. Without appropriate substitutes for cow's milk, inappropriate feeding can lead to nutritional deficiencies of CMA patients. Despite most children outgrow CMA by the age of 3-5 years, they are at a higher risk of developing other atopic diseases such as asthma and rhino-conjunctivitis [4]. Thus, early intervention to prevent CMA development is imperative for augmenting CMA patients and caregivers' quality of life via alleviation of symptoms or acceleration of outgrowth of CMA.

The Learning Early About Peanuts (LEAP) study showed early introduction of peanut to high-risk infants with eczema and/or egg allergy, starting from 4 to 11 months of age, predominantly induced allergen-specific oral tolerance and thus reduced the prevalence of peanut allergy [5-7]. These prevention effects were not found for CMA in the Enquiring About Tolerance (EAT) study [8]. Yet, an observational study reported a protective effect of introducing cow's milk protein to infants within 14 days after birth [9]. Nonetheless, the potential risk of adverse reactions to cow's milk protein presents as a challenge for the prevention of CMA, in particular in children at high inherited risk of developing allergies. Nowadays, partially (or extensively) hydrolyzed cow's milk formulas are recommended for high-risk infants when breastfeeding is not possible. The partially hydrolyzed cow's milk formulas may benefit primary prevention however these effects are inconsistent [2, 10, 11]. In previous studies, a mixture of 18-AA peptides derived from the cow's milk allergenic protein β -lactoglobulin, which may function as T cell epitopes, were shown to induce oral tolerance to whole whey protein in mice [12, 13]. These peptides may be added to enrich hydrolyzed infant milk formulas for non-exclusively breastfed infants at risk, aiming to enhance oral tolerance induction for cow's milk for the purpose of primary prevention. In the current study, we selected only two of these small peptides, which are too small to provoke symptoms, since they are unable to bridge two effector cell bound IgE molecules, hence preventing dimerization and mast cell degranulation [14]. However, they can still be presented in the MHCII

pocket of antigen presenting cells which allows them to provoke allergen specific T-cell responses. The T-cell receptor recognition of mixtures of nine 18-AA synthetic peptide sequences derived from β -lactoglobulin, was tested via their capability to induce human cow's milk specific T cell activation [12]. Oral pre-exposure using four of the nine peptides prior to whole whey protein sensitization rendered oral tolerance to whey in a CMA mouse model [12]. However, due to proteolytic degradation in the gastrointestinal tract, oral pre-exposure to these peptides would require a large dose, which is associated with an instable protective effect. To tackle this issue, Kostadinova *et al.* [13] encapsulated two peptides derived from β -lactoglobulin in poly(lactic-co-glycolic acid) nanoparticles (PLGA NPs) using four BLG peptides. The US Food and Drug Administration (FDA) approved PLGA as generally graded as safe (GRAS) polymer, which would allow further development of the approach for future human oral application. It is likely that the PLGA NP increase not only the survival of the peptides in the gastrointestinal tract but also the uptake by antigen presenting cells in the intestinal mucosa, while skewing the immune response from allergy prone T helper 2 (Th2) towards Th1 and regulatory T cell responses [15, 16].

In this study, we aim to identify the tolerance induction efficacy of only two β -lactoglobulin derived peptides encapsulated PLGA NPs in CMA murine model. To this end, NP size and encapsulation efficiency of these two selected β -lactoglobulin derived peptides loaded PLGA NPs were further optimized. In this study, we investigated oral tolerance induction efficacy and the underlying immunomodulatory mechanism of only two β -lactoglobulin derived peptides encapsulated in PLGA NP using two different dosages in a CMA murine model.

Materials And Methods

Peptides

Two 18-AA-long sequential synthetic peptides, derived from chain B of β -lactoglobulin, were purchased from JPT Peptide Technologies (Berlin, Germany). These two 12-AA overlapping β -lactoglobulin derived peptides are indicated as Peptide 3 and Peptide 4, spanning AAs 25-47 in B variant of β -lactoglobulin (Figure 1A). The peptides were encapsulated in PLGA with double emulsion solvent evaporation method as published previously [13], with applied adaptations to optimize NP size and increase

encapsulation efficiency of the peptide cargos. The detailed methods are described in the supplemental Materials and Methods section.

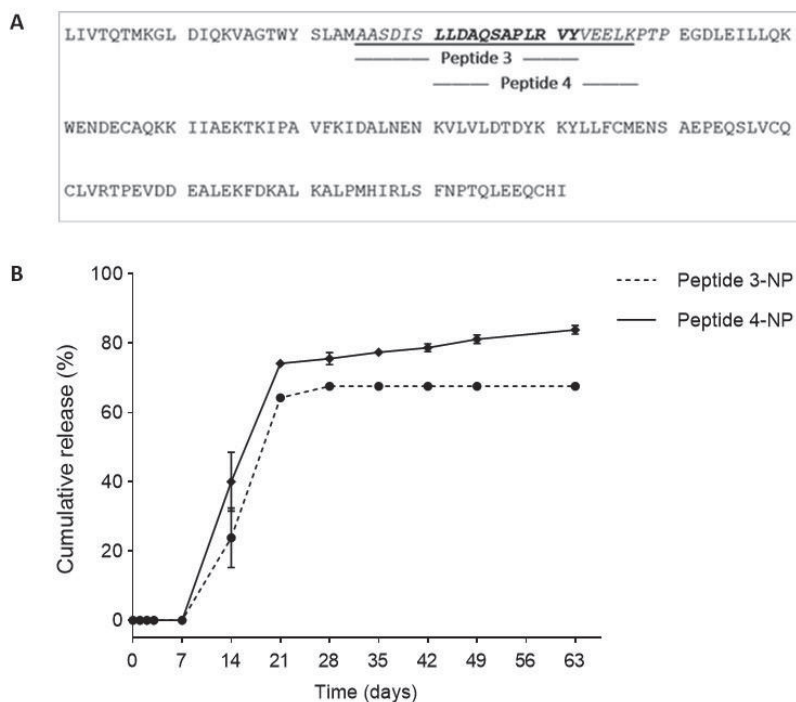


Figure 1. Amino acids sequence of B variant of β -lactoglobulin (A). The two selected sequential peptides (Peptide 3 and Peptide 4) used in the study were underlined and italicized. The bold amino acids sequence is the overlapping 12 amino acids. *In vitro* release of Peptide 3 and Peptide 4 from PLGA NPs in PBS at 37°C was conducted using cumulative method (B). Data is presented as mean \pm SEM, n=3 per formulation.

***In vitro* studies**

Culture of human monocytes-derived dendritic cells (moDCs)

Freshly donated and condensed blood (buffy coat) (time between donation and experiments was 24 h at most) was obtained from Sanquin Blood Supply (Amsterdam, the Netherlands). Human monocytes were isolated and differentiated into human monocytes-derived dendritic cells (moDCs) using the method described in the study by Ayeche Muruzabal *et al.* [17] (see supplemental materials and methods for details).

Stimulation of human moDCs and subsequent cytokine production

On day 8 immature moDCs were used for co-incubation with peptide mix, Peptide-NPs or empty-NP plus Peptide mix as described in the following sections respectively, LPS was used as a positive control for moDCs maturation. 5×10^5 cells in 500 μ L RPMI

1640 medium (Sigma-Aldrich) / 10% FBS+ 1% penicillin /Streptomycin (Gibco, New York, USA) were pulsed with 100 ng/mL Lipopolysaccharide (LPS-EB Ultrapure, from E. coli O111:B4 strain, TLR4-based adjuvant, Invivogen, San Diego, USA), 0.4 mg/mL empty-NP, Peptide mix (containing 1.6 µg/mL Peptide 3 and 1.9 µg/mL Peptide 4), Empty NP plus Peptide mix (containing 1.6 µg/mL Peptide 3, 1.9 µg/mL Peptide 4 and 0.2 mg/mL empty NP), Peptide-NPs (containing 0.2 mg/mL Peptide 3-NP and 0.2 mg/mL Peptide 4-NP) for 24 h at 37°C and 5% CO₂ respectively. Subsequently, supernatants were collected for cytokine analysis. IL-10, IL-12p70, TNF-α and IL-6 were measured with human ELISA Kit (Invitrogen, Fisher Scientific, USA) in accordance with the manufacturer's protocols. Human moDCs were washed to remove free nanoparticles and analyzed with flow cytometry.

Flow cytometry

First, human moDCs were stained with fixable viability dye eFluor 780 (ThermoFisher Scientific, Waltham, USA) to exclude dead cells from analysis. Non-specific staining was excluded by incubating the cells with anti-human Fcγ Receptors (Human BD Fc Block™, BD Pharmingen™, San Jose, USA) in PBS / 1% BSA / 2% FBS for 10 min in the dark at 4°C. For analyzing the percentage of moDC, cells were stained with CD11c-PerCP/eFluor 710 and HLA-DR-PE. To analyze the expression of costimulatory markers, cells were stained with CD80-FITC and CD86-PE/Cy7 (All from Invitrogen, Thermo Fisher Scientific, USA). Results were obtained with BD FACSCanto II flow cytometer (Becton Dickinson, Franklin Lakes, USA) and processed with FlowLogic software (Inivai Technologies, Mentone, Australia).

***In vivo* study**

Animals

3-Week old pathogen free female C3H/HeOuj mice were ordered from Charles River Laboratories (Sulzfeld, Germany) and housed under standard conditions in the animal facility of Utrecht University. The work protocol was approved by the Animal Ethics committee of Utrecht University and the Center Commission for Animal use (CCD) with an approval number of AVD108002015262. Animal care and use in this study follows the guidelines of the Animal Ethics committee of Utrecht University.

Inhibition of CMA development in mice by oral delivered BLG-peptides loaded PLGA NP is associated with systemic whey-specific immune silencing

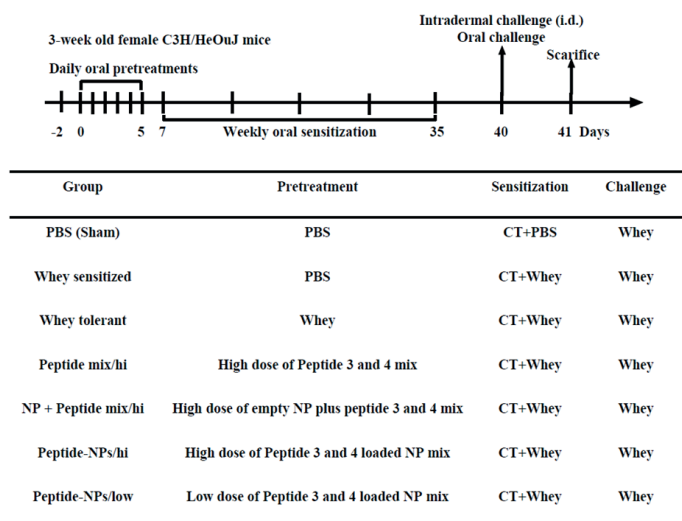


Figure 2. Schematic overview of the animal model for CMA prevention and different treatments per group.

Oral tolerance induction, sensitization and challenge

The CMA prevention murine model has been established previously by van Esch *et al.* [18]. To evaluate oral tolerance induction by Peptide-NPs, mice were randomly allocated into 7 groups (Figure 2) and received 6 consecutive daily oral gavage with 0.5 mL PBS (Sigma-Aldrich, Steinheim, Germany) for Group 1 (sham) and 2 (whey-sensitized), 50 mg whey protein (DMV International, Veghel, the Netherlands) for Group 3 (whey tolerant), 80 µg per Peptide 3 and 4 for Group 4 (Peptide mix), 18.7 mg empty-NP plus 80 µg per Peptide 3 and 4 for Group 5 (NP + Peptide mix/hi), 18.9 mg Peptide-NPs mixture (containing 80 µg per encapsulated Peptide 3 and 4) for Group 6 (Peptide-NPs/hi), and 8.5 mg Peptide-NPs mixture (containing 40 µg encapsulated Peptide 3 and 4) for Group 7 (Peptide-NPs/low) (Figure 3). For oral gavage, the peptides and NPs were dissolved or dispersed respectively in 0.5 mL PBS per mouse. Two days after the last oral administration with the indicated pre-treatment, mice received 5 consecutive weekly oral sensitizations with 20 mg whey plus 10 µg cholera toxin (CT; List Biological Laboratories, Inc. California, USA) as adjuvant in 0.5 mL PBS for Group 2-7 to break oral tolerance for whey, and 10 µg cholera toxin in 0.5 mL PBS for the non-sensitized mice in Group 1. Five days after the last oral sensitization, mice were intradermally and orally challenged with 10 µg or 20 mg whey respectively. The allergic response including acute skin response (Δ ear swelling thickness), body temperature

and anaphylactic shock core within one hour upon intradermal challenge were assessed. 18 H after oral challenge, mice were anesthetized with isoflurane and euthanized.

Evaluation of acute allergic response

To evaluate the efficacy of the allergy prevention of the different pretreatments, the acute allergic skin response upon intradermal challenge with 10 µg whey protein in 20 µL PBS was recorded as the primary outcome. The ear pinnae thickness of the mice was measured twice with a digital micrometer (Mitutoyo, Veenendaal, the Netherlands) before and 1 h after intradermal ear challenge with whey. Mice were under anaesthesia by inhalation of isoflurane prior to measurement of the ear pinnae and injection of whey. Δ Ear pinnae thickness is calculated by subtraction of the basal ear pinnae thickness as indicated in the following formula. Simultaneously, the anaphylaxis symptoms score was determined at 15 min and 1 h after intradermal challenge with whey according to Schouten *et al.* [19]. The evaluation of the acute allergic response was performed with the cage number concealed to avoid bias.

Δ Ear pinnae thickness

$$= \text{Average thickness}_{1h \text{ after } i.d. \text{ challenge}} - \text{Average thickness}_{\text{before } i.d. \text{ challenge}}$$

ELISA detection of serum Whey- and BLG-specific immunoglobulins

Whey-specific and BLG-specific immunoglobulins were measured in the sera collected 18 h after oral challenge with whey using a previously reported method [20].

Cells isolation from spleen

Splenocytes were isolated by sieving the spleens through 70 µm sterile cell strainers (Nylon, Falcon, Germany) and rinsed with 10 mL RPMI 1640 medium. To lyse red blood cells, 1 mL lysis buffer (155 mmol NH₄Cl, 10 mmol KHCO₃ and 0.127 µmol EDTA, filtered with 0.22 µm filter (Cellulose Acetate, Whatman™, GE Healthcare Life Sciences), was added into the splenocyte suspension and incubated on ice for 4 min. The lysis of red blood cells was stopped by addition of RPMI 1640 medium (Sigma-Aldrich, Steinheim, Germany) supplemented with 10% FBS, 1% Penicillin /Streptomycin. The isolated splenocytes were resuspended in RPMI 1640 medium (Sigma-Aldrich) supplemented with 10% FBS, 1% Penicillin /Streptomycin on ice until use.

Ex vivo re-stimulation of splenocytes and cytokine measurements

6×10^5 Splenocytes per well and suspended in 200 μ L RPMI 1640 medium supplemented with 10% FBS + 1% Penicillin / Streptomycin were cultured in a round bottom culture plate, and the cells were stimulated with either 500 μ g/mL whey protein (DMV International, Veghel, the Netherlands), or medium as control and cultured at 37°C, 5% CO₂. After 5-day stimulation with whey protein and medium, the supernatants were collected and stored at -20°C until further analysis. The cytokine concentrations in the collected supernatants were measured with mouse IFN- γ , IL-13, IL-5, IL-17A, IL-10 or TNF- α ELISA kits (ThermoFisher), conforming to the ThermoFisher protocols. Absorbance was measured at 450 nm by a Benchmark plate reader (Bio-Rad, Veenendaal, the Netherlands). In addition, cytokine production were measured in the supernatant after 2-day *ex vivo* stimulation of splenocytes with 1 μ g/mL anti-mouse CD3 antibody (eBioscience, ThermoFisher Scientific, USA) or medium as control and cultured at 37°C, 5% CO₂.

Statistical analysis

The obtained *in vivo* data were analyzed with GraphPad Prism 8.0.1 software (GraphPad Software, San Diego, USA). For each statistical analysis, multiple comparisons were conducted for the selected pairs: the whey-sensitized group was compared to all the other groups and the Peptide-NPs/hi group was compared to all groups except the non-sensitized group. For data sets that were not normal distributed as indicated by the Kolmogorov-Smirnov test or the Shapiro-Wilk test, square root transformation was performed. One-way ANOVA followed by Bonferroni's *post hoc* test for selected pairs was performed. Otherwise, Kruskal-Wallis' non-parametric test followed by Dunn's *post hoc* test for selected pairs was applied. Data are presented as mean \pm SEM for n=9-10 per group except for the non-sensitized group (n=3) and the whey tolerant group (n=6). For correlation analysis of acute allergic skin response and sera immunoglobulins, nonparametric Spearman correlation coefficient test was conducted using GraphPad Prism 8.0.1 software.

Results

Characteristics of empty and BLG-derived Peptides loaded PLGA nanoparticles.

Placebo and PLGA NPs loaded with BLG-derived Peptide 3 or 4 were prepared using a double emulsion solvent evaporation method. Empty NP, Peptide 3-NP and Peptide

4-NP had a close to neutral zeta potential and similar size of 280 ± 28 , 287 ± 40 and 271 ± 30 nm respectively (Table 1). 18 Amino acids sequence of Peptides 3 and 4 were selected from the B variant of β -lactoglobulin protein (adapted from Meulenbroek *et al.* [12]) (Figure 1A). Both Peptide 3-NP and Peptide 4-NP were encapsulated with a high encapsulation efficiency of 78 ± 10 and $84 \pm 7\%$ respectively. Peptide 3-NP and Peptide 4-NP has a loading capacity of 0.8 ± 0.1 and $0.9 \pm 0.1\%$ respectively. Peptide 3-NP and Peptide 4-NP showed no burst release in the *in vitro* release study (Figure 1B). Sustained release profiles of Peptide 3 and 4 from PLGA NP matrices were observed from 1-3 weeks, showing a cumulative release of 68% and 85% respectively (Figure 1B).

Table.1 Characteristics of Peptide 3-NP, Peptide 4-NP and empty NP (mean \pm SD).

Nanoparticles (NP)	Z-Ave (nm)	PDI	Zeta potential (mV)	Encapsulation efficiency (%)	Loading capacity (%)
Empty NP (n=6)	280 ± 28	0.13 ± 0.07	-1.3 ± 0.2	NA	NA
Peptide 3-NP (n=4)	287 ± 40	0.13 ± 0.10	-1.1 ± 0.1	78 ± 10	0.8 ± 0.1
Peptide 4-NP (n=4)	271 ± 30	0.11 ± 0.01	-1.1 ± 0.1	84 ± 7	0.9 ± 0.1

Effect of BLG-derived peptides loaded NPs (Peptide-NPs) on human moDCs activation *in vitro*

Figure 3A shows incubation of medium, LPS, Peptide-NPs, Peptide mix, or empty-NP plus Peptide mix for 24 h did not affect cell viability. Figure 3B shows that incubation of immature human moDCs with Peptide-NPs, Peptide mix or empty-NP plus Peptide mix did not influence HLA-DR expression on. As for human moDCs maturation, pulsing immature human moDCs with Peptide-NPs, Peptide mix, or empty-NP plus Peptide mix did not induce an increase in surface expression of costimulatory molecules CD80 or CD86 compared to the medium control, whereas positive control LPS induced a significant higher surface expression of costimulatory molecules CD80 and CD86 on moDCs than the other groups (Figure 3C-D). MoDCs incubation with LPS elicited a significant increase in production of IL-12p70, IL-10, TNF- α and IL-6 compared to medium controls (Figure 3E-H). Compared to the medium treated group, moDCs co-incubated with empty PLGA-NP also showed a higher cytokine release of IL-12p70, IL-10 and TNF- α . However, this effect was lost when the moDCs were incubated with empty PLGA-NP plus free peptides or the peptide encapsulated-NPs. The free peptide mixture did not provoke cytokine release by moDCs (Figure 3-H).

Inhibition of CMA development in mice by oral delivered BLG-peptides loaded PLGA NP is associated with systemic whey-specific immune silencing

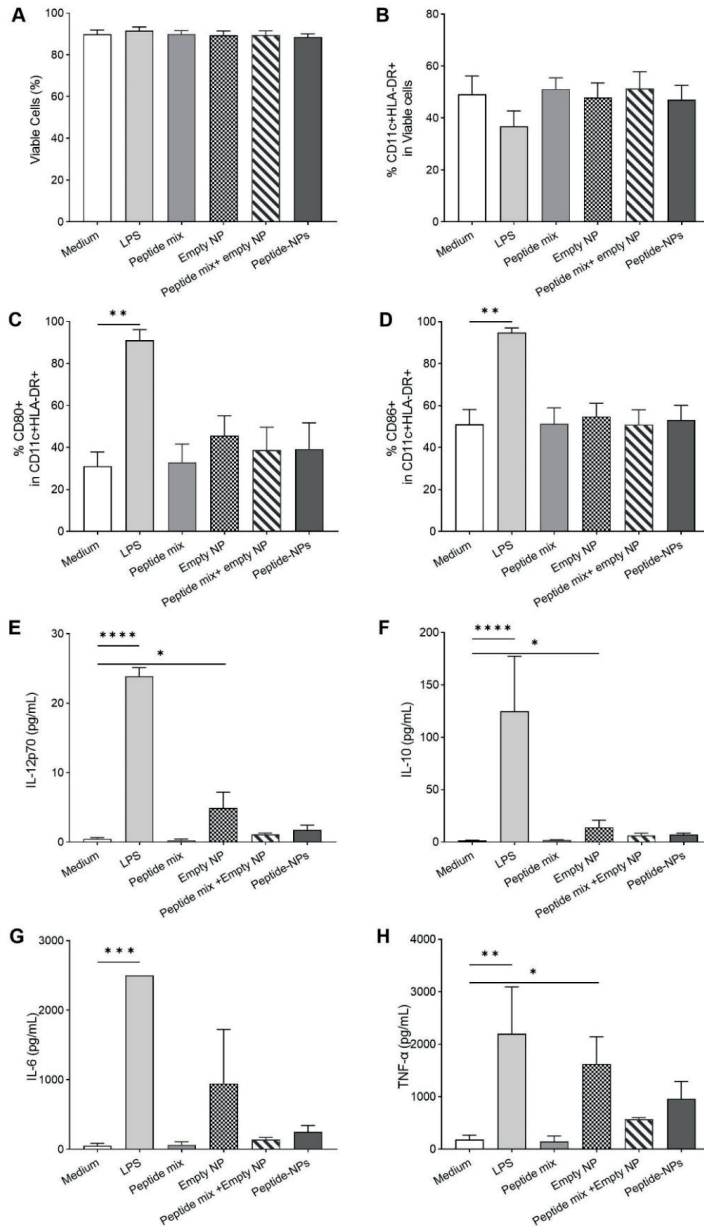


Figure 3. Effect of Peptide-NPs, Peptide mix, empty NP and Peptide mix plus empty NP on human moDCs activation *in vitro*. After incubation of human moDCs with medium, LPS, Peptide mix, empty NP, Peptide mix plus empty NP or Peptide-NPs for 24 h, cell viability (A), % MHC class II expression by human moDCs (B) and surface expression of co-stimulatory molecules in HLA-DR positive moDCs (C-D) were evaluated by flow cytometry. IL12p70 (E), IL-10 (F), and pro-inflammatory IL-6 and TNF- α (G-H) concentrations were measured in the supernatant. Data are presented as mean \pm SEM for n=3 independent experiments per group. Comparison between medium and the other groups were analyzed with one-way ANOVA followed by Bonferroni's post hoc test for selected pairs for (A-D), after square root transformation for (E), (G) and (H) and after log transformation for (F). *P<0.05, **P<0.01, ***P<0.001, ****P<0.0001.

Oral pre-exposure to BLG peptides loaded PLGA nanoparticles dose-dependently induces allergen-specific oral tolerance for whole whey protein

The acute allergic skin response of mice from all groups was measured prior to and 1 h upon i.d. challenge in the ear pinnae with whole whey protein (Figure 4). Notably, the PBS-pretreated whey-sensitized group showed a significantly increased acute skin response when compared to the non-sensitized group ($***P<0.001$), while whole whey-pretreatment largely prevented allergic symptoms indicating oral tolerance induction in this whey-tolerant group. A significant alleviated acute allergic skin response was observed in the high dose Peptide-NPs pretreated group ($*P<0.05$) compared to the whey-allergic mice, the high dose free Peptide mix group and also the low dose of Peptide-NPs group. The latter two interventions were unable to prevent allergy development. However, also the pretreatment with empty-NP plus high dose free Peptide mix tended to reduce the acute allergic skin response in comparison to the whey allergic group, albeit this effect was not significant.

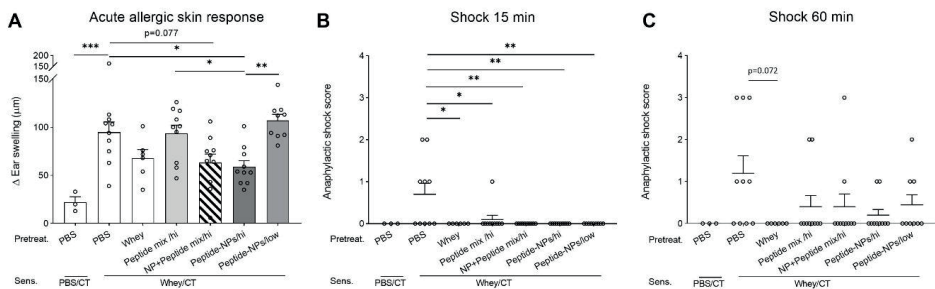


Figure 4. Acute allergic skin response and anaphylaxis score. Five days after last sensitization, mice were i.d. challenged in the ear pinnae with 10 µg whey followed by oral challenge. The acute allergic skin response was measured 60 min afterwards (A), and signs of anaphylaxis were scored after 15 min (B) and 60 min (C). Data are presented as mean ± SEM for the non-sensitized group, n=3 and whey tolerant group, n=6. (A) is analyzed by one-way ANOVA, followed by Bonferroni's *post hoc* test for selected pairs; (B) and (C) are analyzed with Kruskal-Wallis' non-parametric test, followed by Dunn's *post hoc* test for selected pairs. *P<0.05, **P<0.01, ***P<0.001. CT, Cholera toxin.

Anaphylactic shock scores of the mice were recorded 15 min and 60 min upon intradermal challenge with whole whey protein. As a result, the whey-sensitized mice showed a significant higher shock score than the other groups 15 min after the challenge. After 60 min, all the non-sensitized mice and whey-tolerant mice scored 0 for anaphylaxis, while the observed mice with highest shock score 3 were from the whey-allergic and the empty-NP plus high dose Peptide mix pretreated group. The maximum shock score in the high-dose Peptide-NPs group was 1.

Inhibition of CMA development in mice by oral delivered BLG-peptides loaded PLGA NP is associated with systemic whey-specific immune silencing

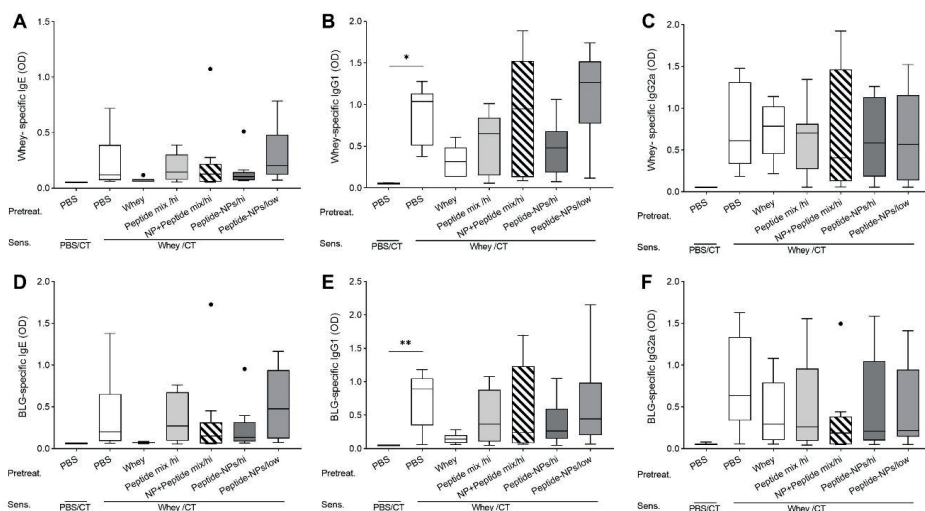


Figure 5. Whey- and BLG-specific serum immunoglobulins levels. Whey- (A-C) and BLG-specific (D-F) IgE, IgG1 and IgG2a levels are measured in sera, which were collected 18 h after last oral challenge with whey in mice from all groups. Data are presented as Tukey box- and-whisker plots for n=9-10 per group except for the non-sensitized group, n=3 and whey tolerant group, n=6. (A-F) are analyzed with the Kruskal-Wallis non-parametric test, followed by Dunn's *post hoc* test for selected pairs; *P<0.05, **P<0.01; BLG, β -lactoglobulin; CT, Cholera toxin.

Whey-specific and BLG-specific serum immunoglobulins

To investigate the influence of the pretreatments on the humoral immune response to whole whey protein or BLG, whey specific- and BLG specific-immunoglobulins were measured in the sera collected 18 h after oral challenge with whole whey protein. The whey-sensitized group showed a significant higher level of whey specific-IgG1 and BLG specific-IgG1 in comparison to that of the non-sensitized group (Figure 5B and E). Even though the different pre-treatments modified the pattern of immunoglobulin release similar to the effects shown on the ear swelling response, no significant results were obtained.

Cytokine production by splenocytes upon *ex vivo* re-stimulation with whey

Upon *ex vivo* whey re-stimulation, the general pattern of the cytokine secretion levels of IFN- γ , IL-13, IL-10 and TNF- α was not significantly different between the non-sensitized, whey-sensitized and whey tolerant group (Figure 6A-D) (for full data set see supplemental Figure S3). However, the high dose Peptide-NPs pretreated group showed

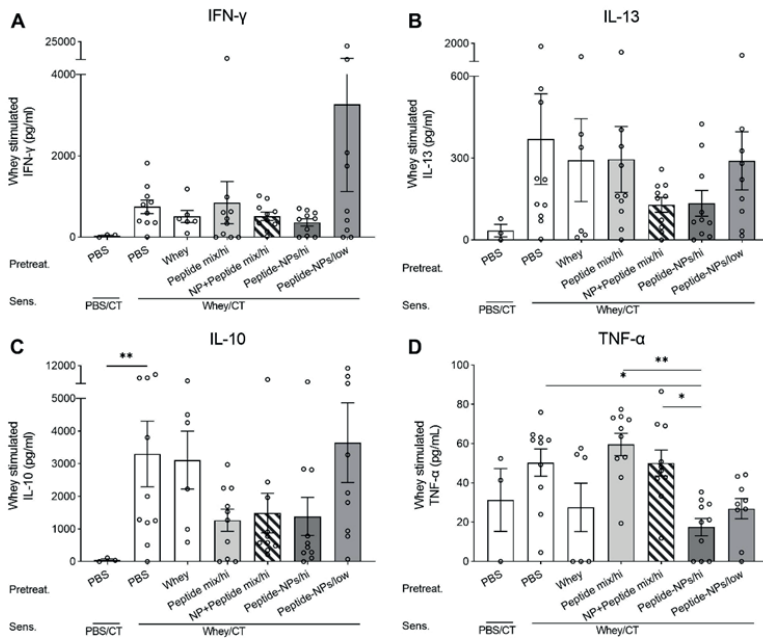


Figure 6. Cytokine production after *ex-vivo* re-stimulation of splenocytes with whole whey protein. Splenocytes were *ex vivo* re-stimulated either with whole whey protein for 5 days, Th1- (A), Th2- (B), regulatory (C) and proinflammatory (D) associated cytokines were measured in supernatants; Data are presented as mean \pm SEM for n=9-10 per group except for the non-sensitized group, n=3 and whey tolerant group, n=6. (A)-(D) are analyzed with one-way ANOVA followed by Bonferroni's *post hoc* test for selected pairs, after log transformation for (A-C) and after square root transformation for (D); * P <0.05, ** P <0.01, *** P <0.001; CT, Cholera toxin.

low levels of IL-13, IL-10 and TNF- α release. Similar to the anti-CD3 stimulated groups (supplemental Figure S4A-D), the high dose Peptide-NPs pretreated group showed significantly lower whey-stimulated TNF- α release than the whey sensitized mice (** P <0.01) as well as the high dose free Peptide mix (** P <0.001), and the empty-NP plus high dose Peptide mix (** P <0.01). In addition, whey and anti-CD3 induced secretion of IL-5 and IL-17A by splenocytes were measured (supplemental Figure S5A-D).

Discussion

CMA is one of the first allergies to develop early in life and disrupts the quality of life of newborns and their caretakers. Gut-associated lymphoid tissues (GALT) have been regarded as an ideal site for oral tolerance induction, as intestinal dendritic cells in the GALT can take up the oral administered antigens and present to T cells in the Peyer's patch and mesenteric lymph nodes to generate systemic immune tolerance [14, 21-25]. Therefore, our study investigated and confirmed the early life allergen-specific tolerance induction effect in a murine CMA prophylactic model via oral pre-exposure to only 160 µg encapsulated two selected 18-AA β-lactoglobulin peptides in PLGA nanoparticles.

Previously, Kostadinova *et al.* [13] reported oral delivery of 4 selected 18-AA β-lactoglobulin derived peptides (40 µg per Peptide), namely Peptide 1 and 2 mix plus PLGA nanoparticles encapsulated Peptide 3 and 4, effective in modulating mucosal immunity by increase in *ex vivo* whey stimulated TGF-β release by intestinal lamina propria cells. The current study only made use of the two selected Peptide 3 and 4 loaded PLGA NPs, which were further optimized in terms of NP size, encapsulation efficiency and *in vitro* release profile. The NP size of ~280 nm (Table 1) is smaller than the previous mean NP size of 320 nm [13], facilitating penetration through the mucus and cellular uptake by intestinal M-cells or enterocytes [26, 27]. In addition, the encapsulation efficiency of Peptide 3 in PLGA nanoparticles has now been improved from 30% in the previous study [13] to 78% in the present study. *In vitro* release study of Peptide 3-NP and Peptide 4-NP in PBS showed no burst release and a lag phase of 7 days, followed by a sustained release from week 1 to 3, which is likely resulting from hydrolysis of the PLGA polymeric matrix [28]. This observed absence of burst release of Peptide 3-NP is likely to be attributed to sufficient washing procedures and/or absence of porosity in the lyophilized Peptide-NPs, confirming the successful and improved encapsulation of these two peptides.

In vitro cellular uptake of empty PLGA NP by murine bone marrow derived dendritic cells and human moDCs was reported previously [13, 29]. *In vitro*, we found human moDCs remained immature phenotype upon stimulation with Peptides-NPs, showing no upregulation of surface expression of co-stimulatory molecules CD80/CD86. This immature human moDCs is often regarded as a prerequisite for tolerance induction. As reported, the CD80^{low}/CD86^{low} human immature dendritic cells have the potential to

induce tolerance by promoting differentiation of naïve T cells into Treg cells after repetitive stimulation under steady conditions [30-32]. Furthermore, empty NP induced a small increase of Th1, pro-inflammatory and regulatory associated cytokines, namely IL-12p70, TNF- α , and IL-10 release by human moDC. Remarkably, this phenomenon was abolished when the moDCs were pulsed with co-administration of the two BLG peptides plus PLGA nanoparticles. This neutralization effect for Th1 associated cytokine IL-12p70 release, but not TNF- α release, was also found when pulsing BMDC with Peptide 1, 3 and 4 loaded PLGA NP in a previous study. It is not unlikely that the previously reported *in vivo* Th1 and Th2 immune silencing effect of Peptide 4, neutralized the Th1 skewing effect of the PLGA nanoparticles [12]. Yet, future studies are warranted to confirm this hypothesis.

In this study, the oral pre-exposure to a relatively low required dose (160 μ g) of Peptide 3 and 4 loaded PLGA NPs (160 μ g) and short duration (6 days) prior to whey sensitizations, significantly reduced the acute allergic skin response upon intradermal whole whey protein challenge. The dose of peptides used in the current study is very small as compared to the 4 mg per Peptide 3 or 4 in the previous murine prophylactic CMA study by Meulenbroek *et al.* [12].

Previous studies showed PLGA nanoparticles exert a Th1 adjuvant effect, but PLGA NP alone did not protect against allergy development [13, 33]. However, simultaneous presence of PLGA NPs and antigen may have facilitated allergen-specific tolerance concomitantly. As reported previously [34-36], nanoparticles of approximately 200 nm or less can efficiently diffuse into the lymphatic system and be internalized by dendritic cells, which may account for the observed improved tolerance induction effect in our study.

Consistent with a previous study by Kim *et al.* [22], this observed preventive effect is dose-dependent, since the dosage of 40 μ g per encapsulated peptide in PLGA NP did not protect against allergy development. Although oral pre-exposure to high dose of Peptide-NPs, prior to whey sensitization, did not lower whey- and BLG-specific IgE, IgG1 and IgG2a compared to the whey allergic group. A similar declining pattern in immunoglobulin levels comparable to the skin response was observed. In accordance with the previous study [19], the acute allergic skin response and whey- and BLG-specific IgE, IgG1 and IgG2a levels were positively correlated (supplemental Figure S1),

connecting the intensity of allergic sensitization and the outcome of the effector response.

In contrast to previous findings of regulatory T-cells development induced by PLGA NP [16], the frequency of the systemic Treg, as well as CD4⁺ cells, Th1 and Th2 subsets in splenocytes remained unaffected in the current study (supplemental Figure S2). However, oral pre-exposure to PLGA NP, with or without peptides incorporation, attributed to an increasing pattern of mRNA expression of regulatory cytokine IL-10 in middle intestines after oral whey challenge (supplemental Figure S6). Regulatory cytokines, such as IL-10, and its increased intestinal expression were found associated with allergy protection.

Despite no significant decrease observed, the high dose Peptide-NPs pretreatment maintained a relative low *ex vivo* whey stimulated IL-13 and IL-10 release by splenocytes compared to the whey-sensitized group. Furthermore, the high dose Peptide-NPs pretreatment, but not the low dose counterpart, significantly reduced the whey-stimulated TNF- α release, indicating allergen specific immune silencing was established in a dose-dependent manner. TNF- α is principally associated with Th1 mediated inflammation [37], but also plays a key role in enhancing Th2-polarizing cytokines release and antigen-specific IgE production [38, 39]. Indeed, the silencing of *ex vivo* whey-stimulated TNF- α release by splenocytes suggests the systemic immunomodulatory effect of oral pre-exposure to Peptide-NPs, in association with the observed ameliorated acute allergic skin response.

Only the high dose Peptide-NPs, but not empty NP plus equal amount of free Peptide mix, showed high efficacy in immune silencing and significant antigen-specific suppression of TNF- α as compared to the whey-sensitized group. This further underlines the relevance and importance of the finding that the high dose of Peptide-NPs (80 μ g per peptide) is capable of largely protecting against whole whey sensitization. Furthermore, it has highlighted the superiority of PLGA NP encapsulated peptides over the treatment with peptides that were co-delivered with PLGA NP, which may be attributed a more potent immunomodulatory effect by the antigen-encapsulated PLGA nanoparticles as was also reported by Gu *et al.* [40]. Indeed, previous studies have shown peptide 3 to be able to activate human T-cells and it also was predicted *in silico* to be presented by human MHCII (HLA-DRB1) [41]. Future studies are needed to confirm

in vivo presentation of the PLGA nanoparticles delivered peptides in the MHCII cleft of the DC and the generation or deletion of T-cells recognizing peptides 3 or 4.

Our findings in the dose-dependent tolerance induction effect of the peptide encapsulated PLGA nanoparticles are consistent with the previous studies [42, 43], suggesting different mechanisms of oral tolerance involved for low and high dose of oral administered antigens. As reported, deletion of antigen reactive Th1 and Th2 cells induced by high dose of oral administered antigens, is abolished when using a lower antigen dosage. Instead, a lower dosage of oral administered antigens showed an active suppression by increasing antigen-stimulated IL-10 release [43]. Nevertheless, the high dose Peptide-NPs group showed both lower *ex vivo* generic T-cell receptor anti-CD3 stimulated regulatory and inflammatory associated cytokine production, IL-10 and TNF- α , than the whey-sensitized group (supplemental Figure S4) and lowered whey-stimulated TNF- α release, while maintaining low levels of whey-specific IL-13, IFN- γ and IL-10. We hypothesize that the underlying mechanism by which Peptide-NPs mediated this immune silencing differs from the mechanism by which whole whey protein facilitated tolerance induction. In the whey-tolerant group the regulatory IL-10 secretion remained unaffected high whereas TNF- α secretion was low, hence shifting the immune balance in favor of the regulatory response which may have dampened allergic sensitization and clinical symptoms. Similarly, the low dose Peptide-NPs also showed this pattern, but in this group the IFN- γ and IL-13 release tended to increase. In contrast to whey pre-treated mice, the low dose Peptide-NPs pretreatment did not tend to lower the whey-immunoglobulin levels. Therefore, the T-cell modulatory effect in the low dose Peptide-NPs may have been insufficient to affect allergic sensitization and whey induced symptoms. Collectively, the high dose Peptide-NPs (160 μ g) or 50 mg whey protein showed similar reduction in acute allergic skin response but disparate whey stimulated cytokine release pattern, indicating a different tolerance induction mechanism.

Ultimately, the current study indicates full tolerance induction/ immune silencing for whole whey protein at the level of the T-cells, while using only 160 μ g two small peptides derived from β -lactoglobulin. This may be accomplished if these peptide 3 or 4 sequences consist of immunodominant epitopes of whey proteins, when processed and expressed in MHCII by DC and presented to the T-cells. The small required dose of these BLG peptides may be attributed to the prolonged retention time of the PLGA NP

encapsulated peptides in dendritic cells as reported in previous studies [33, 44, 45]. Furthermore, the BLG peptides as well as PLGA nanocarriers have been shown to instruct regulatory T-cell development *in vivo* and in the *in vitro* studies [12, 16]. We hypothesize that the two PLGA nanoparticles encapsulated BLG peptides may instruct a tolerogenic DC phenotype, presenting the antigen via their MHC class II, which contributes to the immune silencing effect at the T-cell level even for whole whey protein either in an epitope specific fashion or via bystander suppression.

Silencing of the T-cell response may consequently suppress the generation of whey and BLG specific IgE/IgG1, but here no statistical significance was observed. Allergen specific B-cell selection occurs via direct binding of the allergen to the B-cell receptor. B-cells may therefore be responsive to a broader/different spectrum of epitopes (B-cell epitopes) as compared to T-cells. Hence, to further improve tolerance induction also at the level of the B-cells, supplemental addition of other whey/BLG epitopes may help which needs to be addressed in future studies.

In summary, this study has proven that oral delivery of only two BLG peptides encapsulated in PLGA NP is effective in partial oral tolerance induction for whole whey protein in a dose dependent manner. Our findings substantiate PLGA NP encapsulation of the peptide cargo as a relevant strategy for optimal antigen-specific oral tolerance induction. Oral pretreatment with BLG peptides loaded PLGA NP might be a promising CMA prevention strategy, circumventing the potential adverse effect for children at high risk of CMA while enhancing the chance to develop oral tolerance, that warrants further clinical validation. For future study, incorporation of additional BLG epitopes and a Th1 and Treg skewing adjuvant may further optimize the tolerance induction effect of the current preventive approach or for development of therapeutic purposes.

Acknowledgements: ML is financially supported by China Scholarship Council (CSC), grant number 201707720004 and receive additional bench fee funding is supplied by Danone Nutricia Research B.V., Utrecht, the Netherlands.

Supporting Information

Materials and Method

Preparation of empty NP and peptides loaded NPs.

A double emulsion solvent evaporation method was incorporated to prepare both empty, peptide 3 and peptide 4 loaded PLGA NPs. Briefly, 1.6 mg peptide (Peptide 3 or Peptide 4 separately) was dissolved in 3 mL internal aqueous phase containing 95% milli-Q water, 5% acetonitrile (ACN, HPLC grade, Sigma-Aldrich, Steinheim, Germany) and 0.1% trifluoroacetic acid (TFA, Sigma-Aldrich, Steinheim, Germany). The dissolved peptide was added to 30 mL anhydrous dichloromethane (DCM, Biosolve BV, Valkenswaard, the Netherlands), containing 5% w/v uncapped PLGA (lactide/glycolide molar ratio 50:50, 0.32 - 0.48 dl/g) (PURASORB PDLG 5004A, Corbion, the Netherlands), and the mixture was sonicated using a Sonifier S-450A (3 mm, Branson Ultrasonics B.V., Soest, the Netherlands) at 10% amplitude for 1 min on ice bath to yield a water-in-oil emulsion. Subsequently, the formed water-in-oil emulsion was added to 30 mL external aqueous phase, containing 3% w/v polyvinyl alcohol (87-90% hydrolyzed, Mw 3,000-70,000 Da, Sigma-Aldrich, Steinheim, Germany) and 0.9% w/v NaCl, and the obtained mixture was sonicated using a Sonifier S-450A (first 3 mm, then 13 mm, Branson Ultrasonics B.V., Soest, the Netherlands) at 10% amplitude for 1 min on ice bath to yield a water-in-oil-in-water emulsion. Finally, the formed emulsion was subjected to agitation for 3 h at room temperature to evaporate DCM and to obtain hardened PLGA NPs. The nanoparticles suspension was centrifuged at 20,000×g for 30 min at 4°C and the obtained pellet was washed with 20 mL milli-Q water twice prior to lyophilization using a freeze dryer (Buchi Lyovapor L-200, Hendrik-Ido-Ambacht, the Netherlands).

Characterization of PLGA NPs

One milligram lyophilized empty and peptide loaded NPs were suspended in 2 mL 10 mM HEPES buffer (pH 7.4) for characterization of nanoparticle size, polydispersity index (PDI) and Zeta-potential with Zetasizer Nano S (Malvern Instruments, Malvern, UK) and Zetasizer Nano-Z (Malvern Instruments, Malvern, UK) respectively.

The encapsulation efficiency of peptides 3 and 4 was determined as described previously [13]. In detail, 10-20 mg lyophilized nanoparticles were accurately weighed and dissolved in 0.8 mL DCM, facilitated with sonication for 40 min. Subsequently, 1 mL 5% ACN/0.1% TFA aqueous solution per 10 mg nanoparticles was added to extract the

loaded peptide from the DCM phase under agitation at 41°C for 3 h to evaporate DCM. Afterwards, the obtained aqueous solution was filtered using 0.2 µm RC syringe filter (Phenomenex, CA, USA) prior to Acquity Ultra Performance Liquid Chromatography (UPLC) analysis. The peptide content in the obtained filtered aqueous phase was measured with UPLC using a BEH C18 1.7 µm column (Waters, MA, USA) and UV detection at 210 nm. A gradient elution method was used with a mobile phase A (0.1% TFA, 5% acetonitrile and 95% H₂O) and a mobile phase B (0.1% TFA and acetonitrile). The eluent changed linearly from 20% mobile phase B to 40% mobile phase B in 6 min with a flow rate of 0.25 mL/ min at 25°C.

Peptide standards (1-100 µg/mL, 7.5 µL injection volume) dissolved in mobile phase A were used for calibration. Encapsulation efficiencies (EE) of peptides in PLGA NP are reported as the amount of encapsulated peptides divided by the total amount of peptides used for the preparation of the peptides loaded NPs. Loading capacity[46] of peptides in PLGA NP are reported as weight of the encapsulated peptides divided by the weight of the peptides loaded NPs. Calculation of encapsulation efficiency and loading capacity are indicated as the following equations:

$$\text{Encapsulation Efficiency (\%)} = \frac{\text{Amount of encapsulated peptides}}{\text{Amount of feed peptides used for nanoparticles preparation}} \times 100\%$$

$$\text{Loading Capacity (\%)} = \frac{\text{Amount of encapsulated peptides}}{\text{Amount of nanoparticles}} \times 100\%$$

***In vitro* release of peptide 3 and 4 from PLGA NPs**

The release of the peptides from the PLGA NP was determined as follows. Around 10 mg peptide-loaded PLGA NPs were accurately weighed in triplicate, prior to suspension in 1 mL phosphate saline buffer (PBS, pH 7.4) / 0.06% w/v sodium azide (NaN₃, Sigma-Aldrich, Steinheim, Germany) (release buffer) and incubation at 37°C on a nutating mixer. At different time points, samples were spun down at 20,000×g at 4°C and 500 µL supernatant was withdrawn for UPLC analysis using the method as described in section of characterization of PLGA nanoparticles. Next, 500 µL of fresh release buffer was added, the pelleted NPs were resuspended and the samples were further incubated at 37°C on a nutating mixer. The percentage of released peptide was calculated based on the loaded amount [13].

Flow cytometry

Approximate 8×10^5 isolated splenocytes resuspended in 135 μ L PBS were pipetted into the wells of a 96-well falcon plate. Cells viability was determined by staining with fixable viability dye eFluor™780 (ThermoFisher). Nonspecific binding sites were blocked by incubation with anti-mouse CD16/CD32 (Mouse BD Fc block; BD Pharmingen San Jose, CA USA) for 5 min. For extracellular staining of Th1/Th2 and Treg, cells were incubated with CD4-BV510 (BioLegend, San Diego, CA, USA), CD69-PE/Cy7 (ThermoFisher), T1ST2-FITC (MD Biosciences, Oakdale, MN, USA), CXCR3-PE (ThermoFisher), CD25- PerCP/eFluor710 (ThermoFisher), and CD127-PE/Vio770REA (Miltenyi Biotec, Bergisch Gladbach, Germany). For intracellular staining of Th1/Th2 and Treg, cells were first fixed and permeabilized with FoxP3/Transcription Factor Staining Buffer Set (ThermoFisher), Tbet-Alexa Fluor647 (BioLegend), Gata3 PerCP-eFluor710 (ThermoFisher) and FoxP3-FITC (ThermoFisher). Cells were analyzed with BD FACSCantoll flow cytometer (Becton Dickinson, Franklin Lakes, NJ, USA). Data analysis was conducted with FlowLogic software (Inivai Technologies, Mentone, VIC, Australia).

qPCR analysis of mRNA expression in middle intestine

Middle intestine samples (1 cm) from the mice sacrificed after blood sampling were washed with (Sigma-Aldrich, Steinheim, Germany) and collected in RNAlater (Invitrogen, ThermoFisher Scientific, Waltham, MA, USA) and stored at -20°C . mRNA isolation from the collected middle intestine samples was performed with RNeasy Mini Kit (Qiagen, Venlo, the Netherlands) according to the manufacturer's protocol. DNA was digested by using the On-column RNase-Free DNase Set (Qiagen, Venlo, the Netherlands). cDNA synthesis was performed with iScript™ cDNA Synthesis Kit (Bio-Rad, Switzerland) in accordance with the manufacturer's instruction. Quantitative analysis was performed on a CFX96 real-time PCR detection system by using an iQ SYBR™ Green PCR supermix (Bio-Rad, the Netherlands). Commercial primers for T-box transcription factor 21 (Tbet), Gata3, Tgf β 1 and IL-10 were used (Qiagen, Venlo, the Netherlands). Ribosomal protein S13 (Rps13) (Qiagen, Venlo, the Netherlands) was used as reference gene for all the other genes of interest. The mRNA level was analyzed with CFX Manager software and corrected as $100 \times 2^{-(\Delta\Delta\text{Ct})}$ (Rps13-gene of interest). [47]

Culture of human monocytes-derived dendritic cells (moDCs)

25 mL Fresh human blood was diluted with the same volume of DPBS (Dulbecco's Phosphate Buffered Saline, Sigma-Aldrich) / 2% FBS (Fetal Bovine Serum, Sigma-Aldrich) at room temperature and transferred slowly into Leucosep tubes (VWR, Radnor, Pennsylvania, USA), followed by centrifugation for 13 min at 1000×g at room temperature with slow acceleration and slow deceleration. Subsequently, the interface containing the PBMC (peripheral blood mononuclear cell) was washed with 50 mL PBS/ 2% FBS for 4 times until the supernatant was clear. Next, the lysis of red blood cells in the PBMC fraction were started by addition of 5 mL lysis buffer (8.3 g/L NH₄Cl, 1 g/L KHCO₃ and 37 mg/L EDTA, filtered using a sterile 0.2 µm syringe filter (Cellulose Acetate, Whatman™, GE Healthcare Life Sciences)) for incubation on ice for 4 min and stopped by addition of 45 mL PBS + 2% FBS prior to centrifugation at 1200 rpm at 4°C for 5 min. The obtained PBMC suspension was used for monocytes isolation using negative selection with human Monocyte Isolation Kit II (Miltenyi Biotec B.V. & Co. KG, USA) and MACS column and MACS separator (Miltenyi Biotec B.V. & Co. KG, USA). 1×10⁶ Cells per mL monocytes per donor were cultured in the presence of 100 ng/mL human IL-4 recombinant (Prospec, Rehovot, Israel) and 60 ng/mL recombinant human GM-CSF (granulocyte macrophage colony-stimulating factor) (Prospec, Rehovot, Israel) to induce differentiation into immature monocytes derived dendritic cells (moDCs) in 6-well suspension culture plates (Greiner Bio-one, Solingen, Germany) and incubated at 37°C and 5% CO₂. After every 3 days, half of the medium was withdrawn and replaced with fresh medium containing 100 ng/mL IL-4 and 60 ng/mL GM-CSF.

Supporting Information

Results

Correlation between serum immunoglobulins and acute allergic skin response

To investigate the correlation between the serum immunoglobulins and acute allergic skin reaction, non-parametric Spearman correlation coefficient analyses were conducted using data from 6-7 independent experiments. The serum dilution used to calculate the correlations were: 10 times for whey-and BLG-specific IgE, 40,000 times for whey-specific IgG1, 32,000 times for BLG-specific IgG1, 8,000 times for whey-specific IgG2a and 4,000 times for BLG-specific IgG2a. The acute allergic skin response were found positively correlate with whey-specific IgE (supplemental Figure S1A; $p=0.001$, $r=0.416$, $n=56$), whey-specific IgG1 (supplemental Figure S1B; $p<0.0001$, $r=0.557$, $n=56$), whey-specific IgG2a (supplemental Figure S1C; $p=0.005$, $r=0.371$, $n=56$), BLG-specific IgE (supplemental Figure S1D; $p=0.003$, $r=0.395$, $n=56$), BLG-specific IgG1 (supplemental Figure S1E; $p=0.0003$, $r=0.470$, $n=56$) and BLG-specific IgG2a (supplemental Figure S1F; $p=0.001$, $r=0.423$, $n=56$).

Cytokine production by splenocytes upon *ex vivo* re-stimulation with α -CD3.

Ex vivo stimulation with α -CD3 induced similar secretion of IFN- γ , IL-13, IL-10 and TNF- α in the non-allergic, whey allergic and whey tolerance group, verifying the responsiveness of the isolated splenocytes upon generic T-cell receptor (CD3) activation, despite no differences were observed between the sham and whey-sensitized groups (supplemental Figure S4A-D). Typically, the high dose of Peptide-NPs pretreated group, showed a significantly lower generic IL-13 and IL-10 release than the whey tolerant group upon α -CD3 stimulation. Furthermore, the high dose of Peptide-NPs significantly lowered IL-10 and TNF- α concentrations compared to the whey sensitized- as well as high dose Peptide mix, and empty-NP plus Peptide mix pretreated groups. In addition, α -CD3 induced secretion of IL-5 and IL-17A by splenocytes were measured (supplemental Figure S5A-B).

Supporting Figures

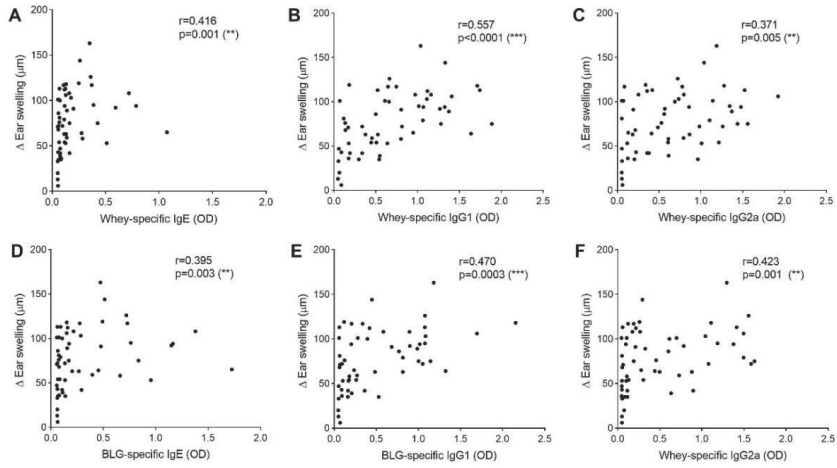


Figure S1. Correlation analysis between ear swelling and whey- and BLG-specific immunoglobulins. Spearman correlation between ear swelling and whey-specific IgE (A) ($p=0.001$, $r=0.416$, $n=56$), whey-specific-IgG1 (B) ($p<0.0001$, $r=0.557$, $n=56$), whey-specific-IgG2a (C) ($p=0.005$, $r=0.371$, $n=56$), BLG-specific IgE (D) ($p=0.003$, $r=0.395$, $n=56$), BLG-specific IgG1 (E) ($p=0.0003$, $r=0.470$, $n=56$) and BLG-specific IgG2a (F) ($p=0.001$, $r=0.423$, $n=56$). (* $p < 0.05$, ** $p < 0.01$, *** $p < 0.001$)

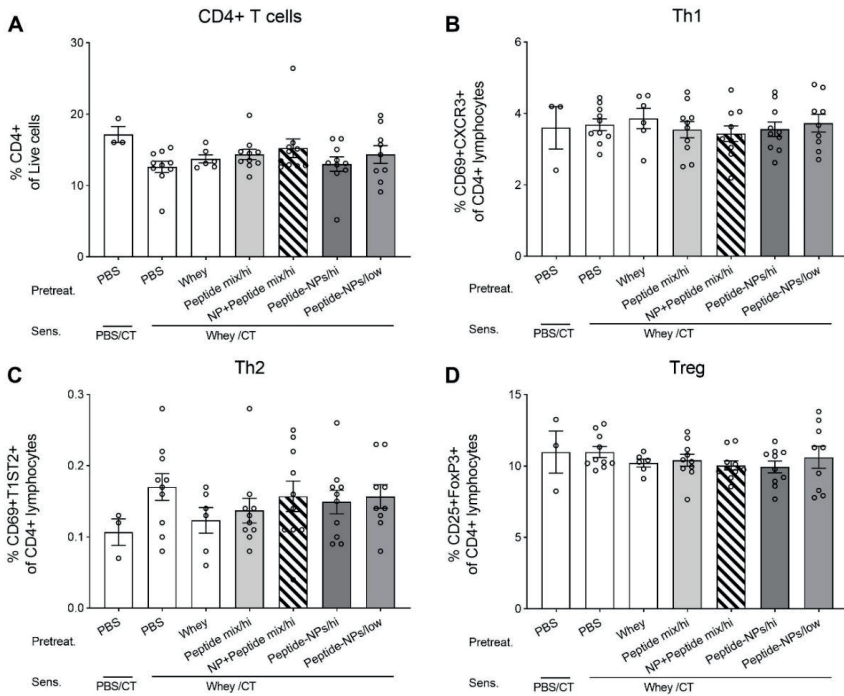


Figure S2. T cell subsets in the splenocytes. 18 h After the last oral challenge with whey, splenocytes were isolated and analyzed by flow cytometry for percentages of CD4+ cells (A), activated Th1 (B), activated Th2 (C) and Treg phenotype (D). Data are presented as mean \pm SEM for n=9-10 per group except for the non-sensitized group, n=3 and whey tolerant group, n=6. (A)-(D) are analyzed with one-way ANOVA for selected pairs, followed by Bonferroni's *post hoc* test; CT, Cholera toxin.

Inhibition of CMA development in mice by oral delivered BLG-peptides loaded PLGA NP is associated with systemic whey-specific immune silencing

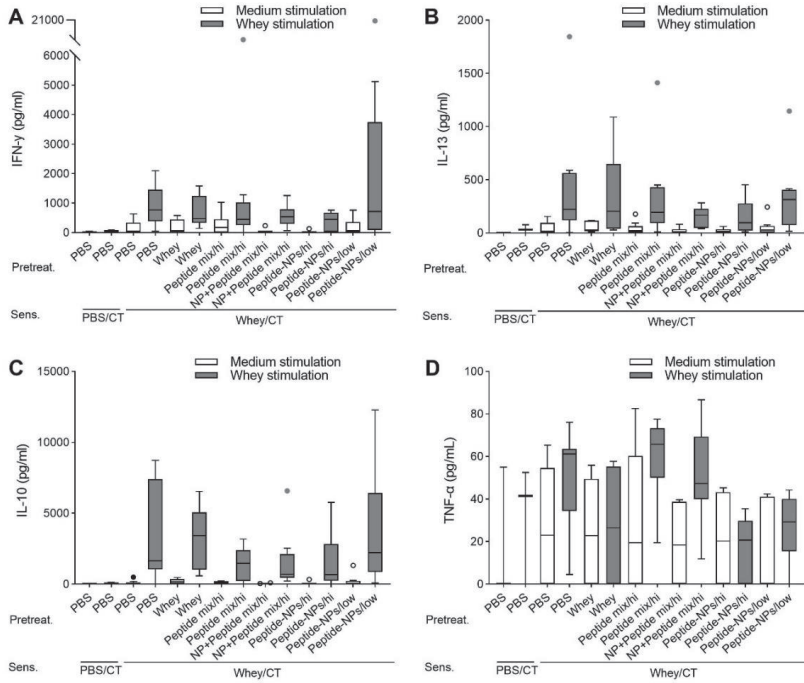


Figure S3. Cytokine production after *ex-vivo* re-stimulation of splenocytes with medium or whole whey protein. Splenocytes were *ex vivo* re-stimulated either with medium or whole whey protein for 5 days, Th1- (A), Th2- (B), regulatory (C) and proinflammatory (D) associated cytokines were measured in supernatants; Data are presented as Tukey box-and whisker plots for n=9-10 per group except for the non-sensitized group, n=3 and whey tolerant group, n=6. CT, Cholera toxin.

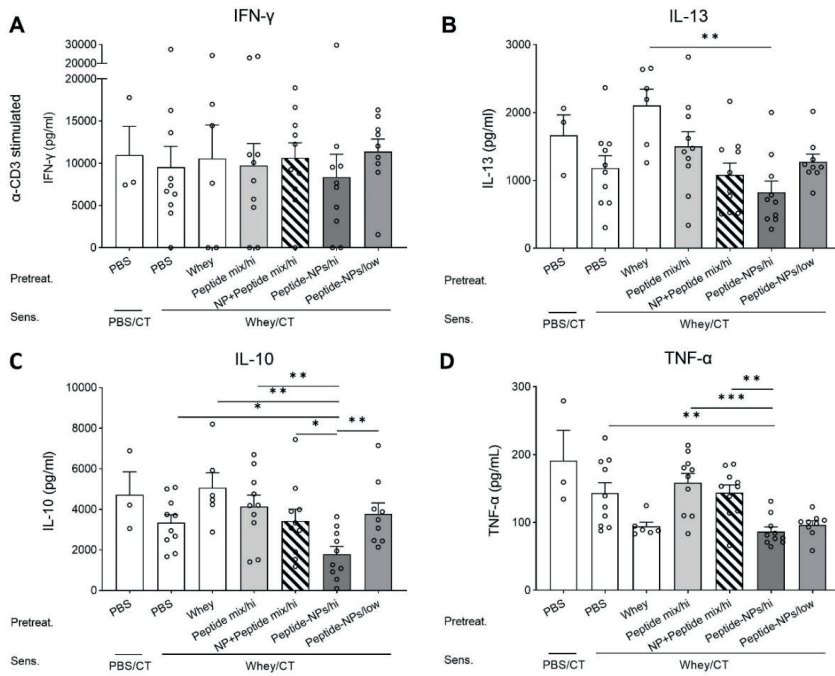


Figure S4. Cytokine production after *ex-vivo* re-stimulation of splenocytes with α -CD3. Splenocytes were *ex vivo* re-stimulated with anti-CD3 monoclonal antibody for 2 days, Th1- (A), Th2- (B), regulatory (C) and proinflammatory (D) associated cytokines were measured in supernatants; Data are presented as mean \pm SEM for n=9-10 per group except for the non-sensitized group, n=3 and whey tolerant group, n=6. (A)-(D) are analyzed with one-way ANOVA followed by Bonferroni's *post hoc* test for selected pairs, after log transformation for (A-C) and after square root transformation for (D); *P<0.05, **P<0.01, ***P<0.001; CT, Cholera toxin.

Inhibition of CMA development in mice by oral delivered BLG-peptides loaded PLGA NP is associated with systemic whey-specific immune silencing

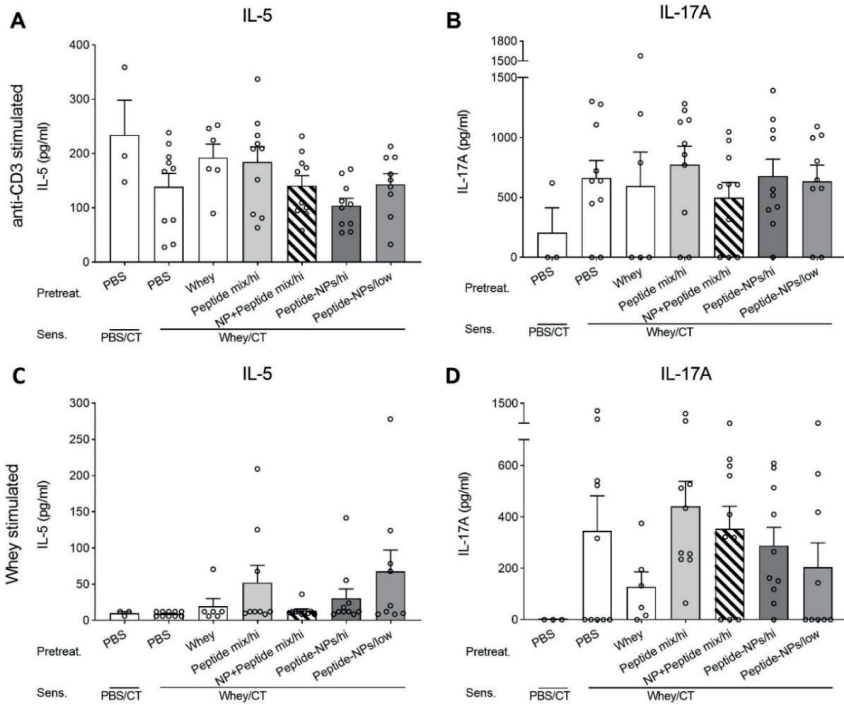


Figure S5. IL-5 and IL-17A production after restimulation of splenocytes with α -CD3 or whole whey protein. Splenocytes were re-stimulated *ex vivo* either with medium or anti-CD3 monoclonal antibody for 2 days, Th2-(A) and Th17A- associated (B) cytokines, or with medium or whole whey protein for 5 days, Th2- (C), Th17A- associated (D) cytokines are measured in supernatants; Data are presented as mean \pm SEM for n=9-10 per group except for non-sensitized group, n=3; whey tolerant group, n=6. (A)-(D) are analyzed with one-way ANOVA followed by Bonferroni's post hoc test for selected pairs, after square root transformation *P<0.05, **P<0.01, ***P<0.001; CT, Cholera toxin.

CHAPTER TWO

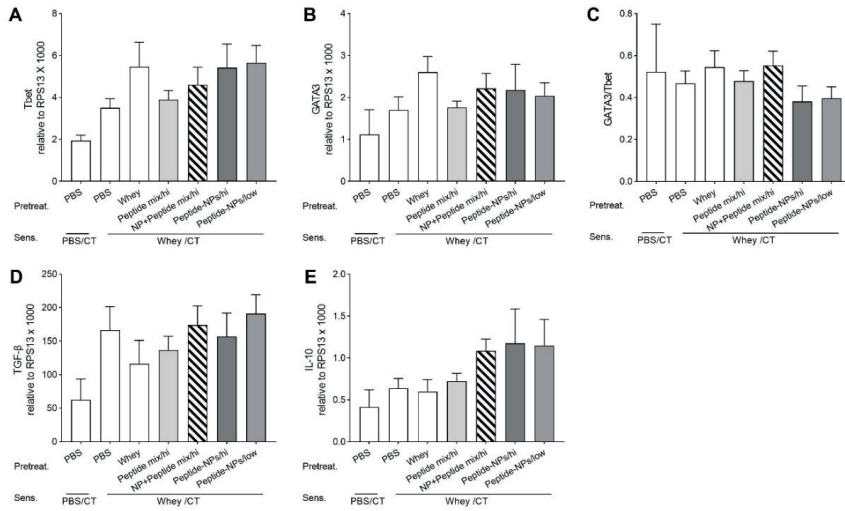


Figure S6. mRNA expression in the middle intestine after oral challenge with whole whey protein. Middle intestines were collected 18 h after oral whey challenge for mRNA isolation and cDNA synthesis. mRNA expression of Th1-associated Tbet (A), Th2-associated GATA3 (B), regulatory TGF- β (D) and IL-10 (E) markers with real-time qPCR. The ratio of Tbet/GATA3 was calculated to represent Th1/Th2 balance. mRNA expression is normalized to RPS13 reference gene expression. Data are presented as mean \pm SEM for n=9-10 per group except for non-sensitized group, n=3; whey tolerant group, n=6.

Inhibition of CMA development in mice by oral delivered BLG-peptides loaded PLGA NP is associated with systemic whey-specific immune silencing

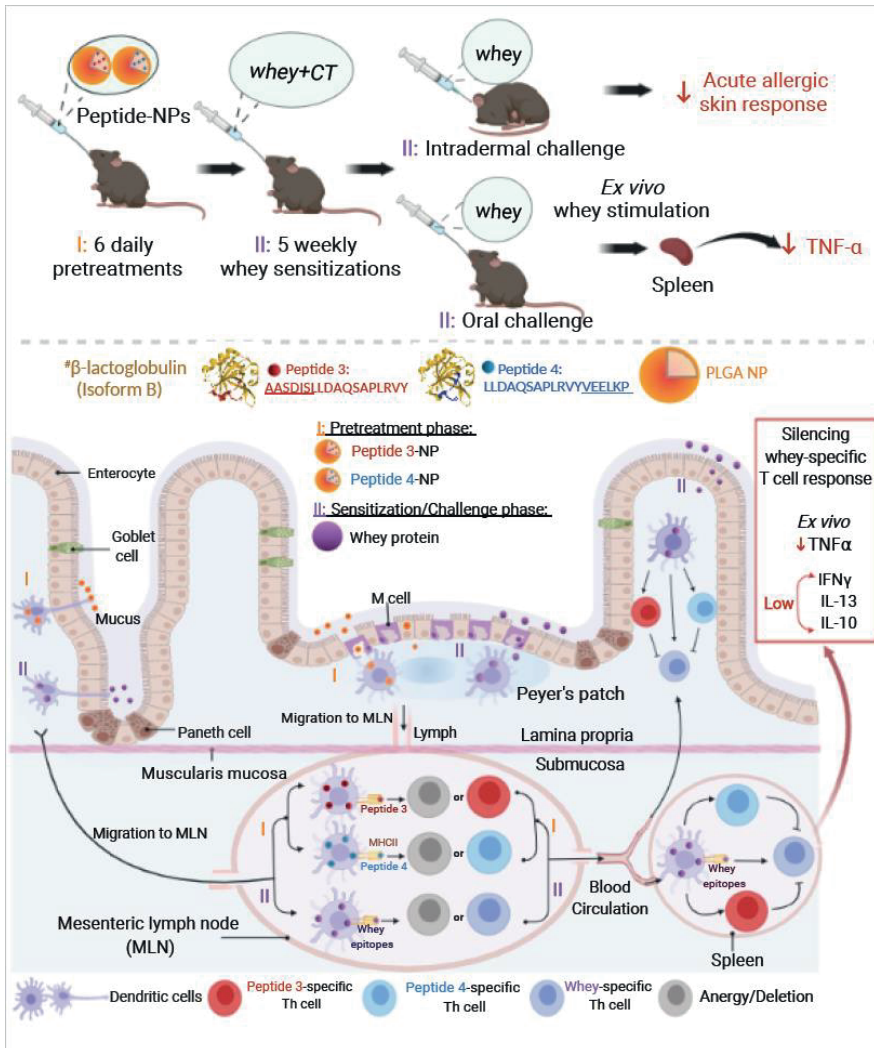


Figure S7. Graphical Abstract. Oral pre-exposure to PLGA nanoparticles encapsulated with two selected 18-AA β -lactoglobulin-derived peptides for 6 days, prior to 5 weekly oral sensitizations to whole whey protein, significantly reduced the acute allergic skin response of 3 week-old female C3H/HeO/J mice upon intradermal whey challenge dose dependently. *Ex vivo* whey stimulation recalled low IL-13, IFN- γ and IL-10 and significantly lowered TNF- α release by splenocytes in the 160 μ g PLGA-encapsulated peptides recipients, but not empty PLGA nanoparticles plus peptides recipients, indicating a systemic whey silencing effect.

References

- [1] D. Luyt, H. Ball, N. Makwana, M.R. Green, K. Bravin, S.M. Nasser, A.T. Clark, A. Standards of Care Committee of the British Society for, I. Clinical, BSACI guideline for the diagnosis and management of cow's milk allergy, *Clin Exp Allergy*, 44 (2014) 642-672.
- [2] C. Lifschitz, H. Szajewska, Cow's milk allergy: evidence-based diagnosis and management for the practitioner, *Eur J Pediatr*, 174 (2015) 141-150.
- [3] P. Restani, C. Ballabio, C. Di Lorenzo, S. Tripodi, A. Fiocchi, Molecular aspects of milk allergens and their role in clinical events, *Anal Bioanal Chem*, 395 (2009) 47-56.
- [4] C. Sackesen, D.U. Altintas, A. Bingol, G. Bingol, B. Buyuktiryaki, E. Demir, A. Kansu, Z. Kuloglu, Z. Tamay, B.E. Sekerel, Current Trends in Tolerance Induction in Cow's Milk Allergy: From Passive to Proactive Strategies, *Front Pediatr*, 7 (2019) 372.
- [5] H.R. Fisher, G. Du Toit, H.T. Bahnson, G. Lack, The challenges of preventing food allergy: Lessons learned from LEAP and EAT, *Ann Allergy Asthma Immunol*, 121 (2018) 313-319.
- [6] G. du Toit, P.H. Sayre, G. Roberts, K. Lawson, M.L. Sever, H.T. Bahnson, H.R. Fisher, M. Feeney, S. Radulovic, M. Basting, M. Plaut, G. Lack, t. Immune Tolerance Network Learning Early About Peanut Allergy study, Allergen specificity of early peanut consumption and effect on development of allergic disease in the Learning Early About Peanut Allergy study cohort, *J Allergy Clin Immunol*, 141 (2018) 1343-1353.
- [7] G. Du Toit, G. Roberts, P.H. Sayre, H.T. Bahnson, S. Radulovic, A.F. Santos, H.A. Brough, D. Phippard, M. Basting, M. Feeney, V. Turcanu, M.L. Sever, M. Gomez Lorenzo, M. Plaut, G. Lack, L.S. Team, Randomized trial of peanut consumption in infants at risk for peanut allergy, *N Engl J Med*, 372 (2015) 803-813.
- [8] M.R. Perkin, K. Logan, T. Marrs, S. Radulovic, J. Craven, C. Flohr, G. Lack, E.A.T.S. Team, Enquiring About Tolerance (EAT) study: Feasibility of an early allergenic food introduction regimen, *J Allergy Clin Immunol*, 137 (2016) 1477-1486 e1478.
- [9] Y. Katz, N. Rajuan, M.R. Goldberg, E. Eisenberg, E. Heyman, A. Cohen, M. Leshno, Early exposure to cow's milk protein is protective against IgE-mediated cow's milk protein allergy, *J Allergy Clin Immunol*, 126 (2010) 77-82 e71.
- [10] D.A. Osborn, J.K. Sinn, L.J. Jones, Infant formulas containing hydrolysed protein for prevention of allergic disease, *Cochrane Database Syst Rev*, 10 (2018) CD003664.
- [11] Y. Vandenplas, Prevention and Management of Cow's Milk Allergy in Non-Exclusively Breastfed Infants, *Nutrients*, 9 (2017).
- [12] L.A. Meulenbroek, B.C. van Esch, G.A. Hofman, C.F. den Hartog Jager, A.J. Nauta, L.E. Willemsen, C.A. Bruijnzeel-Koomen, J. Garssen, E. van Hoffen, L.M. Knippels, Oral treatment with beta-lactoglobulin peptides prevents clinical symptoms in a mouse model for cow's milk allergy, *Pediatr Allergy Immunol*, 24 (2013) 656-664.
- [13] A.I. Kostadinova, J. Middelburg, M. Ciulla, J. Garssen, W.E. Hennink, L.M.J. Knippels, C.F. van Nostrum, L.E.M. Willemsen, PLGA nanoparticles loaded with beta-lactoglobulin-derived peptides modulate mucosal immunity and may facilitate cow's milk allergy prevention, *Eur J Pharmacol*, 818 (2018) 211-220.
- [14] M. Larche, Peptide therapy for allergic diseases: basic mechanisms and new clinical approaches, *Pharmacol Ther*, 108 (2005) 353-361.
- [15] A.L. Silva, R.A. Rosalia, E. Varypataki, S. Sibuea, F. Ossendorp, W. Jiskoot, Poly-(lactic-co-glycolic-acid)-based particulate vaccines: particle uptake by dendritic cells is a key parameter for immune activation, *Vaccine*, 33 (2015) 847-854.
- [16] Q. Liu, X. Wang, X. Liu, S. Kumar, G. Gochman, Y. Ji, Y.P. Liao, C.H. Chang, W. Situ, J. Lu, J. Jiang, K.C. Mei, H. Meng, T. Xia, A.E. Nel, Use of Polymeric Nanoparticle Platform Targeting the Liver To Induce Treg-Mediated Antigen-Specific Immune Tolerance in a Pulmonary Allergen Sensitization Model, *ACS Nano*, 13 (2019) 4778-4794.
- [17] V. Ayechu-Muruzabal, S.A. Overbeek, A.I. Kostadinova, B. Stahl, J. Garssen, B. Van't Land, L.E.M. Willemsen, Exposure of Intestinal Epithelial Cells to 2'-Fucosyllactose and CpG Enhances Galectin Release and Instructs Dendritic Cells to Drive Th1 and Regulatory-Type Immune Development, *Biomolecules*, 10 (2020).
- [18] B.C. van Esch, B. Schouten, G.A. Hofman, T. van Baalen, F.P. Nijkamp, L.M. Knippels, L.E. Willemsen, J. Garssen, Acute allergic skin response as a new tool to evaluate the allergenicity of whey hydrolysates in a mouse model of orally induced cow's milk allergy, *Pediatr Allergy Immunol*, 21 (2010) e780-786.

- [19] B. Schouten, B.C. van Esch, G.A. Hofman, L.W. van den Elsen, L.E. Willemsen, J. Garssen, Acute allergic skin reactions and intestinal contractility changes in mice orally sensitized against casein or whey, *Int Arch Allergy Immunol*, 147 (2008) 125-134.
- [20] B.C. van Esch, B. Schouten, S. de Kivit, G.A. Hofman, L.M. Knippels, L.E. Willemsen, J. Garssen, Oral tolerance induction by partially hydrolyzed whey protein in mice is associated with enhanced numbers of Foxp3+ regulatory T-cells in the mesenteric lymph nodes, *Pediatr Allergy Immunol*, 22 (2011) 820-826.
- [21] K.S. Park, M.J. Park, M.L. Cho, S.K. Kwok, J.H. Ju, H.J. Ko, S.H. Park, H.Y. Kim, Type II collagen oral tolerance; mechanism and role in collagen-induced arthritis and rheumatoid arthritis, *Mod Rheumatol*, 19 (2009) 581-589.
- [22] W.U. Kim, W.K. Lee, J.W. Ryoo, S.H. Kim, J. Kim, J. Youn, S.Y. Min, E.Y. Bae, S.Y. Hwang, S.H. Park, C.S. Cho, J.S. Park, H.Y. Kim, Suppression of collagen-induced arthritis by single administration of poly(lactic-co-glycolic acid) nanoparticles entrapping type II collagen: a novel treatment strategy for induction of oral tolerance, *Arthritis Rheum*, 46 (2002) 1109-1120.
- [23] J.L. Coombes, F. Powrie, Dendritic cells in intestinal immune regulation, *Nat Rev Immunol*, 8 (2008) 435-446.
- [24] A.M. Mowat, To respond or not to respond - a personal perspective of intestinal tolerance, *Nat Rev Immunol*, 18 (2018) 405-415.
- [25] A.M. Mowat, Anatomical basis of tolerance and immunity to intestinal antigens, *Nat Rev Immunol*, 3 (2003) 331-341.
- [26] Y.Y. Luo, X.Y. Xiong, Y. Tian, Z.L. Li, Y.C. Gong, Y.P. Li, A review of biodegradable polymeric systems for oral insulin delivery, *Drug Deliv*, 23 (2016) 1882-1891.
- [27] C. He, L. Yin, C. Tang, C. Yin, Size-dependent absorption mechanism of polymeric nanoparticles for oral delivery of protein drugs, *Biomaterials*, 33 (2012) 8569-8578.
- [28] Y. Xu, C.S. Kim, D.M. Saylor, D. Koo, Polymer degradation and drug delivery in PLGA-based drug-polymer applications: A review of experiments and theories, *J Biomed Mater Res B Appl Biomater*, 105 (2017) 1692-1716.
- [29] S.S. Saluja, D.J. Hanlon, F.A. Sharp, E. Hong, D. Khalil, E. Robinson, R. Tigelaar, T.M. Fahmy, R.L. Edelson, Targeting human dendritic cells via DEC-205 using PLGA nanoparticles leads to enhanced cross-presentation of a melanoma-associated antigen, *Int J Nanomedicine*, 9 (2014) 5231-5246.
- [30] M.K. Levings, S. Gregori, E. Tresoldi, S. Cazzaniga, C. Bonini, M.G. Roncarolo, Differentiation of Tr1 cells by immature dendritic cells requires IL-10 but not CD25+CD4+ Tr cells, *Blood*, 105 (2005) 1162-1169.
- [31] Jonuleit. Helmut, Schmitt. Edgar, Schuler. Gerold, Knop. Jürgen, Enk. Alexander H., Induction of Interleukin 10 producing Nonproliferating CD4+cells with regulatory properties by repetitive stimulation with allogeneic human iDC, *J. Exp. Med.*, 192 (2000) 10.
- [32] K. Kretschmer, I. Apostolou, D. Hawiger, K. Khazaie, M.C. Nussenzweig, H. von Boehmer, Inducing and expanding regulatory T cell populations by foreign antigen, *Nat Immunol*, 6 (2005) 1219-1227.
- [33] K.D. Srivastava, A. Siefert, T.M. Fahmy, M.J. Caplan, X.M. Li, H.A. Sampson, Investigation of peanut oral immunotherapy with CpG/peanut nanoparticles in a murine model of peanut allergy, *J Allergy Clin Immunol*, 138 (2016) 536-543 e534.
- [34] G. Joshi, A. Kumar, K. Sawant, Bioavailability enhancement, Caco-2 cells uptake and intestinal transport of orally administered lopinavir-loaded PLGA nanoparticles, *Drug Deliv*, 23 (2016) 3492-3504.
- [35] J.M. Silva, M. Videira, R. Gaspar, V. Preat, H.F. Florindo, Immune system targeting by biodegradable nanoparticles for cancer vaccines, *J Control Release*, 168 (2013) 179-199.
- [36] M.F. Bachmann, G.T. Jennings, Vaccine delivery: a matter of size, geometry, kinetics and molecular patterns, *Nat Rev Immunol*, 10 (2010) 787-796.
- [37] R.O. Williams, M. Feldmann, R.N. Maini, Anti-tumor necrosis factor ameliorates joint disease in murine collagen-induced arthritis, *Proc Natl Acad Sci U S A*, 89 (1992) 9784-9788.
- [38] J.P. Choi, Y.S. Kim, O.Y. Kim, Y.M. Kim, S.G. Jeon, T.Y. Roh, J.S. Park, Y.S. Gho, Y.K. Kim, TNF-alpha is a key mediator in the development of Th2 cell response to inhaled allergens induced by a viral PAMP double-stranded RNA, *Allergy*, 67 (2012) 1138-1148.
- [39] H.R. Cohn L, Marinov A, Rankin J, and Bottomly K., Induction of Airway Mucus Production By T Helper 2 (Th2) Cells: A Critical Role For Interleukin 4 In Cell Recruitment But Not Mucus Production., *J. Exp. Med.*, 186 (1997) 11.
- [40] P. Gu, A. Wusiman, Y. Zhang, Z. Liu, R. Bo, Y. Hu, J. Liu, D. Wang, Rational Design of PLGA Nanoparticle Vaccine Delivery Systems To Improve Immune Responses, *Mol Pharm*, 16 (2019) 5000-5012.

- [41] J.W. Gouw, J. Jo, L. Meulenbroek, T.S. Heijger, E. Kremer, E. Sandalova, A.C. Knulst, P.V. Jeurink, J. Garsen, A. Rijnierse, L.M.J. Knippels, Identification of peptides with tolerogenic potential in a hydrolysed whey-based infant formula, *Clin Exp Allergy*, 48 (2018) 1345-1353.
- [42] R. Kuo, E. Saito, S.D. Miller, L.D. Shea, Peptide-Conjugated Nanoparticles Reduce Positive Co-stimulatory Expression and T Cell Activity to Induce Tolerance, *Mol Ther*, 25 (2017) 1676-1685.
- [43] J.-i.l. Youhai Chen, Reinhard Marks, Patricia Gonnella, Vijay K. Kuchroo & Howard L. Weiner, Peripheral deletion of antigen-reactive T cells in oral tolerance., *Nature*, 376 (1995) 4.
- [44] S.L. Demento, W. Cui, J.M. Criscione, E. Stern, J. Tulipan, S.M. Kaech, T.M. Fahmy, Role of sustained antigen release from nanoparticle vaccines in shaping the T cell memory phenotype, *Biomaterials*, 33 (2012) 4957-4964.
- [45] A.L. Siefert, A. Ehrlich, M.J. Corral, K. Goldsmith-Pestana, D. McMahon-Pratt, T.M. Fahmy, Immunomodulatory nanoparticles ameliorate disease in the *Leishmania (Viannia) panamensis* mouse model, *Biomaterials*, 108 (2016) 168-176.
- [46] A.P. Walczak, E. Kramer, P.J. Hendriksen, P. Tromp, J.P. Helder, M. van der Zande, I.M. Rietjens, H. Bouwmeester, Translocation of differently sized and charged polystyrene nanoparticles in in vitro intestinal cell models of increasing complexity, *Nanotoxicology*, 9 (2015) 453-461.
- [47] J.J. Garcia-Vallejo, B. Van Het Hof, J. Robben, J.A. Van Wijk, I. Van Die, D.H. Joziassse, W. Van Dijk, Approach for defining endogenous reference genes in gene expression experiments, *Anal Biochem*, 329 (2004) 293-299.

CHAPTER 3

Oral Pretreatment With β -Lactoglobulin Derived Peptide And CpG Co-Encapsulated In PLGA Nanoparticles Prior To Sensitizations Attenuates Cow's Milk Allergy Development In Mice

M. (Mengshan) Liu^{1,2}, S.(Suzan) Thijssen², W.E. (Wim) Hennink¹, J. (Johan) Garssen^{1,3}, C.F. (Cornelus) van Nostrum¹, L.E.M. (Linette) Willemsen^{2*}

1. Division of Pharmaceutics, Utrecht Institute for Pharmaceutical Sciences, Utrecht University, Utrecht, the Netherlands
2. Division of Pharmacology, Utrecht Institute for Pharmaceutical Sciences, Utrecht University, Utrecht, the Netherlands
3. Department of Immunology, Nutricia Research B.V., Utrecht, the Netherlands

This chapter is published in *Front Immunol*, 13 (2023) 1053107.

Abstract

Background. Cow's milk allergy is a common food allergy among infants. Improved hygiene conditions and loss of microbial diversity are associated with increased risk of allergy development. The intestinal immune system is essential for oral tolerance induction. In this respect, bacterial CpG DNA is known to drive Th1 and regulatory T-cell (Treg) development via Toll-Like-Receptor 9 (TLR-9) signaling, skewing away from the allergic Th2 phenotype. **Objective.** We aimed to induce allergen specific tolerance via oral delivery of poly (lactic-co-glycolic acid) nanoparticles (NP) co-encapsulated with a selected β -lactoglobulin derived peptide (BLG-Pep) and TLR-9 ligand CpG oligodeoxynucleotide (CpG). **Methods.** *In vivo*, 3-4-week-old female C3H/HeOuj mice housed in individually ventilated cages received 6-consecutive-daily gavages of either PBS, whey, BLG-Pep/NP, CpG/NP, a mixture of BLG-Pep/NP plus CpG/NP or co-encapsulated BLG-Pep+CpG/NP, before 5-weekly oral sensitizations with whey plus cholera toxin (CT) or only CT (sham) and were challenged with whey 5 days after the last sensitization. **Results.** The co-encapsulated BLG-Pep+CpG/NP pretreatment, but not BLG-Pep/NP, CpG/NP or the mixture of BLG-Pep/NP plus CpG/NP, prevented the whey-induced allergic skin reactivity and prevented rise in serum BLG-specific IgE compared to whey-sensitized mice. Importantly, co-encapsulated BLG-Pep+CpG/NP pretreatment reduced dendritic cell (DC) activation and lowered the frequencies of PD-L1+ DC in the mesenteric lymph nodes compared to whey-sensitized mice. By contrast, co-encapsulated BLG-Pep+CpG/NP pretreatment increased the frequency of splenic PD-L1+ DC compared to the BLG-Pep/NP plus CpG/NP recipients, in association with lower Th2 development and increased Treg/Th2 and Th1/Th2 ratios in the spleen. **Conclusion.** Oral administration of PLGA NP co-encapsulated with BLG-Pep and CpG prevented rise in serum BLG-specific IgE and symptom development while lowering splenic Th2 cell frequency in these mice which were kept under strict hygienic conditions.

Keywords: β -lactoglobulin, cow's milk allergy, CpG oligodeoxynucleotides, individual ventilated cages, poly (lactic-co-glycolic acid), toll-like-receptor 9, whey protein.

Introduction

Cow's milk allergy (CMA) is one of the most common food allergies occurring early in life, with an overall incidence of 0.54% in Europe [1]. Despite most infants can outgrow CMA, affected children need to avoid ingestion of cow's milk proteins, which may restrict nutrient intake and decrease their quality of life. Early introduction of peanuts, between 4 and 11 months after birth, was found effective in prevention of peanut allergy development among high-risk infants [2] in the Learning Early About Peanut Allergy (LEAP) study. Similarly, early introduction of egg proteins between 4 and 6 months of age protected against the development of egg allergy [3]. However, early introduction of cow's milk protein was not found to reduce the risk on cow's milk allergy among the general population in the Enquiring About Tolerance (EAT) observational study [4]. Nevertheless, an earlier timing for cow's milk protein exposure among a general population, in addition to breast feeding, within 14 days after birth [5] and during the first 3 months of life was found to be associated with a decreased risk of CMA [6]. When breastfeeding is not possible, cow's milk formula or hydrolyzed formula milk might be given to the atopic children at risk of CMA development as breastmilk substitute [7]. However, neither cow's milk formula nor hydrolyzed formula milk was proven effective in CMA prevention [7]. Furthermore, early introduction of cow's milk proteins (*i.e.* whole whey protein) might induce adverse reactions among infants that have been sensitized via environmental exposure via skin [8]. Therefore, when breastfeeding is not possible for the high-risk infants, it is of importance to implement a safe and effective approach for CMA prevention. Previously 18-AA long synthetic peptides were identified within the β -lactoglobulin (BLG) sequence and shown to contribute to oral tolerance induction [9]. In pre-clinical studies, BLG derived peptides showed reduced sensitizing capacity as compared to BLG protein [10], and were found capable of inducing oral tolerance to whole whey protein [9, 11]. These peptides are too small to provoke allergic symptoms and therefore safe to provide early in life in children at risk to enrich formula milk.

Our previous study showed a protective effect of BLG derived peptides encapsulated poly(lactic-co-glycolic acid) (PLGA) nanoparticles (NP) against CMA development when mice were housed in open cages [12]. The gut-associated lymphoid tissue (GALT) is prone to induce peripheral immune tolerance to harmless food proteins [13] in the presence of the proper environmental stimuli as co-factors [14]. Allergen loaded PLGA nanoparticles have been extensively exploited via subcutaneous [15] or oral route [16-18] for allergen immunotherapy in mice. In early life, microbial triggers

are suggested to play a pivotal role in immune maturation and development of regulatory T-cells contributing to oral tolerance induction [19]. Noteworthy, bacterial CpG DNA can activate the TLR-9 that is expressed in the endolysosomes of plasmacytoid DC and B-cells [20, 21] and drive regulatory immune maturation [22], skewing away from the allergic type 2 phenotype [23, 24]. However, modern lifestyle and environmental changes, including improved hygiene conditions and use of antibiotics affect intestinal microbial diversity and commensal microbiota composition contributing to an immune imbalance and a rise in allergic diseases including food allergy [25, 26].

Housing mice in individual ventilated cages (IVC) simulates a strict hygienic environment with reduced exposure to bacterial ligands that are essential for immune function and/or contribute to immune maturation [27]. We hypothesized that co-encapsulating TLR-9 ligand CpG together with a selected model synthetic peptide of 18-AA derived from BLG sequence (BLG-peptide, abbreviated as BLG-Pep) [12] in PLGA nanoparticles would improve the allergy preventive capacity of the BLG-Pep as CpG acts as a Th1 and Treg adjuvant [28-30]. Noteworthy, this BLG-Pep was shown previously to be recognized by a cow's milk specific human T-cell line *in vitro* and to reduce allergic skin reactivity to whole whey protein in mice when used in a relatively high dose [31] and at a lower dose when encapsulated in PLGA nanoparticles to optimize oral delivery [32]. To further enhance the efficacy of this approach a strategy was developed to co-encapsulate BLG-Pep, to instruct allergen specificity, together with CpG, as an immunomodulatory adjuvant, into PLGA nanoparticles.

Previously, co-administration of antigen and class B CpG-oligonucleotides (CpG), as a Th1-skewing immune adjuvant, has been harnessed in food allergy [24] and allergic asthma immunotherapy [33] in mice. Current reported strategies for antigen and CpG co-delivery using PLGA carriers either incorporates cationic lipid dioleoyl-3-trimethylammonium propane (DOTAP) [34] or protamine [35]. However, DOTAP functions as a Toll-like receptor 4 (TLR-4) agonist and interferes with the tolerance induction outcome. To preclude the influences from DOTAP and additional protein protamine, we have prepared well-defined CpG and BLG-Pep co-encapsulated PLGA nanoparticles.

In this study, we investigated the effect of orally administered nanoparticles co-encapsulated with CpG and BLG-Pep as a model peptide to prevent whey induced cow's milk allergy in mice kept in IVC housing to mimic increased hygienic conditions.

Materials And Methods

Peptide and CpG

A 18-AA-long sequential synthetic peptide that are derived from the chain B of bovine β -lactoglobulin, BLG-Pep (AASDISLLDAQSAPLRVY), previously indicated as Peptide 3 [12], was purchased from JPT Peptide Technologies (Berlin, Germany). Murine TLR-9 ligand CpG oligonucleotides 1826 (5'-tccatgacgttcctgacgtt-3', further abbreviated as CpG) was purchased from InvivoGen (San Diego, USA).

Preparation and characterization of BLG-Pep and/or CpG encapsulated PLGA nanoparticles and release studies

Nanoparticles were prepared with poly (lactic-co-glycolic acid) (PLGA: lactide/glycolide molar ratio 50:50, 0.32 - 0.48 dL/g; PURASORB PDLG 5004A, Corbion, the Netherlands) using a double emulsion solvent evaporation method, as described in detail in the supplemental information. BLG-Pep (previously indicated as Peptide 3) were encapsulated in PLGA nanoparticles for the animal study as previously published [12, 32]. The *in vitro* release method of BLG-Pep and CpG from the PLGA NP is described in detail in the supplemental method.

Animal study

Sixty 3-4-week-old pathogen free female C3H/HeOJ mice were ordered from Charles River Laboratories (Sulzfeld, Germany). The mice were randomly allocated into 7 treatment groups and housed in individually ventilated cages in the animal facility of Utrecht University. The mice were fed cow's milk protein free control purified diet AIN-93G (contains soy protein and supplemented methionine to replace casein as protein source, Ssniff diet obtained via Bio-services, Uden, the Netherlands) *ad libitum* in the study. Animal care and use in this study follows the guidelines of the Animal Ethics committee and the Center Commission for Animal use (CCD) of Utrecht University, with approval numbers of AVD108002015262-2.

Oral tolerance induction, sensitization and challenge

The CMA prevention murine model was developed and described by Schouten *et al.* [36] and Kostadinova *et al.* [37]. As indicated in Figure 1, mice were randomly allocated into 7 groups and received 6-consecutive-daily oral pretreatments (Table 1) with the selected model BLG peptide (BLG-Pep) and/or CpG encapsulated in PLGA NP in a sterile biosafety cabinet starting 2 days after their arrival. Briefly, the mice received either PBS (Dulbecco's phosphate-buffered saline, Sigma-Aldrich, Zwijndrecht, the Netherlands), 50 mg whey, BLG-Pep/NP (160 µg encapsulated BLG-Pep), CpG/NP (3 µg encapsulated CpG), a mixture of BLG-Pep/NP plus CpG/NP (160 µg BLG-Pep and 3 µg CpG in separate encapsulation form), or co-encapsulated BLG-Pep+CpG/NP (160 µg BLG-Pep and 3 µg CpG in co-encapsulation form) in 0.5 mL PBS via oral gavages. Two days after the tolerance induction phase mice received 5-consecutive-weekly sensitizations with 20 mg whey plus 10 µg cholera toxin (CT) in 0.5 mL PBS for all groups except sham (only CT) to break oral tolerance for whey from day 7 to day 35. Five days after the last whey-sensitization, mice received intradermal challenge with 10 µg whole whey protein in the ears (day 40) and at t=0 h

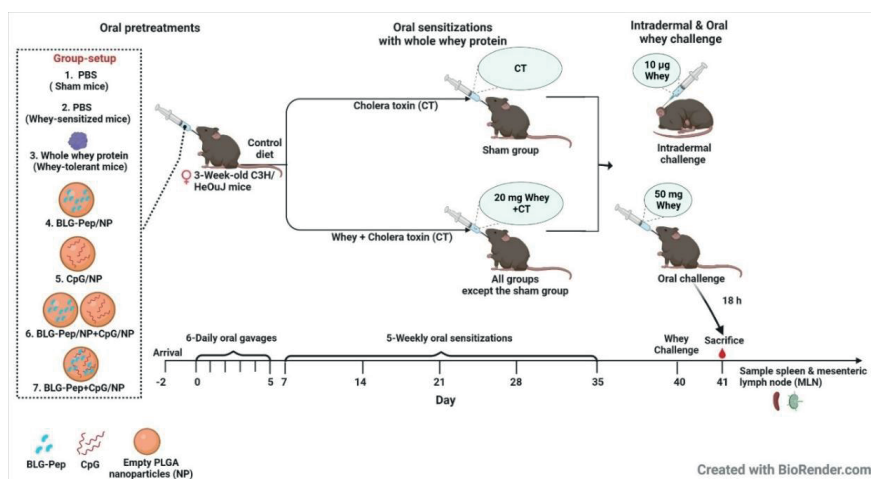


Figure 1. Experimental protocol for pre-treatment, sensitizations and challenge in murine model of cow's milk allergy for the animal study. Three-four-week-old pathogen free female C3H/HeOJ mice were given 6 daily oral pretreatments starting 2 days after arrival of the mice. Two days after the tolerance induction phase mice received 5-consecutive-weekly sensitizations with 20 mg whey plus 10 µg cholera toxin in 0.5 mL PBS for all groups but sham (only cholera toxin) from day 7 to day 35 to break whey tolerance. Five days after the last whey-sensitization, mice received intradermal challenge with 10 µg whole whey protein in the ears and at t=0 h and t=1 h the acute allergic skin response (ear swelling) was determined. Three hours after the intradermal whey challenge, the mice were orally challenged by means of gavage with 50 mg whey in 0.5 mL PBS. Eighteen hours after the oral whey challenge, mice were anesthetized with isoflurane and euthanized after blood sampling. Subsequently, spleen and mesenteric lymph nodes were collected immediately for further analysis. CT: Cholera toxin; NP: nanoparticles

and t=1 h the ear swelling response was measured (acute allergic skin response). Three hours after the intradermal whey challenge, the mice were orally challenged by means of gavage with 50 mg whey in 0.5 mL PBS. Eighteen hours after the oral whey challenge, mice were anesthetized with isoflurane and euthanized after blood sampling.

Table 1. Treatment groups of the animal study in the CMA prevention murine model.

Group	Pretreatment per mouse per dose	Sensitization	Challenge
Sham (n=4)	PBS	Cholera Toxin	Whey
Whey-sensitized (n=10)	PBS	Cholera Toxin + Whey	
Whey-tolerant (n=6)	Whey		
BLG-Pep/NP (n=10)	23 mg BLG-Pep/NP (encapsulating 160 µg BLG-Pep plus 5 mg Empty NP)		
CpG/NP (n=10)	5 mg CpG/NP (encapsulating 3 µg CpG plus 23 mg Empty NP)		
BLG-Pep/NP+CpG/NP (n=10)	23 mg BLG-Pep/NP plus 5 mg CpG/NP (encapsulating 160 µg BLG-Pep and 3 µg CpG)		
BLG-Pep+CpG/NP (n=10)	20 mg BLG-Pep+CpG/NP (encapsulating 160 µg BLG-Pep and 3 µg CpG)		

Assessment of acute allergic skin response

Five days after the last oral sensitization, the acute allergic skin response was recorded with the cage code concealed. Under anaesthesia by inhalation of isoflurane, the ear pinnae thickness of the mice was measured twice using a digital micrometer (Mitutoyo, Veenendaal, the Netherlands), before and 1 h after intradermal ear challenge with 10 µg whey protein in 20 µL PBS. Difference in ear pinnae thickness (ear swelling) was calculated by subtracting the basal ear pinnae thickness before challenge according to Schouten *et al.* [36]. Meanwhile, body temperature and anaphylaxis symptoms score were recorded before and at 30 min and 1 h after intradermal challenge with whole whey protein according to Schouten *et al.* [36].

Serum mucosal mast cell protease-1 (mMCP-1) and allergen specific immunoglobulins

mMCP-1 was measured in serum that was collected 18 h after the oral whey challenge, using the mouse mucosal mast cell protease-1 (MCPT-1) Elisa kit (eBioscience, ThermoFisher, Massachusetts, USA) according to the manufacturer's

protocol. Serum whey- and BLG-specific immunoglobulins were measured a previously reported method [31].

Flow cytometry analysis of T cell subsets from spleen and DC from mesenteric lymph nodes and spleen

Eighteen hours after oral challenge of the mice with whole whey protein, isolation of cells from spleen [11] and mesenteric lymph nodes (MLN) [38] was performed as previously reported.

Approximate 8×10^5 isolated MLN or spleen cells were resuspended in 135 μ L PBS (Sigma-Aldrich) and cultured in 96-wells falcon plates. Cell viability was determined by staining with 100 μ L fixable viability dye (FVD)-eFluor™780 (ThermoFisher) at 2000 times dilution in PBS at 4°C. Nonspecific binding sites were blocked by incubation with 25 μ L anti-mouse CD16/CD32 (Mouse BD Fc block; BD Pharmingen, San Jose, USA) at 100 times dilution in 2% Fetal Bovine Serum (FBS)-1% Bovine Serum Albumin (BSA, Sigma-Aldrich)-PBS buffer for 5 min at 4°C.

For extracellular staining of Th1/Th2 and Th17/Treg (Antibodies concentrations are shown in the Supplemental Table 1 and 2), splenocytes were incubated with CD4-BV510 (BioLegend, San Diego, USA), T1/ST2-FITC (MD Biosciences, Oakdale, USA), CXCR3-PE (ThermoFisher), CD25-PerCP/eFluor710 (ThermoFisher), and CD196-PE (BioLegend) in 1% BSA-PBS buffer overnight at 4°C. For intracellular Treg staining, cells were first fixed and permeabilized with FoxP3/Transcription Factor Staining Buffer Set (ThermoFisher) and then stained with FoxP3-FITC (ThermoFisher).

For extracellular staining of DC (antibodies concentrations are shown in the Supplemental Table 3), MLN and spleen cell suspension were incubated with MHCII-PE (ThermoFisher), CD11c-FITC (ThermoFisher), CD11b-PE/Cy7 (ThermoFisher), CD80-BV421 (BioLegend), CD86-BV510 (BioLegend) and programmed cell death ligand 1 (PD-L1)-PerCP/Cy5.5 (ThermoFisher) 1% BSA-PBS buffer overnight at 4°C. Cells were analyzed with BD FACSCantoll flow cytometer (Becton Dickinson, Franklin Lakes, USA). Data analysis was conducted with FlowLogic software (Invai Technologies, Mentone, Australia).

Ex vivo allergen re-stimulated cytokine release by splenocytes

Splenocytes (6×10^5 cells) were stimulated with either 200 μ L 500 μ g/mL whey protein (DMV International, Veghel, the Netherlands), 290 μ g/mL β -Lactoglobulin B variant (from bovine milk, Sigma-Aldrich), or only blank RPMI 1640 medium supplemented with 10% FBS, 100 U/mL penicillin and 100 μ g/mL streptomycin as control and cultured in a round-bottom culture plate at 37°C, 5% CO₂. After 5-days, supernatants were collected and determined using a Procartaplex kit for mouse IL-13, IL-5, IL-10 and TNF- α and mouse IFN- γ , IL-17A and TGF- β ELISA kits (both from ThermoFisher) according to the manufacturer's protocols and using a GloMax® Discover plate reader (Promega, Wisconsin, USA).

Statistical analysis

The obtained *in vivo* data were analyzed with GraphPad Prism 9.0.0 software (GraphPad Software, San Diego, USA). Normal distribution of the data was assessed by the Shapiro-Wilk test and Kolmogorov-Smirnov test. If required data were log transformed to obtain normal distribution or alternatively a non-parametric test was used. One-way ANOVA followed by Bonferroni's *post hoc* test, or the non-parametric Kruskal-Wallis test followed by Dunn's *post hoc* test was applied for selected pairs (as indicated in the figure legends). In the *post hoc* analyses for selected pairs the whey-sensitized group was compared to all the other groups and the BLG-Pep+CpG/NP group was compared to all groups except the sham group (non-sensitized group).

Results

Characteristics of PLGA nanoparticles

Empty and encapsulated PLGA nanoparticles had average hydrodynamic particle sizes in the range of 240-270 nm. As a parameter that described the size range of nanocarriers [39], low polydispersity indices (PDI) below 0.14 (Table 2) of these nanoparticles demonstrated their narrow size distributions. The particles had close to neutral zeta-potentials (around -1 mV), as a key parameter reflects the electrostatic interactions and stability of the nanoparticles dispersions [40], in 10 mM HEPES buffer (pH7.4). BLG-Pep was encapsulated without CpG (in BLG-Pep/NP) or with CpG (in BLG-Pep+CpG/NP) with encapsulation efficiencies (EE) between 41-65% and loading capacities (LC) between 0.7-0.8%. CpG was encapsulated in CpG/NP (*i.e.*, without peptide) and in BLG-Pep+CpG/NP with EEs between 38-47% and LCs between 0.02-

0.06%. Quantification of the encapsulated BLG-Pep and CpG cargos in the PLGA nanoparticles enabled further *in vitro* release study and dosing for the pretreatments in the animal study.

Table 2. Characteristics of BLG-Pep and/or CpG encapsulated PLGA nanoparticles.

Formulation (Number of combined batches)	Hydrodynamic particle size (nm) (Measurement in triplicate)	Poly dispersity Index (PDI)	Zeta-potential ¹ (mV)	CpG		BLG-Pep	
				EE ² (%)	LC ³ (%)	EE (%)	LC (%)
Empty NP (n=6)	250 ± 15	0.09 ± 0.07	-1.2 ± 0.2	-	-	-	-
BLG-Pep/NP (n=3)	264 ± 3	0.08 ± 0.02	-1.0 ± 0.3	-	-	65	0.7
CpG/NP (n=2)	245 ± 2	0.06 ± 0.04	-1.2 ± 0.4	47	0.06	-	-
BLG-Pep+CpG/NP (n=2)	242 ± 3	0.08 ± 0.03	-0.8 ± 0.6	38	0.02	41	0.8

¹ Zeta-potential: Zeta-potential of the PLGA nanoparticles were characterized in 10 mM HEPES buffer at pH7.4.

² EE: Encapsulation Efficiency = $\frac{\text{Amount of encapsulated BLG-Pep or CpG}}{\text{Amount of feed BLG-Pep or CpG for formulation preparation}} \times 100$ (%)

³ LC: Loading Capacity = $\frac{\text{Amount of encapsulated BLG-Pep or CpG}}{\text{Weight of nanoparticles}} \times 100$ (%)

The *in vitro* release profiles of BLG-Pep/NP were similar to our previous study [12], except for a burst release of 18% BLG-Pep from the BLG-Pep/NP and no burst release of the peptide cargo from the BLG-Pep+CpG/NP used in the animal study (Supplemental Figure 1A). Thereafter, a slow-release phase and accelerated release phase of peptide cargo were observed during 49-58 days. For the release of CpG, a burst release of 20% CpG from CpG/NP and 10% CpG from BLG-Pep+CpG/NP were observed, followed by a sustained release of CpG from day 7 onwards (Supplemental Figure 1B).

Co-encapsulated BLG-Pep+CpG/NP prevented the acute allergic skin response and serum BLG-specific IgE levels

The animal study was performed in IVC housing as indicated in Table 1 and Figure 1. Whey-sensitized (sham-pretreated mice) mice had significantly increased ear thickness one hour after intradermal whey challenge, as compared to the sham (PBS-pretreated mice) and whey-tolerant group (whey-pretreated mice), indicating successful establishment of a prophylactic CMA murine model in this study (Figure 2A and Supplemental Figure 2A). Pretreatments by nanoparticles encapsulated with only BLG-Pep (BLG-Pep/NP) did not prevent the acute allergic skin response (Figure 2A). In the animal study, only co-encapsulated BLG-Pep+CpG/NP, but not pretreatments with, PBS (sham group), BLG-Pep/NP, CpG/NP or BLG-Pep/NP+CpG/NP, effectively prevented

the whey induced acute allergic skin response as compared to the whey-sensitized (sham-pretreated) mice. Moreover, co-encapsulated BLG-Pep+CpG/NP prevented the whey induced acute allergic skin response as compared to separately delivered BLG-Pep/NP+CpG/NP in mice (Figure 2A and Supplemental Figure 2A). No statistic difference was observed in body temperature or anaphylactic shock score of the mice during 1 h after intradermal whey challenge (Supplemental Figure 3). Despite lack of statistical significance, mMCP-1 measured in the serum showed a similar pattern as the acute allergic skin response result (Supplemental Figure 2B).

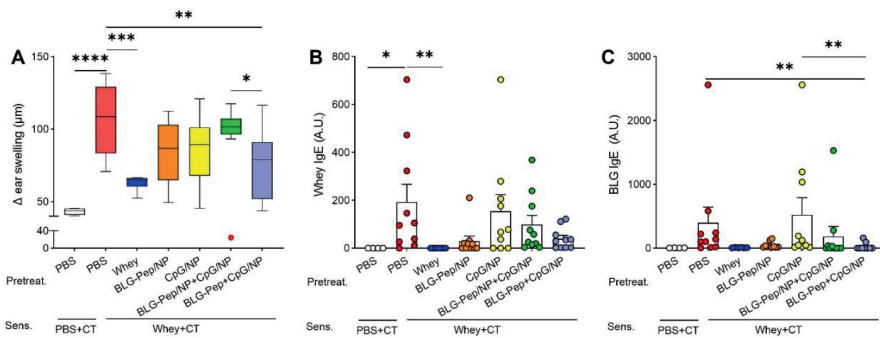


Figure 2. Acute allergic skin response and BLG- and whey-specific serum immunoglobulin E. Five days after last sensitization, mice were intradermally challenged in the ear pinnae with 10 µg whey followed by oral challenge. BLG- (B) and whey-specific (C) IgE levels are measured in serum, which were collected 18 h after last oral challenge with whey in mice from all groups of the animal study. The acute allergic skin response was measured 60 min afterwards in the *in vivo* study (A). Data are presented as box-and-whisker Tukey plots for (A), and mean \pm SEM for (B-C) n=9-10 per group except for the sham group, n=4 and whey-tolerant group, n=6. (A-C) are presented with Y axis formatted in two segments to properly show the relevant part of the window of effect. (A) is analyzed by one-way ANOVA, followed by Bonferroni's *post hoc* test for selected pairs. The outlier (in red) in the BLG-Pep/NP+CpG/NP group is excluded in (A) from statistics; (B-C) are analyzed with the Kruskal-Wallis non-parametric test, followed by Dunn's *post hoc* test for selected pairs; * p <0.05, ** p <0.01, *** p <0.001, **** p <0.0001; BLG, β -lactoglobulin; CT, Cholera toxin.

Consistent with the prevented allergic skin reactivity, mean BLG-specific IgE serum levels 18 h after oral whey challenge were significantly lower in the BLG-Pep+CpG/NP recipients compared to both whey-sensitized (sham-pretreated mice) and CpG/NP groups (Figure 2B). A similar overall pattern was found for whey-specific IgE, albeit this did not reach statistical significance (Figure 2C). In the whey-tolerant group (whey-pretreated mice), BLG- and whey-specific IgG1 and IgG2a remained low (Supplemental Figure 4A-D), but the other pretreatments did not reduce these immunoglobulins levels.

In mesenteric lymph nodes co-encapsulated BLG-Pep+CpG/NP decreased percentages of CD80/CD86+CD11b+ DC

No differences in the mean percentages of CD11c+MHCII+ DC in MLN were found among all pretreatment groups (Figure 3A). The co-encapsulated BLG-Pep+CpG/NP recipients

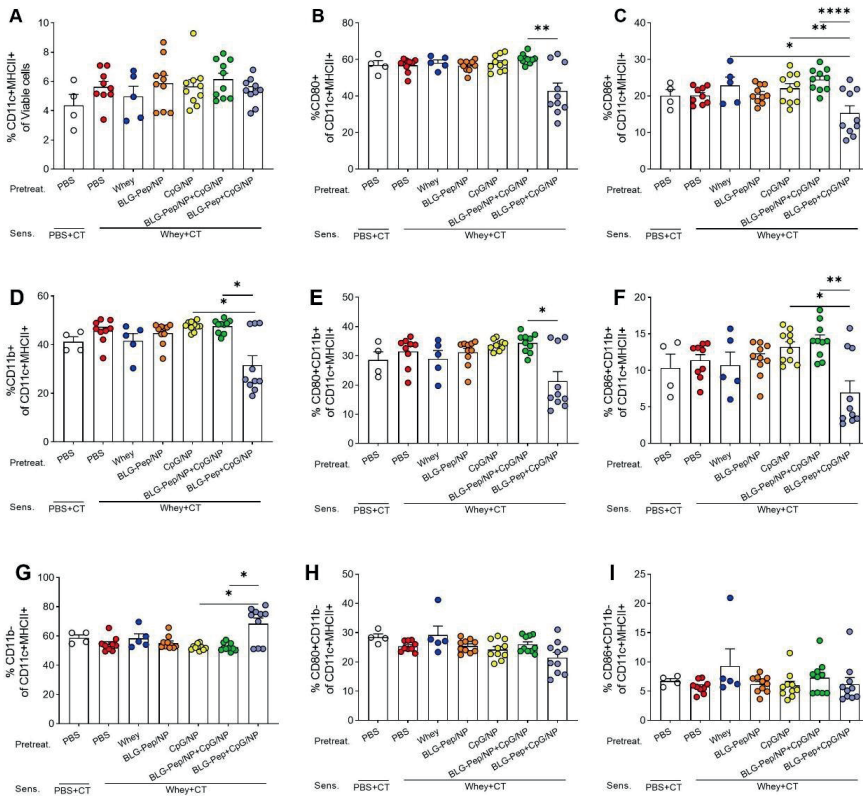


Figure 3. Surface activation markers expression on dendritic cells in mesenteric lymph nodes (MLN). Eighteen hours after oral whey-sensitization, MLN cells were isolated and analyzed using flow cytometry to determine the percentage of CD11c+MHCII+ DC (A) and CD11b+ (D) and CD11b- (G) DC subsets. Surface costimulatory molecules expression of CD80+ (B)(E)(H) and CD86+ (C)(F)(I) on CD11c+MHCII+ DC, CD11b+ and CD11b- DC subsets were determined respectively. Data are presented as mean ± SEM for n=9-10 per group except for the sham group, n=4 and whey-tolerant group, n=5. (A) is analyzed with one-way ANOVA for selected pairs after log transformation, followed by Bonferroni's *post hoc* test; (B) and (D-I) are analyzed with the Kruskal-Wallis non-parametric test, followed by Dunn's *post hoc* test for selected pairs; (C) is analyzed with one-way ANOVA for selected pairs after log transformation, followed by Bonferroni's *post hoc* test; **p*<0.05, ***p*<0.01; CT, Cholera toxin.

showed a lower percentage CD11b+ DC and higher percentage of CD11b- DC subsets compared to both the CpG/NP group and BLG-Pep/NP+CpG/NP group (Figure 3D and

G). The co-encapsulated BLG-Pep+CpG/NP pretreatment reduced the expression of costimulatory molecules CD80 and CD86 on DC and CD11b+ DC compared to BLG-Pep/NP+CpG/NP pretreatment, but not on CD11b- DC in MLN (Figure 3B, C, E, F, H and I). The gating strategy of the flow cytometry analysis for DC from MLN is shown in Supplemental Figure 8.

Co-encapsulated BLG-Pep+CpG/NP reduced percentages of PD-L1+ DC subsets in mesenteric lymph nodes but increased PD-L1+CD11b+ DC frequency in spleen

In MLN, co-encapsulated BLG-Pep+CpG/NP, but not the other pretreatments, significantly decreased surface expression of PD-L1+ on CD11c+MHCII+ DC (Figure 4A) as compared to the whey-sensitized group in CD11b- DC (Figure 4C), and only showed a decreasing tendency in CD11b+ DC subset ($p=0.0655$, Figure 4B). In spleen, however, co-encapsulated BLG-Pep+CpG/NP pretreatment upregulated expression of PD-L1 on CD11b+ DC subset (Figure 4E) and tended to enhance PD-L1 expression on CD11c+MHCII+ DC ($p=0.0617$, Figure 4D), but not on its CD11b- DC subset (Figure 4F), as compared to the BLG-Pep/NP plus CpG/NP group.

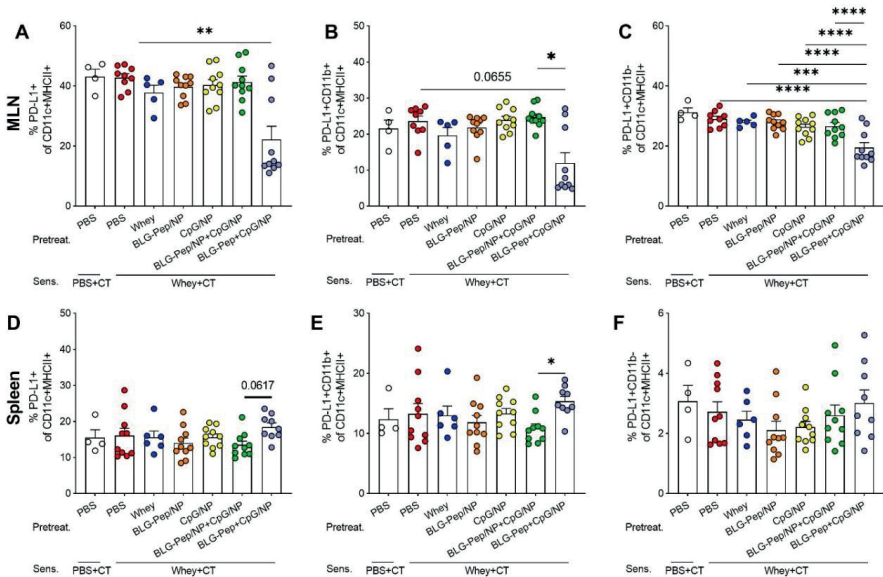


Figure 4. Expression of PD-L1 on dendritic cells from mesenteric lymph nodes (MLN) and spleen. Eighteen hours after the last oral challenge with whey, cells isolated from MLN and spleen were analyzed by flow cytometry for the frequencies of PD-L1+ on CD11c+MHCII+ DC (A) (D), PD-L1+CD11b+ (B) (E) and PD-L1+CD11b- (C) (F) DC subsets in MLN and spleen respectively. Data are presented as mean \pm SEM for n=8-10 per group except for the sham group, n=4 and whey-tolerant group, n=6. (A-B) and (D-F) are analyzed with the Kruskal-Wallis non-parametric test, followed

by Dunn's *post hoc* test for selected pairs; (C) is analyzed with one-way ANOVA for selected pairs after log transformation, followed by Bonferroni's *post hoc* test; * $p < 0.05$, ** $p < 0.01$; CT, Cholera toxin.

In splenocytes co-encapsulated BLG-Pep+CpG/NP lowered the percentage of Th2 cell while increasing ratios Treg/Th2 and Th1/Th2

The co-encapsulated BLG-Pep+CpG/NP pretreatment resulted in an increasing trend in CD25+FoxP3+ Treg percentage as compared to the BLG-Pep/NP+CpG/NP pretreated mice ($p=0.0518$, Figure 5A). The co-encapsulated BLG-Pep+CpG/NP pretreatment reduced the percentage of T1/ST2+ Th2 cells (Figure 5B) compared to the whey-sensitized group, but no difference was found on the frequencies of CXCR3+ Th1 (Figure 5C) and CD196+ Th17 subsets (Data not shown for Th17) in all pretreatment groups. Co-encapsulated BLG-Pep+CpG/NP increased ratios of Treg/Th2 and Th1/Th2 as compared to the whey-sensitized mice (Figure 5D and F), and tended to increase the Treg/Th1 ratio in BLG-Pep+CpG/NP recipients as compared to whey-tolerant mice ($p=0.0647$, Figure 5E). The gating strategy of the flow cytometry analysis for Th1, Th2 and Treg subsets from splenocytes is shown in Supplemental Figure 9.

Co-encapsulated BLG-Pep+CpG/NP decreased whey-restimulated IFN- γ and enhanced IL-10/IFN- γ ratio in splenocyte supernatants

CpG/NP pretreatment reduced whey-restimulated splenocytes release of IL-13 (Figure 5G), while BLG-Pep/NP+CpG/NP and co-encapsulated BLG-Pep+CpG/NP pretreatments lowered whey-restimulated splenocytes release of IFN- γ compared with the whey-sensitized mice (Figure 5H). Whey-sensitized mice showed higher whey-stimulated IL-17A and IL-10 production by splenocytes compared to sham mice (Figure 5I and J), which was prevented in the whey-tolerant group for IL-17A secretion (Figure 5I). Despite no statistical differences were found in IL-10 concentrations or in the ratio of IL-10/IL-13 (Figure 5K), BLG-Pep/NP+CpG/NP and co-encapsulated BLG-Pep+CpG/NP pretreatments significantly increased the ratio of IL-10/IFN- γ compared to whey-sensitized mice (Figure 5L). BLG-Pep+CpG/NP pretreatment also significantly increased the ratio of IL-10/IFN- γ compared to the BLG-Pep/NP+CpG/NP group and whey-tolerant group (Figure 5L). Supplemental Figure 5, 6 and 7 shown medium versus whey-stimulated cytokine responses and additional whey or BLG induced re-stimulation responses.

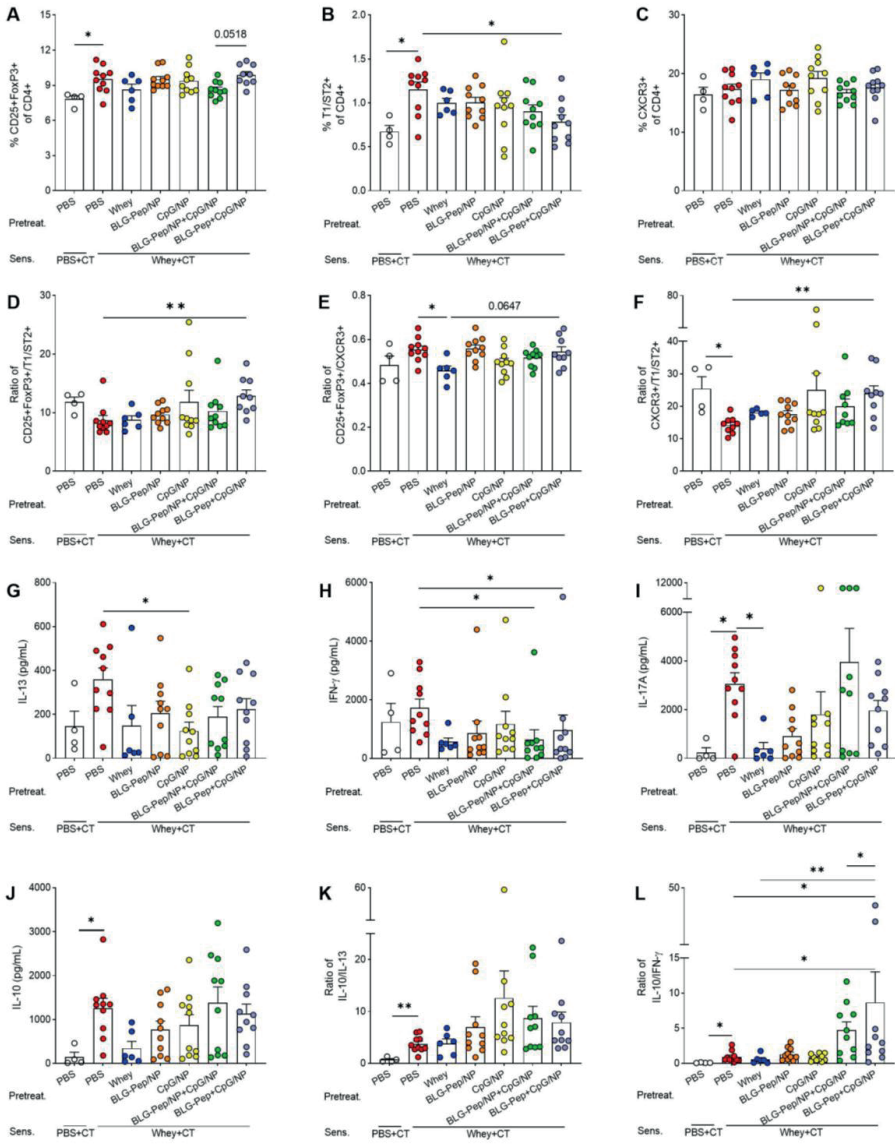


Figure 5. Splenic T-cell subsets and cytokines production of splenocytes upon *ex vivo* stimulation with whey for 5 days. Eighteen hours after the last oral challenge with whey, splenocytes were isolated and analyzed by flow cytometry for the percentages of T-cell subsets including Treg (A), Th2 (B), Th1 (C), ratio of Treg/Th2 (D), ratio of Treg/Th1 (E) and ratio of Th1/Th2 (F) respectively. Splenocytes were restimulated with whole whey protein for 5 days, Th2- (G), Th1- (H), Th17- (I), and Treg- (J) associated cytokines were measured in supernatants. Ratios of Treg-/Th2- associated (K) and Treg-/Th1-associated (L) cytokines were calculated. Data are presented as mean \pm SEM for n=9-10 per group except for the sham group, n=4 and whey-tolerant group, n=6. (A-C) and (E) are analyzed with one-way ANOVA for selected pairs, followed by Bonferroni's *post hoc* test; (D) and (F-K) are analyzed with the Kruskal-Wallis non-parametric test, followed by Dunn's *post hoc* test for selected pairs; (L) is analyzed with one-way ANOVA for selected pairs after log transformation, followed by Bonferroni's *post hoc* test; * $p < 0.05$, ** $p < 0.01$; CT, Cholera toxin.

Discussion

We hypothesized that CpG as an adjuvant can enforce the allergy preventive effect of a model selected BLG peptide co-encapsulated in PLGA (BLG-Pep/NP) under strict hygienic conditions. Previously, this selected BLG peptide (BLG-Pep) was shown to be recognized by a cow's milk specific human T-cell line *in vitro* and to inhibit acute allergic skin response to whey protein in mice pretreated with a relatively high dose [31] and at a lower dose when encapsulated in PLGA nanoparticles to optimize oral delivery [32]. In this study, 3-4-week-old female mice were chosen to investigate the oral tolerance induction in early life using pretreatment of BLG-peptide and CpG co-encapsulated PLGA NP before oral sensitization with whole whey protein. In the 3-4-week-old mice, microfold (M) cells have already reached adult levels, since this is achieved before 2-3 week of age. This will allow access of the PLGA nanoparticles to the Peyer's patch and gut draining mesenteric lymph nodes where nanoparticle uptake and peptide presentation by the DC can instruct T-cell development [41, 42]. Recruitment of T-cells to the neonatal mucosa [43, 44] and microbiome maturation [45] are pivotal for induction of Treg and thus establishment of oral tolerance [46]. To further enhance the allergy preventive effect, a strategy was developed to co-encapsulate BLG peptide (to instruct allergen specificity) together with CpG (as an immunomodulatory adjuvant) into PLGA nanoparticles.

BLG-Pep and CpG were separately dissolved in the water phase (PBS), and both were emulsified with PLGA solubilized in oil phase (dichloromethane) to form two water-in-oil emulsions. This was followed by combining these two water-in-oil emulsions and next via preparing the water-in-oil-in-water emulsion [47] in order to co-encapsulate BLG-Pep and CpG into the PLGA nanoparticles. BLG-Pep and CpG were co-encapsulated in ~250 nm size PLGA nanoparticles with encapsulation efficiencies for both compounds of about 40%. *In vitro*, the BLG-Pep+CpG/NP showed a burst release of about 20% of the CpG, and no burst release of BLG-Pep from the NP matrix, which might be attributed to the insufficient washing and/or diffusion from the microporous channels that were resulted from the freeze drying process [48, 49]. The sustained release of BLG-Pep+CpG/NP from PLGA NP demonstrates that a suitable formulation for *in vivo* evaluation was developed. Similar to many other drugs, there is a therapeutic dose window for CpG as an adjuvant, and toxicity was shown in mice that received a repetitive daily injection of CpG in a dose above 2.4 mg/kg [50]. In this study, a relative low dose of 3 µg encapsulated CpG per daily oral gavage was given to the mice for a

period of 6 days, which is a safe dosing scheme in terms of toxicity as reviewed [51]. PLGA is biodegradable and biocompatible polymer as approved by the US Food and Drug Administration (FDA) for vaccine and drug delivery [52, 53]. PLGA nanoparticles provide protection for the encapsulated BLG-peptide and CpG cargos [54] and facilitate cellular uptake by antigen-presenting cells [54].

As shown by previous studies, intestinal uptake and lymphatic transport of oral delivered nanoparticles are dependent on surface charge, particle size and dose of the administered nanoparticles [55-57]. The similar size and surface charge of the different PLGA NP suggest similar mucus penetration and cellular uptake of these nanoparticles after oral administration. Despite that, only the co-encapsulation gave the allergy preventive effect (*i.e.*, prevented acute allergic skin reactivity and rise in BLG-specific IgE) even compared to the cocktail of BLG-Pep/NP plus CpG/NP. Antigen-encapsulated PLGA nanoparticles can be internalized by DC into phagosomes via endocytosis [58], followed by endosomal degradation for the MHCII pathway [59]. On the other hand, TLR-9 and MHCII are also present in the endolysosomes of plasmacytoid DC and B-cells [21, 30]. Thus, simultaneous internalization and intracellular release of CpG and BLG-Pep from BLG-Pep+CpG/NP in the endolysosomes of DC may facilitate synergistic activation of TLR-9 and antigen-presentation via MHCII pathway in the same DC (see graphical abstract Figure 6).

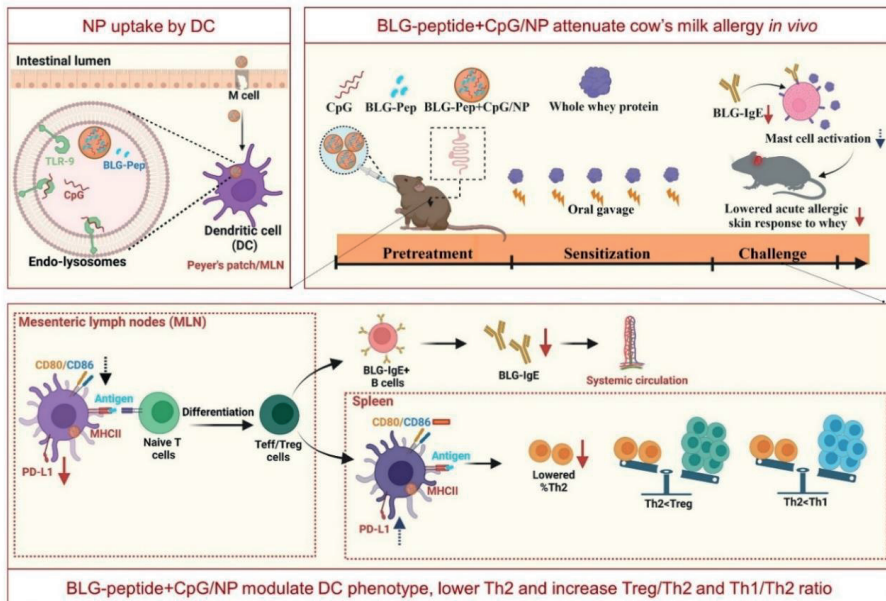


Figure 6. Graphical Abstract (Created with BioRender.com)

Oral pretreatment with a daily dosage of both antigen and adjuvant (160 µg BLG-Pep plus 3 µg CpG) for a short period (6 days) prevented skin reactivity and rise in serum BLG-specific IgE. Srivastava *et al.* [24] reported oral therapy using whole peanut extract encapsulated PLGA nanoparticles with surface conjugation of CpG, inhibited peanut allergic symptoms and facilitated peanut allergy outgrowth [24]. Our study differs from this study substantially in that we investigated the cow's milk allergy prevention effect using BLG-Pep (18-AA) and CpG co-encapsulated PLGA nanoparticles in a cow's milk allergy murine model kept in IVC housing. In this study, BLG-Pep+CpG/NP pretreatment significantly prevented rise in BLG-specific IgE levels, but did not lower whey- or BLG-specific IgG1 and IgG2a levels. Despite the role of allergen-specific IgG1 in allergic diseases remains elusive [60], it is likely that full inhibition of allergen-specific IgE and IgG for both BLG and whey requires additional whey epitopes. Here we used only one small BLG model peptide of 18-AA while BLG protein itself consist of 162-AA (18.4 kDa) and multiple epitopes [61]. Moreover, whole whey protein consists not only of BLG as allergen but also other allergenic proteins such as alpha-lactoglobulin [61]. Thus, in future studies, an additional BLG-peptide from another region in the BLG protein sequence and/or peptides of other whey-derived allergens may be supplemented to the current regime and co-encapsulated with CpG to generate full tolerance for whole whey protein.

DC as antigen presenting cells, capture and recognize microorganisms via pathogen-associated-molecular-patterns (PAMPs) by Toll-Like Receptors (TLRs) [62], mediating tolerance [63] or activation of T-cell responses [64] to various antigens. Co-encapsulated BLG-Pep+CpG/NP recipients showed a lower frequency of the Th2/Th17 immune polarizing CD11b+ DC subset in the MLN [65], and a reduced expression of costimulatory molecules CD80/CD86 on CD11c+MHCII+ DC compared to the BLG-Pep/NP plus CpG/NP group, suggesting a more tolerogenic DC phenotype and consequent constraint of Th2 immunity [66]. Programmed cell death ligand 1 (PD-L1) is expressed on non-lymphoid and lymphoid cells, including resting B-cells, T-cells, macrophages and DC, and regulates immune responses in secondary lymphoid and target organs [67]. In particular, expression of PD-L1 on DC was reported essential for inducing IL-10 secreting T-cells *in vitro* [68], and required for generation of adaptive Treg subsets both *in vitro* and *in vivo* [69]. Despite the diminished frequency of PD-L1+ DC in the MLN of the BLG-Pep+CpG/NP recipients, the simultaneous decreased surface

expression of co-stimulatory molecules CD80/CD86 was previously shown to enforce a tolerogenic phenotype with a reduced maturation status [70].

Given the short lifespan of DC for less than 9 days [71], we speculate that the general DC phenotype may have undergone epigenetic changes and form immune memory responses via a process known as trained immunity resulting in a more tolerogenic DC phenotype [72, 73]. Even though BLG-Pep+CpG/NP pretreatment reduced PD-L1 expression in the MLN compared to the whey-sensitized mice and the BLG-Pep/NP plus CpG/NP recipients, it enhanced the PD-L1 expression on splenic CD11b+ DC as compared to BLG-Pep/NP plus CpG/NP recipients. The latter was associated with an increase in the percentage of CD25+FoxP3+ Treg cells compared to the BLG-Pep/NP plus CpG/NP group. We hypothesize BLG-Pep+CpG/NP pretreatment to have instructed development of Treg that reside in the spleen, upon reactivation these cells may modify the phenotype of local DC resulting in enhanced PD-L1 expression actively contributing to systemic Treg function and a tolerogenic microenvironment [74-77]. Alternatively, the BLG-Pep+CpG/NP pretreatment may have resulted in upregulation of PD-L1 on intestinal DC upon whey challenge, which then may have migrated via the MLN to the spleen for antigen presentation to naive CD4+ T-cells [78, 79], inducing development of regulatory T-cell and memory T-cells [74-77].

Indeed, a high dose CpG (50 µg) was reported to enhance expression of indoleamine 2,3-dioxygenase (IDO) in the plasmacytoid DC [80] after ligation to the Toll-like Receptor-9 in the endolysosomes, and hence activate a suppressor phenotype of Treg cells for tolerance induction [81]. Therefore, we hypothesize the PLGA nanoparticles co-encapsulating only 3 µg CpG and 160 µg BLG-Pep might generate a tolerogenic microenvironment preventing allergy development for whole whey protein via supporting regulatory responses. The provided dose of CpG was relatively low and already effective. The dose-dependency of the BLG-Pep and CpG co-encapsulated PLGA NP for allergy prevention and antigen-specific tolerance induction via oral delivery and possible uptake by plasmacytoid DC warrants further investigation.

As reported, CD11b+ DCs initiate and maintain Th2 immunity towards allergens [82]. However, BLG-Pep+CpG/NP pretreatment upregulated PD-L1 expression on these conventional CD11b+ splenic DC compared to BLG-Pep/NP plus CpG/NP recipients, which might also have promoted Treg development and reduced Th2 immunity upon

re-exposure to whey allergens during sensitization and challenge stages [83, 84]. Indeed, BLG-Pep+CpG/NP pretreatment induced a significant diminished frequency of T1/ST2+ Th2 cells, and higher splenic Treg/Th2, Th1/Th2 and IL-10/IFN- γ ratios compared to the whey-sensitized mice, which may favor a tolerogenic outcome (see graphical abstract Figure 6). The observed constraint of Th2 cells development might be attributed to the immunomodulatory effect from the co-encapsulated Type B CpG. As reported previously [85], systemic administered CpG reduces Th2 associated cytokines production without affecting Th1 cytokines in a murine asthma model. However, in the current study despite the decreased Th2 frequency in the CpG and peptide co-encapsulated group, upon BLG restimulation of the splenocytes the cytokine release was not silenced which was the case in the whey-tolerant group (Supplemental Figure 7). Hence, pretreatment with a single 18-AA BLG peptide may not be sufficient in overruling the immunogenic properties of the full immunogenic T-cell epitope repertoire of the BLG fraction in whey protein.

Collectively, these observations provide evidence that BLG-Pep+CpG/NP pretreatment changes the DC phenotype, reduces Th2 development and drives towards a Th1 and Treg microenvironment, which might contribute to reducing allergen-specific CMA development.

Acknowledgements: ML is financially supported by China Scholarship Council (CSC), grant number 201707720004 and receive additional bench fee funding is supplied by Danone Nutricia Research B.V., Utrecht, the Netherlands.

Supporting Information

Supporting Data

Preparation and characterization of BLG-peptide and/or CpG encapsulated PLGA nanoparticles

Nanoparticles were prepared with PLGA (lactide/glycolide molar ratio 50:50, 0.32-0.48 dl/g; PURASORB PDLG 5004A, Corbion, the Netherlands) using a double emulsion solvent evaporation method [86]. Briefly, 160 mg PLGA was weighed and dissolved in 4 mL dichloromethane (DCM, Biosolve BV, Valkenswaard, the Netherlands) overnight at room temperature. Next, 1) 3.2 mg BLG-Pep in 400 μ L sterile PBS and 65 μ g CpG in 50 μ L PBS for BLG-Pep+CpG/NP or 2) 400 μ L PBS and 200 μ g CpG in 50 μ L PBS for CpG/NP or 3) 400 μ L PBS and 50 μ L PBS for Empty NP, were added dropwise into 3 mL and 1 mL PLGA-solutions, respectively, and sonicated using a Sonifier S-450A (3 mm, Branson Ultrasonics B.V., Soest, the Netherlands) at 20% amplitude for 0.5 min on ice bath. The obtained two water-in-oil emulsions were combined and further sonicated (at 20% amplitude for 0.5 min on ice bath) to yield one single water-in-oil-emulsion. Subsequently, the obtained water-in oil-emulsion was added dropwise into 40 mL external aqueous phase, containing 3 w/v % polyvinyl alcohol (87-90% hydrolyzed, Mw 3,000-70,000 Da, Sigma-Aldrich, Zwijndrecht, the Netherlands) and 0.9 w/v % sodium chloride (NaCl, Sigma-Aldrich), and the obtained mixture was sonicated at 20% amplitude for 1 min on ice bath to yield the final water-in-oil-in-water emulsion. Finally, the formed emulsion was subjected to agitation for 3 h at room temperature to evaporate DCM and to obtain hardened PLGA NPs. The nanoparticle suspension was centrifuged at 20,000 \times g for 30 min at 4°C and the obtained pellet was washed with 20 mL nuclease free water (not DEPC-Treated, Invitrogen, Life Technologies, Carlsbad, USA) twice prior to lyophilization using a freeze dryer (Buchi Lyovapor L-200, Hendrik-Ido-Ambacht, the Netherlands).

Next, 2 μ L of the prepared NP suspensions was added into 998 μ L milliQ water for characterization of nanoparticle size and polydispersity index (PDI) with Zetasizer Nano S (Malvern Instruments, Malvern, UK), or transferred into 998 μ L 10 mM HEPES buffer (pH7.4) for characterization of surface charge of the NP formulations with Zetasizer Nano-Z (Malvern Instruments, Malvern, UK) respectively.

BLG-Pep alone were encapsulated in PLGA nanoparticles as published previously [12, 32]. Encapsulation efficiency of BLG-peptide in the BLG-Pep/NP was measured with a direct method using UPLC as published previously [32]. Encapsulation efficiency of CpG was quantified with a direct method. In detail, around 10-15 mg lyophilized CpG/NP or BLG-Pep+CpG/NP were accurately weighed and hydrolyzed in 450 μ L 0.2N NaOH solution per 5 mg NP overnight (for 17 h) at room temperature under agitation until the PLGA polymers were fully hydrolyzed. Next, 22.5 μ L 20 \times Tris-EDTA (ThermoFisher) buffer per 5 mg NP was added into the hydrolysis solution to stop the hydrolysis and additional volume of 1 \times Tris-EDTA buffer was added to reach 10 mg/mL NP-equivalent of the hydrolysis solution prior to the quantification assay for CpG using Quant-iT™ OliGreen™ ssDNA Assay Kit (ThermoFisher) according to the manufacturer's protocol.

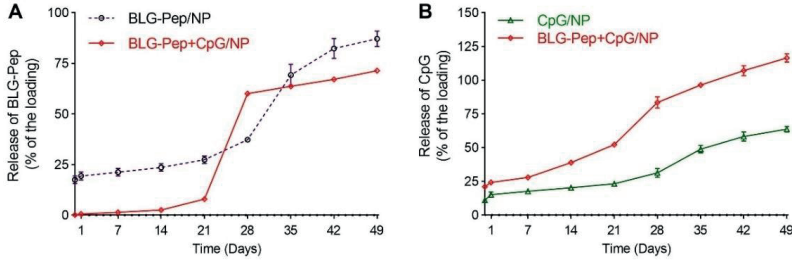
***In vitro* release of BLG-Pep and CpG from PLGA nanoparticles**

The release of BLG-Pep from the PLGA NP from the animal study was determined as follows. Around 10 mg of freeze dried BLG-Pep/NP, CpG/NP and 20 mg BLG-Pep+CpG/NP were accurately weighed in triplicate, prior to suspension in 500 μ L phosphate saline buffer (PBS, pH7.4)-0.06 w/v % sodium azide (NaN₃, Sigma-Aldrich) (release buffer) and incubation at 37°C on a nutating mixer. At different time points (at 30 min, day 1, 7, 14, 21, 28, 35, 42 and 49 time points respectively), samples were centrifuged at 20,000 \times g at 4°C and 400 μ L supernatant was withdrawn. Next, 400 μ L of fresh release buffer was added, the pelleted NPs were resuspended and the samples were further incubated at 37°C on the nutating mixer.

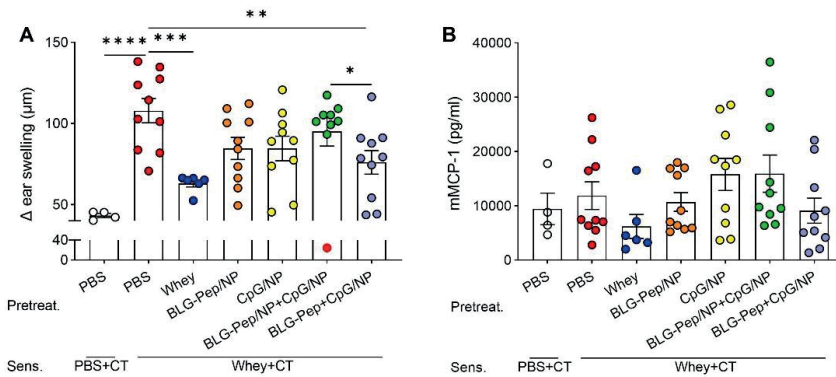
BLG-Peptide (BLG-Pep) and CpG were measured in the different release samples using established UPLC method as described previously [32] and Quant-iT™ OliGreen™ ssDNA Assay Kit (ThermoFisher) according to the manufacturer's protocol, respectively. The percentage of released peptide cargo and CpG were calculated based on the encapsulated amount as described previously [32].

Supporting Figures and Tables

Supporting Figures

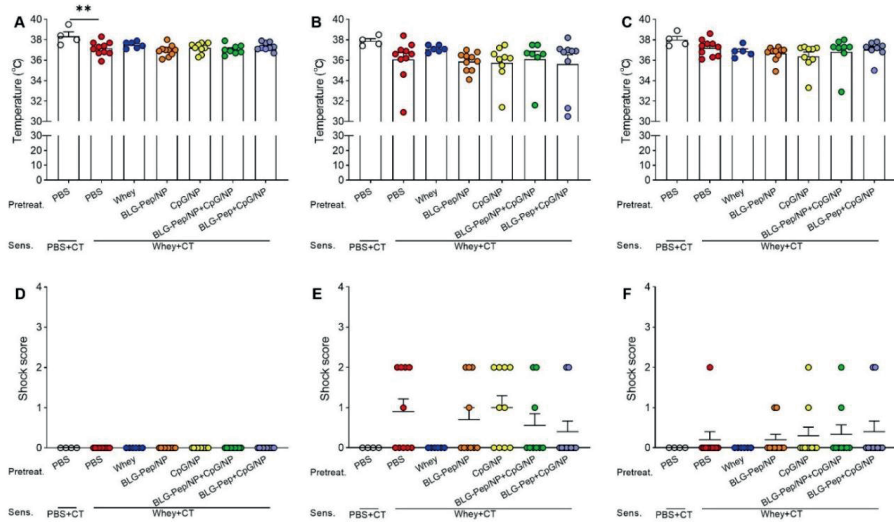


Supplemental Figure 1. *In vitro* release of β -lactoglobulin derived peptide (namely BLG-Pep) (A) and CpG (B) from PLGA NPs used for the animal study in PBS (pH7.4) at 37°C. The release samples were taken at 30 min, day 1, 7, 14, 21, 28, 35, 42 and 49 time points respectively. Data are presented as mean \pm SD, n=3 per formulation.

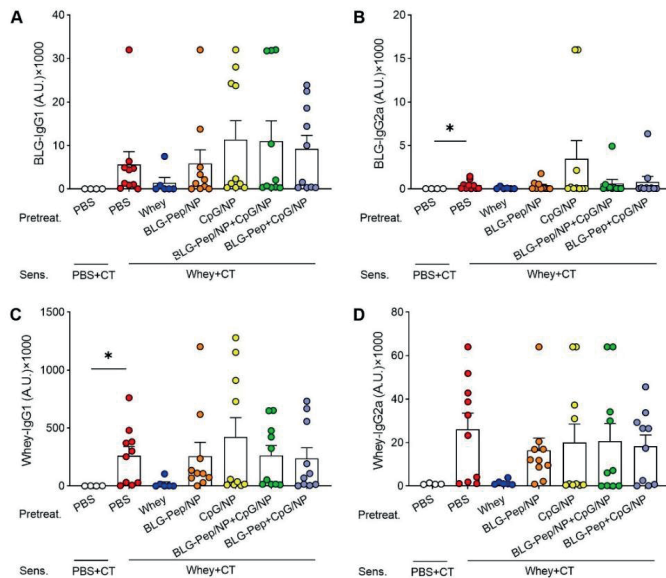


Supplemental Figure 2. Acute allergic skin response and serum murine mucosal mast cell protease-1 (mMCP-1). Five days after last sensitization, mice were intradermally challenged in the ear pinnae with 10 μ g whey and the acute allergic skin response was measured 60 min (A) afterwards. In addition, mMCP-1 (B) was quantified in the collected 18 h after last oral challenge with whey in mice from all groups of the animal study. Data are presented as mean \pm SEM, n=9-10 per group except for the sham group, n=4 and whey-tolerant group, n=6. (A) is presented with Y axis formatted in two segments to properly show the relevant part of the window of effect. (A) is analyzed by one-way ANOVA, followed by Bonferroni's *post hoc* test for selected pairs; The outlier (in red) in the BLG-Pep/NP+CpG/NP group is excluded in (A) from statistics; (B) is analyzed with Kruskal-Wallis' non-parametric test, followed by Dunn's *post hoc* test for selected pairs. * p <0.05, ** p <0.01, *** p <0.001, **** p <0.0001; BLG, β -lactoglobulin; CT, Cholera toxin.

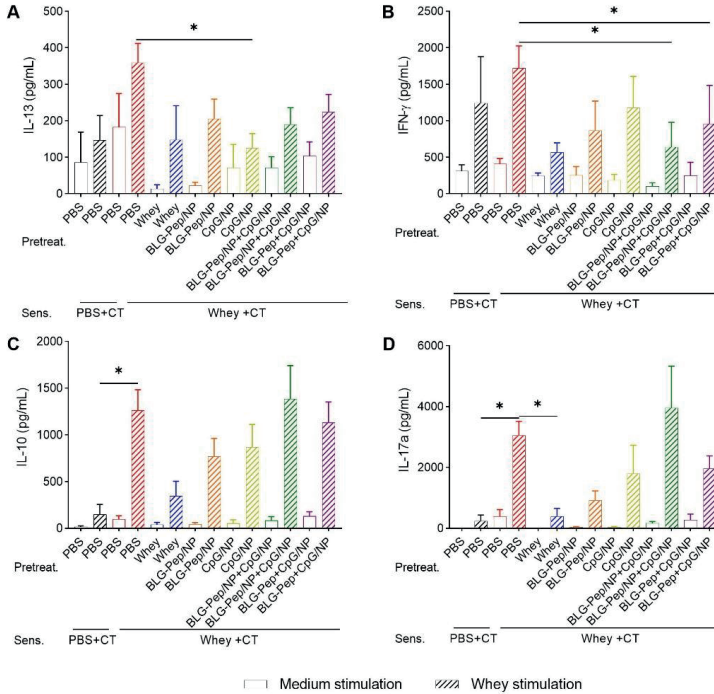
Oral pretreatment with BLG-peptide and CpG co-encapsulated in PLGA NP attenuates CMA development in mice



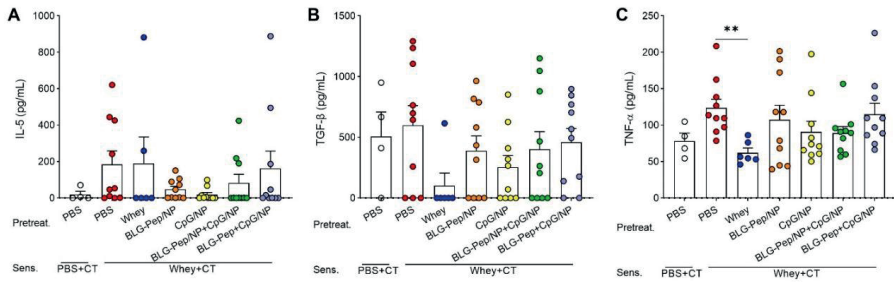
Supplemental Figure 3. Anaphylactic shock score and body temperature after intradermal challenge with whole whey protein. Body temperature and anaphylactic shock score were recorded at 0 h (A) (D), 30 min (B) (E) and 60 min (C) (F) after intradermal whey challenge in mice from all groups of the animal study. Data are presented as mean \pm SEM for n=8-10 per group except for the sham group, n=4 and whey-tolerant group, n=5-6. (A-C) are presented with Y axis formatted in two segments to properly show the relevant window for shock induced body temperature changes. (A) is analyzed with one-way ANOVA for selected pairs after log transformation, followed by Bonferroni's *post hoc* test; (B-E) are analyzed with the Kruskal-Wallis non-parametric test, followed by Dunn's *post hoc* test for selected pairs; ** $p < 0.01$; BLG, β -lactoglobulin; CT, Cholera toxin.



Supplemental Figure 4. BLG- and whey-specific serum immunoglobulin levels. BLG- (A-B) and whey-specific (C-D) IgG1 and IgG2a levels are measured in serum, which were collected 18 h after last oral challenge with whey in mice from all groups of the animal study. Data are presented as mean \pm SEM for n=9-10 per group except for the sham group, n=4 and whey-tolerant group, n=6. (A-D) are analyzed with the Kruskal-Wallis non-parametric test, followed by Dunn's *post hoc* test for selected pairs; * $p < 0.05$; BLG, β -lactoglobulin; CT, Cholera toxin.

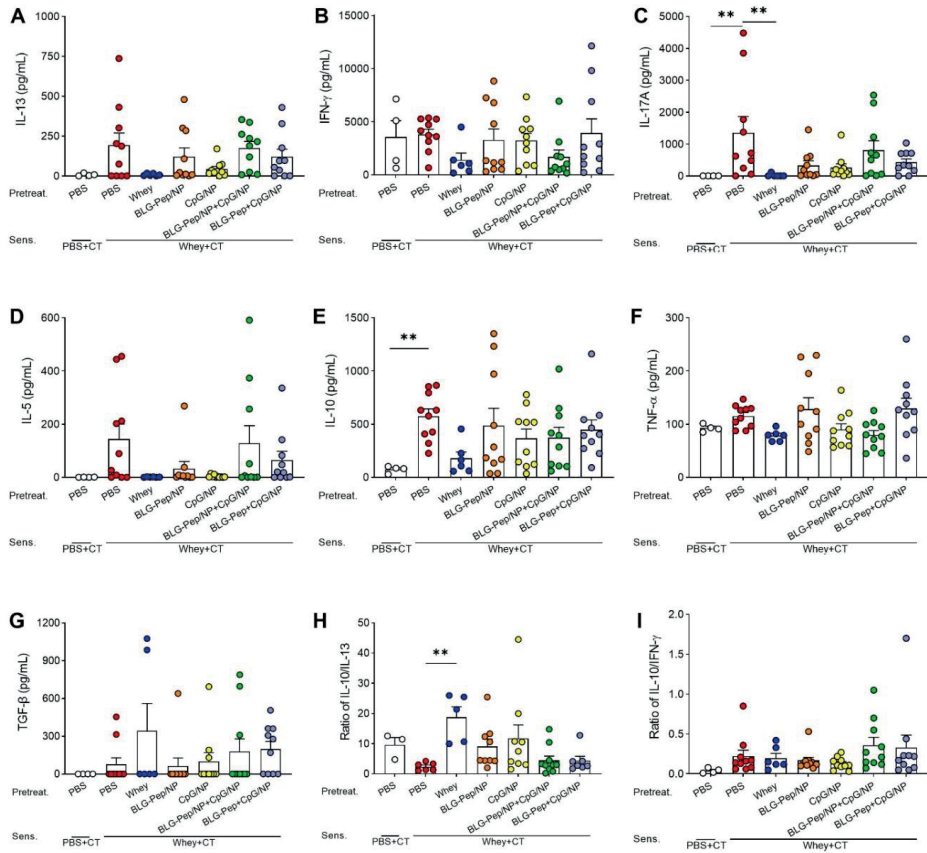


Supplemental Figure 5. Cytokines production of splenocytes after *ex vivo* stimulation with medium or whole whey protein for 5 days. Th2- (A), Th1- (B), Treg- (C), and Th17- (D) associated cytokines were measured in supernatants. Data are presented as mean \pm SEM for n=9-10 per group except for the sham group, n=4 and whey-tolerant group, n=6. (A-D) are analyzed with the Kruskal-Wallis non-parametric test only for whey stimulation, followed by Dunn's *post hoc* test for selected pairs; * p <0.05; CT, Cholera toxin.



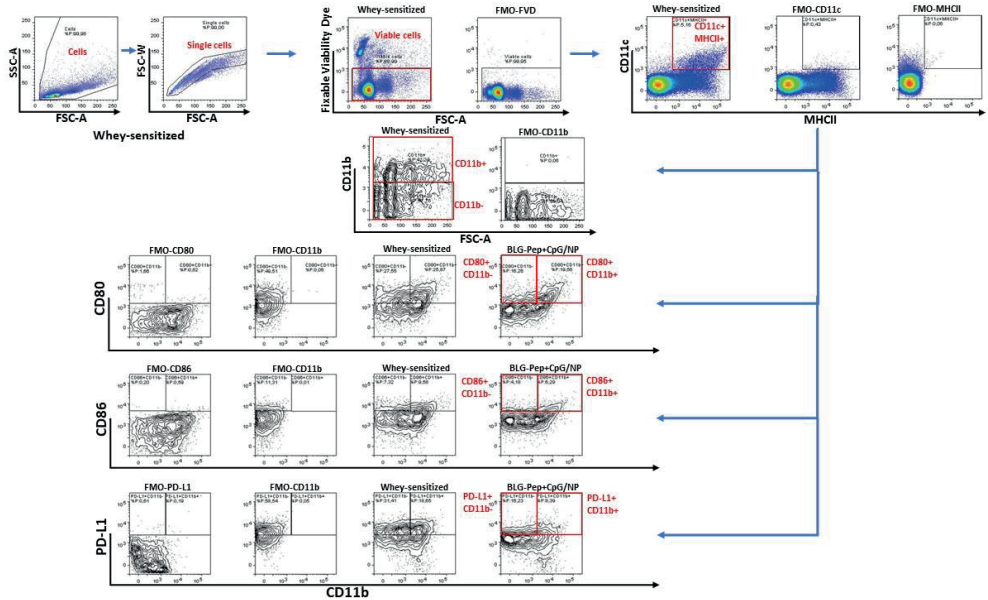
Supplemental Figure 6. Cytokines production of splenocytes after *ex vivo* stimulation with whole whey protein for 5 days. Splenocytes were restimulated with medium or whole whey protein for 5 days, the medium stimulated cytokine release are subtracted. Th2- (A), Treg- (B), pro-inflammatory- (C) associated cytokines were measured in supernatants. Data are presented as mean \pm SEM for n=9-10 per group except for the sham group, n=4 and whey-tolerant group, n=6. (A), (B), (C) are analyzed with the Kruskal-Wallis non-parametric test, followed by Dunn's *post hoc* test for selected pairs; ** p <0.01; CT, Cholera toxin.

Oral pretreatment with BLG-peptide and CpG co-encapsulated in PLGA NP attenuates CMA development in mice

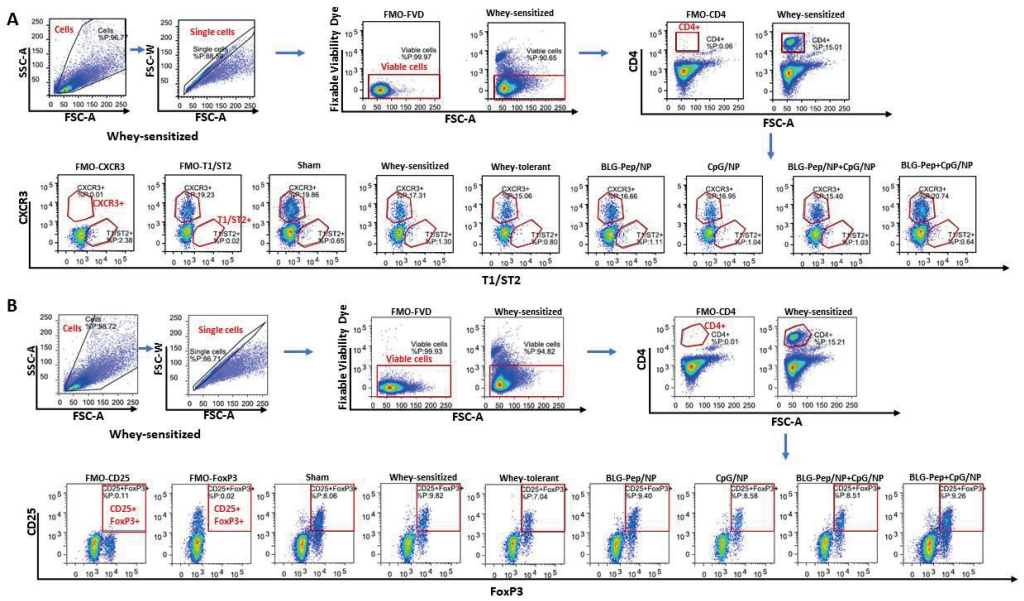


Supplemental Figure 7. Cytokines production of splenocytes after *ex vivo* stimulation with β -lactoglobulin for 5 days. Splenocytes were restimulated with medium or β -lactoglobulin for 5 days, the medium stimulated cytokine release are subtracted. Th2- (A and D), Th1- (B), Th17- (C), Treg- (E and G), proinflammatory (F) associated cytokines were measured in supernatants. Ratios of Treg-/Th2- associated (H) and Treg-/Th1-associated (I) cytokines were calculated. Data are presented as mean \pm SEM for n=9-10 per group except for the sham group, n=4 and whey-tolerant group, n=6. (A-I) are analyzed with the Kruskal-Wallis non-parametric test, followed by Dunn's *post hoc* test for selected pairs; * p <0.05, ** p <0.01; CT, Cholera toxin.

CHAPTER THREE



Supplemental Figure 8. Gating strategy of the flow cytometry analysis of DC from mesenteric lymph nodes (MLN).



Supplemental Figure 9. Gating strategy of the flow cytometry analysis of T helper 1 and 2 (Th1 and Th2) subsets (A) and regulatory T cells (Treg) (B) in splenocytes.

Supporting Tables

Supplemental Table 1. Flow cytometry staining of T helper 1 (Th1) and T helper 2 (Th2) subsets from spleen

Antibodies	Supplier	Cat. no.	Dilution	Buffer
CD4-BV510	BioLegend	100553	1:160	1% Bovine Serum Albumin (BSA) ¹ -Dulbecco's phosphate-buffered saline (PBS) ²
T1/ST2-FITC	mdbioproducts	101001F	1:200	1% BSA-PBS
CXCR3-PE	ThermoFisher	12-1831	1:100	1% BSA-PBS

Supplemental Table 2. Flow cytometry staining of regulatory T-cells (Treg) from spleen

Antibodies	Supplier	Cat. no.	Dilution	Buffer
CD4-BV510	Biolegend	100553	1:160	1% Bovine Serum Albumin (BSA) ¹ -Dulbecco's phosphate-buffered saline (PBS) ²
CD25-PerCP/Cy5.5	ThermoFisher	45-0251	1:1280	1% BSA-PBS
FoxP3-FITC	ThermoFisher	11-5773	1:100	Permeabilization buffer ³

Supplemental Table 3. Flow cytometry staining of surface activation markers staining of dendritic cells from spleen and mesenteric lymph node

Antibodies	Supplier	Cat. no.	Dilution	Buffer
MHCII-PE	ThermoFisher	12-5322	1:640	1% Bovine Serum Albumin (BSA) ¹ -PBS ²
CD11c-FITC	ThermoFisher	11-0114	1:3200	1% BSA-PBS
CD11b-PE/Cy7	ThermoFisher	25-0112	1:2580	1% BSA-PBS
CD80-BV421	BioLegend	104726	1:160	1% BSA-PBS
CD86-BV510	BioLegend	105040	1:320	1% BSA-PBS
PD-L1-PerCP/eFluor710	ThermoFisher	46-5982	1:1000	1% BSA-PBS

¹ Bovine Serum Albumin (BSA) was purchased from Sigma-Aldrich.

² Dulbecco's phosphate-buffered saline (PBS) was purchased from Sigma-Aldrich.

³ Permeabilization buffer was prepared using the FoxP3/Transcription Factor Staining Buffer Set (ThermoFisher) according to the protocol provided by the supplier.

References

- [1] A.A. Schoemaker, A.B. Sprikkelman, K.E. Grimshaw, G. Roberts, L. Grabenhenrich, L. Rosenfeld, S. Siegert, R. Dubakiene, O. Rudzveciene, M. Reche, A. Fiandor, N.G. Papadopoulos, A. Malamitsi-Puchner, A. Fiocchi, L. Dahdah, S.T. Sigurdardottir, M. Clausen, A. Stanczyk-Przyluska, K. Zeman, E.N. Mills, D. McBride, T. Keil, K. Beyer, Incidence and natural history of challenge-proven cow's milk allergy in European children--EuroPrevall birth cohort, *Allergy*, 70 (2015) 963-972.
- [2] G. Du Toit, G. Roberts, P.H. Sayre, H.T. Bahnson, S. Radulovic, A.F. Santos, H.A. Brough, D. Phippard, M. Basting, M. Feeney, V. Turcanu, M.L. Sever, M. Gomez Lorenzo, M. Plaut, G. Lack, L.S. Team, Randomized trial of peanut consumption in infants at risk for peanut allergy, *N Engl J Med*, 372 (2015) 803-813.
- [3] J.J. Koplin, N.J. Osborne, M. Wake, P.E. Martin, L.C. Gurrin, M.N. Robinson, D. Tey, M. Slaa, L. Thiele, L. Miles, D. Anderson, T. Tan, T.D. Dang, D.J. Hill, A.J. Lowe, M.C. Matheson, A.L. Ponsonby, M.L. Tang, S.C. Dharmage, K.J. Allen, Can early introduction of egg prevent egg allergy in infants? A population-based study, *J Allergy Clin Immunol*, 126 (2010) 807-813.
- [4] M.R. Perkin, K. Logan, T. Marrs, S. Radulovic, J. Craven, C. Flohr, G. Lack, E.A.T.S. Team, Enquiring About Tolerance (EAT) study: Feasibility of an early allergenic food introduction regimen, *J Allergy Clin Immunol*, 137 (2016) 1477-1486 e1478.
- [5] Y. Katz, N. Rajuan, M.R. Goldberg, E. Eisenberg, E. Heyman, A. Cohen, M. Leshno, Early exposure to cow's milk protein is protective against IgE-mediated cow's milk protein allergy, *J Allergy Clin Immunol*, 126 (2010) 77-82 e71.
- [6] R.L. Peters, J.J. Koplin, S.C. Dharmage, M.L.K. Tang, V.L. McWilliam, L.C. Gurrin, M.R. Neeland, A.J. Lowe, A.L. Ponsonby, K.J. Allen, Early Exposure to Cow's Milk Protein Is Associated with a Reduced Risk of Cow's Milk Allergic Outcomes, *J Allergy Clin Immunol Pract*, 7 (2019) 462-470 e461.
- [7] S. Halken, A. Muraro, D. de Silva, E. Khaleva, E. Angier, S. Arasi, H. Arshad, H.T. Bahnson, K. Beyer, R. Boyle, G. du Toit, M. Ebisawa, P. Eigenmann, K. Grimshaw, A. Hoest, C. Jones, G. Lack, K. Nadeau, L. O'Mahony, H. Szajewska, C. Venter, V. Verhasselt, G.W.K. Wong, G. Roberts, A. European Academy of, A. Clinical Immunology Food, G. Anaphylaxis Guidelines, EAACI guideline: Preventing the development of food allergy in infants and young children (2020 update), *Pediatr Allergy Immunol*, 32 (2021) 843-858.
- [8] G. Lack, Epidemiologic risks for food allergy, *J Allergy Clin Immunol*, 121 (2008) 1331-1336.
- [9] L.A. Meulenbroek, B.C. van Esch, G.A. Hofman, C.F. den Hartog Jager, A.J. Nauta, L.E. Willemsen, C.A. Bruijnzeel-Koomen, J. Garssen, E. van Hoffen, L.M. Knippels, Oral treatment with beta-lactoglobulin peptides prevents clinical symptoms in a mouse model for cow's milk allergy, *Pediatr Allergy Immunol*, 24 (2013) 656-664.
- [10] K.L. Bogh, V. Barkholt, C.B. Madsen, The sensitising capacity of intact beta-lactoglobulin is reduced by co-administration with digested beta-lactoglobulin, *Int Arch Allergy Immunol*, 161 (2013) 21-36.
- [11] A.I. Kostadinova, A. Pablos-Tanarro, M.A.P. Diks, B. van Esch, J. Garssen, L.M.J. Knippels, L.E.M. Willemsen, Dietary Intervention with beta-Lactoglobulin-Derived Peptides and a Specific Mixture of Fructo-Oligosaccharides and Bifidobacterium breve M-16V Facilitates the Prevention of Whey-Induced Allergy in Mice by Supporting a Tolerance-Prone Immune Environment, *Front Immunol*, 8 (2017) 1303.
- [12] M. Liu, S. Thijssen, C.F. van Nostrum, W.E. Hennink, J. Garssen, L.E.M. Willemsen, Inhibition of cow's milk allergy development in mice by oral delivery of beta-lactoglobulin-derived peptides loaded PLGA nanoparticles is associated with systemic whey-specific immune silencing, *Clin Exp Allergy*, 52 (2022) 137-148.
- [13] A.M. Mowat, To respond or not to respond - a personal perspective of intestinal tolerance, *Nat Rev Immunol*, 18 (2018) 405-415.
- [14] A.M. Mowat, Anatomical basis of tolerance and immunity to intestinal antigens, *Nat Rev Immunol*, 3 (2003) 331-341.
- [15] I. Scholl, A. Weissenbock, E. Forster-Waldl, E. Untersmayr, F. Walter, M. Willheim, G. Boltz-Nitulescu, O. Scheiner, F. Gabor, E. Jensen-Jarolim, Allergen-loaded biodegradable poly(D,L-lactic-co-glycolic) acid nanoparticles down-regulate an ongoing Th2 response in the BALB/c mouse model, *Clin Exp Allergy*, 34 (2004) 315-321.
- [16] F. Walter, I. Scholl, E. Untersmayr, A. Ellinger, G. Boltz-Nitulescu, O. Scheiner, F. Gabor, E. Jensen-Jarolim, Functionalisation of allergen-loaded microspheres with wheat germ agglutinin for targeting enterocytes, *Biochem Biophys Res Commun*, 315 (2004) 281-287.

- [17] F. Roth-Walter, I. Scholl, E. Untersmayr, A. Ellinger, G. Boltz-Nitulescu, O. Scheiner, F. Gabor, E. Jensen-Jarolim, Mucosal targeting of allergen-loaded microspheres by Aleuria aurantia lectin, *Vaccine*, 23 (2005) 2703-2710.
- [18] F. Roth-Walter, I. Scholl, E. Untersmayr, R. Fuchs, G. Boltz-Nitulescu, A. Weissenbock, O. Scheiner, F. Gabor, E. Jensen-Jarolim, M cell targeting with Aleuria aurantia lectin as a novel approach for oral allergen immunotherapy, *J Allergy Clin Immunol*, 114 (2004) 1362-1368.
- [19] T. Gensollen, R.S. Blumberg, Correlation between early-life regulation of the immune system by microbiota and allergy development, *J Allergy Clin Immunol*, 139 (2017) 1084-1091.
- [20] J.L. Round, S.K. Mazmanian, The gut microbiota shapes intestinal immune responses during health and disease, *Nat Rev Immunol*, 9 (2009) 313-323.
- [21] A.M. Krieg, CpG motifs in bacterial DNA and their immune effects, *Annu Rev Immunol*, 20 (2002) 709-760.
- [22] K. Atarashi, T. Tanoue, K. Oshima, W. Suda, Y. Nagano, H. Nishikawa, S. Fukuda, T. Saito, S. Narushima, K. Hase, S. Kim, J.V. Fritz, P. Wilmes, S. Ueha, K. Matsushima, H. Ohno, B. Olle, S. Sakaguchi, T. Taniguchi, H. Morita, M. Hattori, K. Honda, Treg induction by a rationally selected mixture of Clostridia strains from the human microbiota, *Nature*, 500 (2013) 232-236.
- [23] S. de Kivit, E. van Hoffen, N. Korthagen, J. Garssen, L.E. Willemsen, Apical TLR ligation of intestinal epithelial cells drives a Th1-polarized regulatory or inflammatory type effector response in vitro, *Immunobiology*, 216 (2011) 518-527.
- [24] K.D. Srivastava, A. Siefert, T.M. Fahmy, M.J. Caplan, X.M. Li, H.A. Sampson, Investigation of peanut oral immunotherapy with CpG/peanut nanoparticles in a murine model of peanut allergy, *J Allergy Clin Immunol*, 138 (2016) 536-543 e534.
- [25] I. Hanski, L. von Hertzen, N. Fyhrquist, K. Koskinen, K. Torppa, T. Laatikainen, P. Karisola, P. Auvinen, L. Paulin, M.J. Makela, E. Vartiainen, T.U. Kosunen, H. Alenius, T. Haahela, Environmental biodiversity, human microbiota, and allergy are interrelated, *Proc Natl Acad Sci U S A*, 109 (2012) 8334-8339.
- [26] A.T. Stefkra, T. Feehley, P. Tripathi, J. Qiu, K. McCoy, S.K. Mazmanian, M.Y. Tjota, G.Y. Seo, S. Cao, B.R. Theriault, D.A. Antonopoulos, L. Zhou, E.B. Chang, Y.X. Fu, C.R. Nagler, Commensal bacteria protect against food allergen sensitization, *Proc Natl Acad Sci U S A*, 111 (2014) 13145-13150.
- [27] R. Lundberg, M.I. Bahl, T.R. Licht, M.F. Toft, A.K. Hansen, Microbiota composition of simultaneously colonized mice housed under either a gnotobiotic isolator or individually ventilated cage regime, *Sci Rep*, 7 (2017) 42245.
- [28] S.H. Kang, S.J. Hong, Y.K. Lee, S. Cho, Oral Vaccine Delivery for Intestinal Immunity-Biological Basis, Barriers, Delivery System, and M Cell Targeting, *Polymers (Basel)*, 10 (2018) 948.
- [29] S.D. Jazayeri, H.X. Lim, K. Shamel, S.K. Yeap, C.L. Poh, Nano and Microparticles as Potential Oral Vaccine Carriers and Adjuvants Against Infectious Diseases, *Front Pharmacol*, 12 (2021) 682286.
- [30] Y. Krishnamachari, A.K. Salem, Innovative strategies for co-delivering antigens and CpG oligonucleotides, *Adv Drug Deliv Rev*, 61 (2009) 205-217.
- [31] B.C. van Esch, B. Schouten, S. de Kivit, G.A. Hofman, L.M. Knippels, L.E. Willemsen, J. Garssen, Oral tolerance induction by partially hydrolyzed whey protein in mice is associated with enhanced numbers of Foxp3+ regulatory T-cells in the mesenteric lymph nodes, *Pediatr Allergy Immunol*, 22 (2011) 820-826.
- [32] A.I. Kostadinova, J. Middelburg, M. Ciulla, J. Garssen, W.E. Hennink, L.M.J. Knippels, C.F. van Nostrum, L.E.M. Willemsen, PLGA nanoparticles loaded with beta-lactoglobulin-derived peptides modulate mucosal immunity and may facilitate cow's milk allergy prevention, *Eur J Pharmacol*, 818 (2018) 211-220.
- [33] J.D. Campbell, S.A. Kell, H.M. Kozy, J.A. Lum, R. Sweetwood, M. Chu, C.R. Cunningham, H. Salamon, C.M. Lloyd, R.L. Coffman, E.M. Hessel, A limited CpG-containing oligodeoxynucleotide therapy regimen induces sustained suppression of allergic airway inflammation in mice, *Thorax*, 69 (2014) 565-573.
- [34] Z. Xu, S. Ramishetti, Y.C. Tseng, S. Guo, Y. Wang, L. Huang, Multifunctional nanoparticles co-delivering Trp2 peptide and CpG adjuvant induce potent cytotoxic T-lymphocyte response against melanoma and its lung metastasis, *J Control Release*, 172 (2013) 259-265.
- [35] I. Pali-Scholl, H. Szollosi, P. Starkl, B. Scheicher, C. Stremnitzer, A. Hofmeister, F. Roth-Walter, A. Lukschal, S.C. Diesner, A. Zimmer, E. Jensen-Jarolim, Protamine nanoparticles with CpG-oligodeoxynucleotide prevent an allergen-induced Th2-response in BALB/c mice, *Eur J Pharm Biopharm*, 85 (2013) 656-664.
- [36] B. Schouten, B.C. van Esch, G.A. Hofman, L.W. van den Elsen, L.E. Willemsen, J. Garssen, Acute allergic skin reactions and intestinal contractility changes in mice orally sensitized against casein or whey, *Int Arch Allergy Immunol*, 147 (2008) 125-134.
- [37] A.I. Kostadinova, L.A. Meulenbroek, B.C. van Esch, G.A. Hofman, J. Garssen, L.E. Willemsen, L.M. Knippels, A Specific Mixture of Fructo-Oligosaccharides and Bifidobacterium breve M-16V Facilitates

Partial Non-Responsiveness to Whey Protein in Mice Orally Exposed to beta-Lactoglobulin-Derived Peptides, *Front Immunol*, 7 (2016) 673.

[38] L.W. van den Elsen, B.C. van Esch, G.A. Hofman, J. Kant, B.J. van de Heijning, J. Garssen, L.E. Willemsen, Dietary long chain n-3 polyunsaturated fatty acids prevent allergic sensitization to cow's milk protein in mice, *Clin Exp Allergy*, 43 (2013) 798-810.

[39] M. Danaei, M. Dehghankhold, S. Ataei, F. Hasanzadeh Davarani, R. Javanmard, A. Dokhani, S. Khorasani, M.R. Mozafari, Impact of Particle Size and Polydispersity Index on the Clinical Applications of Lipidic Nanocarrier Systems, *Pharmaceutics*, 10 (2018) 57.

[40] M. Kaszuba, J. Corbett, F.M. Watson, A. Jones, High-concentration zeta potential measurements using light-scattering techniques, *Philos Trans A Math Phys Eng Sci*, 368 (2010) 4439-4451.

[41] K.Z. Sanidad, M.Y. Zeng, Neonatal gut microbiome and immunity, *Curr Opin Microbiol*, 56 (2020) 30-37.

[42] K. Zhang, A. Dupont, N. Torow, F. Gohde, S. Leschner, S. Lienenklaus, S. Weiss, M.M. Brinkmann, M. Kuhnel, M. Hensel, M. Fulde, M.W. Hornef, Age-dependent enterocyte invasion and microcolony formation by Salmonella, *PLoS Pathog*, 10 (2014) e1004385.

[43] L.M. D'Cruz, L. Klein, Development and function of agonist-induced CD25+Foxp3+ regulatory T cells in the absence of interleukin 2 signaling, *Nat Immunol*, 6 (2005) 1152-1159.

[44] J.D. Fontenot, J.P. Rasmussen, M.A. Gavin, A.Y. Rudensky, A function for interleukin 2 in Foxp3-expressing regulatory T cells, *Nat Immunol*, 6 (2005) 1142-1151.

[45] Z. Al Nabhani, S. Dulauroy, R. Marques, C. Cousu, S. Al Bounny, F. De Jardin, T. Sparwasser, M. Berard, N. Cerf-Bensussan, G. Eberl, A Weaning Reaction to Microbiota Is Required for Resistance to Immunopathologies in the Adult, *Immunity*, 50 (2019) 1276-1288 e1275.

[46] B. Weström, E. Arévalo Sureda, K. Pierzynowska, S.G. Pierzynowski, F.-J. Pérez-Cano, The Immature Gut Barrier and Its Importance in Establishing Immunity in Newborn Mammals, *Frontiers in Immunology*, 11 (2020).

[47] G. Dordelmann, D. Kozlova, S. Karczewski, R. Lizio, S. Knauer, M. Eppler, Calcium phosphate increases the encapsulation efficiency of hydrophilic drugs (proteins, nucleic acids) into poly(D,L-lactide-co-glycolide acid) nanoparticles for intracellular delivery, *J Mater Chem B*, 2 (2014) 7250-7259.

[48] N. Samadi, C.F. van Nostrum, T. Vermonden, M. Amidi, W.E. Hennink, Mechanistic studies on the degradation and protein release characteristics of poly(lactic-co-glycolic-co-hydroxymethylglycolic acid) nanospheres, *Biomacromolecules*, 14 (2013) 1044-1053.

[49] H. Park, D.H. Ha, E.S. Ha, J.S. Kim, M.S. Kim, S.J. Hwang, Effect of Stabilizers on Encapsulation Efficiency and Release Behavior of Exenatide-Loaded PLGA Microsphere Prepared by the W/O/W Solvent Evaporation Method, *Pharmaceutics*, 11 (2019) 627.

[50] M. Heikenwalder, M. Polymenidou, T. Junt, C. Sigurdson, H. Wagner, S. Akira, R. Zinkernagel, A. Aguzzi, Lymphoid follicle destruction and immunosuppression after repeated CpG oligodeoxynucleotide administration, *Nature Medicine*, 10 (2004) 187-192.

[51] G. Montamat, C. Leonard, A. Poli, L. Klimek, M. Ollert, CpG Adjuvant in Allergen-Specific Immunotherapy: Finding the Sweet Spot for the Induction of Immune Tolerance, *Front Immunol*, 12 (2021) 590054.

[52] Y. Wang, B. Qin, G. Xia, S.H. Choi, FDA's Poly (Lactic-Co-Glycolic Acid) Research Program and Regulatory Outcomes, *AAPS J*, 23 (2021) 92.

[53] J.K. Vasir, V. Labhasetwar, Biodegradable nanoparticles for cytosolic delivery of therapeutics, *Adv Drug Deliv Rev*, 59 (2007) 718-728.

[54] J. Koerner, D. Horvath, M. Groettrup, Harnessing Dendritic Cells for Poly (D,L-lactide-co-glycolide) Microspheres (PLGA MS)-Mediated Anti-tumor Therapy, *Front Immunol*, 10 (2019) 707.

[55] K.S. Kim, K. Suzuki, H. Cho, Y.S. Youn, Y.H. Bae, Oral Nanoparticles Exhibit Specific High-Efficiency Intestinal Uptake and Lymphatic Transport, *ACS Nano*, 12 (2018) 8893-8900.

[56] M. Abdulkarim, N. Agullo, B. Cattoz, P. Griffiths, A. Bernkop-Schnurch, S.G. Borros, M. Gumbleton, Nanoparticle diffusion within intestinal mucus: Three-dimensional response analysis dissecting the impact of particle surface charge, size and heterogeneity across polyelectrolyte, pegylated and viral particles, *Eur J Pharm Biopharm*, 97 (2015) 230-238.

[57] I. Pereira de Sousa, T. Moser, C. Steiner, B. Fichtl, A. Bernkop-Schnurch, Insulin loaded mucus permeating nanoparticles: Addressing the surface characteristics as feature to improve mucus permeation, *Int J Pharm*, 500 (2016) 236-244.

[58] N.D. Donahue, H. Acar, S. Wilhelm, Concepts of nanoparticle cellular uptake, intracellular trafficking, and kinetics in nanomedicine, *Adv Drug Deliv Rev*, 143 (2019) 68-96.

- [59] M. Allahyari, E. Mohit, Peptide/protein vaccine delivery system based on PLGA particles, *Hum Vaccin Immunother*, 12 (2016) 806-828.
- [60] C. Kanagaratham, Y.S. El Ansari, O.L. Lewis, H.C. Oettgen, IgE and IgG Antibodies as Regulators of Mast Cell and Basophil Functions in Food Allergy, *Front Immunol*, 11 (2020) 603050.
- [61] A.R. Madureira, C.I. Pereira, A.M.P. Gomes, M.E. Pintado, F. Xavier Malcata, Bovine whey proteins – Overview on their main biological properties, *Food Research International*, 40 (2007) 1197-1211.
- [62] A.L. Siefert, M.J. Caplan, T.M. Fahmy, Artificial bacterial biomimetic nanoparticles synergize pathogen-associated molecular patterns for vaccine efficacy, *Biomaterials*, 97 (2016) 85-96.
- [63] C. Castenmiller, B.C. Keumatio-Doungtso, R. van Ree, E.C. de Jong, Y. van Kooyk, Tolerogenic Immunotherapy: Targeting DC Surface Receptors to Induce Antigen-Specific Tolerance, *Front Immunol*, 12 (2021) 643240.
- [64] L. Guery, S. Hugues, Tolerogenic and activatory plasmacytoid dendritic cells in autoimmunity, *Front Immunol*, 4 (2013) 59.
- [65] J.U. Mayer, M. Demiri, W.W. Agace, A.S. MacDonald, M. Svensson-Frej, S.W. Milling, Different populations of CD11b(+) dendritic cells drive Th2 responses in the small intestine and colon, *Nat Commun*, 8 (2017) 15820.
- [66] J.G. Li, Y.M. Du, Z.D. Yan, J. Yan, Y.X. Zhuansun, R. Chen, W. Zhang, S.L. Feng, P.X. Ran, CD80 and CD86 knockdown in dendritic cells regulates Th1/Th2 cytokine production in asthmatic mice, *Exp Ther Med*, 11 (2016) 878-884.
- [67] M.A. Galvan Morales, J.M. Montero-Vargas, J.C. Vizueta-de-Rueda, L.M. Teran, New Insights into the Role of PD-1 and Its Ligands in Allergic Disease, *Int J Mol Sci*, 22 (2021) 11898.
- [68] W.W. Unger, S. Laban, F.S. Kleijwegt, A.R. van der Slik, B.O. Roep, Induction of Treg by monocyte-derived DC modulated by vitamin D3 or dexamethasone: differential role for PD-L1, *Eur J Immunol*, 39 (2009) 3147-3159.
- [69] K.P.-L. Li Wang, Victor C. de Vries, Indira Guleria, Mohamed H. Sayegh, and Randolph J. Noelle, Programmed death 1 ligand signaling regulates the generation of adaptive Foxp3^{hi}CD4^{hi} regulatory T cells, *PNAS* 105 (2008) 9331–9336.
- [70] A. Roberts, L. Bentley, T. Tang, F. Stewart, C. Pallini, J. Juvvanapudi, G.R. Wallace, A.J. Cooper, A. Scott, D. Thickett, S.T. Lugg, H. Bancroft, B. Hemming, C. Ferris, G. Langman, A. Robinson, J. Chapman, B. Naidu, T. Pinkney, G.S. Taylor, K. Brock, Z. Stamataki, C.A. Brady, S.J. Curnow, J. Gordon, O. Qureshi, N.M. Barnes, Ex vivo modelling of PD-1/PD-L1 immune checkpoint blockade under acute, chronic, and exhaustion-like conditions of T-cell stimulation, *Sci Rep*, 11 (2021) 4030.
- [71] S.H. Arun T. Kamath, Frank Battye, David F. Tough, and Ken Shortman, Developmental kinetics and lifespan of dendritic cells in mouse lymphoid organs, *Blood*, 100 (2002) 1734-1741.
- [72] H. Michael, Y. Li, Y. Wang, C.T. McCusker, Trained immunity induced by in vivo peptide-based STAT6 inhibition prevents ragweed allergy in mice, *Allergy Asthma Clin Immunol*, 17 (2021) 42.
- [73] D. Boraschi, P. Italiani, R. Palomba, P. Decuzzi, A. Duschl, B. Fadeel, S.M. Moghimi, Nanoparticles and innate immunity: new perspectives on host defence, *Semin Immunol*, 34 (2017) 33-51.
- [74] D. Alvarez, E.H. Vollmann, U.H. von Andrian, Mechanisms and consequences of dendritic cell migration, *Immunity*, 29 (2008) 325-342.
- [75] T.B. Bertolini, M. Biswas, C. Terhorst, H. Daniell, R.W. Herzog, A.R. Pineros, Role of orally induced regulatory T cells in immunotherapy and tolerance, *Cell Immunol*, 359 (2021) 104251.
- [76] M. Tekguc, J.B. Wing, M. Osaki, J. Long, S. Sakaguchi, Treg-expressed CTLA-4 depletes CD80/CD86 by trogocytosis, releasing free PD-L1 on antigen-presenting cells, *Proc Natl Acad Sci U S A*, 118 (2021).
- [77] L.M. Wakim, J. Waithman, N. van Rooijen, W.R. Heath, F.R. Carbone, Dendritic cell-induced memory T cell activation in nonlymphoid tissues, *Science*, 319 (2008) 198-202.
- [78] D. Gatto, K. Wood, I. Caminschi, D. Murphy-Durland, P. Schofield, D. Christ, G. Karupiah, R. Brink, The chemotactic receptor EB12 regulates the homeostasis, localization and immunological function of splenic dendritic cells, *Nat Immunol*, 14 (2013) 446-453.
- [79] E. Umemoto, K. Otani, T. Ikeno, N. Verjan Garcia, H. Hayasaka, Z. Bai, M.H. Jang, T. Tanaka, T. Nagasawa, K. Ueda, M. Miyasaka, Constitutive plasmacytoid dendritic cell migration to the splenic white pulp is cooperatively regulated by CCR7- and CXCR4-mediated signaling, *J Immunol*, 189 (2012) 191-199.
- [80] G. Wingender, N. Garbi, B. Schumak, F. Jungerkes, E. Endl, D. von Bubnoff, J. Steitz, J. Striegler, G. Moldenhauer, T. Tuting, A. Heit, K.M. Huster, O. Takikawa, S. Akira, D.H. Busch, H. Wagner, G.J. Hammerling, P.A. Knolle, A. Limmer, Systemic application of CpG-rich DNA suppresses adaptive T cell immunity via induction of IDO, *Eur J Immunol*, 36 (2006) 12-20.
- [81] B. Baban, P.R. Chandler, M.D. Sharma, J. Pihkala, P.A. Koni, D.H. Munn, A.L. Mellor, IDO activates regulatory T cells and blocks their conversion into Th17-like T cells, *J Immunol*, 183 (2009) 2475-2483.

- [82] M. Plantinga, M. Guillems, M. Vanheerswyngheles, K. Deswarte, F. Branco-Madeira, W. Toussaint, L. Vanhoutte, K. Neyt, N. Killeen, B. Malissen, H. Hammad, B.N. Lambrecht, Conventional and monocyte-derived CD11b(+) dendritic cells initiate and maintain T helper 2 cell-mediated immunity to house dust mite allergen, *Immunity*, 38 (2013) 322-335.
- [83] M.J. Park, K.S. Park, H.S. Park, M.L. Cho, S.Y. Hwang, S.Y. Min, M.K. Park, S.H. Park, H.Y. Kim, A distinct tolerogenic subset of splenic IDO(+)CD11b(+) dendritic cells from orally tolerized mice is responsible for induction of systemic immune tolerance and suppression of collagen-induced arthritis, *Cell Immunol*, 278 (2012) 45-54.
- [84] S. Schulke, Induction of Interleukin-10 Producing Dendritic Cells As a Tool to Suppress Allergen-Specific T Helper 2 Responses, *Front Immunol*, 9 (2018) 455.
- [85] A.M.K. Joel N. Kline, Thomas J. Waldschmidt, Zuhair K. Ballas, Vipul Jain, and Thomas R. Businga., CpG oligodeoxynucleotides do not require TH1 cytokines to prevent eosinophilic airway inflammation in a murine model of asthma, *J Allergy Clin Immunol* 104 (1999) 1258-1264.
- [86] M. Iqbal, N. Zafar, H. Fessi, A. Elaissari, Double emulsion solvent evaporation techniques used for drug encapsulation, *Int J Pharm*, 496 (2015) 173-190.

CHAPTER 4

Live Cell Imaging by Förster Resonance Energy Transfer Fluorescence to Study Trafficking of PLGA Nanoparticles and the Release of a Loaded Peptide in Dendritic Cells

Mengshan Liu ^{1,2}, Chun Yin Jerry Lau ¹, Irene Trillo Cabello ¹, Johan Garssen ^{2,3}, Linette E. M. Willemsen ², Wim E. Hennink ¹ and Cornelus F. van Nostrum ^{1,*}

1. Division of Pharmaceutics, Utrecht Institute for Pharmaceutical Sciences, Utrecht University, Utrecht, the Netherlands

2. Division of Pharmacology, Utrecht Institute for Pharmaceutical Sciences, Utrecht University, Utrecht, the Netherlands

3. Department of Immunology, Nutricia Research B.V., Utrecht, the Netherlands

This chapter is published in *Pharmaceuticals*, 16 (2023).

Abstract

Background. Our previous study demonstrated that a selected β -lactoglobulin-derived peptide (BLG-Pep) loaded in poly(lactic-co-glycolic acid) (PLGA) nanoparticles protected mice against cow's milk allergy development. However, the mechanism(s) responsible for the interaction of the peptide-loaded PLGA nanoparticles with dendritic cells (DCs) and their intracellular fate was/were elusive. **Methods.** Förster resonance energy transfer (FRET), a distance-dependent non-radioactive energy transfer process mediated from a donor to an acceptor fluorochrome, was used to investigate these processes. **Results.** The ratio of the donor (Cyanine-3)-conjugated peptide and acceptor (Cyanine-5) labeled PLGA nanocarrier was fine-tuned for optimal (87%) FRET efficiency. The colloidal stability and FRET emission of prepared NPs were maintained upon 144 h incubation in PBS buffer and 6 h incubation in biorelevant simulated gastric fluid at 37 °C. A total of 73% of Pep-Cy3 NP was internalized by DCs as quantified using flow cytometry and confirmed using confocal fluorescence microscopy. By real-time monitoring of the change in the FRET signal of the internalized peptide-loaded nanoparticles, we observed prolonged retention (for 96 h) of the nanoparticles-encapsulated peptide as compared to 24 h retention of the free peptide in the DCs. **Conclusions.** The prolonged retention and intracellular antigen release of the BLG-Pep loaded in PLGA nanoparticles in murine DCs might facilitate antigen-specific tolerance induction.

Keywords: cyanine-3; cyanine-5; Förster resonance energy transfer; dendritic cells; poly(lactic-co-glycolic acid) nanoparticles; peptide delivery

Introduction

Inducing tolerance against food allergy requires the exposure of the intestinal immune system to specific antigens from food proteins. The intestinal mucosal immune system is the largest immune system in vertebrates and the ideal target site due to its physiological propensity in distinguishing and inducing both local and systemic tolerance to orally administered harmless food proteins [1]. Dendritic cells (DCs) are regarded as the major antigen-presenting cells to contribute to tolerance induction, as they regularly sample antigens from the gastrointestinal environment for presentation to naïve T-cells and instruct adaptive immune response or tolerance thereafter [2]. Indeed, van Esch *et al.* [3] previously reported that oral pre-exposure to partially hydrolyzed whey protein prior to whey sensitizations increased the percentage of regulatory T-cells (Treg) in the mesenteric lymph nodes, leading to a remarkably reduced acute allergic skin response to whole whey protein in a murine prophylactic cow's milk allergy (CMA) model.

Orally delivered peptides are susceptible to degradation due to the acidic pH and proteolytic enzymes in the stomach, which reduce the amount of intact antigen presented to intestinal DC and thus compromise the tolerogenic outcome. Previously, Meulenbroek *et al.* [4] reported that oral administration of a dose of 4 mg β -lactoglobulin-derived peptides (BLG-peptides) prior to whey sensitizations reduced the acute allergic skin response to whole whey protein in mice. To improve the tolerogenic efficacy, we reported that oral pre-exposure to poly(lactic-co-glycolic acid) (PLGA) nanoparticles (NPs) encapsulating 160 μ g BLG-peptides, but not an equivalent dose of BLG-peptides in soluble form, was effective in preventing the development of whey-induced allergy and induced systemic specific tolerance in a prophylactic murine model [5]. This result suggests that PLGA NPs play a dominating role in the improvement of the bioavailability of the encapsulated peptide cargo by its protection against proteolytic degradation in the stomach [6].

Despite the fact that antigen-loaded PLGA NPs have been investigated extensively to trigger immune responses [7-11], only a few studies have addressed their integrity at an acidic pH and under proteolytic conditions in the gastrointestinal tract and their internalization and subsequent intracellular trafficking in dendritic cells. Meulenbroek *et al.* [4] reported that the T-cell epitope containing BLG-Pep (AASDISLLDAQSAPLRVY), from a selection of β -lactoglobulin-derived peptides (BLG-peptides) of 18 amino acids

(AAs), was recognized by a human T-cell line *in vitro* and instructed whey-specific tolerance in mice. More recently, Gouw *et al.* [12] identified that the BLG-Pep (AASDISLLDAQSAPLRVY) contains a sequence that can be presented by the most predominant human MHCII isotype HLR-DRB1 molecule [13]. In other words, the BLG-Pep (AASDISLLDAQSAPLRVY) with an MHCII-restricted T-cell epitope can be presented by human DCs after binding to the MHCII groove. As reviewed by Holland *et al.* [14], the *open-ended* conformation of the MHCII binding groove consists of a core binding 9 AAs, which allows binding to peptides of variable lengths (ranging between 12 and 20 AAs) [15]. MHCII-restricted peptides contain a central binding motif in its core, while the amino acids of outside this core peptide region are called peptide flanking regions (PFRs) [14]. It was shown that the peptide backbone of the central motifs binds to the MHCII groove by hydrogen bonding [14]. Upon the internalization of exogenous peptides by DC, MHCII molecules synthesized in the endoplasmic reticulum (ER) are transported by exocytotic vesicles containing exogenous proteins [16]. Thereafter, the acidic pH and chaperone protein HLA-DM facilitate the binding of endosomal proteolyzed MHCII-restricted peptides to the MHCII groove [17, 18]. In this process, MHCII-restricted peptides undergo peptide editing mediated by HLA-DM and peptide trimming, which determines the length of the PFRs [19, 20]. Hence, in the present study, we aimed to investigate the fate of internalized PLGA NPs loaded with BLG-Pep (AASDISLLDAQSAPLRVY) by murine DC 2.4 cells and the subsequent release of the loaded peptide.

To this end, we applied Förster resonance energy transfer (FRET) imaging using dual-labeled nanocarriers, which consist of donor dye-Cy3-conjugated BLG-Pep encapsulated in PLGA NP labeled with the acceptor dye Cy5 covalently linked to PLGA. Förster resonance energy transfer (FRET) is a non-radioactive energy transfer process between a pair of fluorescent probes, transferring the excess energy from the excited donor fluorochrome to the ground state acceptor by dipole–dipole coupling [21, 22]. Except for the extensive overlap between the donor emission and acceptor excitation wavelengths, FRET efficiency depends predominantly on the distance between the donor and acceptor, ranging typically between 1 and 10 nm to an inverse-sixth power [21]. This strong distance-dependent characteristic enables the investigation of processes that nanoparticles undergo once taken up by cells [21]. FRET has therefore been employed as a tool to obtain insights into the degradation of internalized nanoparticles, cargo release, and particle interaction with cells [23-26]. Recent studies

[25, 27] reported the feasibility of obtaining insight into the intracellular fate of nanoparticles by FRET analysis by means of the co-encapsulation of both FRET donor and acceptor dyes non-covalently in PLGA NPs. Further, Zhang *et al.* [26] investigated the *in vivo* integrity of polymeric micelles by means of dual labeling of only the nanocarrier with a FRET pair dye. However, we hypothesized that the labeling of both the peptide cargo and PLGA nanocarriers in a covalent way could provide more valuable insight into the internalized PLGA nanocarriers and intracellular release of peptide payload. To this end, the peptide cargo was labeled with donor Cy3 and the PLGA nanocarrier with acceptor Cy5, and we analyzed the FRET emission upon internalization by dendritic cells. This could prove to be a biometric tool for understanding the intracellular release of loaded peptides from PLGA nanocarriers in DCs.

Materials And Methods

Materials

Preloaded Fmoc-Tyr (tbu)-Wang resin, 9-fluorenylmethyloxycarbonyl (Fmoc)-protected amino acids, and trifluoroacetic acid (TFA) were purchased from Novabiochem GmbH (Hohenbrunn, Germany). Peptide-grade dimethylformide (DMF), dichloromethane (DCM), piperidine, *N, N'*-diisopropylcarbodiimide (DIC), and HPLC-grade acetonitrile were purchased from Biosolve BV (Valkenswaard, The Netherlands). Ethyl cyanohydroxyiminoacetate (Oxyma pure) was purchased from Manchester Organics Ltd. (Cheshire, UK). Triisopropylsilane (TIPS), BioUltra-grade ammonium bicarbonate, polyvinyl alcohol (PVA, 87–90% hydrolyzed, Mw 30,000–70,000 Da), sodium chloride, Dulbecco's Phosphate Buffered Saline (DPBS), RPMI 1640 medium, Fetal Bovine Serum (FBS), *N, N'*-dicyclohexylcarbodiimide (DCC), *N*-hydroxysuccinimide (NHS), triethylamine (TEA), and lithium chloride (LiCl) were purchased from Sigma-Aldrich Chemie BV (Zwijndrecht, The Netherlands). Cyanine3-labeled Fmoc-Lysine (Fmoc-Lys (Cy3)-OH) was purchased from APPTec (Louisville, USA). Cy5 amine was purchased from Luminprobe (Hannover, Germany). Uncapped poly (DL-lactide-co-glycolide) (PLGA-COOH) (PURASORB PDLG 5004A, lactide/glycolide 50/50, intrinsic viscosity 0.32–0.48 dl/g) was purchased from Corbion (Gorinchem, the Netherlands). Penicillin and streptomycin were purchased from Gibco (New York, USA), and phosphate-buffered saline (10×PBS, containing 1.37 M NaCl, 0.027 M KCl, and 0.119 M phosphates) was obtained from Fisher BioReagents (Pittsburgh, USA) and diluted 10 times with Milli-Q water before use. Bovine serum albumin (BSA) was obtained from Sigma-Aldrich Chemie BV (Zwijndrecht, The Netherlands). Fasted-state-simulated

gastric fluid (FaSSGF) (pH 1.6, without pepsin) was prepared by solubilizing 80 μM NaTc (sodium taurocholate, Santa Cruz biotechnology, Dallas, USA), 20 μM lecithin (phosphatidylcholine from egg, Liphoid GmbH, Ludwigshafen, Germany), and 34.2 μM NaCl (Sigma-Aldrich) in Milli-Q water and adjusted to pH 1.6 with 1N HCl [28]. For the preparation of FaSSGF with pepsin, 0.1 mg/mL pepsin from porcine gastric mucosa (Sigma-Aldrich) was supplemented to the FaSSGF (pH 1.6).

Solid-Phase Peptide Synthesis and Characterization

Cy3-labeled peptide (Pep-Cy3; structure shown in Figure 1B) was obtained using a microwave-assisted solid-phase peptide synthesis method [29] using an H12 liberty blue peptide synthesizer (CEM Corporation, Matthews, USA). DMF was used as the coupling and washing solvent. For each coupling step, Fmoc-amino acids were activated by 5eq of Oxyma pure and DIC to react with the free N-terminal amino acids on the resin for 1 min at 90 °C. After each coupling step, the Fmoc groups were removed by treatment with 20% piperidine for 1 min at 90 °C. Cy3 modification of the β -lactoglobulin-derived peptide (Figure 1A) was performed by introducing Fmoc-Lys (Cy3)-OH residue to the peptide sequence. TFA/H₂O/TIPS (95/2.5/2.5 v/v/v) was used to simultaneously cleave the peptide from the resin and remove the side-chain protecting groups.

Pep-Cy3 was purified by a Prep-HPLC using a Reprosil-Pur C18 column (10 μm , 250 \times 22 mm) and eluted with a water-acetonitrile gradient from 5 to 80% acetonitrile (10 mM ammonium bicarbonate) in 25 min at a flow rate of 15 mL/min with UV detection at 220 nm.

The purity of the obtained Pep-Cy3 was analyzed with ultra-performance liquid chromatography (UPLC) by using a BEH C18 1.7 μm column (Waters®, Milford, USA), UV detection at 210 nm, and fluorescence detection at $\lambda_{\text{ex/em}} = 555/570$ nm. A gradient elution method was used with a mobile phase A (0.1% TFA, 5% acetonitrile, and 95% H₂O) and a mobile phase B (acetonitrile). The eluent changed linearly from 20 to 40% mobile phase B in 6 min with a flow rate of 0.25 mL/min at 25 °C. Mass spectrometry (MS) analysis of the synthesized Pep-Cy3 was performed using a microTOF-Q instrument in positive mode.

Conjugation of Cy5 to PLGA-COOH

The synthesis of PLGA-Cy5 (Figure 2A) was adapted from a method described previously [30]. PLGA-COOH ($M_n = 13,700$ g/mol according to GPC analysis using PEG standards, 211.4 mg) was dissolved in anhydrous DCM (100 mg/mL) at room temperature. Next, DCC (31.0 mg, 150 mmol) in 1 mL anhydrous DCM was added to the PLGA-COOH solution and stirred for 10 min. Subsequently, NHS (17.5 mg, 152 mmol) dissolved in 1 mL anhydrous DCM was added, and the resulting reaction mixture was stirred for 60 min at room temperature. Next, the formed white precipitate *N, N'*-dicyclohexylurea (DCU) was removed by filtration with a 0.2 μm regenerated cellulose (RC) membrane syringe filter (Phenomenex, Torrance, USA). The filtrated PLGA-NHS solution was subsequently added to a mixture of triethylamine (17.3 mg, 0.084 mmol) and Cy5 amine (5.0 mg, 0.0076 mmol) in 0.5 mL anhydrous DCM and stirred for 8 h at room temperature. Next, the synthesized PLGA-Cy5 was precipitated into 80 mL diethyl ether/methanol (1:1 v/v) and centrifuged at $2700\times g$ for 10 min at 4 °C. The supernatant was decanted, and the precipitated product was dried under a nitrogen atmosphere for 10 min to remove residual solvents. Next, the product was dissolved in 4 mL DMSO and transferred into a 3.5 kDa Spectra/Por RC membrane tube (Thermo Fisher Scientific, Washington, USA) for dialysis against 100 mL acetonitrile. The dialysis medium was refreshed daily for 7 days. The obtained PLGA-Cy5 was precipitated by dropping the polymer solution into 100 mL milli-Q water. The formed precipitate was collected and subsequently lyophilized overnight to yield PLGA-Cy5 in the form of small blue pellets. PLGA-Cy5 was analyzed with GPC (Waters® alliance e2695 system, Milford, USA), which was equipped with a UV/Vis detector (Waters® 2489) and refractive index detector (Waters® 2414) using DMF/10 mM LiCl as the solvent, and PEG of a defined molecular weight was used as calibration standards.

Preparation of Nanoparticles

A double emulsion solvent evaporation method was applied to prepare empty PLGA-Cy5 NP, non-labeled PLGA NP loaded with peptide-Cy3 (Pep-Cy3 NP) and PLGA-Cy5 NP loaded with peptide-Cy3 (i.e., FRET NP) [5]. Briefly, 0.125 mL PBS (for PLGA-Cy5 NP) or PBS containing 0.04, 0.2, 0.4, 0.6, or 0.8 mg Pep-Cy3 (corresponding to 0.1, 0.5, 1, 1.5, or 2 wt% Pep-Cy3 NP or FRET NP) as the internal aqueous phase was added to 1.25 mL of anhydrous DCM in which 50 mg of a blend of PLGA-Cy5 (0, 1.5, 2, 4, 7, or 9 wt%) with PLGA-COOH was dissolved prior to sonication using a Sonifier S-450A (3 mm,

Branson Ultrasonics B.V., Soest, The Netherlands) at 20% amplitude for 1 min on an ice bath to yield a water-in-oil emulsion. Next, the emulsion was added to 12.5 mL of the external aqueous phase, containing 3% w/v PVA and 0.9% w/v NaCl, and the obtained mixture was sonicated using a Sonifier S-450A (13 mm, Branson Ultrasonics B.V.) at 20% amplitude for 1 min on an ice bath to yield a water-in-oil-in-water emulsion. Finally, the formed emulsion was stirred for 4 h at room temperature to evaporate DCM and to obtain hardened PLGA NPs. The nanoparticle suspension was centrifuged at 20,000× *g* for 30 min at 4 °C, and the pelleted nanoparticles were washed with 10 mL PBS twice. The nanoparticles were resuspended in 2 mL of Milli-Q water and lyophilized using a freeze dryer (Lyovapor L-200, BUCHI Corporation, New Castle, USA).

Characterization of the Nanoparticles

After the washing step, the nanoparticles pellet was resuspended in 2 mL of Milli-Q water (in Section **Preparation of Nanoparticles**), from which a 6 µL nanoparticle suspension was added to 1994 µL of Milli-Q water for the characterization of nanoparticle size and polydispersity index (PDI) using Zetasizer Nano S (Malvern Instruments, Malvern, UK).

In addition, 100 µL of 100 mM HEPES buffer (pH 7.4) was added into a 900 µL nanoparticles suspension in Milli-Q water for measurement of the zeta potential of nanoparticles, using Zetasizer Nano-Z (Malvern Instruments, Malvern, UK).

To avoid possible inaccuracy caused by the overlapping emission of the laser of the Zetasizer Nano S with Cy5 absorption [31], the size of Cy5-labeled NP was also measured using Nanosight LM14 (Malvern Instruments, Malvern, UK).

Peptide Encapsulation Efficiency

The encapsulation efficiency of Pep-Cy3 was determined using an indirect method [32]. The supernatants collected from the washing steps were filtered using a 0.2 µm RC syringe filter (Phenomenex) prior to Acquity ultra-performance liquid chromatography (UPLC) analysis. The Pep-Cy3 concentration of the collected filtered aqueous phases was determined using a BEH C18 1.7 µm column (Waters) and UV detection at 210 nm and fluorescence detection at $\lambda_{\text{ex/em}} = 555/570$ nm. A gradient elution method was used with mobile phase A (0.1% TFA, 5% acetonitrile, and 95% H₂O)

and mobile phase B (0.1% TFA and acetonitrile). The eluent changed linearly from 20 to 40% mobile phase B in 6 min with a flow rate of 0.25 mL/min at 25 °C.

Peptide standards (1–100 µg/mL Pep-Cy3, 7.5 µL injection volume) dissolved in mobile phase A were used for calibration. The encapsulation efficiency (EE) of Pep-Cy3 in PLGA NP is defined as the amount of encapsulated peptide (which equals the weight of peptide in the feed minus the weight of quantified non-encapsulated peptide) divided by the weight of peptide used for the preparation of the loaded NPs (Equation (2)) [32]. The loading capacity of Pep-Cy3 in PLGA NP is reported as the weight of the encapsulated peptide divided by the weight of the peptide-loaded NPs (Equation (3)) [33].

$$\text{Encapsulation Efficiency (EE) (\%)} = \frac{\text{Weight}_{\text{feed peptide}} - \text{Weight}_{\text{non-encapsulated peptide}}}{\text{Weight}_{\text{feed peptide}}} \times 100\%, \quad (2)$$

$$\text{Loading Capacity (LC) (\%)} = \frac{\text{Weight}_{\text{encapsulated peptide}}}{\text{Weight of nanoparticles}} \times 100\%, \quad (3)$$

Fluorescence Characteristics of Labeled Nanoparticles

Steady-state fluorescence was measured in semi-micro cell quartz cuvettes (10 × 4 × 45 mm, Hellma™ Suprasil™, Thermo Fisher Scientific) in a PCT-818 Automatic 4-position Peltier cell changer equipped Jasco Spectrofluorometer FP-8300 (Easton, USA), from 1 mL 0.5 mg/mL PLGA-Cy5 NP (containing 1.5–9 wt% of Cy5-labeled PLGA), Pep-Cy3 NP (0.1–2 wt% feed Pep-Cy3), or FRET NP (1 wt% feed Pep-Cy3, 1.5–9 wt% PLGA-Cy5) in PBS (pH 7.4). Briefly, the Cy3 fluorophore was excited at $\lambda_{\text{ex}} = 555$ nm using a wavelength width of 5 nm, and the Cy3 fluorescence was recorded at $\lambda_{\text{em}} = 570$ nm. The Cy5 fluorophore was excited at $\lambda_{\text{ex}} = 646$ nm, and fluorescence emission was recorded at $\lambda_{\text{em}} = 662$ nm, using a wavelength width of 5 nm. FRET fluorescence spectra at $\lambda_{\text{em}} = 570$ –900 nm were recorded for 0.5 mg/mL FRET NP (1 wt% feed Pep-Cy3 and 1.5–9 wt% PLGA-Cy5) and PLGA-Cy5 NP as the control (containing 1.5–9 wt% PLGA-Cy5) by the excitation of Cy3 at $\lambda_{\text{ex}} = 555$ nm using a wavelength width of 5 nm.

Fluorescence Intensity of Labeled PLGA NP in PBS or Fasted-State-Simulated Gastric Fluid

The fluorescence intensity of PLGA-Cy5 NP (9 wt% PLGA-Cy5) and FRET NP (0.8:1, i.e., 1 wt% Pep-Cy3, 9 wt% PLGA-Cy5) was monitored upon incubation at 37 °C for 144 h in PBS or fasted-state-simulated gastric fluid (FaSSGF) [28]. Briefly, lyophilized fluorescently labeled PLGA NPs were suspended at 0.2 mg/mL in PBS (pH 7.4), FaSSGF (pH 1.6, with pepsin), or FaSSGF (pH 1.6, without pepsin). Next, 1 mL of NP samples was

pipetted into semi-micro cell quartz cuvettes (10 × 4 × 45 mm, Hellma™ Suprasil™) and closed with a lid for incubation at 37 °C. At different time points (after 0.5, 2, 4, 24, 48, 120, and 144 h), the fluorescence emission of Cy5 and FRET was recorded using Jasco Spectrofluorometer FP-8300.

Culture of Human-Monocytes-Derived Dendritic Cells (moDC)

Freshly donated and condensed blood (buffy coat) (time between donation and experiments was 24 h at most) was obtained from the Dutch blood bank (Amsterdam, The Netherlands). A total of 25 mL of fresh human blood was diluted with the same volume of DPBS-2% FBS at room temperature and slowly transferred into Leucosep tubes (VWR, Radnor, USA), followed by centrifugation for 13 min at 1000× *g* at room temperature with slow acceleration and deceleration. Subsequently, the interface containing the peripheral blood mononuclear cells (PBMCs) was centrifuged for 5 min at 1800 rpm at room temperature, and the supernatant was removed. A total of 50 mL of DPBS-2% FBS was added to resuspend the pellets, and centrifugation was repeated 4 times until the supernatant was clear. Next, 5 mL of the lysis buffer (8.3 g/L NH₄Cl, 1 g/L KHCO₃, and 37 mg/L EDTA), filtered using a sterile 0.22 μm syringe filter (Cellulose Acetate, Whatman™, GE Healthcare Life Sciences, Thermo Fisher Scientific), was added to the pellets and incubated for 4 min on ice to lyse the erythrocytes. Afterward, the obtained PBMC pellet was resuspended in RPMI 1640 medium-10% FBS-1% penicillin/streptomycin and counted using a cell counter (Z1 Coulter Particle Counter, Beckman Coulter™, Indianapolis, USA) prior to the isolation of monocytes by negative selection with human Monocyte Isolation Kit II and MACS column and MACS separator. Per donor, 1 × 10⁶ monocytes per 1 mL were cultured in the presence of 100 ng/mL human recombinant IL-4 and 60 ng/mL recombinant human GM-CSF to induce differentiation into immature-monocytes-derived dendritic cells (moDC) in 6-well suspension culture plates (Greiner Bio-one, Solingen, Germany) and incubated at 37 °C and 5% CO₂. On days 3 and 6, half of the medium was withdrawn and replaced with fresh medium containing 100 ng/mL IL-4 and 60 ng/mL GM-CSF.

Culture of Murine Bone-Marrow-Derived Dendritic Cell Line DC 2.4

Immortalized murine bone-marrow-derived dendritic cell line DC 2.4 (Merck, Kenilworth, USA) was cultured in a T75 flask with RPMI 1640 medium-10% FBS supplemented with 10 μM β-mercapoethanol, 1 × L-glutamine solution, 1 × trypsin-

EDTA solution, MEM non-essential amino acids, and 1 × HEPES solution according to the supplier's instructions.

Internalization of Pep-Cy3/NP by Human moDC Determined by Fluorescence Microscopy and Flow Cytometry

A suspension of Pep-Cy3 NP (with 2 wt% feed Pep-Cy3) dispersed in RPMI 1640 medium-10% FBS-1% penicillin/streptomycin at a concentration of 1 mg/mL was filtered using a 0.2 µm RC membrane filter (Phenomenex). The concentration of the filtrated fluorescent NP suspension was determined after 5 times of dilutions in the RPMI 1640 medium-10% FBS-1% penicillin/streptomycin by measuring the Cy3 fluorescence using Jasco Spectrofluorometer FP-8300. After 7 days of differentiation as indicated in Section **Culture of Human-Monocytes-Derived Dendritic Cells (moDC)**, immature human moDC of 3 healthy donors were seeded at a density of 2.5×10^5 cells per well in a 96-well cell culture plate. On day 7, the immature moDC were incubated with medium or 0.060 mg/mL Pep-Cy3 NP (2 times diluted as indicated in Supplemental Table S1) in 250 µL RPMI 1640 medium-10% FBS-1% penicillin/streptomycin and incubated at 37 °C and 5% CO₂ for 2.5 and 18.5 h, respectively. After incubation, the cells were transferred from the wells into a 15 mL falcon tube and washed twice with 7 mL RPMI 1640 medium-10% FBS-1% penicillin/streptomycin by using centrifugation at 300× *g* for 5 min at room temperature. Approximate 60 µL of RPMI 1640 medium-10% FBS-1% penicillin/streptomycin was added to the cells prior to Yokogawa imaging as described in Section **Cellular Uptake and Intracellular Trafficking of Nanoparticles by Murine DC 2.4**.

In parallel, cellular uptake of Pep-Cy3 NP by the immature moDC was quantified using flow cytometry. The cells were seeded at a density of 2×10^5 cells per well in a 48-well cell culture plate and subsequently incubated at 37 °C and 5% CO₂ for 2.5 h with medium or 0.060 mg/mL Pep-Cy3 NP (2 times diluted as indicated in Supplementary Table S1) in 200 µL of RPMI 1640 medium-10% FBS-1% penicillin/streptomycin. Next, the cells were transferred into a 15 mL falcon tube and washed twice with 7 mL RPMI 1640 medium-10% FBS-1% penicillin/streptomycin by using centrifugation at 300× *g* for 5 min at room temperature. Prior to flow cytometry analysis, the viability of the cells was determined by staining them with the fixable viability dye eFluor™780 (at 2000 times dilution in DPBS) (Thermo Fisher Scientific) and incubated on ice for 30 min. To avoid non-specific binding between the Fc domain of the IgG antibodies and the Fc

receptors expressed on human moDC, the cells were incubated with 25 μ L 1% human Fc-blocking antibody (BD Biosciences) in DPBS-1% bovine serum albumin (BSA)-2% FBS buffer per well for 10 min at 4 °C [34]. For characterization of human CD11c+CD14-moDC, the cells were incubated with CD11c-PerCP/eFluor 710 (at 640 times dilution) (Thermo Fisher Scientific) and CD14-eFluor450 (at 100 times dilution) (BD Biosciences) in DPBS-1% BSA buffer for 45 min at 4 °C in the dark. Cells were analyzed with a BD FACSCantoll flow cytometer (Becton Dickinson, Franklin Lakes, USA). Data analysis was conducted with FlowLogic software (Inivai Technologies, Mentone, Australia).

Cellular Uptake and Intracellular Trafficking of Nanoparticles by Murine DC 2.4

Murine immortalized dendritic cells DC 2.4 were seeded at a density of 5×10^4 per well and cultured in a 96-well light-proof plate for 2 days at 37 °C in 250 μ L RPMI 1640 to reach a density of approximately 2×10^5 cells per well. For reasons explained in Section **Internalization of Pep-Cy3/NP by Human moDC Determined by Fluorescence Microscopy and Flow Cytometry**, the different NP suspensions of PLGA-Cy5 NP (9 wt% labeled polymer), Pep-Cy3 NP (1 wt% feed Pep-Cy3), or FRET NP 0.8:1 (1 wt% Pep-Cy3:9 wt% PLGA-Cy5) dispersed in RPMI 1640 medium at a concentration of 0.5 mg/mL were filtered using a 0.2 μ m RC membrane filter (Phenomenex) to remove NP with a size above 200 nm. The concentration of particles in the filtrated fluorescent NPs suspensions was determined by measuring the Cy3 and Cy5 fluorescence using Jasco Spectrofluorometer FP-8300.

DC 2.4 cells were rinsed twice with DPBS prior to the addition of 200 μ L of the filtered fluorescent NP suspension or a solution of the Pep-Cy3 (concentration 1 μ g/mL, equivalent concentration as in the FRET NP suspension) in RPMI 1640 medium to the wells. After 2.5 h incubation at 37 °C, the nuclei of the DC 2.4 cells were stained with the dye Hoechst 33342 (5 μ g/mL) for 15 min at 37 °C. Subsequently, the stained cells were rinsed 3 times using 200 μ L PBS to remove the extracellular dye and the non-internalized nanoparticles. Finally, live imaging of the cellular uptake and intracellular trafficking of fluorescent nanoparticles by the nuclei-stained cells over 144 h at 37 °C in RPMI 1640 medium was conducted using a confocal laser scanning microscope system (Cell Voyager CV7000S, Yokogawa Electric, Tokyo, Japan) at excitation at 405 ± 5 nm (Hoechst), 561 ± 2 nm (Cy3 or FRET), or 640 ± 4.5 nm (Cy5). Live confocal images were acquired using a water immersion lens 60 \times objective and emission band-pass filters: BP525/50 (Bright field, confocal path), BP445/45 (Hoechst), BP600/37 (Cy3), and

BP676/29 (Cy5 or FRET). Compensation for non-specific fluorescence of the different images was conducted for cells incubated with medium, 1 wt% Pep-Cy3 NP, 9 wt% PLGA-Cy5 NP, and FRET NP (0.8:1, 1 wt% Pep-Cy3:9 wt% PLGA-Cy5) using Columbus Image Data Storage and Analysis System (<http://columbus.science.-uu.nl>).

Results And Discussion

Preparation and Characterization of the Cy3-Labeled β -Lactoglobulin-Derived Peptide and Cy5-Labeled PLGA

The Pep-Cy3 (Figure 1B) was prepared by the solid phase method [35] and purified by preparative HPLC. Ultra-performance liquid chromatography (UPLC) analysis demonstrates that the purified peptide is predominantly a single entity, using UV and fluorescence detection (98.6% purity, Figure 1C). The high-resolution mass spectrometry (MS) analysis (Figure 1D) showed masses of (M^{2+}) = 1172.6 and (M^{3+}) = 782.1 for the purified Pep-Cy3, which is in accordance with its theoretical mass of 2344.6 g/mol. This result demonstrates the successful synthesis and purification of the Pep-Cy3. Of note, the modification of BLG-Pep by dye conjugation would inevitably influence its physicochemical properties. Importantly, the conjugation of a fluorescent dye to the N- or C-terminus of the peptide sequence will alter the resultant charge of the peptide (+1 or -1, respectively), which might influence intracellular processing. Therefore, the hydrophobic aliphatic amino acid leucine located in the middle of the BLG-peptide was substituted by a lysine-Cy3 residue, without alteration of the peptide backbone or overall charge.

Live cell imaging by Förster Resonance Energy Transfer fluorescence to study trafficking of PLGA NP and release of a loaded peptide in DCs

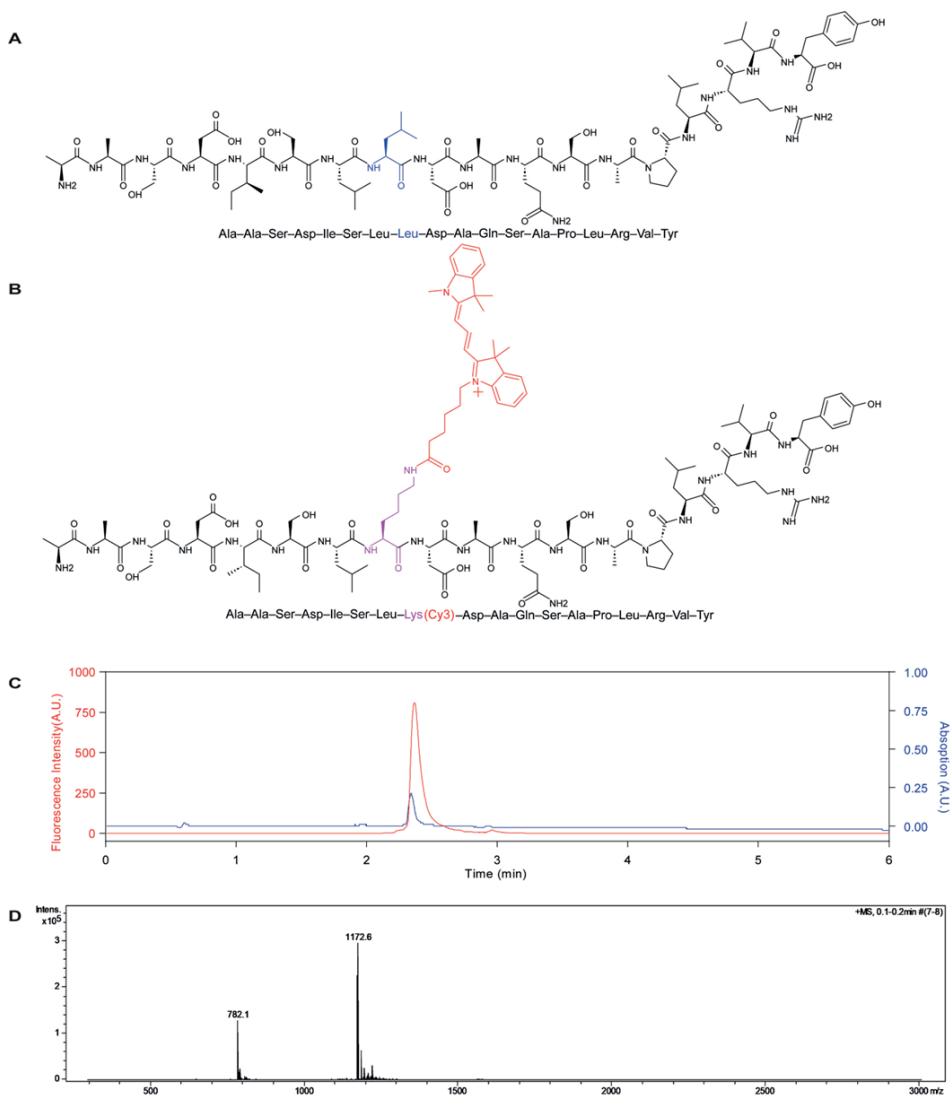


Figure 1. Structures of parent β -lactoglobulin-derived peptide (A) and Pep-Cy3 (B), UPLC chromatograms of Pep-Cy3 (C) used for determination of purity using UV detection at 210 nm (blue curve) and fluorescence detection at $\lambda_{\text{ex/em}} = 555/570$ nm (red curve) and (D) molecular mass of the synthesized Pep-Cy3 by mass spectrometry (Theoretical mass = 2343.3 g/mol; mass found (M2+) = 1172.6 and (M3+) = 782.1; and calculated mass = 2343.2 g/mol or 2343.3 g/mol).

Cy5 was conjugated to PLGA-COOH by using carbodiimide/NHS chemistry as described previously [30] (Figure 2A). Gel permeation chromatography (GPC) of the synthesized PLGA-Cy5 showed overlapping peaks at the same retention time when using the refractive index (RI) and UV detection at 650 nm (Figure 2B,C, respectively), while no free dye was detected (Figure 2C), which demonstrates the successful conjugation of the acceptor dye Cy5 to PLGA-COOH.

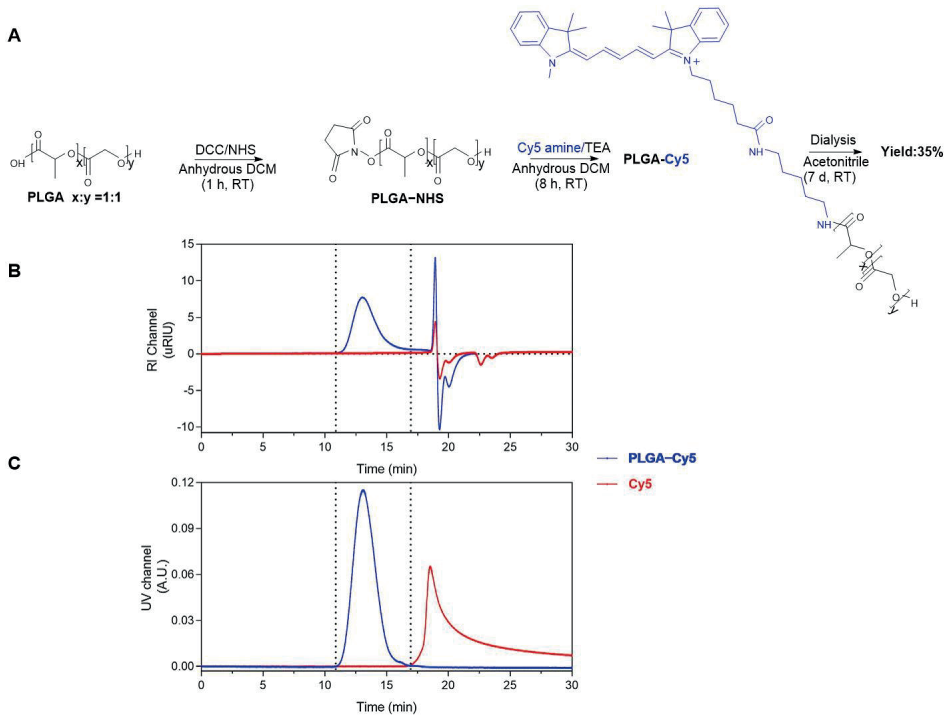


Figure 2. Synthesis and characterization of PLGA-Cy5. (A) Synthesis route of PLGA-Cy5 by conjugation of Cy5 amine to PLGA-COOH using carbodiimide/NHS chemistry. GPC analysis of PLGA-Cy5 conjugate (blue) and free Cy5 (red) by using refractive index (RI) detection (B) and UV detection at 650 nm (C).

Characteristics of Single- and Dual-Labeled PLGA Nanoparticles

The average NP diameter of fluorescent NPs ranged between 340 and 620 nm (Table 1). Positive correlations were found between fluorescence intensities and weight % of PLGA-Cy5 or Pep-Cy3, as well as the concentrations of the PLGA-Cy5 NPs and Pep-Cy3 NPs suspensions (Supplemental Figure S1). The fluorescence intensity of Cy3 or Cy5 leveled off with increasing particle concentration (Supplemental Figure S1) likely due to self-quenching. As reported in previous studies [25, 36], this self-quenching phenomenon is dye-concentration-dependent. To avoid this self-quenching, NPs prepared with a fixed amount of 1 wt% Pep-Cy3 in the feed were selected for the preparation of FRET NPs containing 1.5–9 wt% PLGA-Cy5, corresponding to molar feed ratios of donor dye (Cy3) /acceptor dye (Cy5) (D/A) ranging from 5:1 to 0.8:1. Furthermore, to reduce the particle size, the PLGA concentration in DCM was lowered from 50 to 40 mg/mL, which decreased the average diameter of the obtained NPs from 503 to 342 nm, except for the 7 and 9 wt% PLGA-Cy5 NP (Table 1). The latter NPs had significantly larger diameters of 600–631 nm (with PDI of 0.21-0.29). Nanosight measurements showed significantly smaller mean diameters of the NP, i.e., 361 nm and

170 nm, for the particles with 7 and 9 wt% PLGA-Cy5 NP, respectively, while FRET NP 0.8:1 containing an equivalent weight percentage of PLGA-Cy5 (9%) showed a similar NP size of ~230 nm when using DLS and Nanosight measurements (Table 1). Therefore, the discrepancy in the NP size of 7 and 9 wt% PLGA-Cy5 NP might be attributed to their size distribution that more strongly influences the DLS outcome than for Nanosight [37]. Consistent with our previous study [5], the zeta potentials of the fluorescent NPs (Table 1) ranged from -0.5 to -4.7 mV, demonstrating that they all have close-to-neutral surface charges.

Table 1. Characteristics of Pep-Cy3, PLGA-Cy5 and FRET nanoparticles.

Formulation (n = 1)	Nanosight Analysis ¹		Zetasizer Nano S ²		Zeta-Potential (mV)	EE ³ (%)	LC ⁴ (%)	Actual Molar Ratio Pep-Cy3: PLGA-Cy5	Yield (%)	E _{PR} ⁵ (%)
	D _h (nm)	D _h (nm)	PDI							
0.1% Pep-Cy3 NP *	-	616 ± 24	0.15 ± 0.06	-2.5 ± 0.1	-	-	-	-	63	-
0.5% Pep-Cy3 NP *	-	463 ± 19	0.22 ± 0.01	-2.1 ± 0.2	31	0.16	-	-	82	-
1% Pep-Cy3 NP *	-	338 ± 10	0.15 ± 0.01	-1.9 ± 0.4	31	0.31	-	-	73	-
1.5% Pep-Cy3 NP *	-	526 ± 10	0.20 ± 0.04	-1.8 ± 0.1	44	0.66	-	-	62	-
2% Pep-Cy3 NP *	-	574 ± 22	0.15 ± 0.02	-2.1 ± 0.2	51	1.02	-	-	77	-
Empty PLGA NP	291 ± 5	358 ± 5	0.13 ± 0.01	-2.5 ± 0.4	-	-	-	-	73	-
1.5% PLGA-Cy5 NP	330 ± 7	345 ± 5	0.09 ± 0.05	-2.6 ± 0.3	-	-	-	-	73	-
2% PLGA-Cy5 NP	304 ± 14	372 ± 9	0.12 ± 0.02	-2.5 ± 0.3	-	-	-	-	85	-
4% PLGA-Cy5 NP	309 ± 3	249 ± 6	0.08 ± 0.01	-3.2 ± 0.5	-	-	-	-	66	-
7% PLGA-Cy5 NP	361 ± 10	600 ± 6	0.29 ± 0.01	-2.5 ± 1.6	-	-	-	-	66	-
9% PLGA-Cy5 NP	170 ± 21	631 ± 5	0.21 ± 0.01	-2.1 ± 0.3	-	-	-	-	68	-
1% Pep-Cy3 NP	260 ± 12	253 ± 2	0.08 ± 0.02	-2.7 ± 0.3	30	0.30	-	-	56	-
FRET NP 0.8:1 (1% Pep-Cy3: 9% PLGA-Cy5)	227 ± 26	236 ± 3	0.05 ± 0.01	-2.1 ± 0.3	70	0.70	0.56:1	-	38	60
FRET NP 2:1 (1% Pep-Cy3: 4% PLGA-Cy5)	276 ± 5	240 ± 4	0.10 ± 0.03	-2.5 ± 0.5	24	0.24	0.43:1	-	48	26
FRET NP 4:1 (1% Pep-Cy3: 2% PLGA-Cy5)	295 ± 8	259 ± 2	0.09 ± 0.02	-2.6 ± 0.4	30	0.30	1.11:1	-	60	16
FRET NP 5:1 (1% Pep-Cy3: 1.5% PLGA-Cy5)	265 ± 6	217 ± 6	0.07 ± 0.04	-3.7 ± 1.0	16	0.16	0.77:1	-	58	14

* Formulations marked with * were prepared with 50 mg/mL PLGA in DCM, and the other formulations without * were prepared with 40 mg/mL PLGA in DCM. Percentages mentioned are the weight% of labeled compound within the nanoparticles. ¹ Measurement of hydrodynamic diameter (D_h) in quintuplicate. ² Measurement in triplicate (D_h: hydrodynamic diameter; PDI: Polydispersity Index). ³ EE: Encapsulation Efficiency. ⁴ LC: Loading capacity. ⁵ E_{PR}: FRET Proximity Ratio (Ratiometric FRET efficiency).

The encapsulation efficiency and loading capacity of the NPs increased with increasing feed ratios from 31 to 51% and 0.16 to 1.02%, respectively (Table 1). Similarly, the FRET NPs (Table 1) showed encapsulation efficiencies of the Pep-Cy3 ranging from 16 to 70%, with corresponding loading capacities ranging from 0.16 to 0.70%. The obtained peptide encapsulation and loading efficiencies are in agreement with our previous study [5].

Optimization of FRET Efficiency of the NPs Labeled with the Cy3 and Cy5

The spectra shown in Figure 3 were obtained by irradiating 0.5 mg/mL fluorescent NPs suspensions, namely the single-dye-labeled NPs (labeled with only Pep-Cy3 or PLGA-Cy5) and the FRET NPs (dual-labeled with both Pep-Cy3 and PLGA-Cy5), in PBS (pH 7.4) at the excitation wavelength of the donor dye Cy3 at λ_{ex} = 555 nm. As expected, 1 wt% Pep-Cy3 NP and 9 wt% PLGA-Cy5 NP showed low FRET emission at 662 nm upon excitation at 555 nm (i.e., red and black curves in Figure 3, respectively). Importantly, FRET peaks were clearly observed for Pep-Cy3 loaded in Cy5-labeled NPs prepared with

different feed ratios of donor-dye-labeled peptide cargo and acceptor-dye-labeled PLGA (see FRET NP in Figure 3) upon excitation at 555 nm and emission at 662 nm.

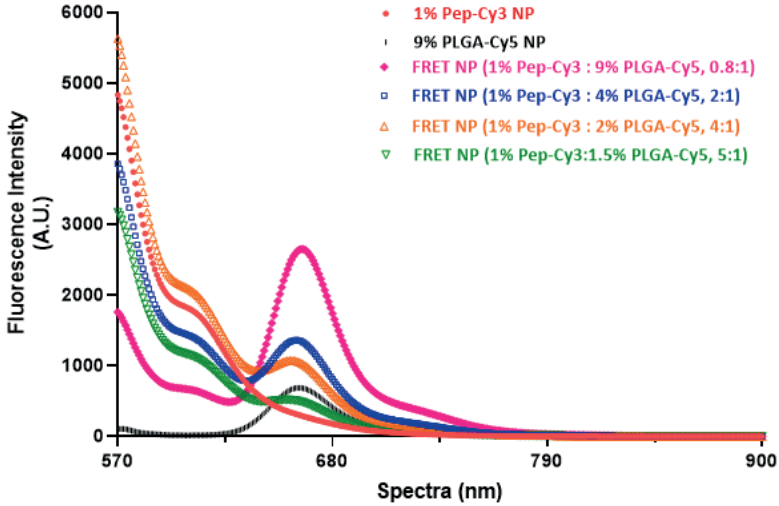


Figure 3. Fluorescence spectra in PBS (pH 7.4) at $\lambda_{ex} = 555$ nm: 0.5 mg/mL 9% PLGA-Cy5 NP (containing 9 wt% labeled polymer), 1% Pep-Cy3 NP (containing 1 wt% feed Pep-Cy3), and FRET NP (containing 1 wt% feed Pep-Cy3 and 1.5–9 wt% PLGA-Cy5).

To compare the ratiometric FRET efficiency of the FRET NPs of different feed Cy3/Cy5 molar ratios, the FRET proximity ratio (E_{PR}) was calculated according to the Equation (1) [38]:

$$E_{PR} = \frac{I_A}{I_A + I_D'} \quad (1)$$

Herein, I_A is acceptor dye Cy5 emission fluorescence intensity, and I_D' is donor dye Cy3 emission fluorescence intensity upon excitation of the donor dye.

As seen in Table 1, the FRET NPs showed increasing E_{PR} with decreasing D/A molar ratio up to 60% for particles prepared with a feed ratio of 1 wt% Pep-Cy3 and 9 wt% PLGA-Cy5 (i.e., 0.8:1, feed molar ratio of D/A). According to the encapsulation efficiency of Pep-Cy3, the actual D/A molar ratio of the FRET pair (Cy3/Cy5) in the FRET NP prepared with a feed ratio of 0.8:1 was 0.56:1 (Table 1), which resembles the highest FRET efficiency from a D/A ratio of about 0.5:1 as found in a previous study [39]. It is indeed likely that the highest loading capacity of Pep-Cy3 of 0.7% and highest weight percentage of PLGA-Cy5 of 9 wt% among the PLGA NPs in FRET NP 0.8:1 of similar NP size (~250 nm) concomitantly enhanced the FRET efficiency (E_{FRET}). In addition, the actual FRET efficiency E_{FRET} of FRET NP 0.8:1 was 87%, from which the average separation distance of the donor and acceptor dye was calculated as 3.6 nm (see Supplemental Materials for the corresponding calculations). In the remainder of this

paper, we used the NPs with this highest FRET efficiency, namely FRET NPs containing the 0.8:1 D/A ratio (i.e., including 1 wt% Pep-Cy3 and 9 wt% PLGA-Cy5). With the control Pep-Cy3 NPs, we refer to NPs loaded with 1 wt% Pep-Cy3, while PLGA-Cy5 NPs contained 9 wt% of the Cy5-labeled PLGA.

Colloidal Stability and Time-Dependent Fluorescence of Labeled PLGA NP in PBS and Biorelevant Fasted-State-Simulated Gastric Fluid

The colloidal stability (size and polydispersity) of a suspension of empty PLGA NP was determined in three different media. Neither changes in the NP size nor in polydispersity (PDI) of the PLGA NPs were observed in the different media over 168 h (Supplemental Figure S2A,B, blue and red and black curves, respectively), in accordance with a previous study [40]. The fluorescence stability of Pep-Cy3 NP, PLGA-Cy5 NP, and FRET NP was determined in the same media.

Supplemental Figure S3 shows the fluorescence spectra upon excitation at 555 nm at $t = 0$ h (top panels), which all have similar shapes and intensities in the different media. Upon incubation for 144 h in PBS (Figure 4C), the FRET peak at 662 nm of the FRET NP (black line) decreased to 72% of the initial value. The kinetics of this decrease is shown in Figure 4C (black squares), which was accompanied by a simultaneous increase in Cy3 fluorescence to 153% (Figure 4A, black dots) and a drop in Cy5 fluorescence intensity to 62% (Figure 4B, black stars) of their initial values. Similar results were obtained with the single-dye-labeled NP; the Cy3 fluorescence of Pep-Cy3 NP increased as well (by 115%, Figure 4A, red dots), whereas the Cy5 fluorescence of PLGA-Cy5 NP (Figure 4B, blue stars) decreased to 65% of its initial value in PBS.

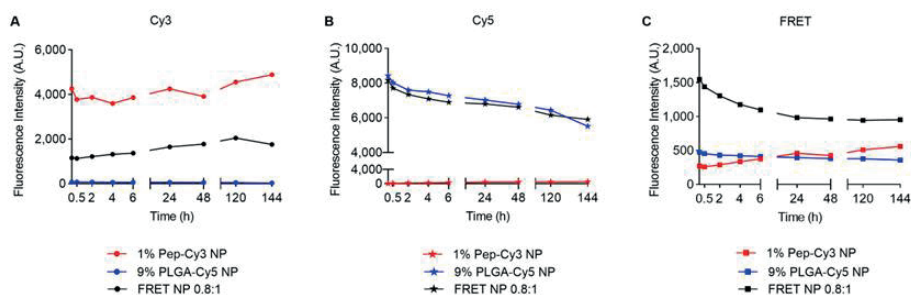


Figure 4. Fluorescence intensity of 0.2 mg/mL 1% Pep-Cy3 NP, 9% PLGA-Cy5 NP and FRET NP 0.8:1 (1 wt% Pep-Cy3:9 wt% PLGA-Cy5) incubated in PBS (pH 7.4) for 144 h at 37 °C. From left to right: fluorescence intensity of (A) Cy3 ($\lambda_{\text{ex/em}} = 555/570$ nm), (B) Cy5 ($\lambda_{\text{ex/em}} = 646/662$ nm), and (C) FRET ($\lambda_{\text{ex/em}} = 555/662$ nm).

In our recent study [41], the non-labeled BLG-peptide-loaded PLGA NP showed a burst release of 17% loading, followed by a slow release to 21% of the loading during the first 7 days in PBS at 37°C. This indicates that Pep-Cy3 in the present study, in line with the previous findings, was partly released from the PLGA NPs. Recently, Yang *et al.* [36] reported dequenching of Dil fluorescence mediated by the release of the Dil dye loaded in Cy5-labeled PLGA NP. In line with the study of Yang *et al.* [36], the observed increase in Cy3 fluorescence of both Pep-Cy3 NP and FRET NP probably points to the dequenching of Cy3 fluorescence due to the release of Pep-Cy3 from the PLGA NP. The release of Pep-Cy3 also resulted in less donor dye present in proximity (less than 10 nm) of the acceptor dye (Cy5)-conjugated PLGA matrix and explains the lower FRET fluorescence intensity over 144 h as shown in Figure 4C (black squares).

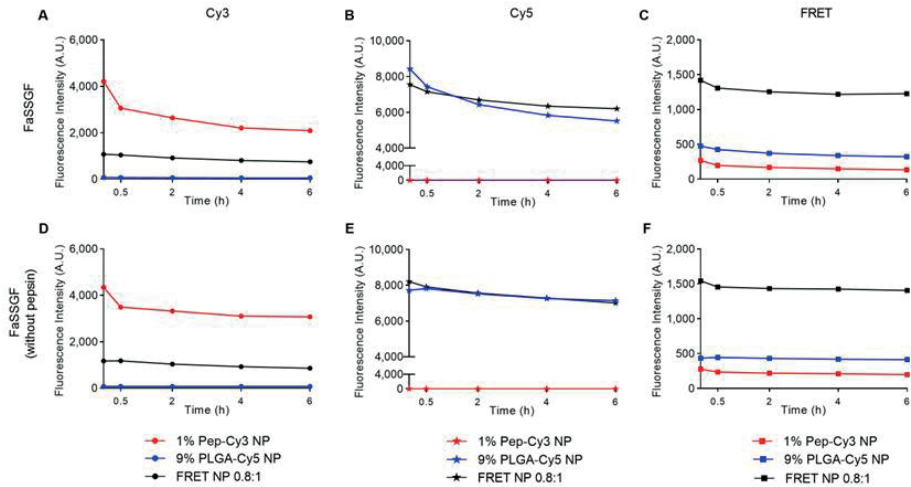


Figure 5. Fluorescence intensity of 0.2 mg/mL 1% Pep-Cy3 NP, 9% PLGA-Cy5 NP, and FRET NP 0.8:1 (1 wt% Pep-Cy3:9 wt% PLGA-Cy5), incubated for 6 h at 37 °C in FaSSGF (pH 1.6, with pepsin) (A–C) and in FaSSGF (pH 1.6, without pepsin) (D–F). From left to right: fluorescence intensity of Cy3 ($\lambda_{\text{ex/em}} = 555/570$ nm), Cy5 ($\lambda_{\text{ex/em}} = 646/662$ nm), and FRET ($\lambda_{\text{ex/em}} = 555/662$ nm).

To investigate the integrity and stability of the nanoparticles in biorelevant simulated gastric fluid, FRET NP and its single-labeled controls were incubated for 6 h in FaSSGF (pH 1.6, with or without pepsin) to predict their integrity during gastric passage. Figure 5C shows that upon incubation of the NPs in FaSSGF with pepsin, the fluorescence FRET intensity of the FRET NP (black squares) decreased slightly during 6 h of incubation to 86% of the initial value, accompanied by a decrease in the fluorescence intensity of Cy3 to 70% (Figure 5A) and of Cy5 to 82% of the initial value (Figure 5B). Similarly, when incubated for 6 h in FaSSGF without pepsin (Figure 5F), the

FRET fluorescence signal of the FRET NP decreased to 91% of the initial value, the fluorescence intensity of Cy3 to 74% (Figure 5D), and that of Cy5 to 85% of the initial value (Figure 5E). This means that the FRET NPs have sufficient stability to survive gastrointestinal conditions after oral administration and to reach their target, namely the intestinal dendritic cells.

Cellular Uptake of FRET NPs by Human Immature moDC and Their Intracellular Trafficking in Murine Dendritic Cells DC 2.4

Cellular uptake of antigen-encapsulated PLGA nanocarriers by human and murine DCs is critical for the effective modulation of the innate and adaptive immune response [8] and induction of allergen-specific tolerance [42]. Thus, we investigated the cellular uptake of FRET NP by both primary human moDC and human immature moDC cells.

Initially, we investigated the uptake of nanoparticles containing only the Cy3 label (on the peptide) by human immature moDC. Figure 6A,B show that the Pep-Cy3 NP did neither affect the cell viability nor the percentage of CD11c+CD14- moDC, as compared to control cells that were exposed to the medium only. This demonstrates that the particles have good cytocompatibility at concentrations below or equal to 0.1 mg/mL NP, as also reported by Kostadinova *et al.* [43]. In line with the previous finding of Waeckerle-Men *et al.* [44] that human immature moDC are capable of internalizing PLGA particles, flow cytometry analysis showed that 73% of the CD11c+CD14- moDC were positive for the Cy3 fluorescence signal (Figure 6C).

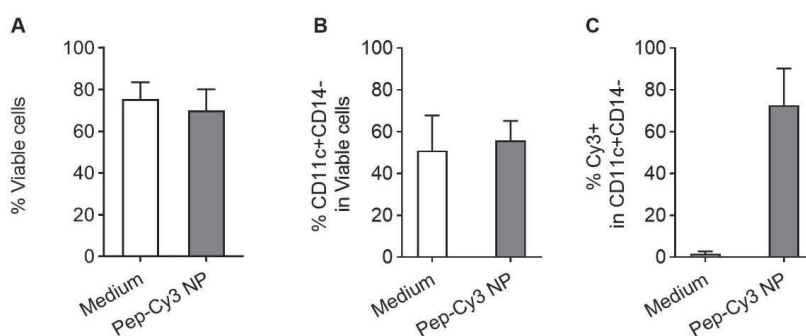


Figure 6. Flow cytometry data of human immature moDC after 2.5 h incubation with 0.06 mg/mL 2% Pep-Cy3 NP at 37 °C. Percentages of viable cells (A), CD11c+CD14- human moDC viable cells (B), and cellular uptake (Cy3-positive CD11c+CD14- cells) (C) were gated using medium-treated human immature moDC as control in the flow cytometry analysis. Data are presented as mean±SEM, $n = 3$. Human immature moDC were derived and cultured from three different donors.

In parallel, confocal fluorescence microscopy (CFM) images of these cells incubated with only the medium (Figure 7A) and Pep-Cy3 NP (Figure 7B) confirmed the internalization of Pep-Cy3 NP after 2.5 h of incubation and showed even higher brightness after 18.5 h of incubation (Figure 7C).

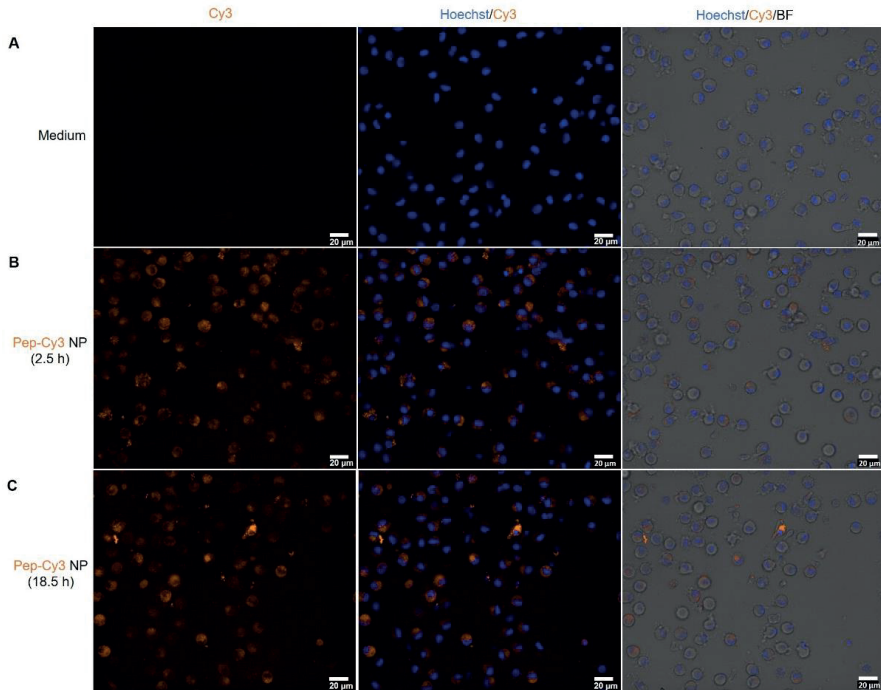


Figure 7. Representative fluorescent microscopy images of cellular uptake of 2% Pep-Cy3 NP (0.06 mg/mL) by day 7 human moDC: medium-treated control (A) and internalized 2% Pep-Cy3 NP after (B) 2.5 and (C) 18.5 h of incubation at 37 °C; bars indicate 20 µm.

As compared to the primary suspension culture of human moDC, the less costly and more accessible immortalized murine DC 2.4 cell line was selected for further investigations of intracellular trafficking of PLGA nanoparticles and encapsulated peptide. Murine DC 2.4 cells were incubated with PLGA-Cy5 NP, Pep-Cy3 NP, and FRET NP and imaged by CFM. It is noted that non-internalized particles of >200 nm could not be separated from the moDC by washing and centrifugation at 300× *g*. Likely, these bigger particles co-sediment with the cells during centrifugation. Therefore, the nanoparticles were filtered before exposure to the cells, using a 0.2 µm RC membrane filter. As shown in Supplemental Table S2, some fluorescence was lost after filtration of the 0.5 mg/mL Pep-Cy3 NP and FRET NP; 0.9 µg/mL of encapsulated Pep-Cy3, corresponding with particle concentrations of 0.30 and 0.14 mg/mL, respectively, remained in the samples after filtration. Therefore, for proper comparison with free

Pep-Cy3 controls, we applied 1 $\mu\text{g}/\text{mL}$ of the free peptide in the following experiments. Even more of the PLGA-Cy5 NP suspension was lost after filtration (Supplemental Table S2) due to their larger mean NP size (631 nm as compared to 236 nm for the FRET NP), resulting in 0.03 mg/mL PLGA-Cy5 NP, which is much lower than 0.14 mg/mL for the FRET NP. This might explain the discrepancy of Cy5 fluorescence intensity observed for cells incubated with the PLGA-Cy5 NP and FRET NP at 2 h after incubation, as shown in the top panels of Figure 8B and the zoomed-out images in Supplemental Figure S4A.

First, images were taken after 2.5 h of exposure of the murine DCs with the NPs, washing, and 2 h of further incubation (top panels of Figure 8B). These images show partial accumulation and heterogeneous distribution of Cy3 fluorescence in DC 2.4 cells incubated with the free Pep-Cy3, while cells incubated with FRET NP showed a more homogeneous intracellular distribution with few separate spots of orange Cy3 fluorescence from internalized FRET NP (see also Cy3 signal only, in the left panel of Figure 8C). These spots might be attributed to the accumulation of free and encapsulated Pep-Cy3 in endosomes of DC. The uptake of soluble antigens by DC is mainly mediated by macropinocytosis [45], while the internalization of PLGA NP with an NP size of ~ 290 nm by the same cells is mediated by phagocytosis, as previously shown by Diwan *et al.* [46], which might explain the observed difference in the intracellular distribution of free Pep-Cy3 and encapsulated Pep-Cy3 in FRET NP.

It is noted that Cy3 fluorescence is diminished in FRET NP (see also Cy3 signal only, in the left panel of Figure 8C) likely due to the self-quenching and quenching effect by non-radioactive energy transfer from the emission of Cy3 to the acceptor Cy5. Indeed, Figure 9A shows Cy3 fluorescence colocalized with the FRET signal, as indicated by the arrows, suggesting the integrity of internalized FRET NP at 2 h post-incubation.

Upon continued incubation, PLGA NP might be partially degraded in the lysosomal compartments of dendritic cells 24 h post incubation [25] and/or endo-lysosomal escape [25, 47, 48]. At the 24 h time point (Figure 8C, right panel), the Cy3 fluorescence of FRET NP retained the spot-like pattern, albeit with lower intensity, while the Cy3 fluorescence was predominantly cleared from cells incubated with free Pep-Cy3. The observed short retention time of internalized free Pep-Cy3 is consistent with the previously reported retention time of less than 24 h for ovalbumin (OVA) taken up by dendritic cells [49, 50]. To maintain intracellular homeostasis, internalized exogenous

proteins and/or nanoparticles are eliminated by energy-dependent lysosome-mediated exocytosis [51, 52], which was found to be faster for low-molecular-weight solutes and slower for PLGA nanoparticles [52]. In fact, Figure 8B demonstrates that the internalized FRET NP remained in the DC for at least 144 h, which demonstrates a significantly longer retention time within the cells as compared to the free Pep-Cy3 at an equivalent dose. To further explain, after internalization of the free Pep-Cy3, it is translocated from macropinosomes to early endosomes, which subsequently matured into late endolysosomes for MHCII presentation on the surface of DCs [53]. On the other hand, after phagocytosis by DC, the internalized FRET NP localized in endosomes [54], which possibly underwent a similar intracellular process as an internalized soluble peptide for MHCII presentation [55].

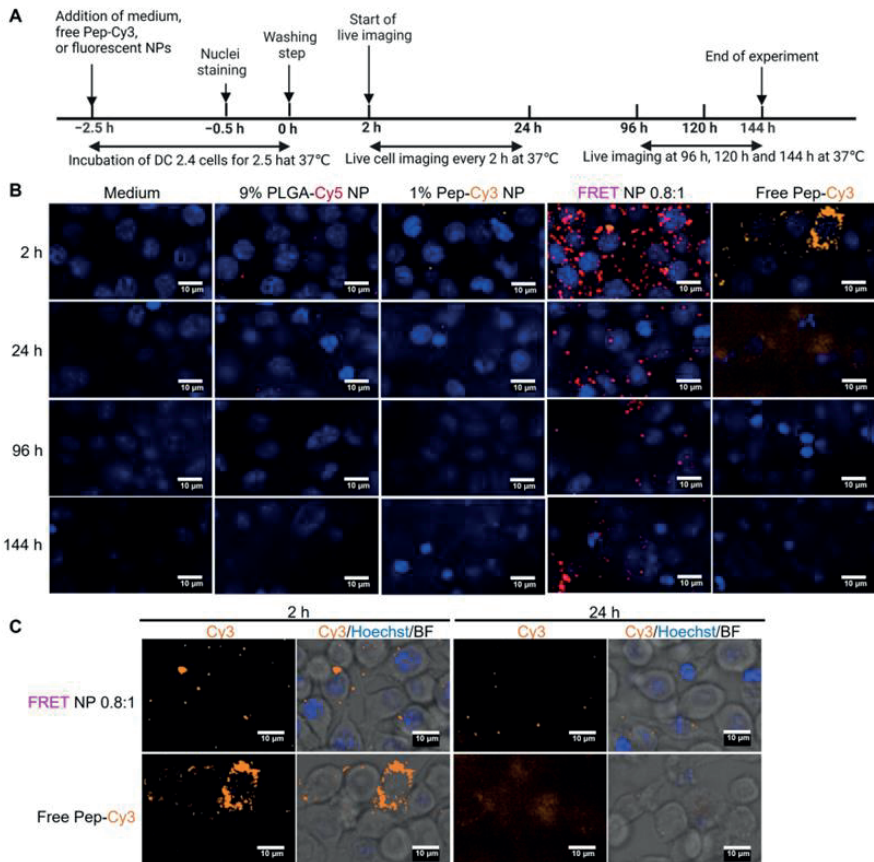


Figure 8. (A) Experimental scheme and (B) cellular images of internalized fluorescent nanoparticles and free Pep-Cy3 by murine DC 2.4. Cells were washed and live-imaged over 144 h after 2.5 h of incubation of DC 2.4 cells with medium, 9% PLGA-Cy5 NP, 1% Pep-Cy3 NP, FRET NP 0.8:1 (1% Pep-Cy3:9% PLGA-Cy5), or 1 $\mu\text{g}/\text{mL}$ free Pep-Cy3. Shown are representative merged confocal fluorescence microscopy images (B) of nuclei (Hoechst, blue, $\lambda_{\text{ex}} = 405 \pm 5$ nm), Cy3 (orange, $\lambda_{\text{ex}} = 561 \pm 2$ nm), Cy5 (red, $\lambda_{\text{ex}} = 640 + 4/-5$ nm), and FRET ($\lambda_{\text{ex}} = 561 \pm 2$ nm) taken 2, 24, 96, and 144 h after

the washing step; bars indicate 10 μm . (C) Fluorescence from the FRET NP 0.8:1 and free Pep-Cy3 treated DC 2.4 cells in confocal image of Cy3 alone and merged confocal images of Cy3 (orange), nuclei (Hoechst, blue), and bright field (BF, confocal path) 2 (left panel) and 24 h (right panel) after the washing step, respectively.

To focus on DC 2.4 cells incubated with FRET NP only, Figure 9 and the same but zoomed-out images in Supplemental Figure 5 show from the left to the right the separate confocal microscopy images of Cy3, Cy5, and FRET fluorescence channels and their merged confocal fluorescence microscopy images at different incubation times. Colocalization of Cy3, Cy5, and the FRET signal was observed and exemplified by the numbered arrows pointing towards the same spot in every image at each time point (2–144 h).

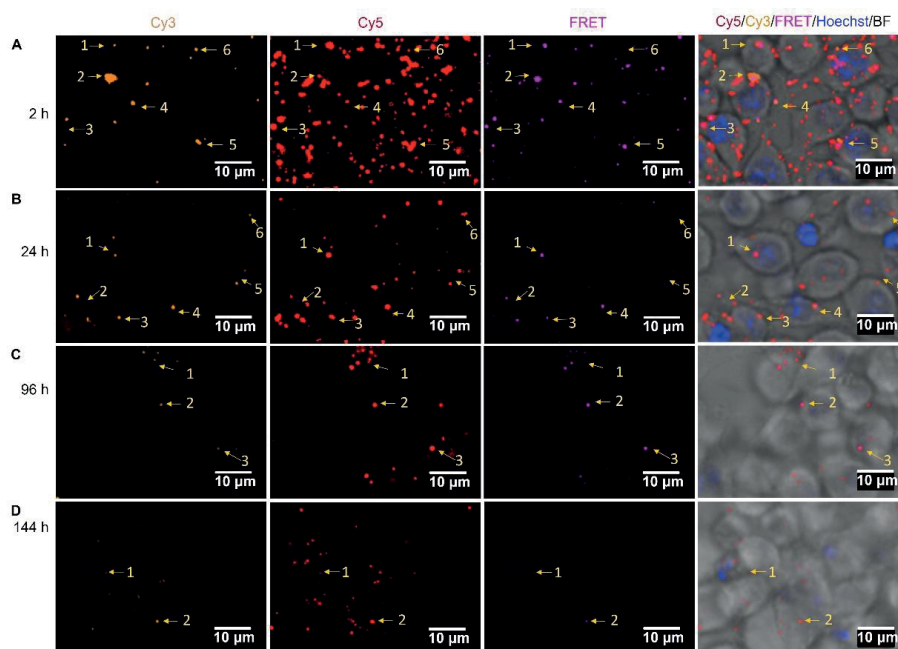


Figure 9. Intracellular localization of FRET NP after internalization by DC 2.4 cells. According to the scheme of Figure 8A, DC 2.4 cells were incubated with FRET NP 0.8:1 (1% Pep-Cy3:9% PLGA-Cy5) for 2.5 h and subsequently washed. Shown are representative confocal fluorescence microscopy images of DC 2.4 cultured with FRET NP (A) 2, (B) 24, (C) 96, and (D) 144 h after the washing step; bars indicate 10 μm . Colocalizations of Cy3 (orange, $\lambda_{\text{ex}} = 561 \pm 2 \text{ nm}$), Cy5 (red, $\lambda_{\text{ex}} = 640 + 4/-5 \text{ nm}$), and FRET (purple, $\lambda_{\text{ex}} = 561 \pm 2 \text{ nm}$) fluorescence are indicated with the yellow arrows and numbers.

Live images in Figure 9B showed a considerable loss of intracellular FRET signal (purple spots) after 24 h, which may be caused by the release of Pep-Cy3 from the FRET NP. At the 96 h time point (Figure 9C), the colocalization of Cy3, Cy5, and the FRET signal was still visible, while at the same time point, full clearance of Cy3 fluorescence was observed for the free Pep-Cy3-incubated DC 2.4 cells (Figure S4C). At 144 h, although Cy5 and Cy3 fluorescence remained detectable, the FRET signal was cleared (Figure 9D

and the same but zoomed-out images in Supplemental Figure S5D), suggesting the quantitative intracellular release of Pep-Cy3 and/or complete degradation of the internalized FRET NP. Our findings demonstrate that PLGA nanoparticles prolong the intracellular presence of encapsulated Pep-Cy3 in dendritic cells, which might be attributed to the endosomal escape of the PLGA nanoparticles into the cytosol [54]. Given the short life span of dendritic cells of less than 9 days [56], the prolonged intracellular presence of the peptide upon incubation with peptide-loaded PLGA nanoparticles may result in a prolonged period of peptide presentation via MHCII by the DC to the T-cell receptor (TCR) of antigen-specific T-cells. This, in turn, may contribute to the efficiency of inducing peptide-specific tolerogenic T-cell responses to induce oral tolerance using a relatively low dose of the peptide.

To investigate whether the β -lactoglobulin-derived peptide-loaded NPs could be internalized and processed by dendritic cells resulting in the intracellular release of the peptide, we exploited nanoparticles with high FRET emission that were obtained by dual labeling of the PLGA nanocarrier (Cy5) and the encapsulated peptide cargo (Cy3). Our study demonstrates sufficient stability and integrity of the peptide-loaded PLGA nanoparticles (FRET NP) in the simulated GI tract conditions, and very efficient cellular uptake of peptide-loaded NP by human moDC as confirmed by fluorescence microscopy imaging and flow cytometry. As compared to a 24 h retention time of the non-encapsulated peptide, prolonged retention of the encapsulated peptide cargo for 96 h by DC 2.4 was demonstrated. Collectively, we show here that NP with a dual FRET labeling strategy of both the peptide cargo and the nanocarriers provides a novel biometric tool to obtain valuable insights on the trafficking and processing of peptide-loaded NPs in DC *in vitro*.

Conclusions

To investigate whether the β -lactoglobulin-derived peptide-loaded NPs could be internalized and processed by dendritic cells resulting in the intracellular release of the peptide, we exploited nanoparticles with high FRET emission that were obtained by dual labeling of the PLGA nanocarrier (Cy5) and the encapsulated peptide cargo (Cy3). Our study demonstrates sufficient stability and integrity of the peptide-loaded PLGA nanoparticles (FRET NP) in the simulated GI tract conditions, and very efficient cellular uptake of peptide-loaded NP by human moDC as confirmed by fluorescence microscopy imaging and flow cytometry. As compared to a 24 h retention time of the non-encapsulated peptide, prolonged retention of the encapsulated peptide cargo for 96 h by DC 2.4 was demonstrated. Collectively, we show here that NP with a dual FRET

labeling strategy of both the peptide cargo and the nanocarriers provides a novel biometric tool to obtain valuable insights on the trafficking and processing of peptide-loaded NPs in DC *in vitro*.

Acknowledgements: ML is financially supported by China Scholarship Council (CSC), grant number 201707720004 and receive additional bench fee funding is supplied by Danone Nutricia Research B.V., Utrecht, the Netherlands.

Supporting Information

Supporting Data

Calculation and interpretation of FRET efficiency of FRET NP 0.8:1

The actual highest E_{FRET} was calculated from the decrease in the Cy3 fluorescence intensity at $\lambda_{ex/em}=555/570$ nm of a suspension of FRET NP 0.8:1, relative to that of a suspension of Pep-Cy3 NP (with 0.7% loading of Pep-Cy3) at a concentration of 0.5 mg/mL in PBS at room temperature (**equation 1** [22, 57]):

$$E_{FRET} = 1 - \frac{\bar{I}_{DA}}{\bar{I}_D}, \quad (1)$$

in which \bar{I}_{DA} and \bar{I}_D are the normalized donor fluorescence (Cy3) intensities at $\lambda_{ex/em}=555/570$ nm in the presence and absence of the acceptor (Cy5), respectively. \bar{I}_{DA} is the donor (Cy3) fluorescence intensity at $\lambda_{ex/em}=555/570$ nm of FRET NP 0.8:1 (1757 A.U.) that was normalized by subtraction of the background signal of 9 wt% PLGA-Cy5 NP (98 A.U.). The donor (Cy3) fluorescence intensity \bar{I}_D (4832 A.U.) was obtained from the 1 wt% Pep-Cy3 NP, however these have a lower loading of Pep-Cy3 (0.3%) than that of the FRET NP 0.8:1 (0.7%). Therefore, we had to correct for this difference and multiplied the measured fluorescence intensity I_D by a factor of 0.7/0.3. These normalizations result finally in the following calculation (**equation 2**):

$$E_{FRET} = 1 - \frac{\bar{I}_{FRET NP 0.8:1} - \bar{I}_{9\% PLGA-Cy5 NP}}{\bar{I}_{1\% Pep-Cy3 NP} \times \frac{LC_{FRET NP 0.8:1}}{LC_{1\% Pep-Cy3 NP}}} = 1 - \frac{1757-98}{4832 \times \frac{0.7}{0.3}} = 0.87 \text{ or } 87\%, \quad (2)$$

Concluding from this, the encapsulation efficiency of Pep-Cy3 is sufficient to obtain a high FRET efficiency (87%) in the dual labeled FRET NP 0.8:1 dispersed in PBS (pH 7.4). The observed FRET fluorescence is contributed to the large spectral overlap of the selected Cy3-Cy5 pair as donor and acceptor, respectively. The large spectral overlap integral $J(\lambda)$ is calculated from the integral of the normalized donor Cy3 emission intensity \bar{I}_D ($\int \bar{I}_D d\lambda = 1$), multiplied by the extinction coefficient of the acceptor Cy5 ε_A (25,000 mol⁻¹ cm⁻¹) [21] and by the wavelength to fourth power according to the **equation 3**[22].

$$J(\lambda) = \int \bar{I}_D \varepsilon_A \lambda^4 d\lambda, \quad (3)$$

The observed Förster distance (R_0) is defined as the separation distance between the donor and acceptor that corresponds to 50% FRET efficiency and is calculated with **equation 4** [25].

$$R_0 = 0.0211(\kappa^2 \Phi_D n^4 J(\lambda))^{1/6}, \quad (4)$$

Herein, $\kappa^2 = 2/3$ is the FRET orientation factor [58], $n = 1.445$ is the refractive index of PLGA [59], $\Phi_D = 0.15$ is the donor Cy3 quantum yield [21] and $J(\lambda)$ (for FRET pair Cy3/Cy5)

is calculated as $7.6 \times 10^{15} \text{ M}^{-1} \text{ cm}^{-1} \text{ nm}^4$ using equation (1). Thus, R_0 is equal to 50 Å (5.0 nm). Practically, efficient non-radioactive energy transfer only occurs when the separation distance between the acceptor and donor is within the range between 0.5-1.5 R_0 (Förster distance) (2.5-7.4 nm) [21, 60]. In conclusion, the occurrence of FRET indicates a proximity (between 2.5-7.4 nm) between the donor and acceptor dyes in the PLGA nanoparticles.

Förster distance (R_0) of 5 nm is the separation distance of D (Cy3) and A (Cy5) in PLGA NP, when assuming a FRET efficiency (E_{FRET}) of 50%. However, the actual E_{FRET} was 87% as calculated by using **equation 3**. Therefore, the actual dye pair distance is smaller. Indeed, the energy transfer mediated by dipole-dipole interactions by the donor and acceptor dye is highly dependent on the separation distance (r), and depends on the Förster distance R_0 as expressed by **equation 5** [21, 22]:

$$E_{\text{FRET}} = \frac{1}{1 + \left(\frac{r}{R_0}\right)^6}, \quad (5)$$

Therefore, from **equation 1** and the previously calculated E_{FRET} (87%) and R_0 (5.0 nm), the actual average separation distance (r) between the donor (Cy3) and acceptor (Cy5) in the FRET NP 0.8:1 is 3.6 nm, which is again between 0.5-1.5 R_0 (Förster distance, 2.5-7.4 nm) to allow occurrence of FRET signal.

Thus, we can conclude that dual labeled FRET nanocarriers of ~250 nm at a D/A ratio of 0.56:1 enables efficient non-radioactive energy transfer from the Cy3 labeled Peptide to the Cy5 labeled PLGA NP matrix with a close average proximity between Cy3 and Cy5 of 3.6 nm.

Supporting Tables and Figures

Supplemental Table 1. Cy3 fluorescence intensity of 1 mg/mL 2% Pep-Cy3 NP in RPMI 1640 medium before and after filtration with 0.2 μ m RC membrane syringe filter.

NP suspension	FI ¹ -Cy3 at $\lambda_{ex/em}$ = 555/570 nm (A.U.)			
	Non-filtered	Filtered	FI ratio of Filtered/Non-filtered	Filtrated NP ² (mg/mL)
2% Pep-Cy3 NP	9006	1071	0.12	0.12

¹ FI: Fluorescence intensity

² $\text{Concentration}_{\text{filtered NP}} \left(\frac{\text{mg}}{\text{mL}} \right) = \frac{\text{FI}_{\text{filtered NP}} (\text{A.U.})}{\text{FI}_{\text{non-filtered NP}} (\text{A.U.})} \times \text{Concentration}_{\text{non-filtered NP}} \left(\frac{\text{mg}}{\text{mL}} \right) = \frac{\text{FI}_{\text{filtered NP}} (\text{A.U.})}{\text{FI}_{\text{non-filtered NP}} (\text{A.U.})} \times 1 \left(\frac{\text{mg}}{\text{mL}} \right)$

Supplemental Table 2.^a Cy3, Cy5 and FRET fluorescence intensity of 0.5 mg/mL 1% Pep-Cy3 NP, 9% PLGA-Cy5 NP and FRET NP 0.8:1 in RPMI 1640 medium before and after filtration with 0.2 μm Regenerated Cellulose membrane syringe filter.

NP suspension	FI ³ -Cy3 at $\lambda_{ex/em}$ = 555/570 nm			FI-Cy5 at $\lambda_{ex/em}$ = 646/662 nm			FI-FRET at $\lambda_{ex/em}$ = 555/662 nm			Loaded Pep-Cy3 in the filtration ⁴ (μg/mL)
	FI (A.U.) Non- filtered	FI Ratio of Filtered/Non- filtered	Filtered NPs (mg/mL)	FI (A.U.) Non- filtered	FI Ratio of Filtered/Non- filtered	Filtered NP (mg/mL)	FI (A.U.) Non- filtered	FI Ratio of Filtered/ Non- filtered	Filtered NP (mg/mL)	
1% Pep-Cy3 NP	1839	0.59	0.30	-	-	-	-	-	-	0.9
9% PLGA-Cy5 NP	-	-	-	10000	0.10	0.05	-	-	-	-
FRET NP 0.8:1	2346	0.26	0.13	10000	0.56	0.28	2752	0.27	0.14	0.9

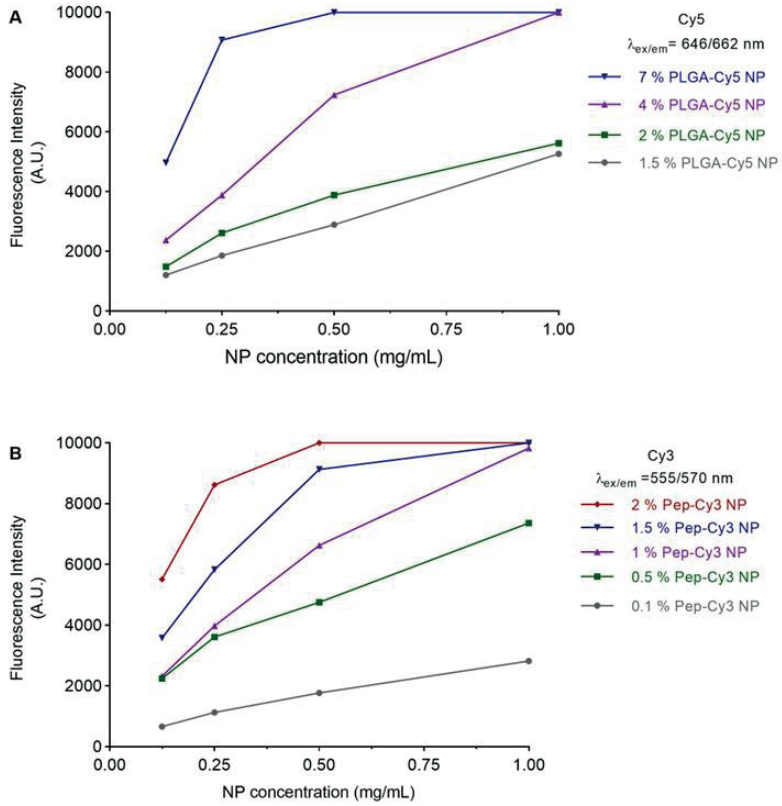
^a Cy5 fluorescence intensity of PLGA-Cy5 and FRET NP before filtration exceeded the maximum of 10,000 A.U. that can be measured by our machine. Measured FI-Cy5 of filtered FRET NPs was 5,583 A.U., showing loss of NPs by filtration. Indeed, from Cy3 and FRET fluorescence data (see Table) it can be concluded that just 26-27% of FRET NPs remained after filtration. Therefore, the Cy5 fluorescence intensity of the stock suspension before filtration was expected to have been 5,583/0.265=21,068 A.U. It is assumed that the stock suspension of PLGA-Cy5 NPs would have given the same FI of 21,068 A.U. as for the FRET NPs, since both contained the same amount of Cy5 labeled polymer. After filtration of the PLGA-Cy5 NPs we measured 1007 A.U., which would suggest that only 5% remained after filtration, which is equal to 0.03 mg/mL.

³ FI: Fluorescence intensity

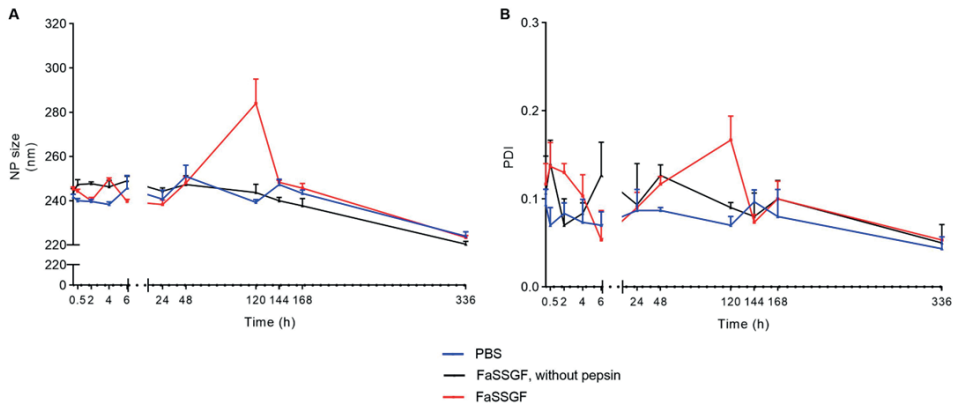
⁴ $\text{Concentration}_{\text{loaded Pep-Cy3}} \left(\frac{\mu\text{g}}{\text{mL}} \right) = \text{Concentration}_{\text{filtered NP}} \left(\frac{\text{mg}}{\text{mL}} \right) \times \text{Loading capacity}_{\text{Pep-Cy3}} (\%) \times 1000$

⁵ $\text{Concentration}_{\text{filtered NP}} \left(\frac{\text{mg}}{\text{mL}} \right) = \frac{\text{FI}_{\text{filtered NP}} (\text{A.U.})}{\text{FI}_{\text{non-filtered NP}} (\text{A.U.})} \times \text{Concentration}_{\text{non-filtered NP}} \left(\frac{\text{mg}}{\text{mL}} \right) = \frac{\text{FI}_{\text{filtered NP}} (\text{A.U.})}{\text{FI}_{\text{non-filtered NP}} (\text{A.U.})} \times 0.5 \left(\frac{\text{mg}}{\text{mL}} \right)$

CHAPTER FOUR

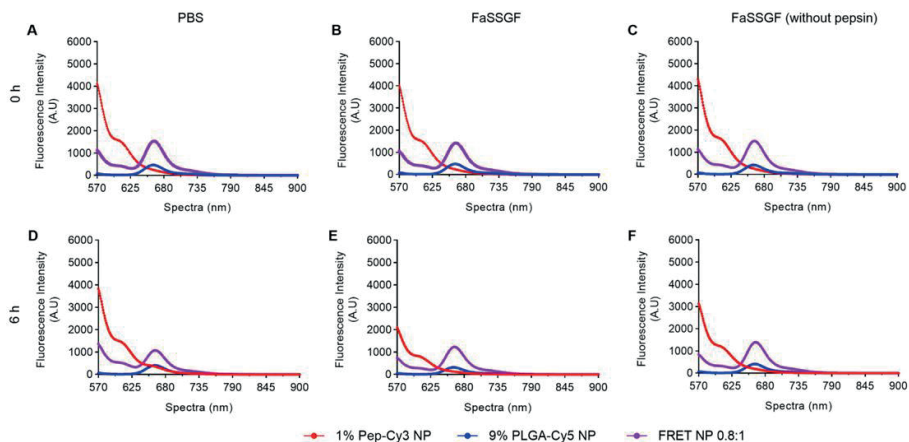


Supplemental Figure 1. Concentration dependent fluorescence intensity of (A) 1.5-7% PLGA-Cy5 NPs at $\lambda_{ex/em}=646/662$ nm and 0.1-2% Pep-Cy3 NPs $\lambda_{ex/em}=555/570$ nm in PBS.

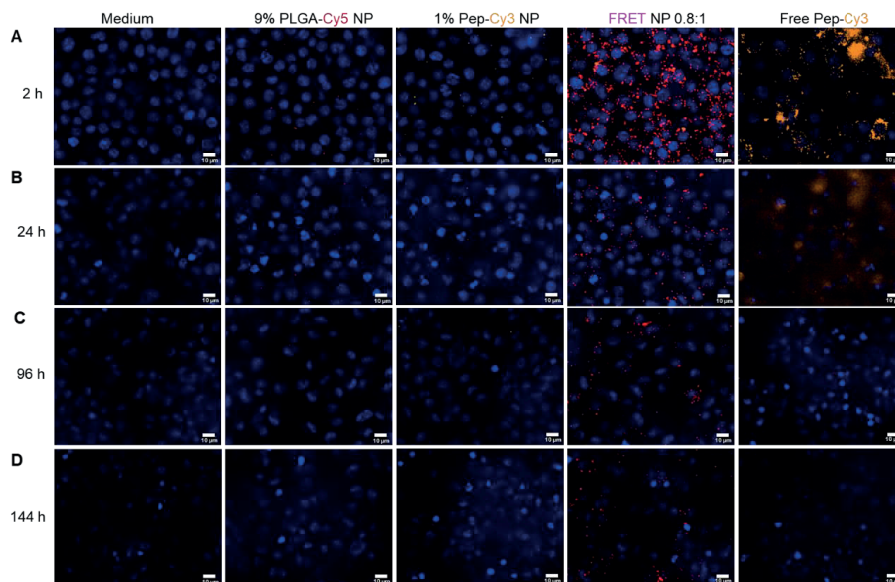


Supplemental Figure 2. Mean NP size (A) and polydispersity index (PDI) (B) of empty PLGA NP incubated in different media at 37 °C over 336 h as determined by Zetasizer Nano S. Data are presented as mean \pm SEM, and SEM is derived from 3 different measurements of one sample.

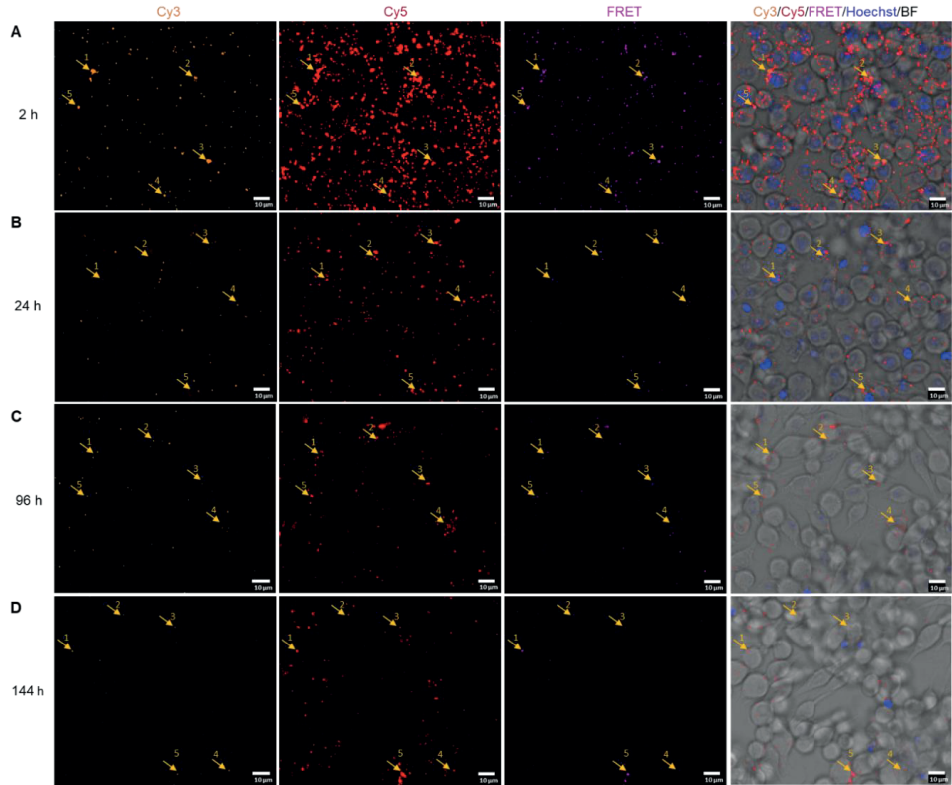
Live cell imaging by Förster Resonance Energy Transfer fluorescence to study trafficking of PLGA NP and release of a loaded peptide in DCs



Supplemental Figure 3. Fluorescence spectra obtained after 0 h (top) and 6 h (bottom) at $\lambda_{ex/em}$ =555/570-900 nm of 0.2 mg/mL 1% Pep-Cy3 NP, 9% PLGA-Cy5 NP and FRET NP 0.8:1 (1% Pep-Cy3:9% PLGA-Cy5) incubated at 37 °C in (A) PBS (pH 7.4), (B) in FaSSGF (pH 1.6) with pepsin and (C) in FaSSGF (pH 1.6) without pepsin for 0 and 6 h.



Supplemental Figure 4. Cellular images of internalized fluorescent nanoparticles and free Pep-Cy3 by murine DC 2.4. According to the scheme of Figure 8A, cells were washed and live imaged over 144 h after 2.5 h-incubation of DC 2.4 cells with medium, 9% PLGA-Cy5 NP, 1% Pep-Cy3 NP, FRET NP 0.8:1 (1% Pep-Cy3:9% PLGA-Cy5) or 1 μg/mL free Pep-Cy3. Shown are representative merged confocal fluorescence microscopy images (B) of nuclei (Hoechst, blue, λ_{ex} =405±5 nm), Cy3 (orange, λ_{ex} =561±2 nm), Cy5 (red, λ_{ex} =640+4/-5 nm) and FRET (λ_{ex} =561±2 nm) taken at (A) 2, (B) 24, (C) 96 and (D) 144 h after the washing step, bars indicate 10 μm.



Supplemental Figure 5. Intracellular localization of FRET NP after internalization by DC 2.4 cells. According to the scheme of Figure 8A, DC 2.4 cells were incubated with FRET NP 0.8:1 (1% Pep-Cy3:9% PLGA-Cy5) for 2.5 h and subsequently washed. Shown are representative confocal fluorescence microscopy images of DC 2.4 cultured with FRET NP at (A) 2, (B) 24, (C) 96 and (D) 144 h after the washing step respectively, bars indicate 10 μm . Colocalizations of Cy3 (orange, $\lambda_{\text{ex}}=561\pm 2$ nm), Cy5 (red, $\lambda_{\text{ex}}=640+4/-5$ nm) and FRET (purple, $\lambda_{\text{ex}}=561\pm 2$ nm) fluorescence are indicated with the yellow arrows and numbers.

References

- [1] Y. Xiong, G. Xu, M. Chen, H. Ma, Intestinal Uptake and Tolerance to Food Antigens, *Front Immunol*, 13 (2022) 906122.
- [2] M.P. Domogalla, P.V. Rostan, V.K. Raker, K. Steinbrink, Tolerance through Education: How Tolerogenic Dendritic Cells Shape Immunity, *Front Immunol*, 8 (2017) 1764.
- [3] B.C. van Esch, B. Schouten, S. de Kivit, G.A. Hofman, L.M. Knippels, L.E. Willemsen, J. Garssen, Oral tolerance induction by partially hydrolyzed whey protein in mice is associated with enhanced numbers of Foxp3+ regulatory T-cells in the mesenteric lymph nodes, *Pediatr Allergy Immunol*, 22 (2011) 820-826.
- [4] L.A. Meulenbroek, B.C. van Esch, G.A. Hofman, C.F. den Hartog Jager, A.J. Nauta, L.E. Willemsen, C.A. Bruijnzeel-Koomen, J. Garssen, E. van Hoffen, L.M. Knippels, Oral treatment with beta-lactoglobulin peptides prevents clinical symptoms in a mouse model for cow's milk allergy, *Pediatr Allergy Immunol*, 24 (2013) 656-664.
- [5] M. Liu, S. Thijssen, C.F. van Nostrum, W.E. Hennink, J. Garssen, L.E.M. Willemsen, Inhibition of cow's milk allergy development in mice by oral delivery of beta-lactoglobulin-derived peptides loaded PLGA nanoparticles is associated with systemic whey-specific immune silencing, *Clin Exp Allergy*, 52 (2022) 137-148.
- [6] A. Miquel-Clopes, E.G. Bentley, J.P. Stewart, S.R. Carding, Mucosal vaccines and technology, *Clin Exp Immunol*, 196 (2019) 205-214.
- [7] P. Gu, A. Wusiman, Y. Zhang, Z. Liu, R. Bo, Y. Hu, J. Liu, D. Wang, Rational Design of PLGA Nanoparticle Vaccine Delivery Systems To Improve Immune Responses, *Mol Pharm*, 16 (2019) 5000-5012.
- [8] A.L.R. Silva, R. A. Varypataki, E. Sibuea, S. Ossendorp, F. Jiskoot, W., Poly-(lactic-co-glycolic-acid)-based particulate vaccines: particle uptake by dendritic cells is a key parameter for immune activation, *Vaccine*, 33 (2015) 847-854.
- [9] G. Cappellano, C. Comi, A. Chiocchetti, U. Dianzani, Exploiting PLGA-Based Biocompatible Nanoparticles for Next-Generation Tolerogenic Vaccines against Autoimmune Disease, *Int J Mol Sci*, 20 (2019).
- [10] T. Chen, W. Liu, S. Xiong, D. Li, S. Fang, Z. Wu, Q. Wang, X. Chen, Nanoparticles Mediating the Sustained Puerarin Release Facilitate Improved Brain Delivery to Treat Parkinson's Disease, *ACS Appl Mater Interfaces*, 11 (2019) 45276-45289.
- [11] S. Rahimian, M.F. Fransen, J.W. Kleinovink, M. Amidi, F. Ossendorp, W.E. Hennink, Particulate Systems Based on Poly(Lactic-co-Glycolic)Acid (pLGA) for Immunotherapy of Cancer, *Curr Pharm Des*, 21 (2015) 4201-4216.
- [12] J.W. Gouw, J. Jo, L. Meulenbroek, T.S. Heijger, E. Kremer, E. Sandalova, A.C. Knulst, P.V. Jeurink, J. Garssen, A. Rijnierse, L.M.J. Knippels, Identification of peptides with tolerogenic potential in a hydrolysed whey-based infant formula, *Clin Exp Allergy*, 48 (2018) 1345-1353.
- [13] E.B. Tiziana Sturniolo, Jiayi Ding, Laura Raddrizzani, Oezlem Tuereci, Ugur Sahin, Michael Braxenthaler, Fabio Gallazzi, Maria Pia Protti, Francesco Sinigaglia, and Juergen Hammer, Generation of tissue-specific and promiscuous HLA ligand databases using DNA microarrays and virtual HLA class II matrices, *Nature Biotechnology*, 17 (1999) 555-561.
- [14] C.J. Holland, D.K. Cole, A. Godkin, Re-Directing CD4(+) T Cell Responses with the Flanking Residues of MHC Class II-Bound Peptides: The Core is Not Enough, *Front Immunol*, 4 (2013) 172.
- [15] M.G. Rudolph, R.L. Stanfield, I.A. Wilson, How TCRs bind MHCs, peptides, and coreceptors, *Annu Rev Immunol*, 24 (2006) 419-466.
- [16] O.J. Landsverk, O. Bakke, T.F. Gregers, MHC II and the endocytic pathway: regulation by invariant chain, *Scand J Immunol*, 70 (2009) 184-193.
- [17] M.S. Schulze, K.W. Wucherpfennig, The mechanism of HLA-DM induced peptide exchange in the MHC class II antigen presentation pathway, *Curr Opin Immunol*, 24 (2012) 105-111.
- [18] B.D.E. Dominique A. Weber, Peter E. Jensen, Enhanced Dissociation of HLA-DR-Bound Peptides in the Presence of HLA-DM, *Science*, 274 (1996) 618-620.
- [19] S.B. Lovitch, Z. Pu, E.R. Unanue, Amino-terminal flanking residues determine the conformation of a peptide-class II MHC complex, *J Immunol*, 176 (2006) 2958-2968.
- [20] A.J. Godkin, K.J. Smith, A. Willis, M.V. Tejada-Simon, J. Zhang, T. Elliott, A.V. Hill, Naturally processed HLA class II peptides reveal highly conserved immunogenic flanking region sequence preferences that reflect antigen processing rather than peptide-MHC interactions, *J Immunol*, 166 (2001) 6720-6727.
- [21] H.C. Ishikawa-Ankerhold, R. Ankerhold, G.P. Drummen, Advanced fluorescence microscopy techniques--FRAP, FLIP, FLAP, FRET and FLIM, *Molecules*, 17 (2012) 4047-4132.

- [22] W.R. Algar, N. Hildebrandt, S.S. Vogel, I.L. Medintz, FRET as a biomolecular research tool - understanding its potential while avoiding pitfalls, *Nat Methods*, 16 (2019) 815-829.
- [23] N. Kaeokhamloed, S. Legeay, E. Roger, FRET as the tool for in vivo nanomedicine tracking, *J Control Release*, 349 (2022) 156-173.
- [24] T. Chen, B. He, J. Tao, Y. He, H. Deng, X. Wang, Y. Zheng, Application of Forster Resonance Energy Transfer (FRET) technique to elucidate intracellular and In Vivo biofate of nanomedicines, *Adv Drug Deliv Rev*, 143 (2019) 177-205.
- [25] E. Swider, S. Maharjan, K. Houkes, N.K. van Riessen, C. Figdor, M. Srinivas, O. Tagit, Forster Resonance Energy Transfer-Based Stability Assessment of PLGA Nanoparticles in Vitro and in Vivo, *ACS Appl Bio Mater*, 2 (2019) 1131-1140.
- [26] H. Zhang, H. Li, Z. Cao, J. Du, L. Yan, J. Wang, Investigation of the in vivo integrity of polymeric micelles via large Stokes shift fluorophore-based FRET, *J Control Release*, 324 (2020) 47-54.
- [27] Z. Lin, L. Xi, S. Chen, J. Tao, Y. Wang, X. Chen, P. Li, Z. Wang, Y. Zheng, Uptake and trafficking of different sized PLGA nanoparticles by dendritic cells in imiquimod-induced psoriasis-like mice model, *Acta Pharm Sin B*, 11 (2021) 1047-1055.
- [28] M. Vertzoni, J. Dressman, J. Butler, J. Hemenstall, C. Reppas, Simulation of fasting gastric conditions and its importance for the in vivo dissolution of lipophilic compounds, *Eur J Pharm Biopharm*, 60 (2005) 413-417.
- [29] G.S. Vanier, Microwave-Assisted Solid-Phase Peptide Synthesis Based on the Fmoc Protecting Group Strategy (CEM), in: K. Jensen, Tofteng Shelton, P., Pedersen, S. (eds) (Ed.) *Peptide Synthesis and Applications*, Humana Press, Totowa, NJ., 2013.
- [30] A. Swami, M.R. Reagan, P. Basto, Y. Mishima, N. Kamaly, S. Glavey, S. Zhang, M. Moschetta, D. Seevaratnam, Y. Zhang, J. Liu, M. Memarzadeh, J. Wu, S. Manier, J. Shi, N. Bertrand, Z.N. Lu, K. Nagano, R. Baron, A. Sacco, A.M. Roccaro, O.C. Farokhzad, I.M. Ghobrial, Engineered nanomedicine for myeloma and bone microenvironment targeting, *Proc Natl Acad Sci U S A*, 111 (2014) 10287-10292.
- [31] S. Bhattacharjee, DLS and zeta potential - What they are and what they are not?, *J Control Release*, 235 (2016) 337-351.
- [32] H. Ali, B. Weigmann, E.M. Collnot, S.A. Khan, M. Windbergs, C.M. Lehr, Budesonide Loaded PLGA Nanoparticles for Targeting the Inflamed Intestinal Mucosa--Pharmaceutical Characterization and Fluorescence Imaging, *Pharm Res*, 33 (2016) 1085-1092.
- [33] J. Monkare, M. Pontier, E.E.M. van Kampen, G. Du, M. Leone, S. Romeijn, M.R. Nejadnik, C. O'Mahony, B. Slutter, W. Jiskoot, J.A. Bouwstra, Development of PLGA nanoparticle loaded dissolving microneedles and comparison with hollow microneedles in intradermal vaccine delivery, *Eur J Pharm Biopharm*, 129 (2018) 111-121.
- [34] C. Macri, H. Morgan, J.A. Villadangos, J.D. Mintern, Regulation of dendritic cell function by Fc-gamma-receptors and the neonatal Fc receptor, *Mol Immunol*, 139 (2021) 193-201.
- [35] B. Merrifield, Solid phase synthesis, *Science*, 232 (1986) 341-347.
- [36] G. Yang, Y. Liu, Y. Hui, Tengjisi, D. Chen, D.A. Weitz, C.X. Zhao, Implications of Quenching-to-Dequenching Switch in Quantitative Cell Uptake and Biodistribution of Dye-Labeled Nanoparticles, *Angewandte Chemie International Edition*, 60 (2021) 15426-15435.
- [37] V. Filipe, A. Hawe, W. Jiskoot, Critical evaluation of Nanoparticle Tracking Analysis (NTA) by NanoSight for the measurement of nanoparticles and protein aggregates, *Pharm Res*, 27 (2010) 796-810.
- [38] S. Preus, L.M. Wilhelmsson, Advances in quantitative FRET-based methods for studying nucleic acids, *Chembiochem*, 13 (2012) 1990-2001.
- [39] H. Chen, H.L. Puhl, 3rd, S.V. Koushik, S.S. Vogel, S.R. Ikeda, Measurement of FRET efficiency and ratio of donor to acceptor concentration in living cells, *Biophys J*, 91 (2006) L39-41.
- [40] N. Rescignano, L. Tarpani, A. Romani, I. Bicchi, S. Mattioli, C. Emiliani, L. Torre, J.M. Kenny, S. Martino, L. Latterini, I. Armentano, In-vitro degradation of PLGA nanoparticles in aqueous medium and in stem cell cultures by monitoring the cargo fluorescence spectrum, *Polymer Degradation and Stability*, 134 (2016) 296-304.
- [41] M. Liu, S. Thijssen, W.E. Hennink, J. Garssen, C.F. van Nostrum, Linette E.M. Willemsen, Oral pretreatment with β -lactoglobulin derived peptide and CpG co-encapsulated in PLGA nanoparticles prior to sensitizations attenuates cow's milk allergy development in mice, *Frontiers in Immunology*, 13 (2023).
- [42] J. Koerner, D. Horvath, M. Groettrup, Harnessing Dendritic Cells for Poly (D,L-lactide-co-glycolide) Microspheres (PLGA MS)-Mediated Anti-tumor Therapy, *Front Immunol*, 10 (2019) 707.

- [43] A.I. Kostadinova, J. Middelburg, M. Ciulla, J. Garssen, W.E. Hennink, L.M.J. Knippels, C.F. van Nostrum, L.E.M. Willemsen, PLGA nanoparticles loaded with beta-lactoglobulin-derived peptides modulate mucosal immunity and may facilitate cow's milk allergy prevention, *Eur J Pharmacol*, 818 (2018) 211-220.
- [44] Y. Waeckerle-Men, E. Scandella, E. Uetz-Von Allmen, B. Ludewig, S. Gillessen, H.P. Merkle, B. Gander, M. Groettrup, Phenotype and functional analysis of human monocyte-derived dendritic cells loaded with biodegradable poly(lactide-co-glycolide) microspheres for immunotherapy, *J Immunol Methods*, 287 (2004) 109-124.
- [45] J.P. Lim, P.A. Gleeson, Macropinocytosis: an endocytic pathway for internalising large gulps, *Immunol Cell Biol*, 89 (2011) 836-843.
- [46] M. Diwan, P. Elamanchili, H. Lane, A. Gainer, J. Samuel, Biodegradable Nanoparticle Mediated Antigen Delivery to Human Cord Blood Derived Dendritic Cells for Induction of Primary T Cell Responses, *Journal of Drug Targeting*, 11 (2008) 495-507.
- [47] J. Panyam, V. Labhasetwar, Biodegradable nanoparticles for drug and gene delivery to cells and tissue, *Adv Drug Deliv Rev*, 55 (2003) 329-347.
- [48] M.S. Cartiera, K.M. Johnson, V. Rajendran, M.J. Caplan, W.M. Saltzman, The uptake and intracellular fate of PLGA nanoparticles in epithelial cells, *Biomaterials*, 30 (2009) 2790-2798.
- [49] D.H. Schuurhuis, A. Ioan-Facsinay, B. Nagelkerken, J.J. van Schip, C. Sedlik, C.J. Melief, J.S. Verbeek, F. Ossendorp, Antigen-antibody immune complexes empower dendritic cells to efficiently prime specific CD8+ CTL responses in vivo, *J Immunol*, 168 (2002) 2240-2246.
- [50] M.G.C. Nadine van Montfoort, Selina Khan, Dmitri V. Filippov, Jimmy J. Weterings, Janice M. Griffith, Hans J. Geuze, Thorbald van Hall, J. Sjeff Verbeek, Cornelis J. Melief, and Ferry Ossendorp,, Antigen storage compartments in mature dendritic cells facilitate prolonged cytotoxic T lymphocyte cross-priming capacity, *PNAS*, 106 (2009) 6730–6735
- [51] E. Frohlich, Cellular elimination of nanoparticles, *Environ Toxicol Pharmacol*, 46 (2016) 90-94.
- [52] J.P.a.V. Labhasetwar, Dynamics of Endocytosis and Exocytosis of Poly(D,L-Lactide-co-Glycolide) Nanoparticles in Vascular Smooth Muscle Cells, *Pharmaceutical Research*, 20 (2003) 212-220.
- [53] Z. Liu, P.A. Roche, Macropinocytosis in phagocytes: regulation of MHC class-II-restricted antigen presentation in dendritic cells, *Front Physiol*, 6 (2015) 1.
- [54] S. Hamdy, A. Haddadi, R.W. Hung, A. Lavasanifar, Targeting dendritic cells with nano-particulate PLGA cancer vaccine formulations, *Adv Drug Deliv Rev*, 63 (2011) 943-955.
- [55] N.D. Donahue, H. Acar, S. Wilhelm, Concepts of nanoparticle cellular uptake, intracellular trafficking, and kinetics in nanomedicine, *Adv Drug Deliv Rev*, 143 (2019) 68-96.
- [56] S.H. Arun T. Kamath, Frank Battye, David F. Tough, and Ken Shortman, Developmental kinetics and lifespan of dendritic cells in mouse lymphoid organs, *Blood*, 100 (2002) 1734-1741.
- [57] K.E. Sapsford, L. Berti, I.L. Medintz, Materials for fluorescence resonance energy transfer analysis: beyond traditional donor-acceptor combinations, *Angew Chem Int Ed Engl*, 45 (2006) 4562-4589.
- [58] H.W. Joseph V. Mersol, Ari Gafni, and Duncan G. Steel, Consideration of dipole orientation angles yields accurate rate equations for energy transfer in the rapid diffusion limit, *Biophys. J.*, 61 (1992) 1647-1655.
- [59] R. Ismail, T. Sovany, A. Gacsi, R. Ambrus, G. Katona, N. Imre, I. Csoka, Synthesis and Statistical Optimization of Poly (Lactic-Co-Glycolic Acid) Nanoparticles Encapsulating GLP1 Analog Designed for Oral Delivery, *Pharm Res*, 36 (2019) 99.
- [60] V.T. Förster, Zwischenmolekulare Energiewanderung und Fluoreszenz, *Annalen der Physik.*, 6 (1948) 9.

CHAPTER 5

***In Vitro* Immunostimulatory Effects of CpG-ODN Encapsulated PLGA Nanoparticles on Human Monocytes Derived Dendritic Cells and Their T-Cells Priming Capacity Using an Allogeneic DC-T-Cell Model**

M. (Mengshan) Liu^{1,2}, S.(Suzan) Thijssen², W.E. (Wim) Hennink¹, J. (Johan) Garssen^{1,3}, C.F. (Cornelus) van Nostrum¹, L.E.M. (Linette) Willemsen^{2*}

1. Division of Pharmaceutics, Utrecht Institute for Pharmaceutical Sciences, Utrecht University, Utrecht, the Netherlands

2. Division of Pharmacology, Utrecht Institute for Pharmaceutical Sciences, Utrecht University, Utrecht, the Netherlands

3. Department of Immunology, Nutricia Research B.V., Utrecht, the Netherlands

Manuscript in preparation.

Abstract

Background. Immunotherapy exploiting nanoparticles has gained increasing attention due to its versatility for the simultaneous delivery of multiple therapeutic components and specific targeting to e.g., dendritic cells (DC). To prevent or treat allergic disease, type 2 prone immune deviation needs to be redirected. CpG oligonucleotides (CpG-ODN) are T helper 1 (Th1) and regulatory T-cells (Treg) adjuvants, which skew away from a type 2 allergic phenotype and promote tolerance induction by modifying DC function in the context of allergen presentation. However, the immunostimulatory effects of different types of CpG-ODNs on dendritic cells when encapsulated in poly(lactic-co-glycolic acid) nanoparticles (PLGA NPs) is currently unknown. **Aim.** Here we aimed to study the immunomodulatory effect of three types of CpG-ODN encapsulated in PLGA NPs (CpG-ODN NP) on human immature monocyte derived dendritic cells (immature moDCs), while studying the function of the primed moDCs in allogeneic DC-T-cell co-cultures. **Methods.** class A-, B- or C- CpG-ODNs were encapsulated in PLGA nanoparticles using a double emulsion solvent evaporation method. *In vitro* immature moDCs were exposed for 48 h in either medium, or with medium in which non-loaded (empty NP) or class A-, B- or C- CpG-ODN encapsulated in PLGA NPs were dispersed. As controls, immature moDCs were exposed to LPS for maturation into DC1 which drive naïve T-cell differentiation towards Th1 cells or a cytokine mixture for maturation into DC2 which drive Th2 cells differentiation. After 48 h of incubation, these primed moDCs were co-cultured with naïve CD4+ T-cells in an allogeneic DC-T-cell co-culture model for 5 days. **Results.** NPs loaded with class A-, B- or C- CpG-ODN had a mean NP size of ~250-290 nm, an encapsulation efficiency of 50-65% and a loading capacity of 0.031-0.040%. DC1 or DC2 controls, and empty NP primed moDCs showed upregulated surface expression of co-stimulatory molecules CD80, CD86 and/or regulatory costimulatory molecule Programmed Death Ligand-1 (PD-L1) as compared to the medium controls, indicating maturation of these moDCs. This was not affected upon incubation with PLGA NPs loaded with class A-, B- or C- CpG-ODN. No significant differences were observed in Th1 and Th2 development in the consecutive DC-T-cell co-cultures. However, only class A CpG-ODN NP primed moDCs increased the Th1/Th2 ratio (CXCR3+/CRTH2+) as well as the Treg/Th2 ratio (CD25+FoxP3+/CRTH2+) as compared to moDCs primed with empty NP. **Conclusion.** The findings indicate that class A CpG-ODN loaded NP are most favorable in the priming of moDCs that shift the balance towards a Th1 and Treg phenotype driving away from the allergy prone Th2 development.

Keywords: Allergy; CpG oligonucleotides; DC-T-cell model; poly(lactic-co-glycolic acid) nanoparticles; moDCs

Introduction

Food allergy is an increasingly prevalent global health concern with an incidence rate of up to 8% of the children in the western countries [1]. In particular, cow's milk allergy (CMA) is one of the most common food allergies that occurs in infancy, which requires strict dietary avoidance to prevent severe allergic symptoms that could be, in some severe cases, life-threatening anaphylaxis for newborns [2]. So far, there is a lack of effective immunotherapeutic or preventive treatments for CMA [3].

Recently, nanoparticle-based immunotherapy has attracted increasing attention for induction of allergen-specific tolerance by the oral route [4]. Oral immunotherapy aims to instruct allergen specific tolerance through the gut-associated lymphoid tissues (GALT), which is prone to develop tolerance towards harmless food proteins [5]. In the GALT, professional antigen-presenting cells (APCs) are regarded as major target cells for orally administered nanoparticle-based immunotherapeutics [6]. APCs play a pivotal role in regulation and connection of innate and adaptive immunity. Upon internalization of pathogens or commensal bacteria, APCs lyse the microbe to result in the intracellular release of evolutionary conserved structures like peptidoglycans, LPS and bacterial DNA (referred as pathogen-associated molecular patterns, PAMPs), which can be recognized by different types of so-called pattern recognition receptors (PRRs) [6, 7]. These PRR are expressed by several types of structural and immune cells including dendritic cells (DC) [7]. PAMPs can activate DC, leading to maturation enabling them to induce adaptive T-cell responses to peptide epitopes (for example of allergens) that are presented by the same DC by MHCII [8]. Depending on the type and structure of the PAMP, the functional outcome of the DC and T-cell response may differ. PAMP may prime DC to induce Th1 type immunity, preferably in the context of additional regulatory T-cell development, driving away from the allergy prone Th2 response [8, 9]. Therefore, these bacterial components may be used as adjuvants to be used in allergen specific strategies to prevent or treat allergies. In this regard, bacterial unmethylated cytosine-guanosine dinucleotides CpG DNA are of interest. These are recognized by Toll-like receptor-9 (TLR-9) in the endo-lysosomal compartments of human plasmacytoid dendritic cells (pDCs) and B lymphocytes (B-cells) [10, 11] as well as by human

monocytes derived dendritic cells (moDC) [12]. In regulation of immune responses [13], DC are central players to drive immunity or tolerance and to shape the phenotype of the generated adaptive immune response.

Synthetic CpG-ODNs are short synthetic single stranded DNA molecules that contain unmethylated CpG-ODN motifs, mimicking the structure of bacterial CpG DNA, have been exploited to activate TLR-9 [14, 15], and were reported to inhibit Th2 immunity and allergic sensitization in mice. Furthermore, activation of TLR-9 by CpG-ODN in antigen-presenting cells (APCs) (*i.e.*, DC) modifies their function (*i.e.*, surface expression of co-stimulatory molecules and cytokine release) and drives differentiation into T helper 1 (Th1) and a regulatory T-cells (Treg) immune response [14, 16]. Hence, the different classes of synthetic CpG-ODN are attractive immune adjuvants for induction of allergen/antigen-specific tolerance [14, 17] and class A- and B- CpG-ODNs have progressed to clinical trials for allergen-specific immunotherapies [18-22]. For use as adjuvant in oral delivery systems, CpG-ODN needs to survive degradation due to nucleases present in the gastrointestinal tract. Therefore, they can be loaded in nanoparticle delivery systems which potentially also can reach DCs [6]. Importantly, encapsulation of CpG-ODN in nanoparticles was reported to enhance its cellular uptake by DC as compared to their soluble form [23].

Poly(lactic-co-glycolic acid) (PLGA) nanoparticles (NPs) have been extensively used for the development of oral vaccines [24, 25] due to several advantages of this polymer and particles derived hereof. To mention, these particles protect the loaded peptides against enzymatic degradation in the GI tract [26-28]. Further, these particles can be taken up by antigen presenting cells (*i.e.*, dendritic cells) and subsequently ideally intracellularly release their content in a sustained manner. Additionally, these particles have a good safety profile and a number of PLGA based drug products have been approved by the U.S. Food and Drug Administration (FDA) and European Medicines Agency (EMA) [29, 30]. Furthermore, cellular uptake of PLGA by DC is dependent on their size and charge [31] and these characteristics can be tailored by the formulation and processing conditions [32]. After oral administration, class B CpG-ODN loaded PLGA NPs were successfully used as adjuvant for peanut protein to induce an antigen-specific adaptive immune response driving away from the T helper 2 (Th2) type allergic response [16]. Moreover, we recently reported whey-specific tolerance induced by oral pretreatments using antigen-encapsulated PLGA NP with and without class B CpG-ODN

co-encapsulation in a prophylactic cow's milk allergy murine model [33]. In addition, exposing intestinal epithelial cells to type C CpG-ODN was found to activate these cells and support the development of regulatory type Th1 response of underlying immune cells [34, 35]. Noteworthy, monocytes derived dendritic cells (moDCs) were reported to express functional TLR-9 and produce IFN- α upon stimulation with class A CpG-ODN [12]. However, the effects of the three different types of CpG-ODNs loaded in PLGA nanoparticles on DC function have not been studied so-far. Furthermore, immature moDCs are known for their potent capacity to internalize nanoparticles [36] and may thus serve as a model to study the effects of adjuvants on moDCs maturation and function. Therefore, in this study, we aimed to investigate the immunomodulatory effects of the three types of CpG-ODN encapsulated in PLGA NPs on human immature moDCs. In addition, using the allogeneic DC-T-cell co-culture model, we also studied in which way these primed moDCs instruct naïve CD4+ T-cells, aiming to identify a proper type of CpG-ODN for the development of nanoparticles-based immunotherapeutics driving away from the Th2-type allergic phenotype.

Materials And Methods

CpG oligonucleotides

Three classes of human Toll-Like Receptor-9 (TLR-9) ligand CpG-ODN, namely class A-, B- and C-, including two types of class C- CpG-ODN, as shown in Table 1, were purchased from InvivoGen (San Diego, USA).

Table 1. Human specific Toll-Like Receptor-9 (TLR-9) ligand CpG oligonucleotides (CpG-ODN) used in this study.

Name	Length (mer)	Sequence (5'→3')	Molecular weight (g/mol)
CpG-ODN A 2216	20	ggGGGACGATCGTCgggggg	6432
CpG-ODN B 2006	24	tcgtcgttttgtcgttttgcgtt	7720
CpG-ODN C 2395	22	tcgtcgttttc <u>ggcgcgcgcgcg</u>	7068
CpG-ODN C M362	25	tcgt <u>cgtcg</u> tttc <u>gaacgac</u> gttgat	8049

Bases shown in capital letters are phosphodiester, and those in lower case are phosphorothioate (nuclease resistant), palindrome is underlined.

Preparation and Characterization of CpG-ODN encapsulated PLGA NPs

Nanoparticles based on PLGA (lactide/glycolide molar ratio 50:50, 0.32 - 0.48 dl/g; PURASORB PDLG 5004A, Corbion, the Netherlands) were prepared using a double emulsion solvent evaporation method [33]. Briefly, 160 mg PLGA was dissolved in 4 mL

dichloromethane (DCM, Biosolve BV, Valkenswaard, the Netherlands). Next, 100 µg CpG-ODN in 50 µL PBS and 400 µL PBS were added dropwise to 1 mL and 3 mL PLGA-solutions, respectively, and sonicated using a Sonifier S-450A (3 mm, Branson Ultrasonics B.V., Soest, the Netherlands) at 20% amplitude for 0.5 min on ice bath. For empty NPs, 50 µL PBS and 400 µL PBS were added dropwise to 1 mL and 3 mL PLGA-solutions, respectively, and sonicated using the same conditions as for preparation of CpG-ODN NPs.

The obtained two water-in-oil emulsions were combined and sonicated (at 20% amplitude for 0.5 min on ice bath) to yield a single water-in-oil-emulsion. Next, the obtained water-in oil-emulsion was added dropwise to 40 mL external aqueous phase, containing 3 w/v % PVA (87-90% hydrolyzed polyvinyl alcohol, Mw 3,000-70,000 Da, Sigma-Aldrich, USA) and 0.9 w/v % NaCl (Sigma-Aldrich), and the obtained mixture was sonicated at 20% amplitude for 1 min on ice bath to yield a water-in-oil-in-water emulsion. The formed emulsion was subjected to agitation for 3 h at room temperature to evaporate DCM and to obtain hardened PLGA NPs. The NP suspension was spun down at 20,000×g for 30 min at 4°C and the obtained pellet was washed with 20 mL nuclease free water (not DEPC-Treated, Invitrogen, USA) twice prior to resuspension in 3 mL nuclease free water (Invitrogen). Next, 2 µL of the prepared NP suspensions was added to 998 µL milliQ water for characterization of nanoparticle size and polydispersity index (PDI) with Zetasizer Nano S (Malvern Instruments, Malvern, UK), or transferred into 998 µL 10 mM HEPES buffer (pH 7.4) for characterization of the zeta-potential of the nanoparticles using Zetasizer Nano-Z (Malvern Instruments, Malvern, UK) respectively. The remaining NP suspension was lyophilized using a freeze dryer (Buchi Lyovapor L-200, Hendrik-Ido-Ambacht, the Netherlands).

The encapsulation efficiency of CpG-ODN was quantified with a direct method. In detail, 16 mg lyophilized NPs and mixed with 1440 µL 0.2N NaOH under agitation overnight to hydrolyze PLGA. Next, 22.5 µL 20×Tris-EDTA (ThermoFisher) buffer per 5 mg NP was added to the obtained solution. An additional volume of 1×Tris-EDTA buffer was added to reach 10 mg/mL NP-equivalent prior to the quantification assay for CpG-ODN using Quant-iT™ OliGreen™ ssDNA Assay Kit (ThermoFisher) according to the manufacturer's protocol. The encapsulation efficiency (EE) and loading capacity (LC) of CpG-ODN were calculated by the following formulas:

$$\text{Encapsulation Efficiency} = \frac{\text{Amount of encapsulated CpG-ODN}}{\text{Amount of feed CpG-ODN for formulation preparation}} \times 100 (\%)$$

$$\text{Loading Capacity} = \frac{\text{Amount of encapsulated CpG-ODN}}{\text{Weight of nanoparticles}} \times 100 (\%)$$

***In vitro* release of CpG-ODN from PLGA NPs**

The release of CpG-ODN from PLGA NPs was determined as follows. Around 10 mg of freeze dried CpG-ODN NPs were accurately weighed in triplicate and suspended in 500 μ L phosphate saline buffer (PBS, pH 7.4)/0.06 w/v % sodium azide (NaN₃, Sigma-Aldrich) (release buffer) followed by incubation at 37°C on a nutating mixer. At different time points (at 30 min, and at day 1, 7, 14, 21, 28, 35, 42 and 49), samples were centrifuged at 20,000 \times g at 4 °C and 400 μ L of the supernatant was withdrawn. Next, 400 μ L of fresh release buffer was added, the pelleted NPs were resuspended, and the samples were further incubated at 37 °C. The concentration of CpG-ODN in the different release samples was determined using Quant-iT™ OliGreen™ ssDNA Assay Kit (ThermoFisher) according to the manufacturer's protocol, respectively. The percentage of released CpG-ODN was calculated based on the encapsulated amount.

Isolation of Peripheral Blood Mononuclear Cell (PBMCs)

Freshly donated human whole blood (time between donation and isolation was less than 24 h) was obtained from the Dutch Blood bank (Amsterdam, the Netherlands) and diluted 1:1 with DPBS-2% FBS at room temperature and transferred into Leucosep tubes (VWR, Radnor, USA), followed by centrifugation for 13 min at 1000 \times g at room temperature. The fraction with the lymphocytes was washed with DPBS supplemented with 2% FBS for 5 times. Next, the remaining erythrocytes were lysed using a red blood cell lysis buffer (8.3 g/L NH₄Cl, 1 g/L KHCO₃ and 37 mg/L EDTA, sterile filtered, pH 7.4) on ice for 4 min. The obtained PBMCs suspension was resuspended in RPMI 1640 medium supplemented with 10% FBS, 100 U/mL penicillin and 100 μ g/mL streptomycin.

Isolation of Monocytes and Differentiation of moDCs

CD14⁺ monocytes were isolated from the PBMC suspension by means of negative selection with classical monocyte isolation kit human following the manufacturer's protocol (Miltenyi Biotec, Bergisch Gladbach, Germany). CD14⁺ cells were cultured at a density of 1 \times 10⁶ cells/mL per well in 1 mL RPMI medium supplemented with 100 ng/mL

IL-4 and 60 ng/mL GM-CSF (both from Prospec, East Brunswick, USA) in 6-well suspension culture plates (Greiner Bio-one, Solingen, Germany). The medium was refreshed at day 3 and 6. The human immature moDCs were harvested at day 7.

Stimulation of Human Immature MoDCs

Human immature moDCs collected at day 7 were seeded at a density of 2×10^6 cells/mL per well in 200 μ L culture medium (RPMI 1640 medium supplemented with 10% FBS, 100 U/mL penicillin and 100 μ g/mL streptomycin) into a 24-wells suspension culture plate. The cells were subsequently incubated with either 1.4 mg/mL empty NP, or 0.4 μ g/mL encapsulated CpG-ODN in PLGA NPs (refer to details in Table 2).

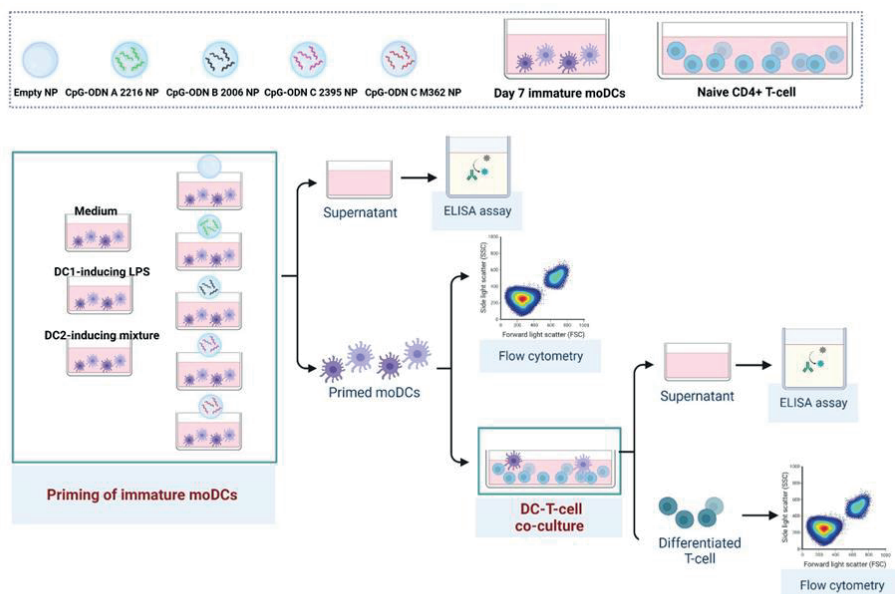
Table 2. Composition of different stimulation media for the priming of immature human monocytes derived dendritic cells (immature moDCs).

Stimulation group	Components for controls	Concentration of Encapsulated CpG-ODN (μ g/mL)	Concentration of PLGA NPs (mg/mL)
Medium	Blank culture medium ¹	-	-
DC1-inducing LPS	100 ng/mL LPS ² in culture medium	-	-
DC2-inducing mix	50 ng/mL TNF- α , 25 ng/mL IL-1b, 10 ng/mL IL-6 and 1 μ g/mL prostaglandin E2 ³	-	-
Empty NP	-	0	1.4
CpG-ODN A 2216 NP	-	0.4	1.2
CpG-ODN B 2006 NP	-	0.4	1.4
CpG-ODN C 2395 NP	-	0.4	1.1
CpG-ODN C M362 NP	-	0.4	1.0

¹: Culture medium: RPMI 1640 medium supplemented with 10% FBS, 100 U/mL penicillin and 100 μ g/mL streptomycin. ²: LPS: Lipopolysaccharide (LPS-EB Ultrapure, from E. coli O111:B4 strain, TLR4-based adjuvant, Invivogen). ³: All these cytokines were purchased from Prospec (East Brunswick, USA).

As control, immature moDCs were incubated with either 1) blank culture medium or 2) DC1-inducing LPS, containing 100 ng/mL lipopolysaccharide (LPS), or 3) DC2 inducing mix [37], containing 50 ng/mL TNF- α , 25 ng/mL IL-1b, 10 ng/mL IL-6 and 1 μ g/mL prostaglandin E2 (detailed in Table 2). After 48 h-incubation, the supernatants were collected for cytokine concentrations as described in the below section of **Cytokine detection** (as shown in Figure 1). On the other hand, the primed moDCs were harvested for analysis using flow cytometry and further co-incubation with freshly isolated allogeneic naïve CD4+ T-cells, respectively.

In vitro immunostimulatory effects of CpG encapsulated PLGA NP on human moDCs and their T-cells priming capacity using an allogenic DC-T-cell model



Created with BioRender.com

Figure 1. Experimental setup for *in vitro* priming of human moDCs using PLGA NP encapsulated human specific CpGs and their influence of these primed moDCs and differentiation of naïve CD4+ T-cells in the DC-T-cell co-cultures.

Naïve CD4+ T-cells Isolation

At the second day of moDCs exposure, naïve CD4+ T-cells were isolated from the freshly isolated PBMCs (as described in the above section) using negative selection using magnetic depletion of memory CD4+ T-cells and non-CD4+ T-cells. PBMCs were incubated with a cocktail of biotinylated CD45RO, CD8, CD14, CD15, CD16, CD19, CD25, CD34, CD36, CD56, CD123, anti-TCR γ/δ , anti-HLA-DR, and CD235a (glycophorin A) antibodies and subsequently labeled with Anti-Biotin MicroBeads for depletion according to the manufacturer's protocol (naïve CD4+ T-cells isolation kit II, human, Miltenyi Biotec).

DC-T-cell Co-culture

The primed moDCs that had been exposed for 48 h to CpG-ODN encapsulated NPs or the control treatments were harvested for the DC-T-cell co-culture as shown in Figure 1. The freshly isolated naïve CD4+ T-cells (1×10^6 cells/well) were co-cultured 10:1 with the primed moDCs (0.1×10^6 cells/well) in IMDM medium supplemented with 10% FCS, 100 U/mL penicillin, 100 μ g/mL streptomycin, 20 μ g/ml apo-transferrin and 50 μ M β -

mercapoethanol in 24-well plates. In addition, 5 ng/mL IL-2 [38, 39] (Prospec, East Brunswick, USA) and 150 ng/mL anti-CD3[39-41] antibody (BD) were added to the DC-T-cell co-cultures, to facilitate clonal expansion of T-cells by activation of the TCR. After incubation for 5 days, the cells were stained for flow cytometry analysis (as described in the next section), and the supernatant was stored for further analysis.

Flow cytometry

The 2-days primed moDCs and 5-days DC-T-cell co-cultured immune cells were stained for flow cytometry analysis. Briefly, the dead cells were excluded from the analysis using Fixable Viability Dye eFluor 780 (ThermoFisher). Cells were incubated with Fc receptor blocking antibody (Biolegend, San Diego, USA) for 10 min on ice to avoid non-specific binding.

The 48 h primed moDCs were extracellularly stained with CD11c-PerCP/eFluor 710, HLA-DR-PE, CD80-FITC, CD86-PE/Cy7 and PD-L1-eFluor450 according to the manufacturer's protocol (All from ThermoFisher).

Approximate 2×10^5 cells collected from the 5 days primed DC-T-cell co-cultures were extracellularly stained for Th1/Th2 with CD4-PerCP Cy5.5, CD69-PE, CXCR3-Alexa Fluor 488, and CRTH2-APC (all from ThermoFisher except CXCR3-Alexa Fluor 488 from BD Biosciences).

In addition, approximately 3×10^5 cells were extracellularly stained for Treg/Th17 cells with CD4-PerCP Cy5.5 and CD25-AF488. For intracellular staining of Treg/Th17, the cells were first fixed and permeabilized with FoxP3/Transcription Factor Staining Buffer Set (ThermoFisher) and then stained with FoxP3-eFluor 660 and ROR γ -PE (ThermoFisher). Stained cells were measured by FACS Cantoll (BD Biosciences) and analyzed using Flowlogic software version 7.3 (Inivai Technologies, Mentone, Australia).

Cytokine detection

In the supernatants collected from the primed moDCs IL-12p70, IL-10 and IP-10 (IFN- γ -inducible protein-10) (also known as CXCL10) were measured according to the manufacturer's protocols (All ELISA kits were purchased from ThermoFisher). IFN- γ , IL-13 and IL-10 (ThermoFisher) were measured in the supernatants collected from the DC-T-cell co-cultures. The samples were measured at 450 nm using Promega™ GloMax® Plate Reader (Madison, USA).

Statistical analysis

Statistical analysis was performed using GraphPad Prism software version 9.5.1 (San Diego, USA). For (log transformed) data sets that were normal distributed as indicated by the Kolmogorov–Smirnov test or the Shapiro–Wilk test, repeated measures one-way ANOVA followed by Bonferroni’s *post hoc* test for selected pairs was performed. Otherwise, Friedman non-parametric test followed by Dunn’s *post hoc* test was applied. The selected pairs were statistically analyzed being the medium controls compared to DC1, DC2 conditions and empty PLGA NP compared to medium, and the CpG-ODN A, B or C loaded PLGA NP conditions as indicated by the dotted line in Figure 3-6 and Supplemental Figure 1.

Results

Characteristics of CpG oligonucleotides encapsulated PLGA NPs

Empty and PLGA NPs encapsulated with class A-, B- or C- CpG-ODN (characteristics given in Table 1) were prepared using a double emulsion solvent evaporation method. The obtained NPs had a close to neutral zeta-potential and similar size ranging between 250 - 290 nm (Table 3). The NPs had a narrow size distribution indicated by polydispersity index ranging between 0.05-0.10. The different CpG-ODNs were loaded with similar encapsulation efficiency (EE) of 53, 49, 57 and 64% respectively, resulting in loading capacities (LC) between 0.031% and 0.040% (Table 3).

Table 3. Characteristics PLGA NPs loaded with the different CpG-ODNs.

Formulation (Number of batches, n=1)	Hydrodynamic particle size (nm) (n=3)	Poly dispersity index (PDI) (n=3)	Zeta-potential (mV) (n=3)	EE (%)	LC (%)
Empty NP	256 ± 1	0.05 ± 0.02	-1.2 ± 0.1	-	-
CpG-ODN A 2216 NP	267 ± 3	0.08 ± 0.02	-1.6 ± 0.2	53	0.033
CpG-ODN B 2006 NP	289 ± 5	0.10 ± 0.01	-1.9 ± 0.1	49	0.031
CpG-ODN C 2395 NP	255 ± 4	0.09 ± 0.00	-1.7 ± 0.1	57	0.036
CpG-ODN C M362 NP	268 ± 2	0.10 ± 0.02	-1.8 ± 0.2	64	0.040

Hydrodynamic particle size, polydispersity and zeta-potential were measured in triplicate.

***In vitro* release of CpG-ODN from PLGA NPs**

CpG-ODN A NP and CpG-ODN C M362 NP showed a burst release of 11-15% of the loading, and CpG-ODN B NP and CpG-ODN C 2395 NP showed a burst release of 26-38% of the loading in the *in vitro* release study (Figure 2). After a lag phase of about two weeks, sustained-release of CpG-ODN from the different PLGA NPs was observed up to 6 weeks. At day 49 the loaded CpG-ODNs were (almost) fully released, *i.e.*, 93% and 90% for CpG-ODN A NP and CpG-ODN C M362 and of 133% and 116 % for CpG-ODN B and CpG-ODN C 2395 respectively (Figure 2). The cumulative release of CpG-ODN B NP and CpG-ODN C 2395 NP above 100% can be ascribed to the error of the analytical method to determine the concentration of CpG-ODN in the different release samples.

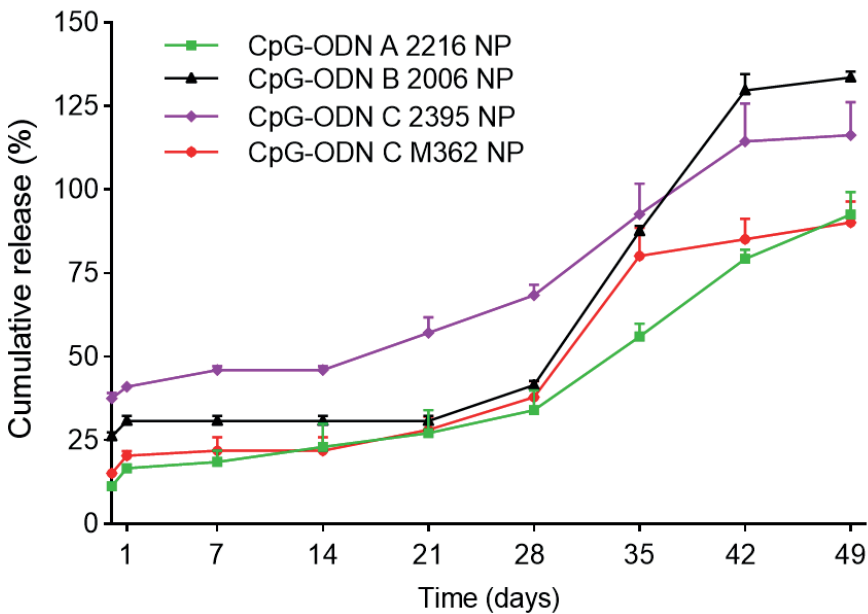


Figure 2. *In vitro* release of Type A B C CpG-ODN from PLGA NPs in PBS at 37°C. Data are presented as mean \pm SD, n = 3 per formulation.

Surface expression of activation markers on stimulated moDCs

The viability of moDCs was not affected by different treatments ranging between 60-80% (data not shown). Figure 3A shows that DC1 and DC2, but not empty NP primed moDCs, had slightly lowered frequency of the CD11c+HLA-DR+ moDC among the viable cells as compared to the medium primed moDCs. The different types of CpG-ODN

loaded NPs did not affect the frequency of CD11c+HLA-DR+ among viable cells as compared to the empty NP control. Incubation of immature moDCs with DC1-inducing LPS or DC2-inducing cytokine mixture increased the surface expression of CD80 and PD-L1 on the CD11c+HLA-DR+ moDCs as compared to the medium control (Figure 3B and D). Exposure of immature moDCs to empty NP upregulated surface expression of co-stimulatory molecules CD80 and CD86 and PD-L1 of the primed moDCs (Figure 3B, C and D) as compared to the medium controls. Meanwhile, stimulation of immature moDCs with different types of CpG NP did not influence the surface expression of CD80, CD86 or PD-L1 as compared to those incubated with empty NP (Figure 3B, C and D).

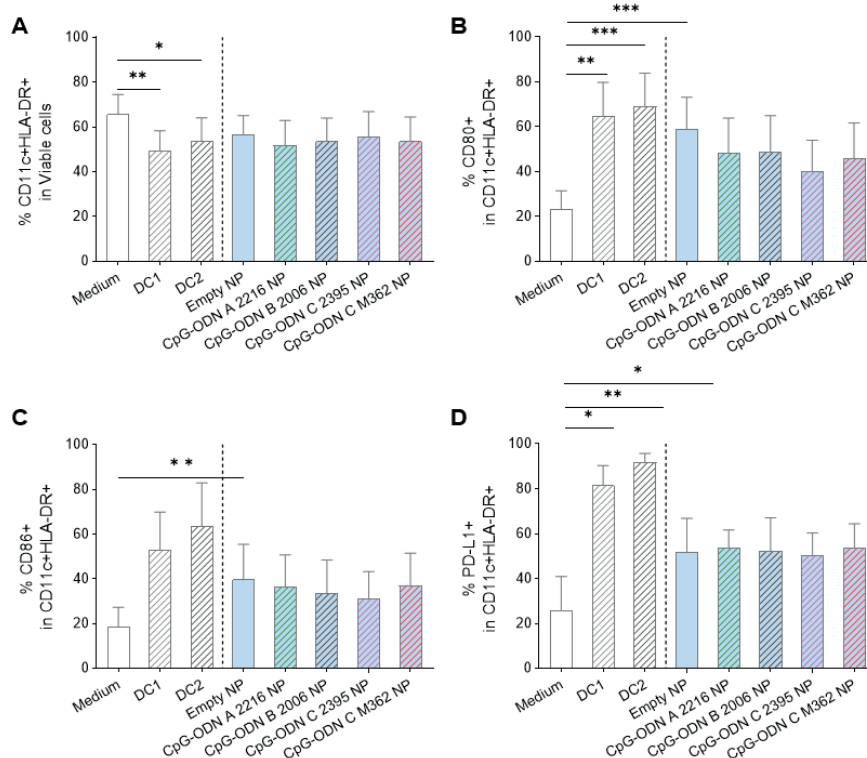


Figure 3. Surface expression of activation markers on the primed moDCs. The day 7 human immature monocytes derived dendritic cells (immature moDCs) were stimulated with either medium, DC1-inducing LPS, or DC2-inducing mixture, empty and class A-, B- or C- CpG-ODN loaded PLGA NPs for 48 h at 37 °C. Subsequently, these primed moDCs were analyzed using flow cytometry to determine the percentages of CD11c+HLA-DR+ moDCs (A) on the viable cells, and the percentages of CD80+ (B), CD86+ (C) and PD-L1+ (D) expressed on the surface of CD11c+HLA-DR+ moDCs. Data are presented as mean \pm SEM, n = 6 independent moDCs donors for (A-C) and n = 4 independent donors for (D); * p <0.05, ** p <0.01, *** p <0.001; DC1: LPS primed moDCs; DC2: DC2-inducing mixture primed moDCs.

Cytokine production by stimulated DCs

After 48 h-incubation of immature moDCs with medium, DC1-inducing LPS or DC2-inducing mixture, empty NP or CpG-ODN loaded PLGA NPs, IL-12p70, IP-10 and IL-10 were measured in the supernatants. The LPS-induced DC1 secreted higher amounts of IL-12p70 as compared to the medium primed moDCs, and empty NP primed moDCs slightly increased IL-12p70 (Figure 4A). This figure also shows that the release of IL-12p70 was not significantly affected by CpG-ODN loaded NPs compared to empty NP. The matured DC2 did not secrete higher levels of IL-12p70, IP-10 nor IL-10 as compared to the medium primed moDCs (Figure 4A, B and C). Incubation of immature moDCs with empty NP did not affect the release of IP-10 or IL-10. Empty NP primed moDCs showed a slightly enhanced the ratio of IL-12p70/IL-10 as compared to the medium control (Figure 4D).

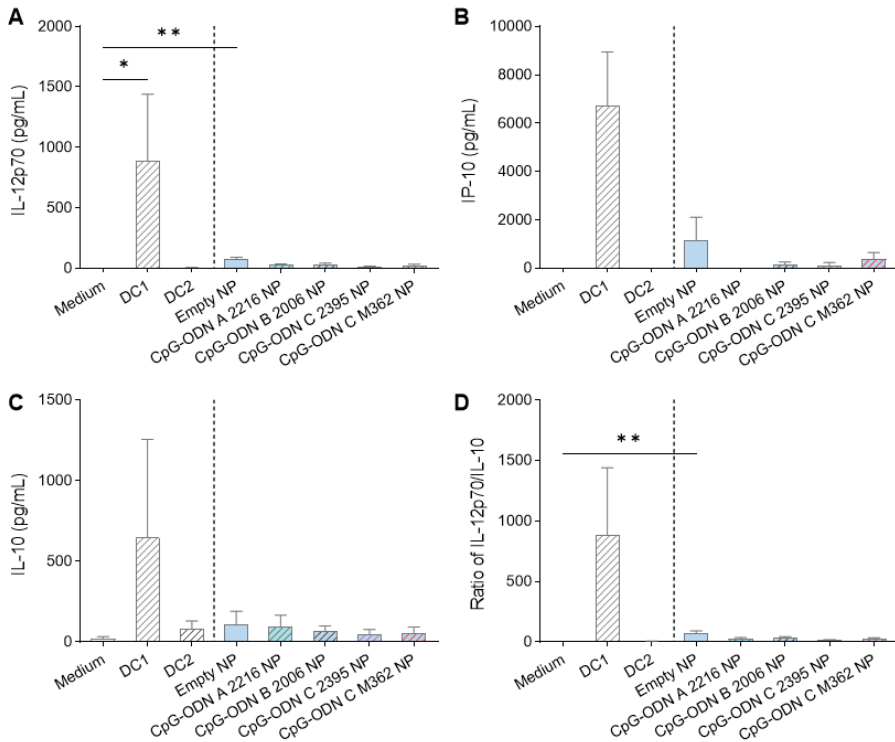


Figure 4. Cytokine and chemokine secretion of the primed moDCs. The day 7 human immature monocytes derived dendritic cells (moDCs) were incubated with medium, DC1-inducing LPS, DC2-inducing mixture, empty NP, and class A-, B- and C- CpG-ODN encapsulated PLGA NPs for 48 h. Supernatants were collected and measured for IL-12p70 (A), IP-10 (B) and IL-10 (C) secretion. The ratio of IL-12p70/IL-10 was calculated and shown in (D). Data are presented as mean \pm SEM, $n = 4$ independent moDCs donors; * $p < 0.05$, ** $p < 0.01$; DC1: LPS primed moDCs; DC2: DC2-inducing mixture primed moDCs.

Th1- and Th2- subsets and cytokine release in the DC-T-cell co-cultures

Using the allogeneic DC-T-cell co-cultures, it was studied whether the primed moDCs exposed to medium, DC1-inducing LPS, DC2-inducing mixture, empty or CpG-ODN loaded NPs, were able to instruct development of Th1 and Th2 immune polarization. Therefore, these primed moDCs were co-cultured with freshly isolated naïve CD4⁺ T-cells of allogeneic donors for 5 days (as shown in Figure 1), after which the frequency of Th1 and Th2 cells (the gating strategy is shown in Supplemental Figure 3) and associated cytokines secretion were studied using flow cytometry and ELISA, respectively.

The co-cultures of T-cells with the primed moDCs from different treatments showed neither differences in viability nor frequency of the CD4⁺ T-cells, nor activation marker expression of CD69 on CD4⁺ T-cells (Figure 5A, B and C). The percentage of CXCR3⁺ (Th1), CRTH2⁺ (Th2) subsets within the CD4⁺ T-cells population was not affected (Figure 5D, E). In contrast, incubation of naïve T-cells with CpG-ODN A NP primed moDCs resulted in a higher Th1/Th2 ratio (Figure 5F), as compared to empty NP primed moDCs in the DC-T-cell co-culture. Th1-associated cytokine IFN- γ and Th2-associated cytokine IL-13 and regulatory type IL-10 secretion in the DC-T-cell co-cultures were not significantly affected (Supplemental Figure 1A, B and C).

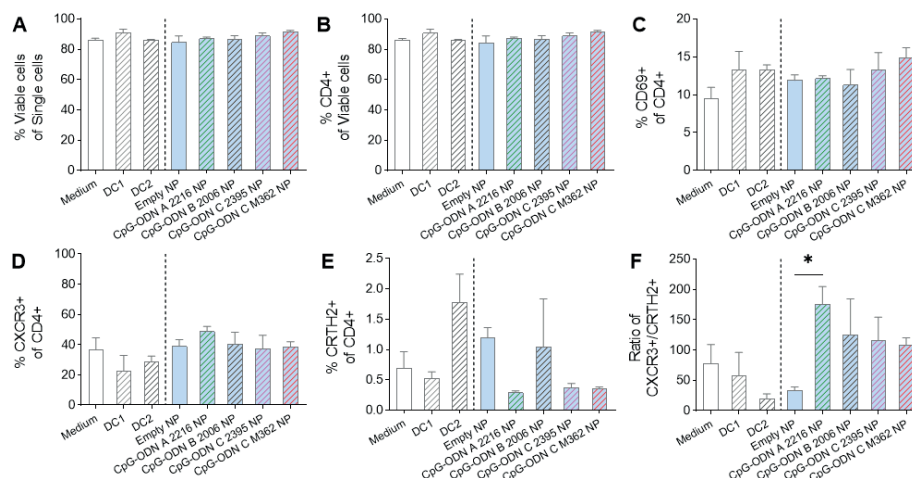


Figure 5. Analysis of T helper 1 (Th1-) and T helper 2 (Th2-) subsets in DC-T-cell co-cultures. After 5-day co-culture of naïve CD4⁺ T-cells with the 48 h-primed moDCs, the cells were collected and analyzed with flow cytometry for viability (A), percentages of CD4⁺ among viable cells (B), percentages of CD69⁺ (C), CXCR3⁺ Th1 (D), CRTH2⁺ Th2 (E) subset, Th1/Th2 ratio of CXCR3⁺/CRTH2⁺ (F) in CD4⁺ T-cells. Data are presented as mean \pm SEM, n = 3 different DC-

T-cell co-cultures with allogeneic combinations using 2 independent naïve CD4⁺ T-cells donors and 2 independent moDCs donors; **p*<0.05; DC1: LPS primed moDCs; DC2: DC2-inducing mixture primed moDCs.

Treg- and Th17-subsets and Treg/Th2 ratio in the DC-T-cell co-cultures

In the allogeneic DC-T-cell co-cultures, it was also investigated whether the moDCs primed with different treatments were able to instruct development of regulatory T-cells (Treg) and T helper 17 (Th17) cells. To this end, the primed moDCs were co-cultured with naïve CD4⁺ T-cells for 5 days (as shown in Figure 1), after which the frequency of FoxP3⁺ Treg and RORγ⁺ Th17 cells (the gating strategy is shown in Supplemental Figure 4) and associated cytokines secretion were studied using flow cytometry and ELISA, respectively. Co-culture of naïve CD4⁺ T-cells with primed moDCs derived from different treatments did not affect the percentage of CD25⁺FoxP3⁺ Treg cells in the DC-T-cell co-culture (Figure 6A).

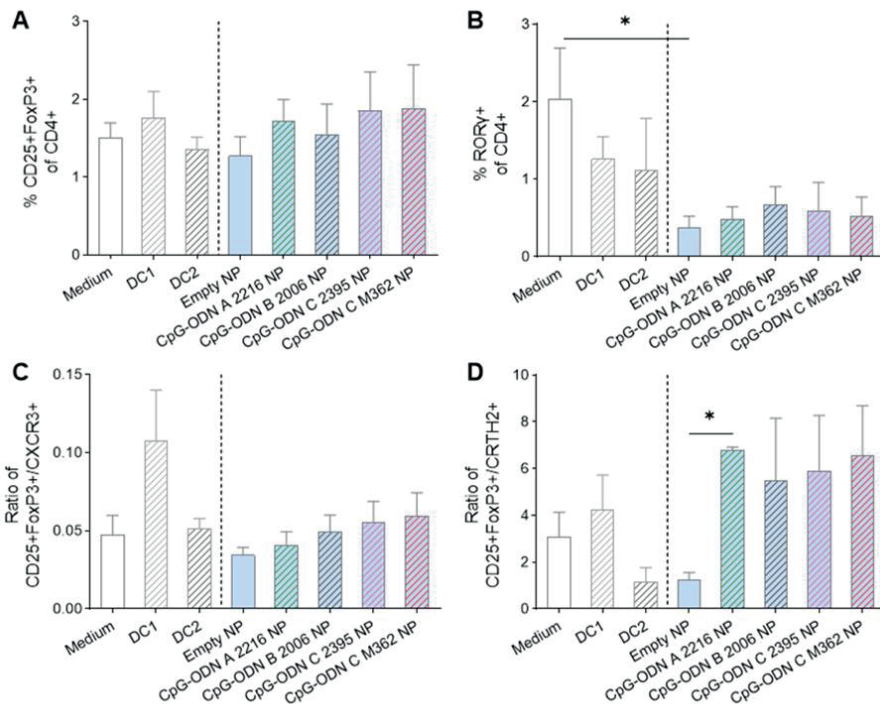


Figure 6. Flow cytometry analysis of regulatory T-cells (Treg), T helper 17 (Th17) subsets, and ratios of Treg over Th1 and Th2 in the DC-T-cell co-cultures. After 5-day co-culture of naïve CD4⁺ T-cells with the primed moDCs, the cells were collected and analyzed with flow cytometry for CD25⁺FoxP3⁺ Treg (A), RORγ⁺ Th17 (B) subsets of CD4⁺ T-cell, the Treg/Th1 ratio of CD25⁺FoxP3⁺/CXCR3⁺ (C) and the Treg/Th2 ratio of CD25⁺FoxP3⁺/CRTH2⁺ (D). Data are presented as mean ± SEM, n = 3 different co-cultures of DC-T-cell with allogeneic combinations using 2 independent naïve CD4⁺ T-cells donors and 2 independent moDCs donors; **p*<0.05; DC1: LPS primed moDCs; DC2: DC2-inducing mixture primed moDCs.

In the DC-T-cell co-culture, the frequency of ROR γ ⁺ cells was downregulated by the empty NP primed moDCs as compared to the medium primed moDCs (Figure 6B), but no additional influence was observed upon incubation of naïve CD4⁺ T-cells with PLGA NPs loaded with different types of CpG-ODN as compared to the empty NP. The primed moDCs derived from different treatments, when co-cultured with naïve CD4⁺T-cells for 5 days, did significantly alter the ratios of Treg/Th17 (CD25⁺FoxP3⁺/ROR γ ⁺) (not shown) nor Treg/Th1 (CD25⁺FoxP3⁺/CXCR3⁺) among CD4⁺ T-cells (Figure 6C). Co-incubation of naïve CD4⁺ T-cells with CpG-ODN A NP primed moDCs increased the Treg/Th2 ratio (CD25⁺FoxP3⁺/CRTH2⁺ in CD4⁺ cells) as compared to the empty NP control (Figure 6D).

Discussion

As reported by previous studies [42, 43], human DC are capable of internalizing PLGA nanoparticles with a size <300 nm. Besides size [44], their surface charge [43, 44] is a key factor that determines their cellular uptake [44]. Because the NPs used in the present study had similar size, zeta potential and loading capacity, difference in priming the immature moDCs using equivalent dose of PLGA NP encapsulated CpG-ODN of different types was expected not to be caused by differences in cellular uptake by phagocytosis [45, 46] and intracellular fate [47]. In line with our previous study [33], the observed burst release of CpG, might be caused by surface adsorbed ODNs that were not removed by the applied washing procedure. This burst release was followed by a phase no release from day 1 to day 14 followed by a sustained release of the loading up to day 49 (see Figure 2). This indicates that the CpG-ODN loading is released during degradation of the PLGA NPs [48] and be explained by the low mobility of the hydrophilic nature and large size of CpG-ODN in non-degraded PLGA matrices. It is however likely that this *in vitro* release profile is not predictive for the intracellular release of internalized PLGA NPs which release their content faster than in PBS buffer of pH 7.4 and 37°C. To illustrate this, Swider *et al.* [49] reported DC-internalized PLGA nanoparticles degraded within 72 hours intracellularly, while PLGA NPs incubated in PBS buffer were stable for more than 2 weeks.

After two days exposure of the immature moDCs, moDCs primed under different conditions showed a similar viability compared the medium controls which was 70-80% as expected [50]. Consistent with previous studies, exposure to the neutrally charged empty PLGA NP caused maturation of DC as shown by upregulated surface expression

of the costimulatory molecules CD80 and CD86 [43, 51], but it did not influence the expression of HLA-DR [51] (MHCII molecule) on DC. Kostadinova *et al.* [52] and Fischer *et al.* [53] however reported that PLGA nano- and micro- particles did not induce maturation of murine derived both bone marrow derived dendritic cells (BMDCs) and moDCs. Therefore, it is plausible that in the current study LPS contamination of the empty NP might have contributed to the observed moDCs maturation. Alternatively, the protein corona coating on the empty NP, formed due to absorption of proteins in the cell culture medium on the hydrophobic surface of PLGA NP [54, 55] may have functioned as danger signal known as nanoparticles associated molecular patterns (NAMPs) [56-58].

Programmed cell death ligand 1 (PD-L1) is ubiquitously expressed on non-lymphoid and lymphoid cells (*i.e.*, DC, resting B-cell and T-cells) and regulates immune responses in secondary lymphoid tissues and target organs [59]. As a negative regulatory co-stimulatory molecule, upregulation of PD-L1 expression on DC is regarded as an indication for their tolerance inducing capacity [60]. The tolerogenic property of the PD-L1+ DC was reported as essential for inducing IL-10 secreting T-cells *in vitro* [61], and generation of adaptive Treg subsets both *in vitro* and *in vivo* [62]. In line with the previous studies, we observed upregulated PD-L1 expression on DC1 [63, 64] and DC2 [65, 66]. Notably, empty NP also increased PD-L1 expression on moDCs [43]. However, empty NP also enhanced expression of costimulatory molecules CD80 and CD86, which was also observed on LPS (100 ng/mL) primed DC1. However, these DC1 produced high concentrations of IL-12p70, which remained low in the medium of the empty NP primed moDCs. It is reported that CpG-ODN can activate TLR-9 in human moDCs [12] and induce secretion of IFN- α , which subsequently upregulates PD-L1 expression [67]. However, PD-L1 expression was not further affected by the encapsulation of different classes of CpG.

It is therefore likely that the dose of CpG-ODN (0.4 μ g/mL encapsulated CpG), was too low to act through this pathway. Indeed, as reported by Jaehn *et al.* [68], the used dose in our study is much lower than the effective dose of 5 μ g/mL CpG-ODN that increased PD-L1 expression on human DC. In line herewith, a dose-dependent TLR-9-mediated response was reviewed by Montamat *et al.* [14]. The high dose of CpG-ODN mediated TLR-9 signaling by TRIF [69] induces secretion of anti-inflammatory molecules (*i.e.*, TGF- β and indoleamine 2, 3 dioxygenase (IDO)), which activate a suppressor

phenotype of Treg cells for tolerance induction [70]. On the other hand, the low concentration of CpG-ODN mediates TLR-9 signaling by the common TLR adaptor protein myeloid differentiation antigen 88 (MyD88) pathway in plasmacytoid dendritic cells (pDCs). A CpG-ODN induced TLR-9-MyD88 signaling in DC was reported by Alberca *et al.* [15] to inhibit Th2 immunity and allergic sensitization in mice.

Even though it was not predictable from the phenotypic changes of the primed moDCs or their cytokine release, consistently, the DC-T-cell assay indicated CpG-ODN A NP (at a dose of 0.4 µg/mL encapsulated CpG) primed moDCs, skewed away from Th2 polarization by enhancing the ratios of Th1/Th2 and Treg/Th2. This change in function of moDC was only significantly induced by CpG-ODN A NP, but not CpG-ODN B nor C albeit a similar pattern was shown. This enhanced Th1/Th2 and Treg/Th2 ratio is consistent with our *in vivo* finding using antigen and CpG-ODN co-encapsulated PLGA NP [33]. Considering the dose-dependent immunomodulatory effect of CpG [71], additional studies are needed to further elucidate the immunostimulatory properties of CpG loaded NPs.

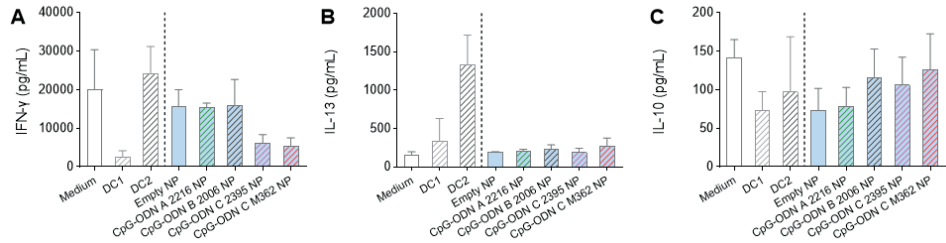
The primed moDCs may modify the T-cells phenotype via secretion of mediators and their expression of costimulatory molecules thereby shaping the outcome of immune polarization. Empty NP-primed moDCs lowered the frequency of Th17 subset ROR γ + cells as compared to the medium control in the DC-T-cell co-culture. This finding suggests that empty NP primed moDCs to skew away from Th17 development. Since Th17 cells can cause the development of inflammation and autoimmune diseases [72, 73], the observed lowered frequency of Th17 cells by empty NP primed moDCs is therefore beneficial with respect to its safety profile. However, ROR γ is not only a marker for T helper 17 cells (Th17), in CD4+ cells it can also be expressed by Treg [74, 75]; thus further investigation is required to support this hypothesis.

Noteworthy, the DC-T-cell assay is an *in vitro* allogeneic model devoid of other relevant immune cells, such as resting B-cells [76] and pDCs [76], which also express TLR-9 and play a pivotal role in mediating humoral responses, effector T-cells immune response and tolerance induction [77]. Therefore, B-cells and pDC need to be included for investigation of the immunostimulatory effects of the different classes of CpG-ODN loaded NP in future studies. Also, DC-T-cell modifying effects of PLGA NP co-encapsulating CpG-ODN plus antigen should be studied, which could include T cells of

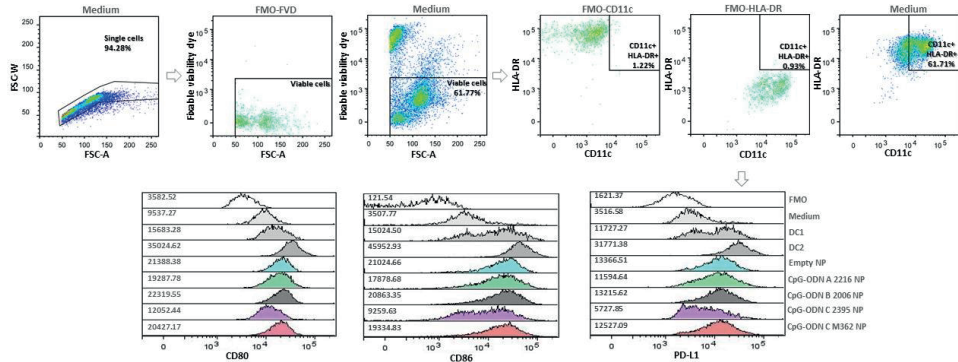
allergic patients to allow for allergen specific autologous DC/T-cell interaction. In conclusion, the findings suggest that priming of moDCs with CpG-ODN A NP is most effective in skewing away from Th2 polarization as shown in the allogeneic DC-T-cell assay. These preliminary results have shed light onto the immunomodulatory effect of CpG loaded PLGA nanoparticles on the function of DC.

Acknowledgments: ML is financially supported by China Scholarship Council (CSC), grant number 201707720004, and additional bench fee funding is supplied by Danone Nutricia Research B.V., Utrecht, the Netherlands.

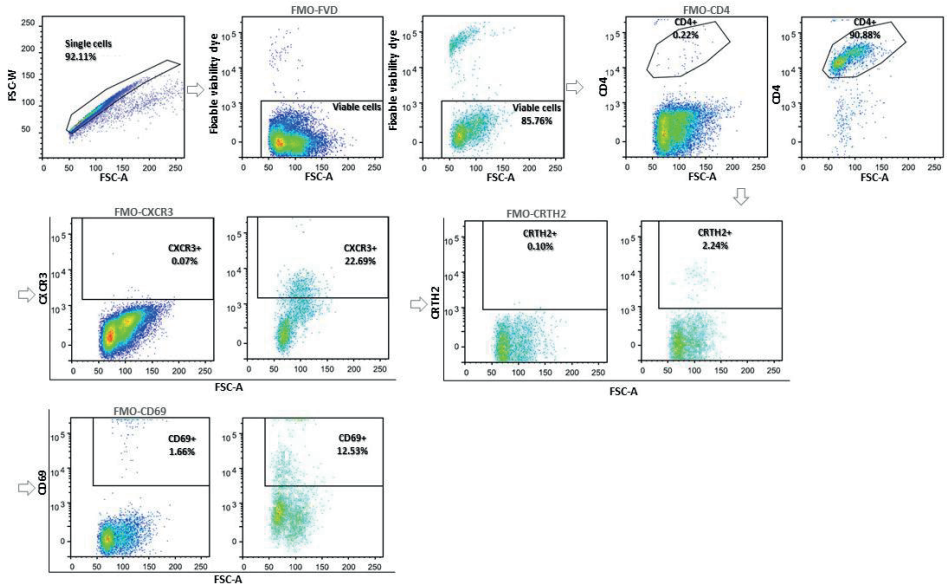
Supporting Figures



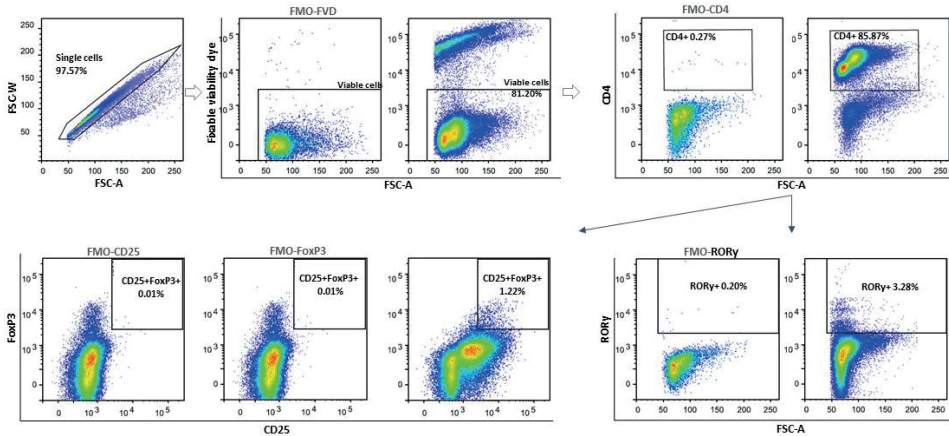
Supplemental Figure 1. Analysis of T helper 1 (Th1), T helper 2 (Th2) and regulatory T (Treg)- associated cytokines production in the DC-T-cell co-cultures. After 5-day co-culture of naïve CD4⁺ T-cells with the 48 h-primed moDCs, Th1-associated IFN- γ (A), Th2-associated IL-13 (B) and Treg-associated IL-10 (C) cytokines were measured in the supernatant collected from the DC-T-cell co-cultures. Data are presented as mean \pm SEM, n = 3 different DC-T-cell co-cultures with allogeneic combinations using 2 independent naïve CD4⁺ T-cells donors and 2 independent moDC donors; * p <0.05, ** p <0.01, *** p <0.001; DC1: LPS primed moDCs; DC2: DC2-inducing mixture primed moDCs.



Supplemental Figure 2. Representative gating plots of primed moDCs including median fluorescence intensity (MFI). The day 7 human immature monocytes derived dendritic cells (immature moDCs) were primed with either medium, DC1-inducing LPS, DC2-inducing mixture, empty NP and PLGA NPs loaded with class A-, B- or C- CpG-ODN encapsulated for 48 h at 37 °C.



Supplemental Figure 3. Representative gating plots of Th1-, Th2- and CD69+ T-cells subsets from the DC-T cell co-cultures. After 5-day co-culture of naïve CD4+ T-cells with the 48 h-primed moDCs, the cells were collected and analyzed with flow cytometry. The DC2 and T-cells co-culture was used for demonstration of the gating strategy.



Supplemental Figure 4. Representative gating plots of regulatory T-cells (Treg), T helper 17 (Th17) subsets from the DC-T cell co-cultures. After 5-day co-culture of naïve CD4+ T-cells with the 48 h-primed moDCs, the cells were collected and analyzed with flow cytometry for CD25+FoxP3+ Treg and RORγ+ Th17 subsets of CD4+ T-cells. The medium primed moDCs and T-cells co-culture was used for demonstration of the gating strategy.

References

- [1] R.L. Peters, M. Krawiec, J.J. Koplin, A.F. Santos, Update on food allergy, *Pediatr Allergy Immunol*, 32 (2021) 647-657.
- [2] P.J. Turner, N. Patel, D.E. Campbell, H.A. Sampson, M. Maeda, T. Katsunuma, J. Westerhout, W.M. Blom, J.L. Baumert, G.F. Houben, B.C. Remington, Reproducibility of food challenge to cow's milk: Systematic review with individual participant data meta-analysis, *J Allergy Clin Immunol*, (2022).
- [3] H.R. Fisher, G. Du Toit, H.T. Bahnson, G. Lack, The challenges of preventing food allergy: Lessons learned from LEAP and EAT, *Ann Allergy Asthma Immunol*, 121 (2018) 313-319.
- [4] D.I. Mitsias, P. Xepapadaki, M. Makris, N.G. Papadopoulos, Immunotherapy in allergic diseases - improved understanding and innovation for enhanced effectiveness, *Curr Opin Immunol*, 66 (2020) 1-8.
- [5] A.M. Mowat, To respond or not to respond - a personal perspective of intestinal tolerance, *Nat Rev Immunol*, 18 (2018) 405-415.
- [6] M.L. Saiz, V. Rocha-Perugini, F. Sanchez-Madrid, Tetraspanins as Organizers of Antigen-Presenting Cell Function, *Front Immunol*, 9 (2018) 1074.
- [7] T.H. Mogensen, Pathogen recognition and inflammatory signaling in innate immune defenses, *Clin Microbiol Rev*, 22 (2009) 240-273, Table of Contents.
- [8] M.L. Kapsenberg, Dendritic-cell control of pathogen-driven T-cell polarization, *Nat Rev Immunol*, 3 (2003) 984-993.
- [9] O. Joffre, M.A. Nolte, R. Sporri, C. Reis e Sousa, Inflammatory signals in dendritic cell activation and the induction of adaptive immunity, *Immunol Rev*, 227 (2009) 234-247.
- [10] V. Hornung, S. Rothenfusser, S. Britsch, A. Krug, B. Jahrsdorfer, T. Giese, S. Endres, G. Hartmann, Quantitative expression of toll-like receptor 1-10 mRNA in cellular subsets of human peripheral blood mononuclear cells and sensitivity to CpG oligodeoxynucleotides, *J Immunol*, 168 (2002) 4531-4537.
- [11] A. Iwasaki, R. Medzhitov, Toll-like receptor control of the adaptive immune responses, *Nat Immunol*, 5 (2004) 987-995.
- [12] V. Hoene, M. Peiser, R. Wanner, Human monocyte-derived dendritic cells express TLR9 and react directly to the CpG-A oligonucleotide D19, *J Leukoc Biol*, 80 (2006) 1328-1336.
- [13] M.P. Domogalla, P.V. Rostan, V.K. Raker, K. Steinbrink, Tolerance through Education: How Tolerogenic Dendritic Cells Shape Immunity, *Front Immunol*, 8 (2017) 1764.
- [14] G. Montamat, C. Leonard, A. Poli, L. Klimek, M. Ollert, CpG Adjuvant in Allergen-Specific Immunotherapy: Finding the Sweet Spot for the Induction of Immune Tolerance, *Front Immunol*, 12 (2021) 590054.
- [15] R.W. Alberca, E. Gomes, M. Russo, CpG-ODN Signaling via Dendritic Cells-Expressing MyD88, but Not IL-10, Inhibits Allergic Sensitization, *Vaccines (Basel)*, 9 (2021).
- [16] K.D. Srivastava, A. Siefert, T.M. Fahmy, M.J. Caplan, X.M. Li, H.A. Sampson, Investigation of peanut oral immunotherapy with CpG/peanut nanoparticles in a murine model of peanut allergy, *J Allergy Clin Immunol*, 138 (2016) 536-543 e534.
- [17] M.E. Kirtland, D.C. Tsitoura, S.R. Durham, M.H. Shamji, Toll-Like Receptor Agonists as Adjuvants for Allergen Immunotherapy, *Front Immunol*, 11 (2020) 599083.
- [18] A. Mansson, O. Bachar, M. Adner, L.O. Cardell, Nasal CpG oligodeoxynucleotide administration induces a local inflammatory response in nonallergic individuals, *Allergy*, 64 (2009) 1292-1300.
- [19] G. Senti, P. Johansen, S. Haug, C. Bull, C. Gottschaller, P. Muller, T. Pfister, P. Maurer, M.F. Bachmann, N. Graf, T.M. Kundig, Use of A-type CpG oligodeoxynucleotides as an adjuvant in allergen-specific immunotherapy in humans: a phase I/IIa clinical trial, *Clin Exp Allergy*, 39 (2009) 562-570.
- [20] L. Klimek, J. Willers, A. Hammann-Haenni, O. Pfaar, H. Stocker, P. Mueller, W.A. Renner, M.F. Bachmann, Assessment of clinical efficacy of CYT003-QbG10 in patients with allergic rhinoconjunctivitis: a phase IIb study, *Clin Exp Allergy*, 41 (2011) 1305-1312.
- [21] T.B. Casale, J. Cole, E. Beck, C.F. Vogelmeier, J. Willers, C. Lassen, A. Hammann-Haenni, L. Trokan, P. Saudan, M.E. Wechsler, CYT003, a TLR9 agonist, in persistent allergic asthma - a randomized placebo-controlled Phase 2b study, *Allergy*, 70 (2015) 1160-1168.
- [22] M. Hessenberger, R. Weiss, E.E. Weinberger, C. Boehler, J. Thalhamer, S. Scheibhofer, Transcutaneous delivery of CpG-adjuvanted allergen via laser-generated micropores, *Vaccine*, 31 (2013) 3427-3434.
- [23] D.L. Miren Kerkmann, Jörg Weyermann, Anja Marschner, Hendrik Poeck, Moritz Wagner, Julia Battiany, Andreas Zimmer, Stefan Endres, And Gunther Hartmann, Immunostimulatory Properties of

- CpG-Oligonucleotides Are Enhanced by the Use of Protamine Nanoparticles, *Oligonucleotides* 16 (2006) 313–322
- [24] G. Cappellano, C. Comi, A. Chiocchetti, U. Dianzani, Exploiting PLGA-Based Biocompatible Nanoparticles for Next-Generation Tolerogenic Vaccines against Autoimmune Disease, *Int J Mol Sci*, 20 (2019).
- [25] J. Koerner, D. Horvath, M. Groettrup, Harnessing Dendritic Cells for Poly (D,L-lactide-co-glycolide) Microspheres (PLGA MS)-Mediated Anti-tumor Therapy, *Front Immunol*, 10 (2019) 707.
- [26] F. Sarti, G. Perera, F. Hintzen, K. Kotti, V. Karageorgiou, O. Kammona, C. Kiparissides, A. Bernkop-Schnürch, In vivo evidence of oral vaccination with PLGA nanoparticles containing the immunostimulant monophosphoryl lipid A, *Biomaterials*, 32 (2011) 4052-4057.
- [27] D.R.R. Daqing Wang, Glen S. Kwon and John Samuel, Encapsulation of plasmid DNA in biodegradable poly(D,L-lactic-coglycolic acid) microspheres as a novel approach for immunogene delivery, *Journal of Controlled Release* 57 (1999) 9-18.
- [28] J.M. Carreno, C. Perez-Shibayama, C. Gil-Cruz, A. Printz, R. Pastelin, A. Isibasi, D. Chariatte, Y. Tanoue, C. Lopez-Macias, B. Gander, B. Ludewig, PLGA-microencapsulation protects *Salmonella typhi* outer membrane proteins from acidic degradation and increases their mucosal immunogenicity, *Vaccine*, 34 (2016) 4263-4269.
- [29] H.O. Alsaab, F.D. Alharbi, A.S. Alhibs, N.B. Alanazi, B.Y. Alshehri, M.A. Saleh, F.S. Alshehri, M.A. Algarni, T. Almugaitieb, M.N. Uddin, R.M. Alzhrani, PLGA-Based Nanomedicine: History of Advancement and Development in Clinical Applications of Multiple Diseases, *Pharmaceutics*, 14 (2022).
- [30] M. Mir, N. Ahmed, A.U. Rehman, Recent applications of PLGA based nanostructures in drug delivery, *Colloids Surf B Biointerfaces*, 159 (2017) 217-231.
- [31] N. Benne, J. van Duijn, J. Kuiper, W. Jiskoot, B. Slutter, Orchestrating immune responses: How size, shape and rigidity affect the immunogenicity of particulate vaccines, *J Control Release*, 234 (2016) 124-134.
- [32] D. Ding, Q. Zhu, Recent advances of PLGA micro/nanoparticles for the delivery of biomacromolecular therapeutics, *Mater Sci Eng C Mater Biol Appl*, 92 (2018) 1041-1060.
- [33] M. Liu, S. Thijssen, W.E. Hennink, J. Garssen, C.F. van Nostrum, L.E.M. Willemsen, Oral pretreatment with beta-lactoglobulin derived peptide and CpG co-encapsulated in PLGA nanoparticles prior to sensitizations attenuates cow's milk allergy development in mice, *Front Immunol*, 13 (2023) 1053107.
- [34] S. de Kivit, E. van Hoffen, N. Korthagen, J. Garssen, L.E. Willemsen, Apical TLR ligation of intestinal epithelial cells drives a Th1-polarized regulatory or inflammatory type effector response in vitro, *Immunobiology*, 216 (2011) 518-527.
- [35] S. de Kivit, A.D. Kraneveld, L.M. Knippels, Y. van Kooyk, J. Garssen, L.E. Willemsen, Intestinal epithelium-derived galectin-9 is involved in the immunomodulating effects of nondigestible oligosaccharides, *J Innate Immun*, 5 (2013) 625-638.
- [36] Y. Waeckerle-Men, E. Scandella, E. Uetz-Von Allmen, B. Ludewig, S. Gillessen, H.P. Merkle, B. Gander, M. Groettrup, Phenotype and functional analysis of human monocyte-derived dendritic cells loaded with biodegradable poly(lactide-co-glycolide) microspheres for immunotherapy, *J Immunol Methods*, 287 (2004) 109-124.
- [37] W.E. Kalinski P, Muthuswamy R, De Jong E., Generation of stable Th1/CTL-, Th2-, and Th17-inducing human dendritic cells, 2010.
- [38] K. Fujimura, A. Oyamada, Y. Iwamoto, Y. Yoshikai, H. Yamada, CD4 T cell-intrinsic IL-2 signaling differentially affects Th1 and Th17 development, *J Leukoc Biol*, 94 (2013) 271-279.
- [39] T. Hoppenbrouwers, V. Fogliano, J. Garssen, N. Pellegrini, L.E.M. Willemsen, H.J. Wichers, Specific Polyunsaturated Fatty Acids Can Modulate in vitro Human moDC2s and Subsequent Th2 Cytokine Release, *Front Immunol*, 11 (2020) 748.
- [40] J.D.M. Bruce L. Levine, James L. Riley, Richard G. Carroll, Maryanne T. Vahey, Linda L. Jagodzinski, Kenneth F. Wagner, Douglas L. Mayers, Donald S. Burke, Owen S. Weislow, Daniel C. St. Louis, Carl H. June, Antiviral Effect and Ex Vivo CD4+ T Cell Proliferation in HIV-Positive Patients as a Result of CD28 Costimulation, *SCIENCE*, 272 (1996) 1939-1943.
- [41] A. Trickett, Y.L. Kwan, T cell stimulation and expansion using anti-CD3/CD28 beads, *J Immunol Methods*, 275 (2003) 251-255.
- [42] M. Diwan, P. Elamanchili, H. Lane, A. Gainer, J. Samuel, Biodegradable Nanoparticle Mediated Antigen Delivery to Human Cord Blood Derived Dendritic Cells for Induction of Primary T Cell Responses, *Journal of Drug Targeting*, 11 (2008) 495-507.

- [43] S. Barillet, E. Fattal, S. Mura, N. Tsapis, M. Pallardy, H. Hillaireau, S. Kerdine-Romer, Immunotoxicity of poly (lactic-co-glycolic acid) nanoparticles: influence of surface properties on dendritic cell activation, *Nanotoxicology*, 13 (2019) 606-622.
- [44] H. Hillaireau, P. Couvreur, Nanocarriers' entry into the cell: relevance to drug delivery, *Cell Mol Life Sci*, 66 (2009) 2873-2896.
- [45] M. Yoshida, J.E. Babensee, Molecular aspects of microparticle phagocytosis by dendritic cells, *J Biomater Sci Polym Ed*, 17 (2006) 893-907.
- [46] D.R.R. M. E. Christine Lutsiak, Conrad Coester, Glen S. Kwon, and John Samuel, Analysis of Poly(D,L-Lactic-Co-Glycolic Acid) Nanosphere Uptake by Human Dendritic Cells and Macrophages In Vitro, *Pharmaceutical Research*, 19 (2002) 1480-1487.
- [47] E. Frohlich, Cellular elimination of nanoparticles, *Environ Toxicol Pharmacol*, 46 (2016) 90-94.
- [48] J. Panyam, M.M. Dali, S.K. Sahoo, W. Ma, S.S. Chakravarthi, G.L. Amidon, R.J. Levy, V. Labhasetwar, Polymer degradation and in vitro release of a model protein from poly(D,L-lactide-co-glycolide) nano- and microparticles, *J Control Release*, 92 (2003) 173-187.
- [49] E. Swider, S. Maharjan, K. Houkes, N.K. van Riessen, C. Figdor, M. Srinivas, O. Tagit, Forster Resonance Energy Transfer-Based Stability Assessment of PLGA Nanoparticles in Vitro and in Vivo, *ACS Appl Bio Mater*, 2 (2019) 1131-1140.
- [50] A. Mohammadi, J. Mehrzad, M. Mahmoudi, M. Schneider, A. Haghparast, Effect of culture and maturation on human monocyte-derived dendritic cell surface markers, necrosis and antigen binding, *Biotech Histochem*, 90 (2015) 445-452.
- [51] M. Yoshida, J.E. Babensee, Poly(lactic-co-glycolic acid) enhances maturation of human monocyte-derived dendritic cells, *J Biomed Mater Res A*, 71 (2004) 45-54.
- [52] A.I. Kostadinova, J. Middelburg, M. Ciulla, J. Garssen, W.E. Hennink, L.M.J. Knippels, C.F. van Nostrum, L.E.M. Willemsen, PLGA nanoparticles loaded with beta-lactoglobulin-derived peptides modulate mucosal immunity and may facilitate cow's milk allergy prevention, *Eur J Pharmacol*, 818 (2018) 211-220.
- [53] S. Fischer, E. Uetz-von Allmen, Y. Waeckerle-Men, M. Groettrup, H.P. Merkle, B. Gander, The preservation of phenotype and functionality of dendritic cells upon phagocytosis of polyelectrolyte-coated PLGA microparticles, *Biomaterials*, 28 (2007) 994-1004.
- [54] R. Gossmann, E. Fahrlander, M. Hummel, D. Mulac, J. Brockmeyer, K. Langer, Comparative examination of adsorption of serum proteins on HSA- and PLGA-based nanoparticles using SDS-PAGE and LC-MS, *Eur J Pharm Biopharm*, 93 (2015) 80-87.
- [55] K. Partikel, R. Korte, N.C. Stein, D. Mulac, F.C. Herrmann, H.U. Humpf, K. Langer, Effect of nanoparticle size and PEGylation on the protein corona of PLGA nanoparticles, *Eur J Pharm Biopharm*, 141 (2019) 70-80.
- [56] A.L. Silva, C. Peres, J. Connot, A.I. Matos, L. Moura, B. Carreira, V. Sainz, A. Scomparin, R. Satchi-Fainaro, V. Preat, H.F. Florindo, Nanoparticle impact on innate immune cell pattern-recognition receptors and inflammasomes activation, *Semin Immunol*, 34 (2017) 3-24.
- [57] D.F. Moyano, M. Goldsmith, D.J. Solfiell, D. Landesman-Milo, O.R. Miranda, D. Peer, V.M. Rotello, Nanoparticle hydrophobicity dictates immune response, *J Am Chem Soc*, 134 (2012) 3965-3967.
- [58] B. Fadeel, Clear and present danger? Engineered nanoparticles and the immune system, *Swiss Med Wkly*, 142 (2012) w13609.
- [59] M.A. Galvan Morales, J.M. Montero-Vargas, J.C. Vizuet-de-Rueda, L.M. Teran, New Insights into the Role of PD-1 and Its Ligands in Allergic Disease, *Int J Mol Sci*, 22 (2021) 11898.
- [60] R. Kuo, E. Saito, S.D. Miller, L.D. Shea, Peptide-Conjugated Nanoparticles Reduce Positive Co-stimulatory Expression and T Cell Activity to Induce Tolerance, *Mol Ther*, 25 (2017) 1676-1685.
- [61] W.W. Unger, S. Laban, F.S. Kleijwegt, A.R. van der Slik, B.O. Roep, Induction of Treg by monocyte-derived DC modulated by vitamin D3 or dexamethasone: differential role for PD-L1, *Eur J Immunol*, 39 (2009) 3147-3159.
- [62] K.P.-L. Li Wang, Victor C. de Vries, Indira Guleria, Mohamed H. Sayegh, and Randolph J. Noelle, Programmed death 1 ligand signaling regulates the generation of adaptive Foxp3^{hi}CD4^{hi} regulatory T cells, *PNAS* 105 (2008) 9331-9336.
- [63] J.C. Mbongue, E. Vanterpool, A. Firek, W.H.R. Langridge, Lipopolysaccharide-Induced Immunological Tolerance in Monocyte-Derived Dendritic Cells, *Immuno*, 2 (2022) 482-500.
- [64] F. Salazar, D. Awuah, O.H. Negm, F. Shakib, A.M. Ghaemmaghami, The role of indoleamine 2,3-dioxygenase-aryl hydrocarbon receptor pathway in the TLR4-induced tolerogenic phenotype in human DCs, *Sci Rep*, 7 (2017) 43337.

- [65] M.A. Frias, M.C. Rebsamen, C. Gerber-Wicht, U. Lang, Prostaglandin E2 activates Stat3 in neonatal rat ventricular cardiomyocytes: A role in cardiac hypertrophy, *Cardiovasc Res*, 73 (2007) 57-65.
- [66] S. Goto, S. Konnai, Y. Hirano, J. Kohara, T. Okagawa, N. Maekawa, Y. Sajiki, K. Watari, E. Minato, A. Kobayashi, S. Gondaira, H. Higuchi, M. Koiwa, M. Tajima, E. Taguchi, R. Uemura, S. Yamada, M.K. Kaneko, Y. Kato, K. Yamamoto, M. Toda, Y. Suzuki, S. Murata, K. Ohashi, Upregulation of PD-L1 Expression by Prostaglandin E(2) and the Enhancement of IFN-gamma by Anti-PD-L1 Antibody Combined With a COX-2 Inhibitor in *Mycoplasma bovis* Infection, *Front Vet Sci*, 7 (2020) 12.
- [67] A.V. Bazhin, K. von Ahn, J. Fritz, J. Werner, S. Karakhanova, Interferon-alpha Up-Regulates the Expression of PD-L1 Molecules on Immune Cells Through STAT3 and p38 Signaling, *Front Immunol*, 9 (2018) 2129.
- [68] P.S. Jaehn, K.S. Zaenker, J. Schmitz, A. Dzionek, Functional dichotomy of plasmacytoid dendritic cells: antigen-specific activation of T cells versus production of type I interferon, *Eur J Immunol*, 38 (2008) 1822-1832.
- [69] C. Volpi, F. Fallarino, M.T. Pallotta, R. Bianchi, C. Vacca, M.L. Belladonna, C. Orabona, A. De Luca, L. Boon, L. Romani, U. Grohmann, P. Puccetti, High doses of CpG oligodeoxynucleotides stimulate a tolerogenic TLR9-TRIF pathway, *Nat Commun*, 4 (2013) 1852.
- [70] B. Baban, P.R. Chandler, M.D. Sharma, J. Pihkala, P.A. Koni, D.H. Munn, A.L. Mellor, IDO activates regulatory T cells and blocks their conversion into Th17-like T cells, *J Immunol*, 183 (2009) 2475-2483.
- [71] G. Wingender, N. Garbi, B. Schumak, F. Jungerkes, E. Endl, D. von Bubnoff, J. Steitz, J. Striegler, G. Moldenhauer, T. Tuting, A. Heit, K.M. Huster, O. Takikawa, S. Akira, D.H. Busch, H. Wagner, G.J. Hammerling, P.A. Knolle, A. Limmer, Systemic application of CpG-rich DNA suppresses adaptive T cell immunity via induction of IDO, *Eur J Immunol*, 36 (2006) 12-20.
- [72] R.P. Singh, S. Hasan, S. Sharma, S. Nagra, D.T. Yamaguchi, D.T. Wong, B.H. Hahn, A. Hossain, Th17 cells in inflammation and autoimmunity, *Autoimmun Rev*, 13 (2014) 1174-1181.
- [73] J.P. McAleer, B. Liu, Z. Li, S.M. Ngoi, J. Dai, M. Oft, A.T. Vella, Potent intestinal Th17 priming through peripheral lipopolysaccharide-based immunization, *J Leukoc Biol*, 88 (2010) 21-31.
- [74] J.-H.P. Caspar Ohnmacht, Sascha Cording, James B. Wing, Koji Atarashi, Yuuki Obata, Valérie Gaboriau-Routhiau, Rute Marques, Sophie Dulauroy, Maria Fedoseeva, Meinrad Busslinger, Nadine Cerf-Bensussan, Ivo G. Boneca, David Voehringer, Koji Hase, Kenya Honda, Shimon Sakaguchi, Gérard Eberl, The microbiota regulates type 2 immunity through ROR γ ⁺ T cells, *Science*, 349 (2015) 989-993.
- [75] N.G.-Z. Esen Sefik, Sungwhan Oh, Liza Konnikova, David Zemmour, Abigail Manson McGuire, Dalia Burzyn, Adriana Ortiz-Lopez, Mercedes Lobera, Jianfei Yang, Shomir Ghosh, Ashlee Earl, Scott B. Snapper, Ray Jupp, Dennis Kasper, Diane Mathis, Christophe Benoist, Individual intestinal symbionts induce a distinct population of ROR γ ⁺ regulatory T cells, *Science*, 349 (2015) 993-997.
- [76] M.E.S. Udo Holtick, Michael S von Bergwelt-Baildon & Martin R Wehrauch, Toll-like receptor 9 agonists as cancer therapeutics, *20* (2011) 361-372.
- [77] B. Wittig, M. Schmidt, W. Scheithauer, H.J. Schmoll, MGN1703, an immunomodulator and toll-like receptor 9 (TLR-9) agonist: from bench to bedside, *Crit Rev Oncol Hematol*, 94 (2015) 31-44.

CHAPTER 6

Summary And Perspectives

Summary

This thesis presents the results of the investigation of poly(lactic-co-glycolic acid) PLGA nanoparticles (NP) loaded with BLG-peptides with or without co-loaded synthetic CpG-ODN as oral delivery system for allergen-specific tolerance induction in mice. To get mechanistic insights into the observed findings, the intracellular fate and immunomodulatory effects of these PLGA NPs were investigated *in vitro*. In this chapter, the major outcomes of this thesis are summarized and their implications, relevance and suggested directions for further research are discussed.

In **Chapter 1**, the management guidelines and current progress in prevention approaches for the development of early life cow's milk allergy (CMA) are discussed. Early life introduction of allergen/antigen provides a window of opportunity for oral tolerance induction. In this regard, advantages of PLGA NP based oral delivery of antigens in presence or absence of CpG-ODN in triggering allergen-specific tolerance are underlined. Previous dissertations of our department investigated the successful possibility to induce oral tolerance using a cocktail of BLG-peptides, either in their free form [1] or separately loaded in PLGA NPs [2]. To investigate tolerance induction using less BLG-peptides, in **Chapter 2**, two BLG-peptides (of 18 amino acids, 18-AA) were selected for separate encapsulation in PLGA NPs using a double emulsion solvent evaporation technique. The CMA prevention outcomes of these orally administered peptides loaded PLGA NPs, were investigated in a whey-protein induced murine model for CMA. *In vivo*, pretreatment of 3-week-old female C3H/HeOuJ mice with high-dose (160 µg encapsulated BLG-peptides), but not low-dose (80 µg encapsulated BLG-peptides) nor empty NP plus 160 µg free BLG-peptides-mix, protected the mice from anaphylaxis and lowered the acute allergic skin response upon intradermal whey challenge compared to sham-pretreated whey-sensitized mice. The high-dose BLG-peptides/NPs-pretreatment, but not the low dose pre-treatment, inhibited *ex vivo* whey-stimulated pro-inflammatory cytokine TNF-α release by splenocytes as compared to the free BLG-peptides-mix or empty NP plus BLG-peptides-mix whey-sensitized recipients.

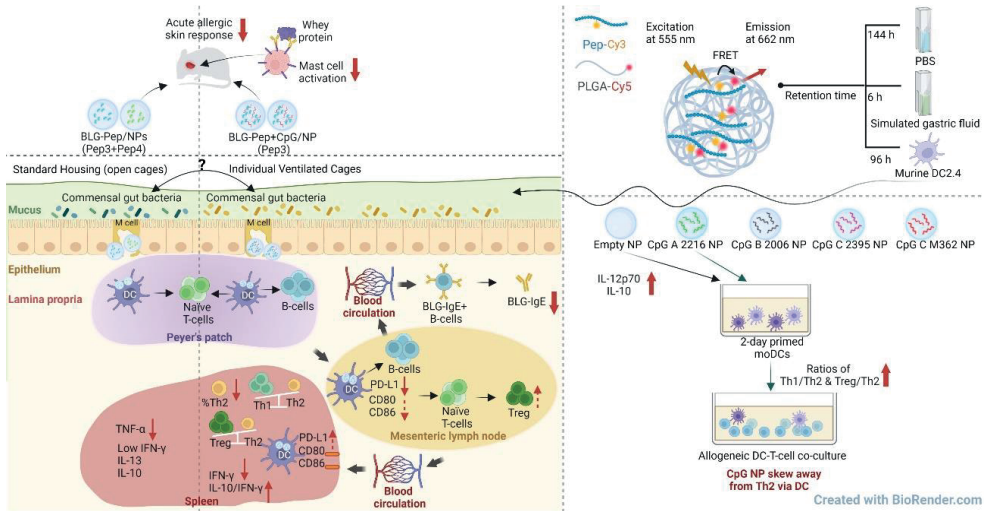
Improved hygiene conditions and loss of microbial diversity are associated with increased risk of allergy development that is mediated by a Th2 predominant immune response. In this respect, bacterial CpG DNA is known to drive Th1 and regulatory T-cell (Treg) development *via* Toll-Like-Receptor 9 (TLR-9) signaling, skewing away from the allergic Th2 phenotype. **Chapter 3** describes co-encapsulation of one selected β-

lactoglobulin derived peptide (BLG-Pep, AASDISLLDAQSAPLRVY) and TLR-9 ligand class B-CpG-ODN in PLGA NP using a double emulsion solvent evaporation technique. In this chapter, CMA prevention outcomes of different oral pretreatments were investigated in the whey-induced CMA murine model. In this experiment the mice were housed in individually ventilated cages simulating a strict hygienic environment. The pretreatment with co-encapsulated BLG-Pep+CpG/NP, but not with BLG-Pep/NP, CpG/NP or the mixture of BLG-Pep/NP plus CpG/NP, prevented both the whey-induced acute allergic skin response and the rise in serum BLG-specific IgE compared to sham-pretreated whey-sensitized mice. Importantly, pretreatment with co-encapsulated BLG-Pep+CpG/NP reduced dendritic cells (DCs) activation and lowered the frequencies of PD-L1+ DCs in the mesenteric lymph nodes compared to whey-sensitized mice. Conversely pretreatment with co-encapsulated BLG-Pep+CpG/NP increased the frequency of splenic PD-L1+ DCs compared to the separately encapsulated BLG-Pep/NP plus CpG/NP recipients. This was associated with the lower Th2 frequency and increased Treg/Th2 and Th1/Th2 ratios in the spleen of the co-encapsulated BLG-Pep+CpG/NP recipients as compared to the whey-sensitized mice. Oral administration of co-encapsulated BLG-Pep+CpG/NP prevented rise in serum BLG-specific IgE and development of whey-allergic symptoms while lowering splenic Th2 cell frequency in these mice.

Despite DCs play a pivotal role in mediating peripheral tolerance *via* sampling particulate (*i.e.*, antigen loaded PLGA NP) and antigen presentation, the mechanism(s) responsible for the interaction of the peptide loaded PLGA nanoparticles with DCs and their intracellular fate is/are elusive. In **Chapter 4**, Förster Resonance Energy Transfer (FRET), a distance-dependent non-radioactive energy transfer process mediated from a donor to an acceptor fluorochrome, was exploited to investigate these processes. Ratio of donor (Cyanine-3) conjugated peptide and acceptor (Cyanine-5) labeled PLGA in the prepared nanocarrier was fine-tuned for optimal FRET efficiency. The colloidal stability and FRET emission of prepared NPs were maintained upon 144 h-incubation in phosphate buffered saline and 6 h-incubation in biorelevant simulated gastric fluid at 37 °C. Real-time tracking of the peptide loaded PLGA nanoparticles and peptide release from the internalized nanoparticles in DCs were monitored from the change in the FRET signal. This confirmed their internalization and prolonged retention of the PLGA nanoparticles encapsulated peptide as compared to the free peptide in the DCs.

As shown in **Chapter 3**, orally administered PLGA NP co-encapsulating BLG-Pep and class B CpG-ODN gave rise to phenotypic changes on DCs as compared to the sham-pretreated whey-sensitized mice. Nevertheless, neither the immunostimulatory effect of class B-CpG-ODN encapsulated PLGA nanoparticles on DCs nor differences in efficacy between class A-, B- or C- CpG-ODN encapsulated in PLGA NPs (CpG/NPs) is known. In **Chapter 5**, we describe preparation of empty and class A-, B- or C- CpG-ODNs encapsulated PLGA NPs using a double emulsion solvent evaporation method. These NPs showed similar mean NP size of ~250-290 nm, zeta potential of -1 mV and encapsulation efficiency of 50-65%. *In vitro*, as maturation controls, human immature monocytes derived DCs (moDCs) were incubated using LPS to induce DC1 which drive naïve T-cell differentiation towards Th1 cells and a cytokine mixture for 48 h to induce DC2 which drive Th2 cells differentiation. In addition, the immature moDCs were exposed to empty NP or CpG-ODN A, B or C loaded NPs. The phenotype of primed moDCs was characterized by analyzing maturation markers expression of CD80, CD86 and/or Programmed Death Ligand-1 (PD-L1). Incubation of immature moDCs with empty NPs, also with DC1- and DC2- maturation controls, resulted in the upregulated expression of the mentioned markers on these moDCs, indicating maturation of these cells. Furthermore, costimulatory expression of CD80, CD86 and PD-L1 on CpG/NPs exposed moDCs was similar to empty NP exposed DC. Intriguingly, when co-cultured with naïve CD4+ T-cells, class A-CpG NP primed moDCs increased the ratios of Th1/Th2 (CXCR3+/CRTH2+) and the Treg/Th2 (CD25+FoxP3+/CRTH2+) as compared to empty NP primed DC. This indicates that class A-CpG NP primed moDCs skew T-cell polarization away from Th2 development.

Finally, the findings from Chapter 2 to 5 are summarized and illustrated in the **Summarizing figure** below.



Summarizing figure.

An overview of the implicated mechanisms of the poly(lactic-*co*-glycolic acid) PLGA nanoparticles-based pretreatments described in this thesis. *In vitro*, PLGA nanoparticles protect the encapsulated peptide cargo against digestion in simulated gastric fluid for up to 6 h. This substantiates an enhanced chance of the encapsulated peptide to be internalized by intestinal DC. In addition, the PLGA nanoparticles prolonged the retention time of the internalized and loaded peptide cargo to 96 h as compared to the non-encapsulated peptide (24 h) in murine DC2.4. Besides the physical protection and prolonged retention time of the cargo in DC, *in vitro*, empty PLGA nanoparticles increased Th1- (IL-12p70) and Treg- (IL-10) associated cytokine release by human moDCs or induced moDCs maturation as shown by increased expression of co-stimulatory molecules. In particular, CpG-A loaded NP primed moDCs enhanced the ratios of Treg/Th2 and Th1/Th2 thus skewing away from the Th2 allergic phenotype.

In vivo, oral pre-exposure to BLG-Pep/NPs protected the mice against whey-sensitizations and acute allergic skin response toward intradermal challenge with whole whey protein. In addition, the *ex vivo* whey-restimulation recalled a significant lower level of TNF- α and relative low levels of IFN- γ , IL-13, and IL-10 by the splenocytes in BLG-Pep/NPs recipients as compared to the whey-allergic mice. This whey-specific systemic silencing induced by pre-exposure to BLG-Pep/NPs might have contributed to the inhibited development of whey-induced allergy.

Influence of standard housing in open cages and individual ventilated cages (IVC) on the commensal gut bacteria remains to be clarified. Despite that, co-encapsulation of CpG as immune adjuvant and a selected model BLG-peptide in PLGA nanoparticles (BLG-Pep+CpG/NP), but not an equivalent dose of CpG/NPs or BLG-Pep/NP alone or as a mixture, lowered expression of co-stimulatory molecules CD80/CD86 and PD-L1 on MLN DC as compared to the whey-allergic mice. Concomitantly, co-encapsulated BLG-Pep+CpG/NP increased expression of PD-L1 on splenic DC and regulatory T-cells. In addition, *ex vivo* whey-restimulation of splenocytes recalled a lower secretion of IFN- γ and higher ratio of IL-10/IFN- γ in co-encapsulated BLG-Pep+CpG/NP recipients as compared to the whey-allergic mice.

Perspectives

In **Chapter 2**, the two synthetic BLG-peptides (referred as peptide 3 and 4) of 18-AA length (with an overlapping sequence of 12-AA) were encapsulated separately in PLGA NP. The NP were optimized in terms of a smaller size (280 nm vs 320 nm in the previous study [3]), higher encapsulation efficiency of peptide 3 (78% vs 30% [3]) and absent burst release of the two encapsulated peptides in the *in vitro* release assay. The observed absence of burst release of BLG-peptide might be attributed to sufficient washing procedures and/or absence of porosity in the lyophilized peptide-NPs. The slightly smaller NP size might facilitate a better penetration through the mucus as well as better cellular uptake by intestinal M-cells or enterocytes [4, 5]. Lowering the size of the NP is certainly possible but this is associated with a lower encapsulation efficiency of the peptides [6]. Therefore, we selected PLGA NPs with a mean NP size between 250-290 nm for dosing the mice in the preclinical study in **Chapter 2 and 3**. PLGA NP of 300 nm or less are ideal for oral delivery since they have a good loading capacity and tend to be taken up by enterocytes and M-cells in the small intestine [4, 5, 7]. Hence, PLGA NP of the size of 250-290 nm [8-10], with a narrow size distribution and with a neutral surface charge [11] are preferred for crossing the mucus, and to subsequently being taken up by the M-cells and possibly also by the intestinal DCs. In the Peyer's Patches (PP) beneath M-cells, DCs can internalize the peptide loaded NP as well and instruct T-cell development. In the meanwhile, these DCs also migrate to the mesenteric lymph nodes (MLN) and instruct T-cells. In case of active tolerance induction, the induced Tregs in MLN will traffic *via* the bloodstream and home back to the intestine, while they can also convert oral tolerance systemically [12, 13].

In **Chapter 2**, 3-4-week-old female C3H/HeO_uJ mice were chosen to investigate the oral tolerance induction using PLGA NP encapsulating the selected BLG-peptides[14]. The mice were given 6-daily oral-pretreatments prior to 5-consecutive-weekly-sensitizations to whole whey protein. As a portal of entry into the intestinal immunity [15], microfold cells (M-cells), already matured and reached adult levels before 2-3-week of age in mice [16]. It is known that nanoparticles can get access *via* the M-cells to the Peyer's Patches (PP) of the GALT where uptake and peptide presentation by the DC is facilitated, which in turn can instruct T-cell development in the PP or mesenteric lymph nodes (MLN) [16, 17]. The developed T-cells migrate from MLN to the systemic bloodstream and due to imprinted homing markers they will travel back to the lamina propria [12]. Noteworthy, during the neonatal period, the immature gut barrier [18] may facilitate delivery of the peptide loaded PLGA NP to the intestinal immune system. In the meanwhile, recruitment of T-cells to the neonatal mucosa [19, 20] and microbiome maturation [21] further contribute to development of regulatory T-cells (Treg) and establishment of oral tolerance [18]. In support of this notion, we observed that early pre-exposures to the peptide loaded PLGA NP [14] protected the mice from development of whey-induced allergy. In addition, **Chapter 2** demonstrated that oral pre-exposure to NP loaded with the two selected BLG-peptides, but not equivalent doses of the free peptides, protected the recipients from acute allergic skin response upon intradermal whey-challenge in a dose-dependent manner. Despite the underlying mechanism remains elusive, this observed preventive effect may be associated with systemic immune silencing for whole whey protein since a reduced allergen specific pro-inflammatory cytokine TNF- α production upon *ex vivo* whey-stimulation was observed. This may be achieved if the two selected-peptides contain immunodominant epitopes of the whole whey protein, when processed and subsequently presented by DC in the MHCII groove for recognition by T-cells. Despite no effect was found in the frequency of Th1, Th2, Th17 and Treg in the spleen, **Chapter 2** demonstrated that BLG-peptides/NPs pretreatment significantly reduced the whey-stimulated TNF- α release in a dose-dependent manner, since it was not effective in the low dose group. Previous studies suggested that TNF- α is predominantly associated with Th1-mediated inflammation [22], but it also plays a pivotal role in upregulation of Th2-polarizing cytokine release and antigen-specific IgE levels [23, 24]. Thus, the silencing of *ex vivo* whey-stimulated TNF- α release by splenocytes, which models silencing of the systemic immune response for whey protein, might associate with the observed reduction in acute allergic skin response among the BLG-peptides/NPs recipient mice.

To further enhance the tolerogenic capacity of the PLGA NP loaded with BLG-peptides, in **Chapter 3** we investigated the oral tolerogenic and/or immune maturation capacity of the NPs by co-encapsulating a model BLG-peptide with CpG-ODN in the prophylactic murine CMA model. Previously reported approaches for codelivery of an antigen and CpG-ODN using PLGA carriers implemented the cationic lipid dioleoyl-3-trimethylammonium propane (DOTAP) [25] or protamine [26] in the preparation of the formulation. However, these are then also co-loaded in the obtained NPs. DOTAP functions as a Toll-like receptor 4 (TLR-4) agonist and therefore most likely interferes with the tolerance induction outcome. To preclude the influences from DOTAP and additional protein protamine, in **Chapter 3**, we prepared well-defined PLGA nanoparticles co-loaded with CpG-ODN and the selected peptide using a double emulsion solvent evaporation method. This enables proper comparison of the pretreatment using co-encapsulated BLG-Pep+CpG/NP and separately encapsulated BLG-Pep/NP and CpG/NP of the same dose, in prevention of CMA development *in vivo*. Only co-encapsulated BLG-Pep+CpG/NP, but not the mixture of PLGA NP, effectively attenuated the acute allergic skin reactivity to whole whey protein as compared to the whey-sensitized mice. Previous studies have reported that the intestinal uptake and lymphatic transport of orally delivered nanoparticles are dependent on the physicochemical properties of NP in terms of surface charge, particle size and dosage [27-29]. As described in **Chapter 3**, PLGA NP without or with encapsulation of BLG-Pep and/or CpG displayed similar size and surface charge, which implicated similar mucus penetration and cellular uptake of these nanoparticles after oral administration. BLG-peptide loaded PLGA nanoparticles can be endocytosed by DC into phagosomes [30], followed by endosomal degradation of the carrier and loaded/released peptide for presentation *via* MHCII proteins [31]. Of note, TLR-9 and MHCII are also present in the endo-lysosomal compartments of plasmacytoid DC [32, 33], which enable binding of co-encapsulated CpG-ODN to TLR-9 and activating TLR-9 signaling. Thus, simultaneous internalization and intracellular release of CpG-ODN and BLG-Pep from the internalized PLGA NPs in the endolysosomes of DC may facilitate simultaneous activation of TLR-9 signaling as well as antigen-presentation *via* MHCII in the same DC. Previously, Heit *et al.* [34] indeed reported that PLGA microspheres co-encapsulating an antigen and CpG-ODN were phagocytosed into murine DC phago-endosomal compartments, followed by antigen degradation and concomitant activation of endosomal TLR. In the same study it was also reported that only antigen plus CpG co-encapsulated PLGA microspheres, but not empty or antigen encapsulated microparticles [34], induced secretion of large

amounts of IL-12 and IL-6 by DC and full DC maturation *in vitro*. Nevertheless, future studies warrant to verify the immunomodulatory effect that PLGA NP loaded with both the BLG-peptides and CpG-ODN exert on DC.

The pretreatment with NP loaded with both peptide and CpG prevented increase in BLG-specific IgE concentrations, which would lower BLG-specific IgE-bound Fc receptor (FcεRI) on mast cells and basophils and subsequent allergic reactions upon whey challenge. Nevertheless, in **Chapter 3**, this pretreatment did not alter whey- or BLG-specific IgG1 and IgG2a levels. Although the underlying mechanism via which IgG antibodies mediate to promote or inhibit IgE-dependent allergic reactions remains elusive [35], many recent studies have also shown a positive correlation between natural resolution of food allergies and elevated food-specific IgG levels in both murine and human subjects [36, 37]. The IgG antibodies can bind to inhibitory IgG Fc receptors (FcγRIIb), that are also expressed on the mast cells and basophils, and thus suppress IgE-mediated allergic reactions *via* the inhibitory signaling upon allergen crosslinking [37]. In support of this notion, Srivastava *et al.* [38] reported that orally administered PLGA NP loaded with a peanut extract to peanut allergic mice increased peanut-specific Th1-associated IgG2a while reducing peanut-specific IgE, Th2-associated IgG1 levels and IL-13 release. Indeed, we found in **Chapter 3** that pretreatment with co-encapsulated BLG-Pep+CpG/NP lowered Th2 development and increased Treg/Th2 and Th1/Th2 ratios in the spleen, but it did not influence *ex vivo* BLG- or whey-stimulated Th2-associated IL-13 or Treg-associated IL-10 release by the splenocytes.

In **Chapters 3** it is shown that the PLGA NP loaded with the BLG-peptide do not fully protect the allergic effect of whey protein. On the other hand, Srivastava *et al.* [38] showed that PLGA NP loaded with a full protein extract gave full protection against peanut allergy. NP encapsulation of the whole protein would circumvent its digestion in the gastro-intestinal tract; however, this will lead to exposure of unprocessed whole proteins to mucosal DC, which in turn may lead to the further unwanted development of allergies and elicitation of symptoms. Our strategy is much more controlled than encapsulation of peanut extract as allergen [38] since the exact peptide sequence is known. Small peptides enhance chances of natural tolerance development with limited

risk on side effects as the peptides cannot provoke effector cell degranulation. Therefore, although it is now tested in a preventive setting, it may also be considered for already allergic infants. Also, from a pharmaceutical and regulatory point of view, encapsulation of a peptide with a known structure is preferred above the entrapment of a poorly characterized protein extract which potentially shows large batch-to batch variations.

As described in **Chapter 3**, we used only one small BLG peptide of 18-AA for pretreatment, while the BLG protein consists of 162-AA and possesses multiple T-cell epitopes [39]. In addition, NP encapsulation of the whole protein would circumvent its digestion in the gastro-intestinal tract. However, this will lead to exposure of unprocessed whole proteins to mucosal DC, which in turn may lead to the further unwanted development of allergies and elicitation of symptoms. Furthermore, the developed peptide-NP formulations can be further improved. Considering the previous findings, we speculate that acquisition of full allergen-specific tolerance might require delivery of broader panel of T-cell epitopes containing peptides for recognition by T-cells from the target allergen. Hence, in future studies, beyond an additional peptide sequence containing another T-cell epitope from the BLG protein[40], peptides from α -lactalbumin may be included in the current regime.

The effective dose of only 160 μ g encapsulated BLG-peptides (referred as peptide 3 or 4 in **Chapter 2**) is very small as compared to the 4 mg dose of the same soluble peptides as reported in the study by Meulenbroek *et al.* [40]. Therefore, in **Chapter 4**, we further investigate how PLGA NP loaded with the peptide are distributed after entry into DC, and their intracellular fate was studied using a FRET pair NP. The donor dye was covalently coupled to the peptide whereas the acceptor was coupled to PLGA. Intriguingly, it was found that the FRET signal of the dually labeled NP remained stable upon 6 h-incubation in the biorelevant fasted-state simulated gastric fluid (pH 1.6). Considering the gastric retention time is about 2 h in mice and human [41, 42], this observation demonstrates sufficient stability of the PLGA NP for protecting the peptide cargo against the gastric ingestion prior to uptake by the intestinal dendritic cells. In addition, **Chapter 4** also demonstrates, using confocal fluorescence microscopy, highly efficient internalization of PLGA NP encapsulated Pep-Cy3 by human immature moDCs. On top of that, we observed a prolonged retention of the peptide PLGA NP (96 h) as compared to the free Pep-Cy3 (24 h) in murine DC2.4. In line with our finding, Waeckerle-Men *et al.* [43] reported that peptides loaded in PLGA microspheres

remarkably prolonged its availability within DCs and enhanced antigen-presentation capacities as compared to soluble peptides internalized by DCs. These findings suggest that encapsulation of antigen into PLGA NP does not only protect the encapsulated antigen from proteolytic degradation in biorelevant simulated gastric fluid, but it also prolongs its retention in DC. The latter is known to favor long-term T-cell responses [44], which is important to develop persistent oral tolerance induction.

To further increase the chances of full tolerance induction for whole whey protein, CpG-ODN as Th1 and regulatory T-cell (Treg) adjuvant, can be co-encapsulated with antigen to skew away from the allergic Th2 phenotype. In **Chapter 3**, the observed protective effect PLGA NP loaded with both class B CpG-ODN and BLG-peptide against acute allergic symptoms to whole whey protein in C3H/HeO_uJ mice might be associated with inhibition of generic Th2 immunity and the enhanced systemic ratios of Th1/Th2 and Treg/Th2. However, the underlying mechanism is not fully understood yet and therefore requires further investigation. Importantly, CpG-ODN was reported to mediate TLR-9-signalling *via* the MyD88- (low dose) or the TRIF- (high dose) pathway in a dose-dependent manner [45]. In line with our finding, Diwan *et al.* [46] reported that CpG-ODN and tetanus toxoid co-encapsulated in PLGA NP skewed Th1 immune response away from Th2 immune response. In an earlier study, Kline *et al.* [47] reported that systemic administered CpG-ODN reduced Th2-associated cytokines production without affecting Th1 cytokines in a murine asthma model. More recently, Alberca *et al.* [48] reported that subcutaneously administered CpG at a dose of 0.45 mg/kg, inhibited Th2 allergic immunity *via* TLR-9-MyD88-expressing DC. Hence, it is likely that the co-encapsulated class B CpG-ODN indeed reduced Th2 cells development *via* its immunomodulatory effect on DC. In an earlier study, Kitagaki *et al.* [49] reported that orally administered CpG-ODN at a dose of 4.5 mg/kg suppressed antigen-induced asthma in mice. In **Chapter 3**, a much lower dose of 3 µg encapsulated CpG-ODN, namely 0.23 mg/kg per dose (body weight of approximate 13 g per 3-4-week-old mouse), was administered orally for tolerance induction in mice. However, it is not known whether the orally administered 3 µg co-encapsulated class B CpG-ODN in PLGA nanoparticles activated signaling *via* the MyD88 pathway or the TRIF pathway. Noteworthy, there is a therapeutic dose window for CpG-ODN as an adjuvant in immunotherapy, and toxicity was observed in mice that received a consecutive daily injection of CpG-ODN in a dose higher than 2.4 mg/kg [50]. Despite the influence from different administration routes for CpG-ODN remains unclear [45], bioavailability is by

definition 100% after intravenous administration, which is always higher or at best equal to that of oral administration. In this regard, notwithstanding the improved bioavailability of conferred by the PLGA NP encapsulation, a dose of 0.23 mg/kg encapsulated CpG-ODN administered by oral route in **Chapter 3** to the mice is low and safe. In light of the therapeutic dose window, the dose-related immunomodulatory effect of CpG-ODN warrants further investigation.

To investigate the immunomodulatory effect of blank PLGA NP or PLGA NP encapsulated with BLG-peptides or CpG-ODN exerts on human moDC *in vitro*, cytokine production and surface expression of activation markers by human moDC were determined. Human immature moDCs incubated with empty PLGA NP secrete higher levels of Th1-associated cytokine IL-12p70 (for 24 h in **Chapter 2** and for 48 h in **Chapter 5**) and Treg-associated cytokine IL-10 (in **Chapter 2**) as compared to the medium control. Moreover, in **Chapter 2** exposure with empty NP did not influence surface expression of the co-stimulatory molecules CD80 and CD86, which suggests an immature moDC phenotype. The CD80^{low}/CD86^{low} human immature dendritic cells are regarded as a prerequisite for tolerance induction *via* promoting differentiation of naïve T-cells into Treg cells after repetitive stimulation under steady conditions [51-53]. In **Chapter 5**, however, 48 h-incubation with empty NP did enhance surface expression of the co-stimulatory molecules CD80, CD86 and PD-L1 on human moDC as compared to the medium control. Alternatively, the formed protein corona on the hydrophobic surface of the PLGA NP may act as a danger signal, also known as nanoparticles' associated molecular patterns (NAMPs) [54-56]. In support of this notion, Barillet *et al.* [57] reported that stimulation of human moDCs *in vitro* with empty NP enhanced surface expression of the costimulatory molecules CD80, CD86 and PD-L1, in the absence of endotoxin. Indeed, PLGA NP have been shown to possess Th1 polarizing capacity themselves [58, 59].

There are three major classes (A, B and C) of synthetic CpG-ODN, which are classified according to their sequence motifs and secondary and tertiary structures [60, 61]. Their different capacities to induce IFN- α secretion and pDCs maturation [62, 63] are endowed by their structural differences, which result in their different compartmentalization of TLR-9 induced signaling cascades. However, after incubation of moDC *in vitro* with the different CpG-ODN encapsulated in PLGA NPs no effect on surface expression of CD80, CD86 and PD-L1 was found. This might be attributed to the low dose of CpG-ODN (0.4 μ g/mL encapsulated CpG) which was much lower than the

effective dose of 5 µg/mL CpG used in human DCs cultures in which PD-L1 expression was increased as reported by Jaehn *et al.* [64]. Thus, further investigation is required to clarify the dose-related immunomodulatory effect of the different classes CpG-ODN loaded in PLGA NPs.

As demonstrated in **Chapter 5**, only class A CpG-ODN loaded in NP primed moDCs skewed T-cell differentiation away from Th2 as indicated by the increased ratios of Th1/Th2 and Treg/Th2. This is in line with our *in vivo* finding in **Chapter 3**, which showed that pretreatment of 3-4-week-old mice with PLGA NP loaded with both BLG-peptide and CpG-ODN inhibited the development of Th2 immune response in spleen. Therefore, it is likely that the orally administered NP encapsulated CpG were internalized by intestinal DC and primed the DC for synergistic antigen presentation to naïve T-cells and T-cell polarization away from Th2 immune response. Future studies are therefore warranted to further investigate the interplay between DC-T-cells upon exposure to different classes of CpG loaded in PLGA NP. In addition, also effects on B-cells may be studied as in particular class B CpG is known to instruct B-cells to produce regulatory type IL-10 [65, 66] which may also impact the outcome of the DC-T-cell response and contribute to oral tolerance induction *in vivo*.

Overall Conclusion

This thesis demonstrates the hypothesis that PLGA nanoparticles improved the stability of the encapsulated peptide cargo in the gastrointestinal lumen and retention in intestinal DC upon internalization. Indeed, we observed a dose-dependent effect of only 160 µg BLG-peptides encapsulated in PLGA nanoparticles to protect mice recipients against CMA upon whey-sensitizations. This lowered allergic symptoms as shown by a reduced acute allergic skin response which was associated with a systemic silencing of *ex vivo* whey-stimulated TNF-α release by splenocytes. More importantly, this thesis highlights the superior tolerogenic effect of orally administered PLGA nanoparticles co-loaded with T-cell epitopes containing peptide and a CpG adjuvant as compared to the separately encapsulated peptide and CpG counterpart. This was associated with the observed reduction in splenic Th2 frequency and increased Treg/Th2 and Th1/Th2 ratios. Furthermore, in the *in vitro* DC-T-cell coculture assay, the immature moDCs primed with CpG-ODN loaded PLGA NP also effectively increased the ratios of Treg/Th2 and Th1/Th2. This finding supports the hypothesis that the co-encapsulated CpG-ODN facilitates the inhibition of Th2 immunity also *in vivo*. In

conclusion, our findings substantiate the translational potential of PLGA nanoparticles in which T-cell epitopes containing peptides are encapsulated for future development of effective and safe strategies for early life CMA prevention (*i.e.*, supplementing hydrolyzed formula milk for infants at risk). In addition, besides BLG-peptides also CpG-ODN motives, which may include bacterial DNA of selected bacterial strains, can be co-loaded in the PLGA NP to increase the efficacy of the formulations in oral tolerance induction. This strategy may be further developed as a modality to treat cow's milk allergy for example as adjunct treatment for allergen specific oral immunotherapy.

References

- [1] L. Meulenbroek, BUILDING TOLERANCE: T cell epitopes as a treatment for cow's milk allergy, in: Utrecht Institute for Pharmaceutical Sciences and Danone Research Centre for Specialised Nutrition, Utrecht University, Utrecht, 2013.
- [2] A. Kostadinova, TAKES TWO TO BUILD TOLERANCE: T cell epitopes and specific dietary synbiotics - together towards early life cow's milk allergy prevention, in: Nutricia Research and the Utrecht Institute for Pharmaceutical Sciences, Utrecht University, Utrecht, 2018.
- [3] A.I. Kostadinova, J. Middelburg, M. Ciulla, J. Garssen, W.E. Hennink, L.M.J. Knippels, C.F. van Nostrum, L.E.M. Willemsen, PLGA nanoparticles loaded with beta-lactoglobulin-derived peptides modulate mucosal immunity and may facilitate cow's milk allergy prevention, *Eur J Pharmacol*, 818 (2018) 211-220.
- [4] Y.Y. Luo, X.Y. Xiong, Y. Tian, Z.L. Li, Y.C. Gong, Y.P. Li, A review of biodegradable polymeric systems for oral insulin delivery, *Drug Deliv*, 23 (2016) 1882-1891.
- [5] C. He, L. Yin, C. Tang, C. Yin, Size-dependent absorption mechanism of polymeric nanoparticles for oral delivery of protein drugs, *Biomaterials*, 33 (2012) 8569-8578.
- [6] A. Budhian, S.J. Siegel, K.I. Winey, Haloperidol-loaded PLGA nanoparticles: systematic study of particle size and drug content, *Int J Pharm*, 336 (2007) 367-375.
- [7] A. Banerjee, J. Qi, R. Gogoi, J. Wong, S. Mitragotri, Role of nanoparticle size, shape and surface chemistry in oral drug delivery, *J Control Release*, 238 (2016) 176-185.
- [8] P. Foroozandeh, A.A. Aziz, Insight into Cellular Uptake and Intracellular Trafficking of Nanoparticles, *Nanoscale Res Lett*, 13 (2018) 339.
- [9] M.J. Mitchell, M.M. Billingsley, R.M. Haley, M.E. Wechsler, N.A. Peppas, R. Langer, Engineering precision nanoparticles for drug delivery, *Nat Rev Drug Discov*, 20 (2021) 101-124.
- [10] J. Koerner, D. Horvath, M. Groettrup, Harnessing Dendritic Cells for Poly (D,L-lactide-co-glycolide) Microspheres (PLGA MS)-Mediated Anti-tumor Therapy, *Front Immunol*, 10 (2019) 707.
- [11] C.J. Genito, C.J. Batty, E.M. Bachelder, K.M. Ainslie, Considerations for Size, Surface Charge, Polymer Degradation, Co-Delivery, and Manufacturability in the Development of Polymeric Particle Vaccines for Infectious Diseases, *Adv Nanobiomed Res*, 1 (2021) 2000041.
- [12] A.M. Mowat, Anatomical basis of tolerance and immunity to intestinal antigens, *Nat Rev Immunol*, 3 (2003) 331-341.
- [13] A.M. Mowat, To respond or not to respond - a personal perspective of intestinal tolerance, *Nat Rev Immunol*, 18 (2018) 405-415.
- [14] M. Liu, S. Thijssen, C.F. van Nostrum, W.E. Hennink, J. Garssen, L.E.M. Willemsen, Inhibition of cow's milk allergy development in mice by oral delivery of beta-lactoglobulin-derived peptides loaded PLGA nanoparticles is associated with systemic whey-specific immune silencing, *Clin Exp Allergy*, 52 (2022) 137-148.
- [15] D.J. Brayden, M.A. Jepson, A.W. Baird, Keynote review: intestinal Peyer's patch M cells and oral vaccine targeting, *Drug Discov Today*, 10 (2005) 1145-1157.
- [16] K. Zhang, A. Dupont, N. Torow, F. Gohde, S. Leschner, S. Lienenklaus, S. Weiss, M.M. Brinkmann, M. Kuhnel, M. Hensel, M. Fulde, M.W. Hornef, Age-dependent enterocyte invasion and microcolony formation by Salmonella, *PLoS Pathog*, 10 (2014) e1004385.
- [17] K.Z. Sanidad, M.Y. Zeng, Neonatal gut microbiome and immunity, *Curr Opin Microbiol*, 56 (2020) 30-37.
- [18] B. Weström, E. Arévalo Sureda, K. Pierzynowska, S.G. Pierzynowski, F.-J. Pérez-Cano, The Immature Gut Barrier and Its Importance in Establishing Immunity in Newborn Mammals, *Frontiers in Immunology*, 11 (2020).
- [19] L.M. D'Cruz, L. Klein, Development and function of agonist-induced CD25+Foxp3+ regulatory T cells in the absence of interleukin 2 signaling, *Nat Immunol*, 6 (2005) 1152-1159.
- [20] J.D. Fontenot, J.P. Rasmussen, M.A. Gavin, A.Y. Rudensky, A function for interleukin 2 in Foxp3-expressing regulatory T cells, *Nat Immunol*, 6 (2005) 1142-1151.
- [21] Z. Al Nabhani, S. Dulauroy, R. Marques, C. Cousu, S. Al Bounny, F. De Jardin, T. Sparwasser, M. Berard, N. Cerf-Bensussan, G. Eberl, A Weaning Reaction to Microbiota Is Required for Resistance to Immunopathologies in the Adult, *Immunity*, 50 (2019) 1276-1288 e1275.
- [22] R.O. Williams, M. Feldmann, R.N. Maini, Anti-tumor necrosis factor ameliorates joint disease in murine collagen-induced arthritis, *Proc Natl Acad Sci U S A*, 89 (1992) 9784-9788.

- [23] J.P. Choi, Y.S. Kim, O.Y. Kim, Y.M. Kim, S.G. Jeon, T.Y. Roh, J.S. Park, Y.S. Gho, Y.K. Kim, TNF-alpha is a key mediator in the development of Th2 cell response to inhaled allergens induced by a viral PAMP double-stranded RNA, *Allergy*, 67 (2012) 1138-1148.
- [24] H.R. Cohn L, Marinov A, Rankin J, and Bottomly K. , Induction of Airway Mucus Production By T Helper 2 (Th2) Cells: A Critical Role For Interleukin 4 In Cell Recruitment But Not Mucus Production., *J. Exp. Med.*, 186 (1997) 11.
- [25] Z. Xu, S. Ramishetti, Y.C. Tseng, S. Guo, Y. Wang, L. Huang, Multifunctional nanoparticles co-delivering Trp2 peptide and CpG adjuvant induce potent cytotoxic T-lymphocyte response against melanoma and its lung metastasis, *J Control Release*, 172 (2013) 259-265.
- [26] I. Pali-Scholl, H. Szollosi, P. Starkl, B. Scheicher, C. Stremnitzer, A. Hofmeister, F. Roth-Walter, A. Lukschal, S.C. Diesner, A. Zimmer, E. Jensen-Jarolim, Protamine nanoparticles with CpG-oligodeoxynucleotide prevent an allergen-induced Th2-response in BALB/c mice, *Eur J Pharm Biopharm*, 85 (2013) 656-664.
- [27] K.S. Kim, K. Suzuki, H. Cho, Y.S. Youn, Y.H. Bae, Oral Nanoparticles Exhibit Specific High-Efficiency Intestinal Uptake and Lymphatic Transport, *ACS Nano*, 12 (2018) 8893-8900.
- [28] M. Abdulkarim, N. Agullo, B. Cattoz, P. Griffiths, A. Bernkop-Schnurch, S.G. Borros, M. Gumbleton, Nanoparticle diffusion within intestinal mucus: Three-dimensional response analysis dissecting the impact of particle surface charge, size and heterogeneity across polyelectrolyte, pegylated and viral particles, *Eur J Pharm Biopharm*, 97 (2015) 230-238.
- [29] I. Pereira de Sousa, T. Moser, C. Steiner, B. Fichtl, A. Bernkop-Schnurch, Insulin loaded mucus permeating nanoparticles: Addressing the surface characteristics as feature to improve mucus permeation, *Int J Pharm*, 500 (2016) 236-244.
- [30] N.D. Donahue, H. Acar, S. Wilhelm, Concepts of nanoparticle cellular uptake, intracellular trafficking, and kinetics in nanomedicine, *Adv Drug Deliv Rev*, 143 (2019) 68-96.
- [31] M. Allahyari, E. Mohit, Peptide/protein vaccine delivery system based on PLGA particles, *Hum Vaccin Immunother*, 12 (2016) 806-828.
- [32] A.M. Krieg, CpG motifs in bacterial DNA and their immune effects, *Annu Rev Immunol*, 20 (2002) 709-760.
- [33] Y. Krishnamachari, A.K. Salem, Innovative strategies for co-delivering antigens and CpG oligonucleotides, *Adv Drug Deliv Rev*, 61 (2009) 205-217.
- [34] A. Heit, F. Schmitz, T. Haas, D.H. Busch, H. Wagner, Antigen co-encapsulated with adjuvants efficiently drive protective T cell immunity, *Eur J Immunol*, 37 (2007) 2063-2074.
- [35] C. Kanagaratham, Y.S. El Ansari, O.L. Lewis, H.C. Oettgen, IgE and IgG Antibodies as Regulators of Mast Cell and Basophil Functions in Food Allergy, *Front Immunol*, 11 (2020) 603050.
- [36] E.M. Savilahti, V. Rantanen, J.S. Lin, S. Karinen, K.M. Saarinen, M. Goldis, M.J. Makela, S. Hautaniemi, E. Savilahti, H.A. Sampson, Early recovery from cow's milk allergy is associated with decreasing IgE and increasing IgG4 binding to cow's milk epitopes, *J Allergy Clin Immunol*, 125 (2010) 1315-1321 e1319.
- [37] O.T. Burton, S.L. Logsdon, J.S. Zhou, J. Medina-Tamayo, A. Abdel-Gadir, M. Noval Rivas, K.J. Koleoglou, T.A. Chatila, L.C. Schneider, R. Rachid, D.T. Umetsu, H.C. Oettgen, Oral immunotherapy induces IgG antibodies that act through FcγRIIb to suppress IgE-mediated hypersensitivity, *J Allergy Clin Immunol*, 134 (2014) 1310-1317 e1316.
- [38] A.L. Siefert, A. Ehrlich, M.J. Corral, K. Goldsmith-Pestana, D. McMahon-Pratt, T.M. Fahmy, Immunomodulatory nanoparticles ameliorate disease in the *Leishmania (Viannia) panamensis* mouse model, *Biomaterials*, 108 (2016) 168-176.
- [39] A.R. Madureira, C.I. Pereira, A.M.P. Gomes, M.E. Pintado, F. Xavier Malcata, Bovine whey proteins – Overview on their main biological properties, *Food Research International*, 40 (2007) 1197-1211.
- [40] L.A. Meulenbroek, B.C. van Esch, G.A. Hofman, C.F. den Hartog Jager, A.J. Nauta, L.E. Willemsen, C.A. Bruijnzeel-Koomen, J. Garssen, E. van Hoffen, L.M. Knippels, Oral treatment with beta-lactoglobulin peptides prevents clinical symptoms in a mouse model for cow's milk allergy, *Pediatr Allergy Immunol*, 24 (2013) 656-664.
- [41] J.J. Lee, J.C. Price, A. Duren, A. Shertzer, R. Hannum, F.A. Akita, S. Wang, J.H. Squires, O. Panzer, J. Herrera, L.S. Sun, N.A. Davis, Ultrasound Evaluation of Gastric Emptying Time in Healthy Term Neonates after Formula Feeding, *Anesthesiology*, 134 (2021) 845-851.
- [42] M. Fernandes, I.C. Goncalves, S. Nardecchia, I.F. Amaral, M.A. Barbosa, M.C. Martins, Modulation of stability and mucoadhesive properties of chitosan microspheres for therapeutic gastric application, *Int J Pharm*, 454 (2013) 116-124.
- [43] Y. Waeckerle-Men, E.U. Allmen, B. Gander, E. Scandella, E. Schlosser, G. Schmidtke, H.P. Merkle, M. Groettrup, Encapsulation of proteins and peptides into biodegradable poly(D,L-lactide-co-glycolide)

- microspheres prolongs and enhances antigen presentation by human dendritic cells, *Vaccine*, 24 (2006) 1847-1857.
- [44] S.L. Demento, W. Cui, J.M. Criscione, E. Stern, J. Tulipan, S.M. Kaech, T.M. Fahmy, Role of sustained antigen release from nanoparticle vaccines in shaping the T cell memory phenotype, *Biomaterials*, 33 (2012) 4957-4964.
- [45] G. Montamat, C. Leonard, A. Poli, L. Klimek, M. Ollert, CpG Adjuvant in Allergen-Specific Immunotherapy: Finding the Sweet Spot for the Induction of Immune Tolerance, *Front Immunol*, 12 (2021) 590054.
- [46] M. Diwan, M. Tafaghodi, J. Samuel, Enhancement of immune responses by co-delivery of a CpG oligodeoxynucleotide and tetanus toxoid in biodegradable nanospheres, *J Control Release*, 85 (2002) 247-262.
- [47] A.M.K. Joel N. Kline, Thomas J. Waldschmidt, Zuhair K. Ballas, Vipul Jain, and Thomas R. Businga., CpG oligodeoxynucleotides do not require TH1 cytokines to prevent eosinophilic airway inflammation in a murine model of asthma, *J Allergy Clin Immunol* 104 (1999) 1258-1264.
- [48] R.W. Alberca, E. Gomes, M. Russo, CpG-ODN Signaling via Dendritic Cells-Expressing MyD88, but Not IL-10, Inhibits Allergic Sensitization, *Vaccines (Basel)*, 9 (2021).
- [49] K. Kitagaki, T.R. Businga, J.N. Kline, Oral administration of CpG-ODNs suppresses antigen-induced asthma in mice, *Clin Exp Immunol*, 143 (2006) 249-259.
- [50] M. Heikenwalder, M. Polymenidou, T. Junt, C. Sigurdson, H. Wagner, S. Akira, R. Zinkernagel, A. Aguzzi, Lymphoid follicle destruction and immunosuppression after repeated CpG oligodeoxynucleotide administration, *Nature Medicine*, 10 (2004) 187-192.
- [51] M.K. Levings, S. Gregori, E. Tresoldi, S. Cazzaniga, C. Bonini, M.G. Roncarolo, Differentiation of Tr1 cells by immature dendritic cells requires IL-10 but not CD25+CD4+ Tr cells, *Blood*, 105 (2005) 1162-1169.
- [52] Jonuleit. Helmut, Schmitt. Edgar, Schuler. Geroold, Knop. Jürgen, Enk. Alexander H., Induction of Interleukin 10 producing Nonproliferating CD4+cells with regulatory properties by repetitive stimulation with allogeneic human iDC, *J. Exp. Med.*, 192 (2000) 10.
- [53] K. Kretschmer, I. Apostolou, D. Hawiger, K. Khazaie, M.C. Nussenzweig, H. von Boehmer, Inducing and expanding regulatory T cell populations by foreign antigen, *Nat Immunol*, 6 (2005) 1219-1227.
- [54] A.L. Silva, C. Peres, J. Conniot, A.I. Matos, L. Moura, B. Carreira, V. Sainz, A. Scomparin, R. Satchi-Fainaro, V. Preat, H.F. Florindo, Nanoparticle impact on innate immune cell pattern-recognition receptors and inflammasomes activation, *Semin Immunol*, 34 (2017) 3-24.
- [55] D.F. Moyano, M. Goldsmith, D.J. Solfiell, D. Landesman-Milo, O.R. Miranda, D. Peer, V.M. Rotello, Nanoparticle hydrophobicity dictates immune response, *J Am Chem Soc*, 134 (2012) 3965-3967.
- [56] B. Fadeel, Clear and present danger? Engineered nanoparticles and the immune system, *Swiss Med Wkly*, 142 (2012) w13609.
- [57] S. Barillet, E. Fattal, S. Mura, N. Tsapis, M. Pallardy, H. Hillaireau, S. Kerdine-Römer, Immunotoxicity of poly (lactic-co-glycolic acid) nanoparticles: influence of surface properties on dendritic cell activation, *Nanotoxicology*, 13 (2019) 606-622.
- [58] M. Yoshida, J.E. Babensee, Differential effects of agarose and poly(lactic-co-glycolic acid) on dendritic cell maturation, *J Biomed Mater Res A*, 79 (2006) 393-408.
- [59] J.S. K.D. Newman, G. Kwon, Ovalbumin peptide encapsulated in Poly(d,l lactic-co-glycolic acid) microspheres is capable of inducing a T helper type 1 immune response, *Journal of Controlled Release*, 54 (1998) 49-59.
- [60] C. Guiducci, G. Ott, J.H. Chan, E. Damon, C. Calacsan, T. Matray, K.D. Lee, R.L. Coffman, F.J. Barrat, Properties regulating the nature of the plasmacytoid dendritic cell response to Toll-like receptor 9 activation, *J Exp Med*, 203 (2006) 1999-2008.
- [61] J. Vollmer, A.M. Krieg, Immunotherapeutic applications of CpG oligodeoxynucleotide TLR9 agonists, *Adv Drug Deliv Rev*, 61 (2009) 195-204.
- [62] A.H. Dalpke, S. Zimmermann, I. Albrecht, K. Heeg, Phosphodiester CpG oligonucleotides as adjuvants: polyguanosine runs enhance cellular uptake and improve immunostimulative activity of phosphodiester CpG oligonucleotides in vitro and in vivo, *Immunology*, 106 (2002) 102-112.
- [63] S. Chakarov, N. Fazilleau, Monocyte-derived dendritic cells promote T follicular helper cell differentiation, *EMBO Mol Med*, 6 (2014) 590-603.
- [64] P.S. Jaehn, K.S. Zaenker, J. Schmitz, A. Dzionek, Functional dichotomy of plasmacytoid dendritic cells: antigen-specific activation of T cells versus production of type I interferon, *Eur J Immunol*, 38 (2008) 1822-1832.

Summary And Perspectives

[65] D. Verthelyi, R.A. Zeuner, Differential signaling by CpG DNA in DCs and B cells: not just TLR9, *Trends Immunol*, 24 (2003) 519-522.

[66] B. He, X. Qiao, A. Cerutti, CpG DNA Induces IgG Class Switch DNA Recombination by Activating Human B Cells through an Innate Pathway That Requires TLR9 and Cooperates with IL-10, *The Journal of Immunology*, 173 (2004) 4479-4491.

APPENDICES

Nederlandse Samenvatting

Dit proefschrift presenteert de resultaten van het onderzoek naar poly(melkzuur-co-glycolzuur) nanodeeltjes (PLGA NP) beladen met beta-lactoglobuline (BLG)-peptiden met of zonder synthetische CpG-oligodeoxynucleotides (CpG-ODN), als oraal toedieningssysteem voor allergeenspecifieke tolerantie-inductie bij muizen ter preventie van koemelkallergie (KMA). Om mechanistisch inzicht te krijgen in de waarnemingen, werden de intracellulaire verwerking en de immunomodulerende effecten van deze PLGA NP's *in vitro* onderzocht. In dit hoofdstuk worden de belangrijkste uitkomsten van dit proefschrift samengevat.

In **hoofdstuk 1** worden de managementrichtlijnen en de huidige vooruitgang in de preventie van KMA voor jonge kinderen besproken. Introductie van allergeen/antigeen in het vroege leven biedt een kans voor inductie van orale tolerantie. Beta-lactoglobuline (BLG) is een van de belangrijkste allergenen in koemelkeiwit wei. Korte peptides uit de aminozuursequentie hiervan (BLG peptides) bleken in eerder onderzoek geschikt voor het induceren van orale tolerantie waardoor het ontwikkelen van koemelkallergie, in muizen grotendeels werd voorkomen. In dit verband worden in hoofdstuk 1 de voordelen onderstreept van orale toediening van antigenen met behulp van PLGA NP en de toevoeging van een immuunstimulerend adjuvant CpG-ODN, wat bacterieel DNA nabootst, bij het activeren van allergeenspecifieke tolerantie. Eerdere studies van onze afdeling onderzochten met succes de mogelijkheid om orale tolerantie te induceren met behulp van een cocktail van BLG-peptiden, hetzij in hun vrije vorm [1] of afzonderlijk geladen in PLGA NP's [2]. Om de mogelijkheid van tolerantie-inductie met minder verschillende BLG-peptiden te onderzoeken, werden in **hoofdstuk 2** twee BLG-peptiden (van 18 aminozuren lengte) geselecteerd voor afzonderlijke inkapseling in PLGA NP's met behulp van een dubbele emulsie-solventverdampingstechniek. De KMA-preventie door middel van deze oraal toegediende, met peptiden beladen PLGA NP's werd onderzocht in een wei-eiwit geïnduceerd muizenmodel voor KMA. Voorbehandeling van drie weken oude vrouwelijke C3H/HeOJ-muizen met hoge dosis (160 µg ingekapselde BLG-peptiden), maar niet met lage dosis (80 µg ingekapselde BLG-peptiden) noch lege NP plus 160 µg vrije BLG-peptiden-mix, gaf muizen bescherming tegen anafylaxie en verlaagde de acute allergische huidrespons bij intradermale wei-blootstelling in vergelijking met controle-voorbehandelde wei-geïnduceerde muizen. De hoge dosis BLG-peptiden/NPs-voorbehandeling, maar niet de lage dosis voorbehandeling, remde de *ex vivo* wei-gestimuleerde afgifte van pro-inflammatoir

cytokine TNF- α door splenocyten, ten opzicht van de vrije BLG-peptiden-mix of lege NP plus BLG-peptiden-mix voorbehandelde wei-gesensibiliseerde muizen.

Verbeterde hygiënische omstandigheden en verlies van microbiële diversiteit zijn geassocieerd met een verhoogd risico op de ontwikkeling van allergieën die ontstaan door een overheersende immuunrespons van Thelper (Th)2 cellen. In dit opzicht is bekend dat bacterieel CpG-DNA de ontwikkeling van Th1 en regulerende T-cel (Treg) stimuleert *via* Toll-Like-Receptor 9 (TLR-9) signalering, hierdoor verschuift de balans weg van het allergische Th2-fenotype. **Hoofdstuk 3** beschrijft de inkapseling van één geselecteerd peptide afgeleid van β -lactoglobuline (BLG-Pep, AASDISLLDAQSAPLRVY) samen met TLR-9 ligand klasse B-CpG-ODN in PLGA NP met behulp van een dubbele emulsie-solventverdampingstechniek. In dit hoofdstuk werd de KMA-preventie door verschillende orale voorbehandelingen onderzocht in het door wei geïnduceerde KMA-muizenmodel. In dit experiment werden de muizen gehuisvest in individueel geventileerde kooien die een strikt hygiënische omgeving simuleerden. De voorbehandeling met co-ingekapselde BLG-Pep+CpG/NP, maar niet met BLG-Pep/NP, CpG/NP of het mengsel van BLG-Pep/NP plus CpG/NP, voorkwam zowel de door wei geïnduceerde acute allergische huidrespons als de stijging van BLG-specifiek serum-IgE in vergelijking met controle-voorbehandelde wei-gesensibiliseerde muizen. Belangrijk is dat voorbehandeling met co-ingekapselde BLG-Pep plus CpG/NP de activering van dendritische cellen (DC's) verminderde en de frequenties van PD-L1+ DC's in de mesenterische lymfeklieren verlaagde in vergelijking met wei-gevoelige muizen. Omgekeerd verhoogde de voorbehandeling met co-ingekapselde BLG-Pep+CpG/NP de frequentie van milt PD-L1+ DC's in vergelijking met de muizen die afzonderlijk ingekapselde BLG-Pep/NP plus CpG/NP ontvingen. Dit was geassocieerd met een lager percentage Th2-cellen en een verhoogde ratio Treg/Th2- en Th1/Th2 in de milt van de muizen die co-ingekapselde BLG-Pep plus CpG/NP-ontvingen als voorbehandeling voor de allergische sensibilisatie in vergelijking met controle-voorbehandelde wei-gesensibiliseerde muizen. Orale toediening van co-ingekapselde BLG-Pep plus CpG/NP voorkwam stijging van BLG-specifiek serum-IgE en de ontwikkeling van wei-allergische symptomen, terwijl het percentage van Th2-cellen in de milt bij deze muizen werd verlaagd.

DC's spelen een cruciale rol bij het ontstaan van perifere tolerantie door middel van het fagocyteren en de intracellulaire verwerking van antigene deeltjes, waaronder

in dit geval de peptide beladen PLGA NP's, wat leidt tot antigeenpresentatie. Dezemechanismen zijn verantwoordelijk voor de interactie van de peptidebeladen PLGA-nanodeeltjes met DC's, echter hun intracellulaire verwerking is onbekend. In **hoofdstuk 4** werd de *Förster Resonance Energy Transfer* (FRET), een afstandafhankelijk niet-radioactief energieoverdrachtsproces van een donor naar een acceptor fluorochroom, gebruikt om deze processen te onderzoeken. De verhouding van donor (Cyanine-3)-geconjugeerd peptide en acceptor (Cyanine-5)-gelabeld PLGA in de nanodeeltjes werd verfijnd voor optimale FRET-efficiëntie. De colloïdale stabiliteit en FRET-emissie van de NP's werden gehandhaafd bij 144 uren incubatie in fosfaat-gebufferde zoutoplossing en 6 uren incubatie in biorelevante gesimuleerde maagvloeistof bij 37 °C. De peptidebeladen PLGA nanodeeltjes en peptideafgifte van de geïnternaliseerde nanodeeltjes in DC's werden *real-time* gemonitord met behulp van de verandering in het FRET-sigitaal. Dit bevestigde de internalisatie en langdurige retentie van het peptide in de DC's als het peptide in PLGA nanodeeltjes was ingekapseld ten opzicht van het vrije peptide.

Zoals aangetoond in **hoofdstuk 3**, gaf oraal toegediend PLGA NP met ingekapseld BLG-Pep en klasse B CpG-ODN aanleiding tot fenotypische veranderingen op DC's in de darm en milt van wei-ge-sensibiliseerde muizen in vergelijking met de controle-voorbehandelde muizen. Niettemin is noch het immunostimulerende effect van klasse B-CpG-ODN beladen PLGA-nanodeeltjes op DC's, noch het verschil in effect tussen klasse A-, B- of C- CpG-ODN beladen PLGA NP's (CpG/NP's) op de functie van DC's bekend. In **hoofdstuk 5** beschrijven we de bereiding van lege en klasse A-, B- of C- CpG-ODN's beladen PLGA NP's met behulp van de dubbele emulsie-solventverdamingsmethode. Deze NP's vertoonden een vergelijkbare gemiddelde NP-grootte van ca. 250-290 nm, zeta-potentiaal van -1 mV en inkapselingsefficiëntie van 50-65%. Ongedifferentieerde monocyt-afgeleide DC's (moDC's) werden blootgesteld aan lege NP's of aan CpG-ODN A-, B- of C-geladen NP's. Het rijpingsproces van de moDC's werd vervolgens vergeleken met de rijping van moDC's die geïncubeerd werden met LPS om een type DC1 te induceren, deze sturen naïeve T-celdifferentiatie naar Th1 type cellen, of met een cytokinemengsel type DC2 te induceren die Th2-celdifferentiatie aanstuurt. Het fenotype van de geprimeerde moDC's werd vastgesteld aan de hand van expressie van de rijpingsmarkers CD80, CD86 en/of *Programmed Death Ligand-1* (PD-L1). Incubatie van ongedifferentieerde moDC's met lege NP's, alsmede de DC1- en DC2-controles, resulteerde in expressietoename van de genoemde costimulatorische markers

op deze moDC's, wat wijst op rijping van deze cellen. Bovendien was de co-stimulatoire expressie van CD80, CD86 en PD-L1 op moDC's die waren blootgesteld aan CpG/NP's vergelijkbaar met DC's die waren blootgesteld aan lege NP. Intrigerend is dat wanneer ze samen met naïeve CD4+ T-cellen werden gekweekt, klasse A-CpG NP geprimeerde moDC's de verhoudingen van Th1/Th2 (CXCR3+/CRTH2+) en de Treg/Th2 (CD25+FoxP3+/CRTH2+) verhoogden in vergelijking met lege NP geprimeerde DC's. Dit geeft aan dat klasse A-CpG NP geprimeerde moDC's de T-celpolarisatie wegtrekt van Th2-ontwikkeling.

Referenties

- [1] L. Meulenbroek, BUILDING TOLERANCE: T cell epitopes as a treatment for cow's milk allergy, in: Utrecht Institute for Pharmaceutical Sciences and Danone Research Centre for Specialised Nutrition, Utrecht University, Utrecht, 2013.
- [2] A. Kostadinova, TAKES TWO TO BUILD TOLERANCE: T cell epitopes and specific dietary synbiotics - together towards early life cow's milk allergy prevention, in: Nutricia Research and the Utrecht Institute for Pharmaceutical Sciences, Utrecht University, Utrecht, 2018.

中文总结

本文介绍了包载了 β -乳球蛋白 (BLG) 衍生肽及其与 CpG 寡聚核苷酸 (CpG-ODN) 共包载的聚乳酸-羟基乙酸共聚物纳米粒 (PLGA NP) 的口服给药系统诱导小鼠过敏原特异性耐受以预防牛奶过敏的研究结果。为了深入了解动物实验所观察结果的机制,我们在体外研究了这些 PLGA 纳米粒 (NP) 在细胞内命运及其免疫调节作用。本章对本论文的主要议题进行了总结。

第一章介绍了早期牛奶过敏的管理指南和预防方法的研究进展。早期引入过敏原/抗原为口服耐受诱导提供了机会。 β -乳球蛋白 (BLG) 是牛奶蛋白乳清蛋白中的主要过敏原之一。先前的研究表明,氨基酸序列中的短肽(即 BLG 衍生肽)可诱导口服耐受,从而基本上预防了牛奶过敏在小鼠中的发生。在这个层面上,第一章中着重强调了以 PLGA NP 口服递送抗原以及共传递模拟细菌 DNA 的免疫刺激佐剂 CpG-ODN 在诱导过敏原特异性耐受的优势。我们部门以前的论文研究了使用 BLG 衍生肽的混合物,以它们的游离形式 [1] 或分别地包封在 PLGA NP 中 [2], 去成功诱导口服耐受的可能性。为了研究使用较少不同种的 BLG 衍生肽诱导耐受性,在第二章中,我们采用双乳液溶剂蒸发技术将所选择的两种 BLG 衍生肽(长度为 18 个氨基酸)单独包封在 PLGA NP 中。在乳清蛋白诱导的牛奶过敏小鼠模型中,我们研究了通过口服这些包载 BLG 衍生肽的 PLGA NP 来预防牛奶过敏。在体内,用高剂量 (160 μ g 封装的 BLG 衍生肽),而不是低剂量 (80 μ g 封装的 BLG 衍生肽)或空 NP 加 160 μ g 游离的 BLG 衍生肽混合物预处理 3 周龄雌性 C3H/HeOuj 小鼠,保护小鼠免于过敏反应并降低与空白对照预处理的乳清蛋白致敏小鼠相比,皮内乳清蛋白激发的急性过敏性皮肤反应。相对于游离态的 BLG 衍生肽混合物或空 NP 加 BLG 衍生肽混合物预处理的乳清蛋白致敏的小鼠,高剂量的包载 BLG 衍生肽的 NP 预处理(而非低剂量的预处理)抑制了脾脏细胞离体乳清蛋白刺激的促炎细胞因子 TNF- α 释放。

卫生条件的改善和微生物多样性的丧失与由 Th2 主要免疫反应介导的过敏发展的风险增加有关。在这方面,已知细菌 CpG DNA 通过 Toll 样受体-9 (TLR-9) 信号传导驱动 Th1 和调节性 T 细胞 (Treg) 的发育,从而使其偏离过敏性 Th2 表型。第三章描述了通过使用双乳液溶剂蒸发技术共包封一种选择的 BLG 衍生肽 (BLG-Pep, AASDISLLDAQSAPLRVY) 和 B 型 TLR-9 配体 CpG-ODN 到 PLGA NP 中。本章在乳清蛋白诱导的牛奶过敏小鼠模型中研究了不同口服预处理对牛奶过敏的预防效果。在

这个实验中，小鼠被安置在单独通风的笼子里，以模拟严格的卫生环境。用共包封的 BLG-Pep+CpG/NP 预处理 (而非 BLG-Pep/NP, CpG/NP 或 BLG-Pep/NP 加 CpG/NP 的混合物预处理) 可以预防与对照组预处理的乳清致敏小鼠相比，乳清蛋白诱导的急性过敏性皮肤反应以及 BLG 特异性血清 IgE 的反应和升高。重要的是，与乳清蛋白致敏小鼠相比，共包封的 BLG-Pep+CpG/NP 预处理减少了树突状细胞 (DC) 的活化并降低了肠系膜淋巴结中 PD-L1+ DC 的频率。与单独包封的 BLG-Pep/NP 加 CpG/NP 受体相比，用共包封的 BLG-Pep+CpG/NP 预处理增加了脾脏 PD-L1+ DC 的频率。与对照预处理的乳清蛋白致敏小鼠相比，这与共包封的 BLG-Pep+CpG/NP 受体的脾脏中 Th2 细胞百分比比较低和 Treg/Th2 和 Th1/Th2 比率增加有关。口服共封装的 BLG-Pep+CpG/NP 可防止血清 BLG 特异性 IgE 的升高和乳清蛋白过敏症状的发生，同时降低这些小鼠脾脏中 Th2 细胞的百分比。

DC 通过吞噬和细胞内处理抗原颗粒 (包括本例中的负载肽的 PLGA NP)，从而导致抗原呈递，在外周耐受的发展中发挥着至关重要的作用。这些机制主导了负载肽的 PLGA NP 与 DC 的相互作用，但它们的细胞内处理尚不明确。在第四章中，荧光共振能量转移 (FRET) 是一种从供体到受体荧光染料距离依赖性非放射性能量转移过程，用于研究这些过程。在制备的 NP 载体中，对供体 (Cyanine-3) 结合肽和受体 (Cyanine-5) 标记的 PLGA 的比例经过优化，以获得最佳的 FRET 效率。37°C 下，在磷酸盐缓冲生理盐水中孵育 144 小时，和生物相关模拟胃液中孵育 6 小时，NP 的胶体稳定性和 FRET 荧光信号保持不变。使用 FRET 信号的变化实时监测负载肽的 PLGA NP 和 DC 中内化 NP 的肽释放。这证实了当肽被封装在 PLGA NP 中时，相对于游离肽，肽在 DC 中的内化和保留时间的延长。

如第三章所示，与对照预处理的乳清蛋白致敏小鼠相比，口服 BLG-Pep 和 B 型 CpG-ODN 共包封的 PLGA NP 引起 DC 的表型变化。然而，B 型 CpG-ODN 包封的 PLGA NP 对 DC 的免疫刺激作用以及包封在 PLGA NP 中的 A, B 或 C 型 CpG-ODN 之间的功效差异都是未知的。在第五章中，我们描述了使用双乳液溶剂蒸发法制备空的和 A、B 或 C 型 CpG-ODN 封装的 PLGA NP (CpG NPs)。这些 NP 的平均粒径约为 250 – 290 nm，zeta 电位为 -1 mV 和 CpG-ODN 的封装率为 50 – 65%。将未分化的单核细胞衍生的 DC (moDC) 暴露于空 NP 或负载 A、B 或 C 型 CpG-ODN 的 NP。然后将 moDC 的成熟过程，和与 LPS 一起孵育以诱导的 DC1 型 (引导初始 T 细胞分化为 Th1 型细胞) 或与细胞因子混合物一起孵育以诱导的 DC2 型 (引导 Th 2 细胞分化) 的 moDC 的成熟过程进行比较。通过成熟标记 CD80、CD86 和/或程序性死亡配体-1 (PD-L1) 的表达来确定引发的 moDC 的表型。将未分化的 moDC 与空 NP 以

及与 DC1 和 DC2 成熟对照一起孵育，导致这些 moDC 的表面表达的上述标记物的表达增加，表明这些细胞的成熟。此外，暴露于 CpG/NP 的 moDC 上的 CD80、CD86 和 PD-L1 的共刺激表达与暴露于空 NP 的 DC 相似。有趣的是，当与初始 CD4+T 细胞共培养时，与空 NP 孵育过的 DC 相比，A 型 CpG NP 孵育过的 moDC 增加了 Th1/Th2 (CXCR3+/CRTH2+) 和 Treg/Th2 (CD25+ FoxP3+/CRTH2+) 的比率。这表明 A 型 CpG NP 孵育过的 moDC 使 T 细胞极化远离 Th2 发育。

引用文献

- [1] L. Meulenbroek, BUILDING TOLERANCE: T cell epitopes as a treatment for cow's milk allergy, in: Utrecht Institute for Pharmaceutical Sciences and Danone Research Centre for Specialised Nutrition, Utrecht University, Utrecht, 2013.
- [2] A. Kostadinova, TAKES TWO TO BUILD TOLERANCE: T cell epitopes and specific dietary synbiotics - together towards early life cow's milk allergy prevention, in: Nutricia Research and the Utrecht Institute for Pharmaceutical Sciences, Utrecht University, Utrecht, 2018.

Curriculum Vitae

Mengshan Liu was born in 1991 in Guangdong, China. After graduating from high school (Shenzhen Long Cheng High School, Shenzhen, China) in 2009, she started her bachelor's study in Pharmacy at Jinan University. In 2014, she started her research master in Medical and Pharmaceutical Drug Innovation at University of Groningen and gained the UMCG scholarship during her two-year master study. Her first master internship project "SMK-1 interacts with DAF-16 and mediates longevity in Insulin/IGF-1 signaling pathway" was performed at University of Groningen under the supervision of Dr. Christian Riedel. Her internship project aimed to investigate the hypothesized interaction between SMK-1 and DAF-16 in the longevity-mediated Insulin/IGF-1 signaling pathway in *C. elegans*. Her second master internship project "Polymeric nanoparticles loaded with novel GSK leads to improve the therapy against Multi-Drug Resistant Tuberculosis" was performed at Utrecht University under the supervision of Prof. dr. Jan-Willem Alffenaar and Dr. Cornelus F. van Nostrum. Her internship project aimed to synthesize polymer PEGylated poly(lactic-co-hydroxymethyl glycolic acid) for improvement of the therapy against Multi-Drug Resistant Tuberculosis. In 2017, she started her PhD study at the division of Pharmaceutics and the division of Pharmacology at Utrecht University under the co-supervision of Prof. dr. Wim E. Hennink and Dr. Cornelus F. van Nostrum, Prof. dr. Johan Garssen and Dr. Linette E.M. Willemsen. For her PhD study she focused on investigating PLGA based nanoparticles for oral delivery of β -lactoglobulin derived peptide and CpG oligodeoxynucleotides aiming to prevent early life cow's milk allergy. The results from the PhD are compiled in this thesis.

List Of Publications

- [1] M. Liu, S. Thijssen, C.F. van Nostrum, W.E. Hennink, J. Garssen, L.E.M. Willemsen, Inhibition of cow's milk allergy development in mice by oral delivery of beta-lactoglobulin-derived peptides loaded PLGA nanoparticles is associated with systemic whey-specific immune silencing, *Clin Exp Allergy*, 52 (2022) 137-148.
- [2] M. Liu, S. Thijssen, W.E. Hennink, J. Garssen, C.F. van Nostrum, Linette E.M. Willemsen, Oral pretreatment with β -lactoglobulin derived peptide and CpG co-encapsulated in PLGA nanoparticles prior to sensitizations attenuates cow's milk allergy development in mice, *Frontiers in Immunology*, 13 (2023).
- [3] M. Liu, C.Y.J. Lau, I.T. Cabello, J. Garssen, L.E.M. Willemsen, W.E. Hennink, C.F. van Nostrum, Live Cell Imaging by Förster Resonance Energy Transfer Fluorescence to Study Trafficking of PLGA Nanoparticles and the Release of a Loaded Peptide in Dendritic Cells, *Pharmaceuticals*, 16 (2023).
- [4] M. Liu, S. Thijssen, W.E. Hennink, J. Garssen, C.F. van Nostrum, Linette E.M. Willemsen, In Vitro Immunostimulatory Effects of CpG-ODN Encapsulated PLGA Nanoparticles on Human Monocytes Derived Dendritic Cells and Their T-Cells Priming Capacity Using an Allogeneic DC-T-Cell Model. Manuscript in preparation.

Acknowledgements

Thanks to the opportunity provided by my dear supervisor **Rene** in my master internship project, I have this honor to pursue this doctoral research at the same University. Now, this journey is officially ending. Throughout the past years, I have received lots of support and thus I would like to express my gratitude to all those people.

To my promoters and co-promoters:

First, I would like particularly to thank my promoters and supervisors **Wim** and **Johan** for giving me the opportunity to perform my PhD study in the division of Pharmaceutics. Dear **Wim**, it is your consistent dedication and rigorous guidance that tremendously contributed to this work. From the regular progress meetings, I am impressed by your knowledge and endless enthusiasm in the scientific discussion. Although it has been challenging, I have been proud to be your student since you are a great scientist with honorable integrity, critical thinking, and genuine curiosity in research. Many midnight emails regarding the manuscript comments, reflected your admirable dedication to science and inspired me in conducting my scientific research. Dear **Johan**, it is my pleasure to have your guidance during this PhD journey. I particularly thank you for being always supportive and positive and your efforts in providing constrictive support and building the amazing environment of team-spirit in the division of Pharmacology. This work could not have been finished without the teamwork that you have established.

Secondly, I would like to express my sincere gratitude to my co-promoters and daily supervisors **Rene** and **Linette**. Dear **Rene**, I am grateful for your trust and offering me the precious opportunity to work in both master and PhD studies. All along the way, your wisdom, kindness, and endless patience always could resolve the miscommunication in our discussions. When it comes to manuscript revision, I am impressed by your simplicity philosophy, which improved its clarity and inspired me profoundly. Your mild character, dedication, integrity, efficient and professional work style are all impressive qualities for me to admire. Dear **Linette**, my deep gratitude for your consistent support in these years is more than words can tell. Still, I would like to thank you for your valuable input and enlightening discussions in this process. You taught me not only the knowledge in the immunology field in our meetings, but also how to accurately interpret the data. In the good or tough times, you kept the faith that

there are valuable indications/clues from our data. Your positive attitude is contagious, and I am so thankful for your regular organizations of some fun activities (e.g., bowling).

To my collaborators:

Dear **Suzan T.**, I would like to thank you for teaching a lot in the practical experimental skills in handling mice and giving oral gavages, flow cytometry analysis and consistent support in all animal studies and cell studies. It was my pleasure to collaborate with you in the past years. During the sectioning days, you have always been there for me and stayed strong even until the midnights. I would like to express my heartfelt gratitude to your enormous contribution to not only the work but also those laughter and joyful moments we shared. Dear **Jerry**, I would like to thank you for your sharing of your knowledge, time, and efforts in Chapter 4. Your broad knowledge in design, synthesis, characterization, and analysis of peptide has been of immense help in accomplishment of this chapter. Your friendliness, enthusiasm, ambition, and dedication have made you a great scientist and an impressive colleague that can lift the spirits.

To my students:

I would like to acknowledge my students for collaborating with me in my project. Dear **Chantal**, thank you for spending time in my project and I wish you success in your pursuit in study and work. Dear **Irene**, thank you for choosing my project as your internship project and your contribution in the Chapter 4. It was such a wonderful experience to collaborate with you and I have also learned a lot from you in this process. I would like to thank you for helping with the sectioning days and your optimism raised my spirits even during the busy days.

To my paranympths and girls:

Dear **Yan** and **Xiaoli**, it was so great to have met you in this journey and thank you for being my paranympths of my PhD defense. Dear **Yan**, I recalled the very first weeks upon arrival in Utrecht that we had a cozy gathering, with nice dinner and fun Karaoke. As fume hood neighbors, I really enjoyed our occasional Chinese chats and the laughter in coffee breaks or lunch time. I especially admired your open-mind, diligence, and enthusiasm in learning (Dutch, swimming, etc). This has also inspired me to explore more possibilities in life and work. On top of that, you have such as good heart that you directly corrected me when necessary and recommended books that I enjoyed reading

a lot. Dear **Xiaoli**, it is always delightful to chat with you. Your enthusiasm for Yoga, and passion for life and work are contagious. During your work trip in Guangzhou, it was so great to meet you again and to know your new life journey. I hope we can spend more fun time together soon.

Dear **Xiangjie**, I am thankful for your support in life and work ever since the very beginning and enjoyed our chats, laughter on the lunch breaks and dinners together. You are always friendly and help me whenever I turned to you. I hope everything goes well with you and I am looking forward to meeting you again. Dear **Blessing**, it was so pleasant to know you since my master internship in the same department. I already missed your good heart, positivity, chats, and laughter as good neighbors at home and as colleagues at work. Dear **Cristina** and **Barbara**, thanks for being so kind and friendly in the lab work, and I missed the chats and your laughter in the borrel.

To my colleagues:

Special thanks go to **Jeffrey, Atanaska, Laura, Yanna, Bo**. Dear **Jeffrey**, thank you for providing me help as lab buddy in the first week of my PhD study and your daily supervision during my master internship. Dear **Atanaska**, thank you very much for helping me to follow up your previous work and the DEC, and your generosity in sharing your knowledge. I have learned a lot from your thesis and admired your work. Dear **Laura**, thank you very much for your scientific advice in the meeting in Nutricia and I also have learned a lot of form reading your previous work. Dear **Yanna**, thanks for your scientific suggestions and your kindness in providing help. Your perseverance, diligence, positivity, and dedication for scientific research have always been encouraging me. Dear **Bo**, thank you for your generous help in giving scientific suggestions in tackling a synthetic problem. Your intelligence, enthusiasm, ambition, and dedication for science have made you such a good scientist. It was so great of you to invited us to your place for the celebration of the Chinese New Year Eve.

Dear **Mies**, thank you for your instruction in the synthesis lab and broad knowledge of various equipment and advice for trouble shooting in the regular synthesis meeting. Dear **Esmeralda**, thank you for your instruction in the Yokogawa and live imaging. It was of immense help for me to start my FRET project by means of fluorescence microscopy. Dear **Kim**, thank you very much for your instruction about the cell culture techniques.

Acknowledgements

Dear **Roel**, thank you for your instruction for working at the cell culture lab. Dear **Feiko, Louis, Imro, Gemma and Koen**, thank you for your help in placing orders for me during these years. Dear **Barbara**, I would like to thank you for scheduling the regular meeting for me and arrangements of the paperwork.

Dear **Tina, Enrico and Robbert Jan**, thanks for your scientific feedbacks during the Tuesday's morning colloquiums.

Dear **Mara**, special thanks for your help in the oral sensitizations when I did not fully comprehend this technique. Dear **Mara, Negisa, Mirelle and Xiaoli**, I would like to thank you all for your help on the whey challenge day in my animal studies, spending your time to collect the allergy-associated readouts. Dear **Suzanne A.**, thank you very much for sharing your knowledge and helping with the preparation of cell isolation from the lamina propria in my second animal study. Dear **Veronica**, thank you for infinite patience in answering my questions and your generous sharing of your knowledge in culture of human monocytes derived dendritic cells and co-culture with T-cells. I enjoyed our talks and laughter in lunch time during laboratory animal science in my first year of the PhD journey. Dear **Marit**, thank you so much for your help in the sectioning day even when you were taking a course, which means a lot to me. I have always admired your optimism, positivity and enjoyed your sharing of some funny stories. Dear **José, Lei, Manou, Monika, Ingrid, and Gemma**, thank you so much for your help in the sectioning days of my animal studies. Dear **Sandra, Alinda, Roos and Robine**, thank you for your chats and all the fun time we spent in the events organized by Linette.

Dear **Haili, Yinan, Dandan, Weiluan, Feilong, Lucia, Andhyk, Karina, Marzieh, Aida, Sjaak, Lies, Mahsa, Desiree, Thijs, Martina, Yong, Boning, Mingjuan, Carl, Charis, Ada, Erik, Mert, Danny, Johanna, Stefania, Yulong, Ling, Jing Chen, Yang, Puqiao, Yuanpeng, Deguang, and Yi**, I am glad to work with you in the UIPS during my master and PhD studies and thankful for your help and/or scientific discussions. Dear **Linglei, Yanyan, Jianming Chen, Jing Li, Wenjing Lu, Donglong Fu, and Qianrao Fu**, it was nice to know you in Utrecht and thankful for the chats and/or help.

To Emanuel Lacko and your families:

Dear **Emanuel**, I could not have accomplished this journey without your infinite support, love, and patience. You have the best heart for me as my partner and always

being there for me in the good or tough times. Dear **Igor, Andrea** and **Raphael**, thanks for making it home for me during the Christmas holidays in your place and showing me around in Frankfurt. Dear **Usch**, thanks for your greetings and sang me birthday songs, which melt my heart like a grandma I never met.

To my families:

Last but not the least, I would like to express my gratitude to my families. 亲爱的爸爸，妈妈和哥哥，感谢你们对我远赴他乡读博深造的支持。虽然相隔万里，你们就是我心里最深的牵挂。亲爱的哥哥刘穗超，感谢你在我读博期间承担起照顾父母的责任，让我能在外安心求学。我也不会辜负你们对我的厚爱，会成为你们最坚定的后盾！

Mengshan Liu (刘梦珊)

2023-08-08

